Techniques expérimentales

…pour les réactions directes

P. Roussel-Chomaz
GANIL
patricia@ganil.fr

Sources des documents:

- INPC2007 (http://www.inpc2007.jp)
- DREB2007(http://ribf.riken.go.jp/DREB2007)
- mes collègues du GANIL, IPNO, SPhN Saclay
- Collaborations MUST2, MAYA

Ecole Joliot Curie, 17-21 Septembre 2007
« Les réactions nucléaires comme sonde de la structure »

Plan du cours

1) Les réactions avec les faisceaux secondaires
Réactions directes: diffusion élastique et inélastique, transfert, knock-out
cinématique directe/inverse

2) Faisceaux secondaires : méthodes de production en vol et en ligne (ISOL).
Avantages et inconvénients de chacune.
Exemples à GANIL, GSI, CERN-ISOLDE, Louvain la Neuve,
TRIUMF, Oak Ridge, RIKEN

3) Cibles :
- cibles solides
- cibles cryogéniques (gaz, liquide, solide pour H et D)
- cibles polarisées

4) Détecteurs de faisceaux

Techniques expérimentales

5) Systèmes de détection et exemples d'expériences :

- ensembles pour particules chargées (MUST, MUST2, TIARA, HIRA….)
- cibles actives (MAYA) :
  - principe de fonctionnement.
  - Comparaison avec les ensembles de détecteurs à base de Silicium
- spectromètres (VAMOS/SPEG) :
  - caractéristiques, optiques, systèmes de détection du plan focal.
- Détecteur γ (EXOGAM)

Méthode de masse manquante, Méthode de masse invariante

Section efficace, Distribution angulaire, Distribution en moment

6) Les machines du futur: nouveaux accélérateurs, nouveaux détecteurs

Japon: RIBF RIKEN

USA: RIA (light)

Europe: SPIRAL2, FAIR, EURISOL

Part 1:

Reactions induced with secondary beams

Why study nuclear reactions between the barrier and 100 MeV/A?

- Elastic Scattering
  - optical model potentials
  - nuclear densities
  - effective nucleon-nucleon potentials

  } E. Baugie
- Inelastic scattering
  - electromagnetic excitation is sensitive "only" to protons while proton scattering is mainly sensitive to neutrons
  - compare proton with e.m. excitation to disentangle proton and neutron deformations and transition matrix elements $M_{n(p)}$
- Transfer reactions (N. Keeley) / Knock-out reactions (D. Baye, L. Cortina)
  - Microscopic structure of ground and excited states
  - Study of unbound nuclei beyond the drip lines
- Deep inelastic reactions
  - Very efficient to produce exotic nuclei
- Fusion reactions (C. Simenel)
  - Explore the influence of novel structures on reaction mechanisms
  - Search for new paths towards heavy elements

Direct reactions with exotic beams

A(B,C)D

Direct reactions (Two-body): elastic, inelastic scattering, transfer reactions

Proceed directly from initial to final state,

generally in one step as opposed to compound nucleus reactions.

Exotic beams

Exotic nuclei do not live long enough to make targets

⇒ secondary beam

To determine the properties of a given nucleus:

interaction with simple structure particles (e^-,p,d,α)

⇒ Inverse kinematics

⇒ Detection of the heavy ejectile

or/and

the light recoil

or/and

the deexcitation γ

Direct reactions with inverse kinematics

Detection of the heavy residue

- Emission at forward angles in the laboratory frame
  - good detection efficiency even with limited angular coverage
  - angular resolution difficult to achieve
- Impossible when not bound (does not give information on the structure)

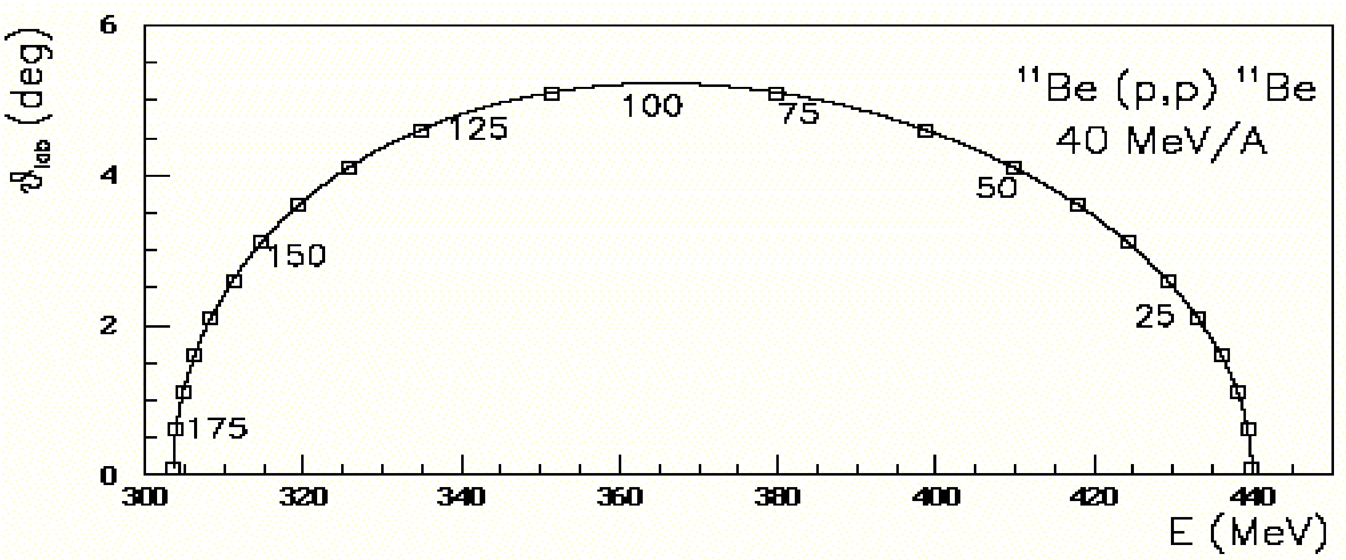

P. Roussel-Chomaz

GANIL Spiral 2

Direct reactions with inverse kinematics: recoil nucleus

^{6}He+p system

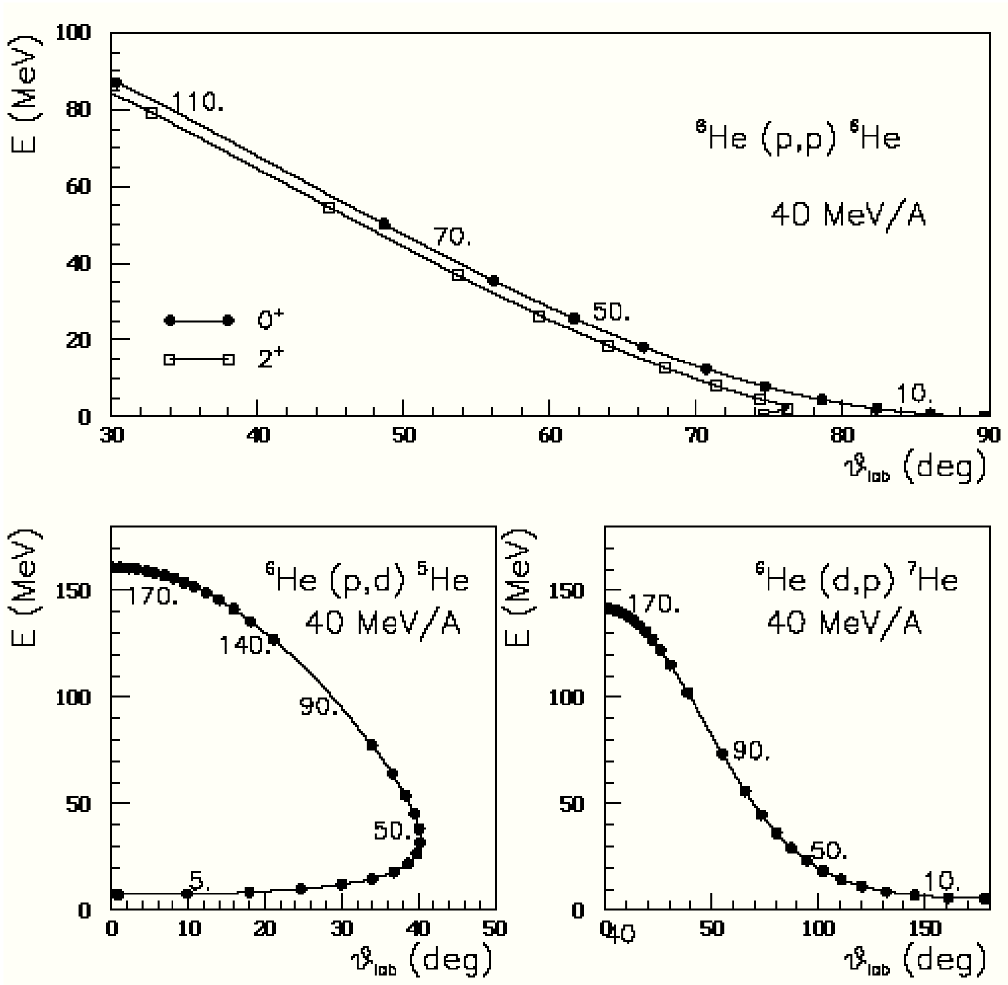

Elastic and Inelastic scattering: small angles correspond to 90° (lab)

Pick-up: Recoil emitted to forward angles

Stripping: Small CM angles correspond to backward lab angles

Direct reactions in Inverse Kinematics

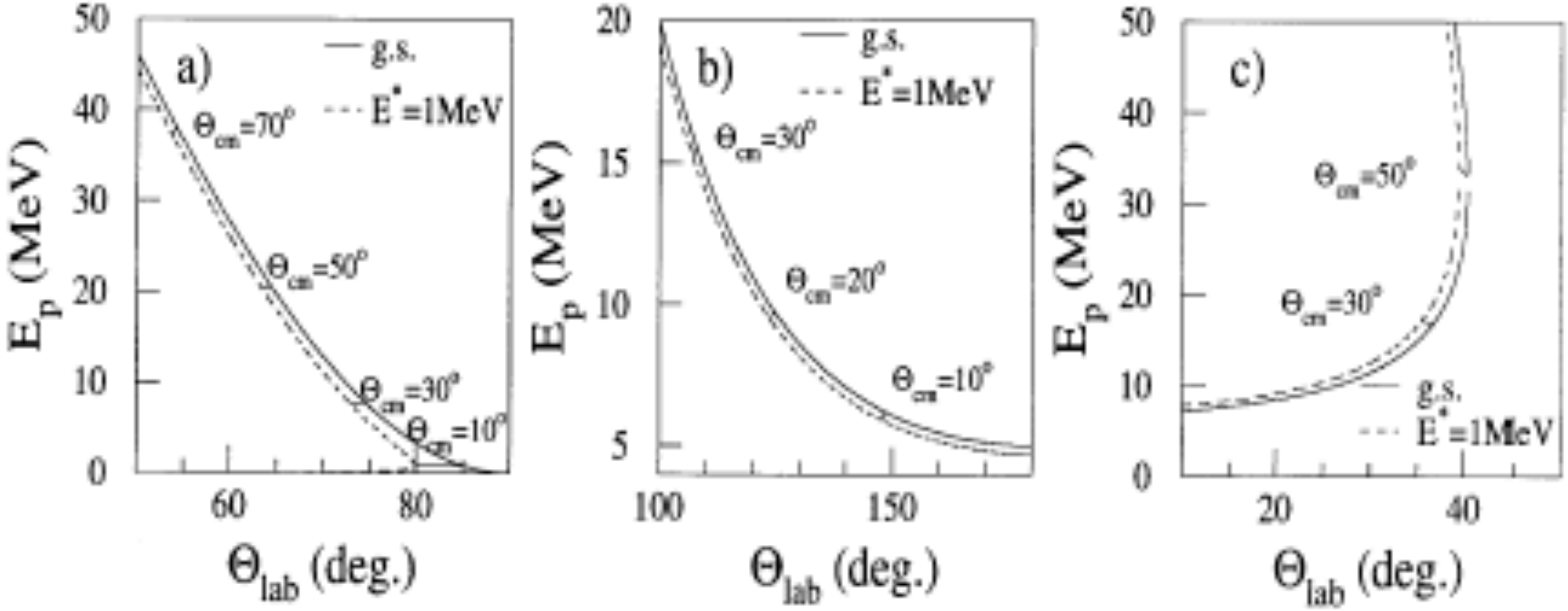

$^{32}Mg(p,p')$ ^{32}Mg (d,p) $^{32}Mg(p,d)$

30 MeV/nucleon

Two-body direct reactions as spectroscopic tools

A [target] (B [projectile], C [measured]) D

Example: ^{32}Mg(p,d)^{31}Mg → p(^{32}Mg,d)^{31}Mg

- Q value : position of level
- Angular distribution : L of the transition
- Cross section : B(EL) or spectroscopic factor (or ANC)

- Detection
  - Ejectile: spectrometer
  - Light recoil: Si array
  - Deexcitation γ : Ge array

A Typical Direct Reaction Experiment

MUST: Y. Blumenfeld et al., *NIM* **A366** (1999) 298
CATS: S. Ottini-Hustache et al., *NIM* **A431** (1999) 476

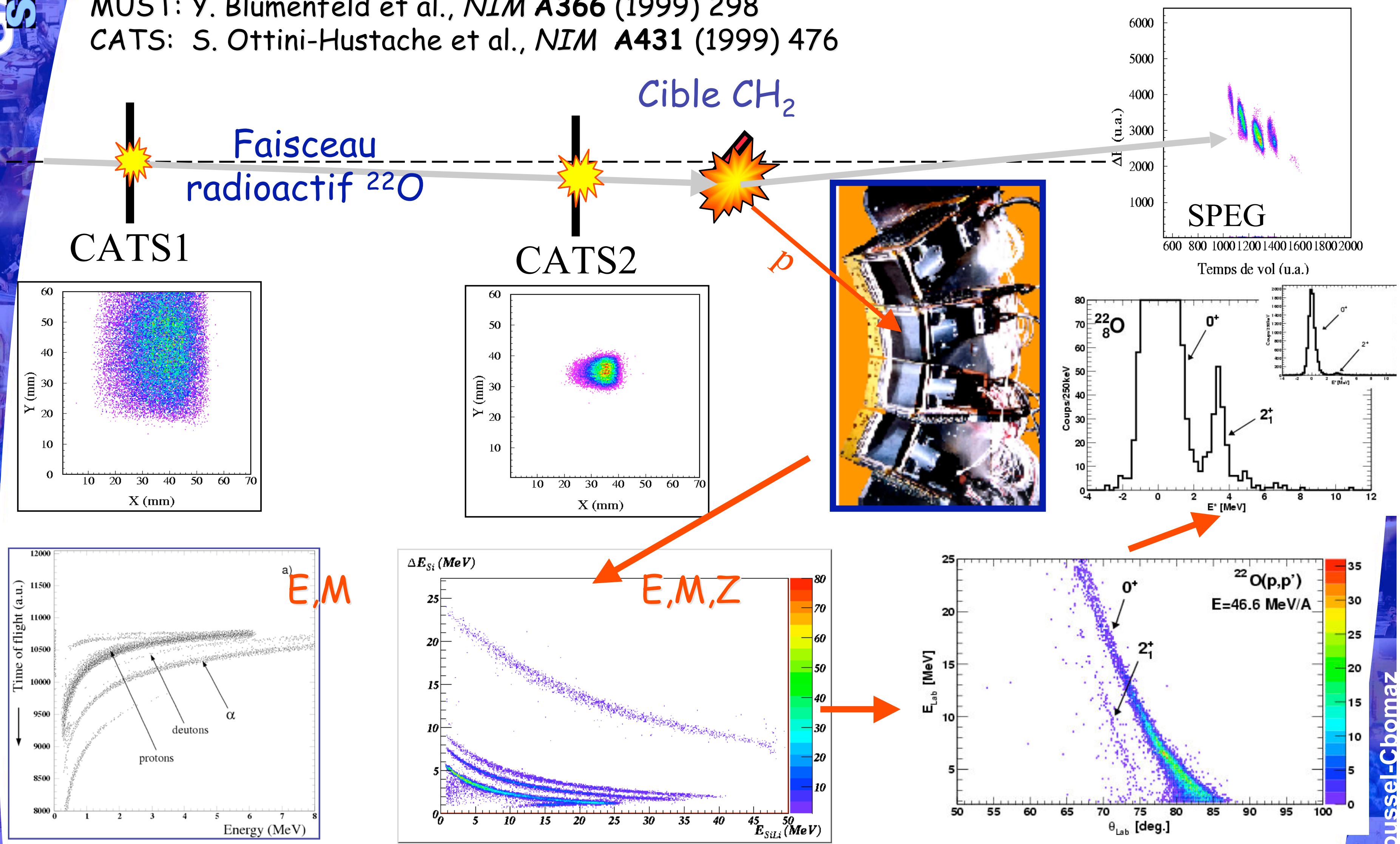

TIARA+EXOGAM+VAMOS

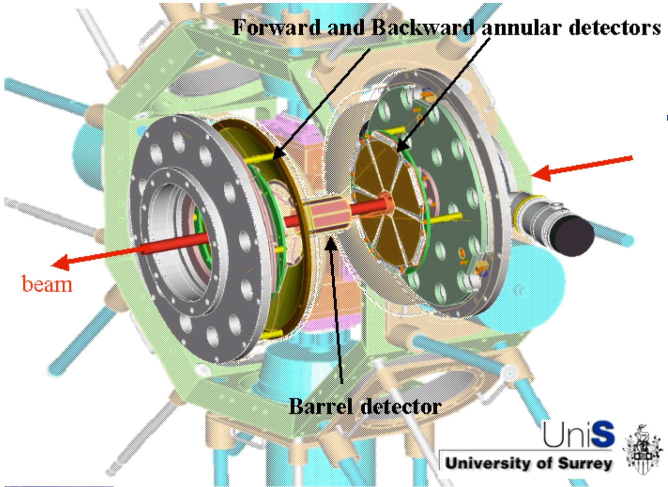

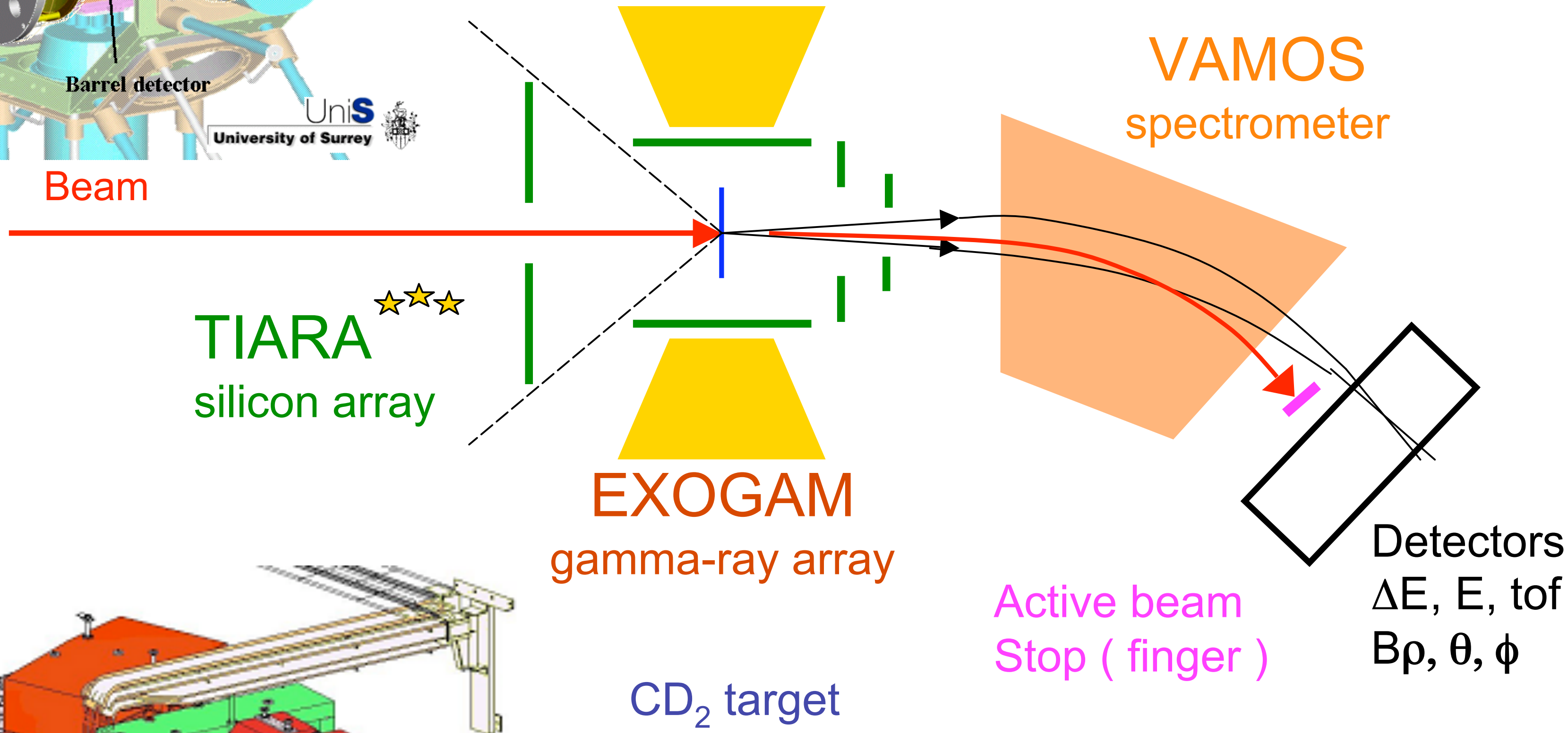

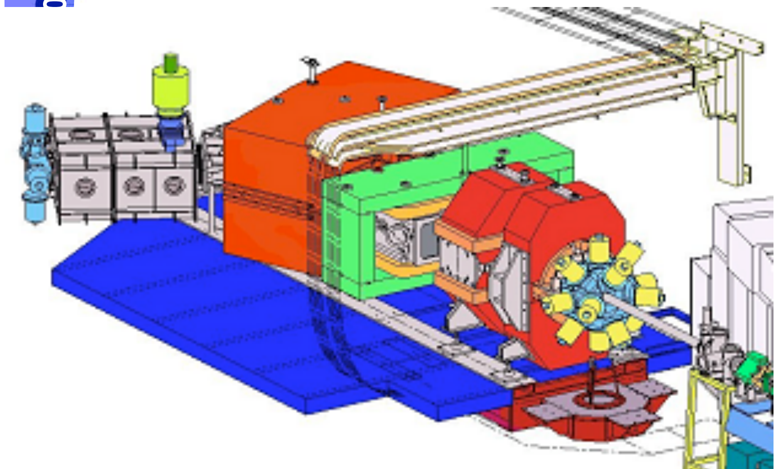

Triple coincidences:
Target-like particles - TIARA
Beam-like particles - VAMOS
Gammas - EXOGAM

P. Roussel-Chomaz

Part 2:

Production of radioactive/exotic/secondary beams

Radioactive beam production

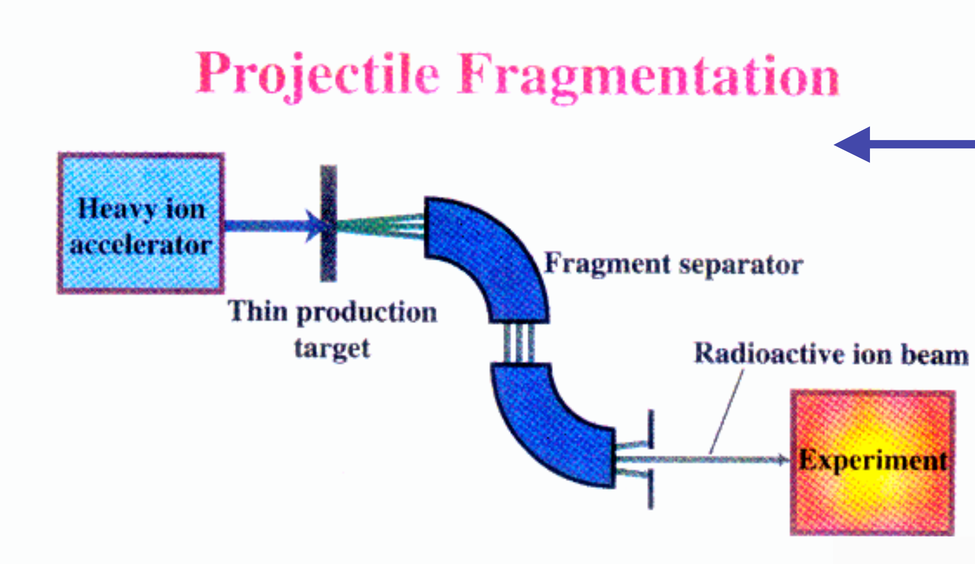

GANIL/SISSI, GSI(FAIR), RIKEN, NSCL/MSU

High energy, large variety of species
Poor optical qualities

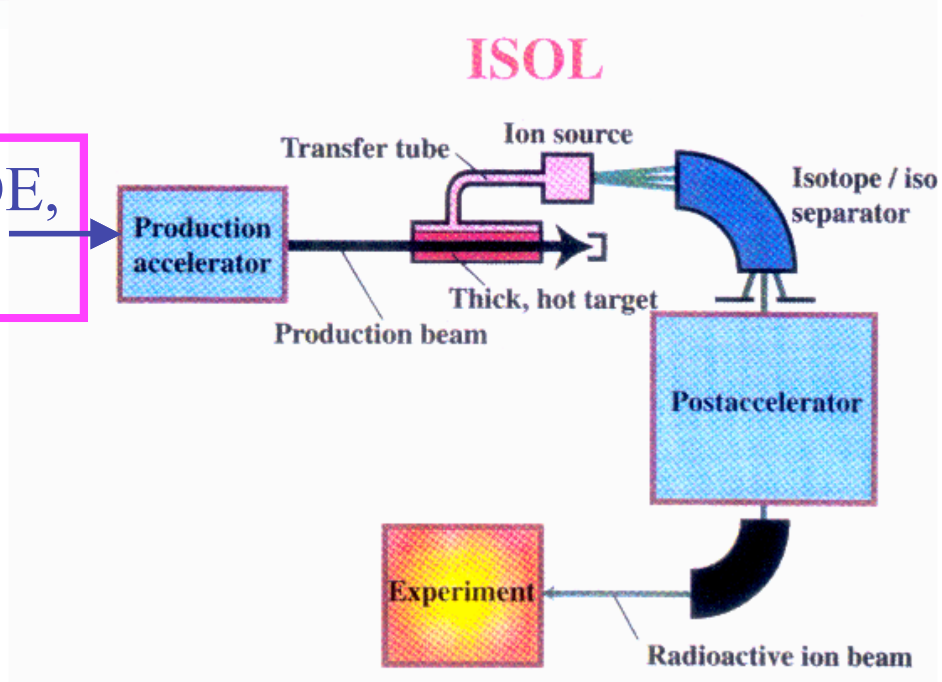

GANIL/SPIRAL(2), REX/ISOLDE, ISAC/ISAC2/TRIUMF

Low energy, chemistry is difficult, good beam qualities

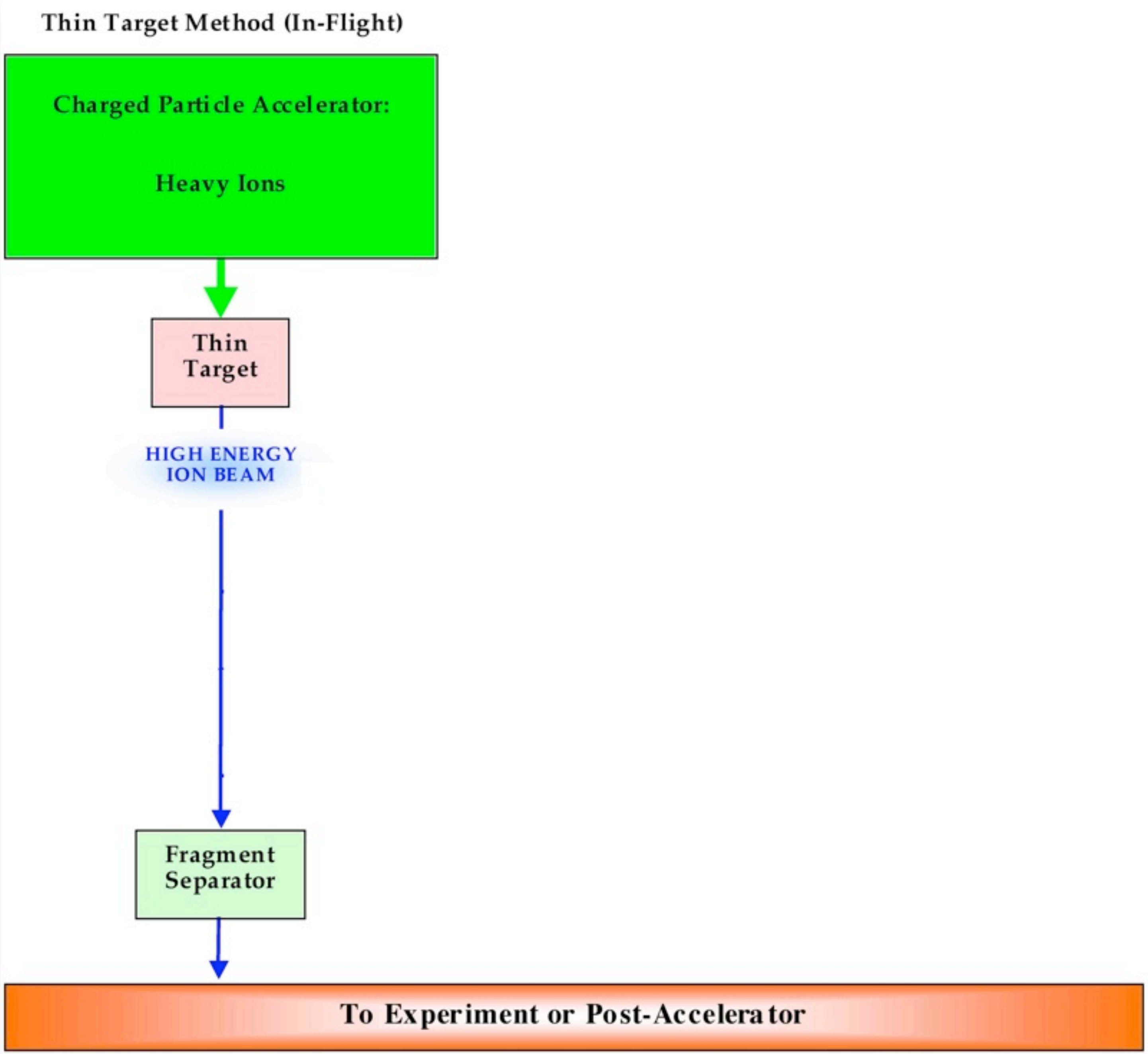

A. Villari, INPC 2007

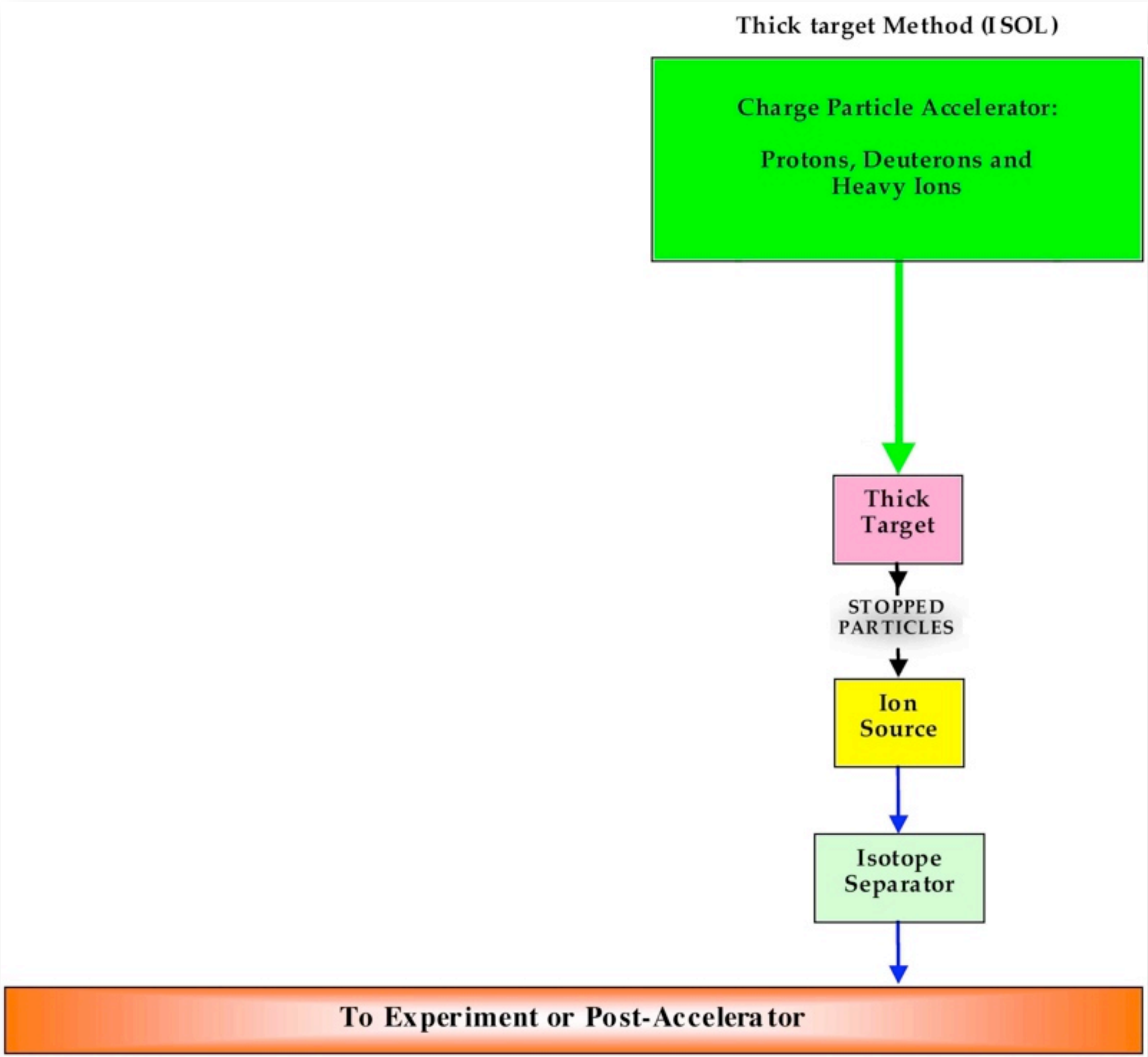

A. Villari, INPC 2007

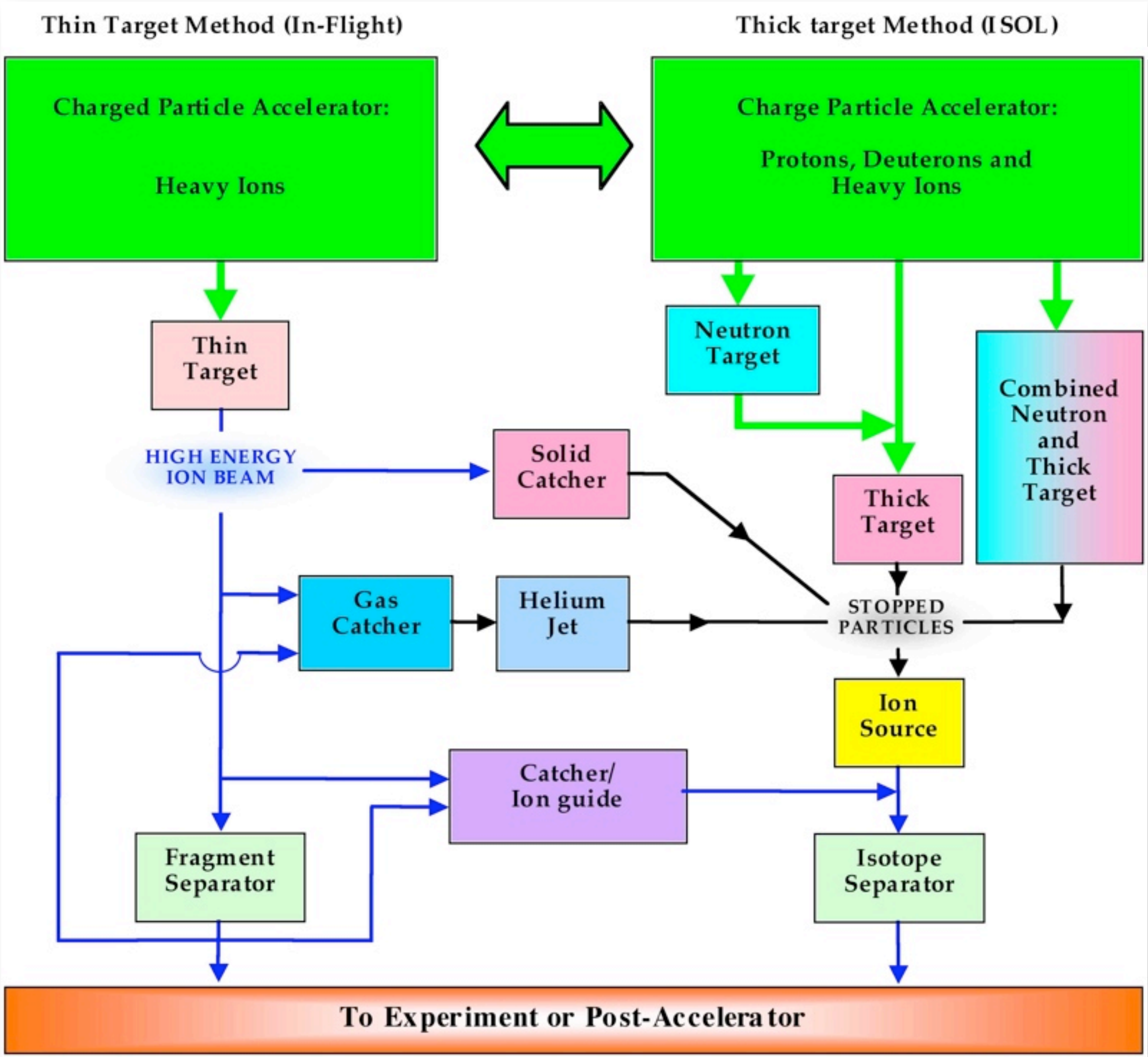

A.C.C. Villari and R. Bennett, Comptes Rendus. Physique (2003) (no.4-5t.4) p. 595

A. Villari, INPC 2007

ISOL + post accelerator

- Provides “high intensity” beams with good optical properties
- Can produce “pure” beams
- Poor efficiency for short living nuclei, but progress is being done
- For refractory elements, only possible in “IGISOL” mode
- MANY ways to get lost what you produced...

Efficiency is an important issue.
Different methods - different facilities - developed complementary techniques, guaranteeing better efficiency and reliability

Selected ISOL Facilities : CRC - LLN

Mass sep: 2 10^{-4}
Transmission: 3 to 5%

For low energy
0.1 to 1 MeV/u
No longer in op.

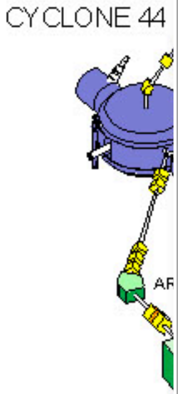

Element	Half live, $T_{1/2}$	charge state	beam intensity [pps on target]	energy range [MeV]
^{6}Helium	0.8 s	1+ 2+	$9 \cdot 10^{6}$ $3 \cdot 10^{5}$	5.3 - 18 30 - 73
^{7}Beryllium	53 days	1+ 2+	$2 \cdot 10^{7}$ $4 \cdot 10^{6}$	5.3 - 12.9 25 - 62
^{10}Carbon	19.3 s	1+ 2+	$2 \cdot 10^{5}$ $1 \cdot 10^{4}$	5.6 - 11 24 - 44
^{11}Carbon	20 min	1+	$1 \cdot 10^{7}$	6.2 - 10
^{13}Nitrogen	10 min	1+ 2+ 3+	$4 \cdot 10^{8}$ $3 \cdot 10^{8}$ $1 \cdot 10^{8}$	7.3 - 8.5 11 - 34 45 - 70
^{15}Oxygen	2 min	2+	$6 \cdot 10^{7}$	10 - 29
^{18}Fluorine NO LONGUER AVAILABLE	110 min	2+	$5 \cdot 10^{6}$	11 - 24
^{18}Neon	1.7 s	2+ 3+	$6 \cdot 10^{6}$ $4 \cdot 10^{6}$	11 - 24 24 - 33,45 - 55
^{19}Neon	17 s	2+ 3+ 4+ 6+	$2 \cdot 10^{9}$ $1.5 \cdot 10^{9}$ $8 \cdot 10^{8}$ $3 \cdot 10^{7}$	11 - 23 23 - 35,45 - 50 60 - 93 171
^{35}Argon	1.8 s	3+ 5+	$2 \cdot 10^{6}$ $1 \cdot 10^{5}$	20 - 28 50 - 79

30 MeV p
300 microA

www.cyc.ucl.ac.be

Selected ISOL facilities: SPIRAL - GANIL

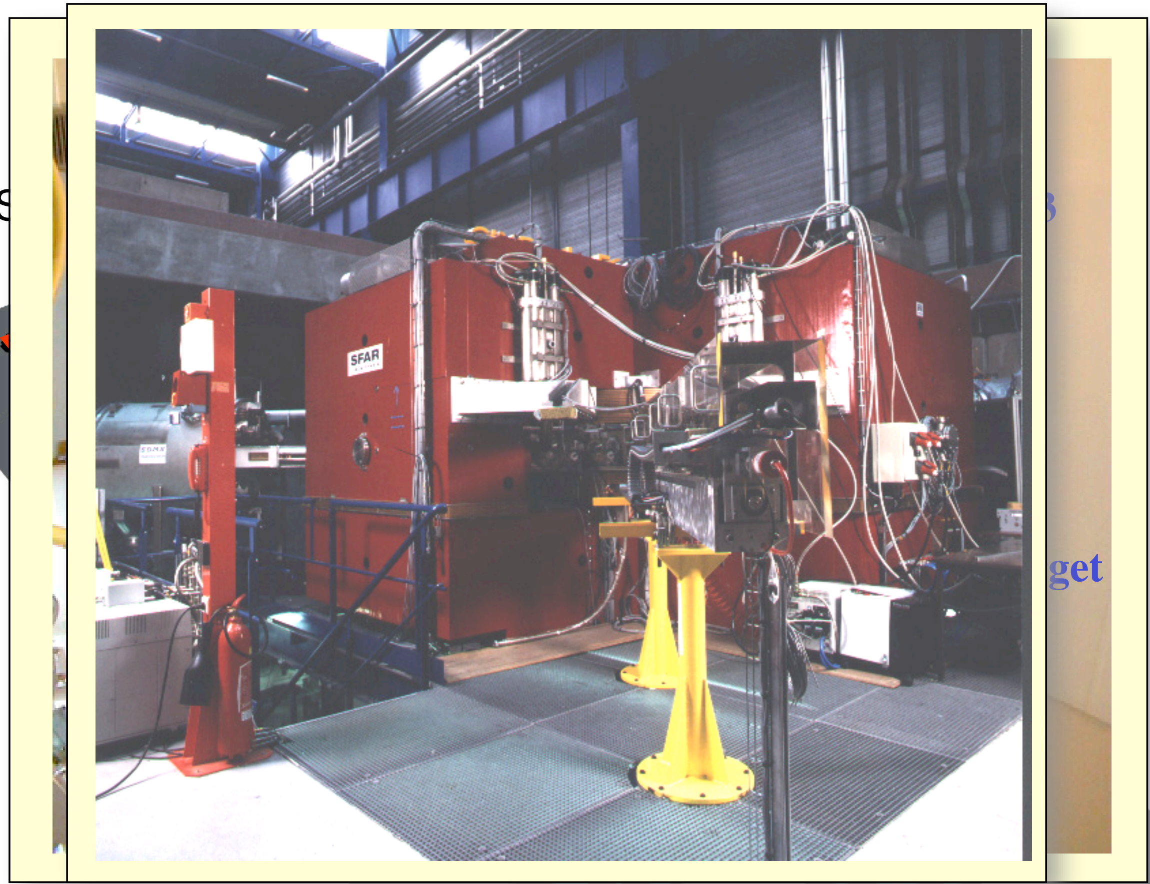

ISOL
E = ~ 1.7A - 25A MeV

ACCV, Nucl.Phys. A693, 465 (2001)

Selected ISOL Facilities: SPIRAL - GANIL

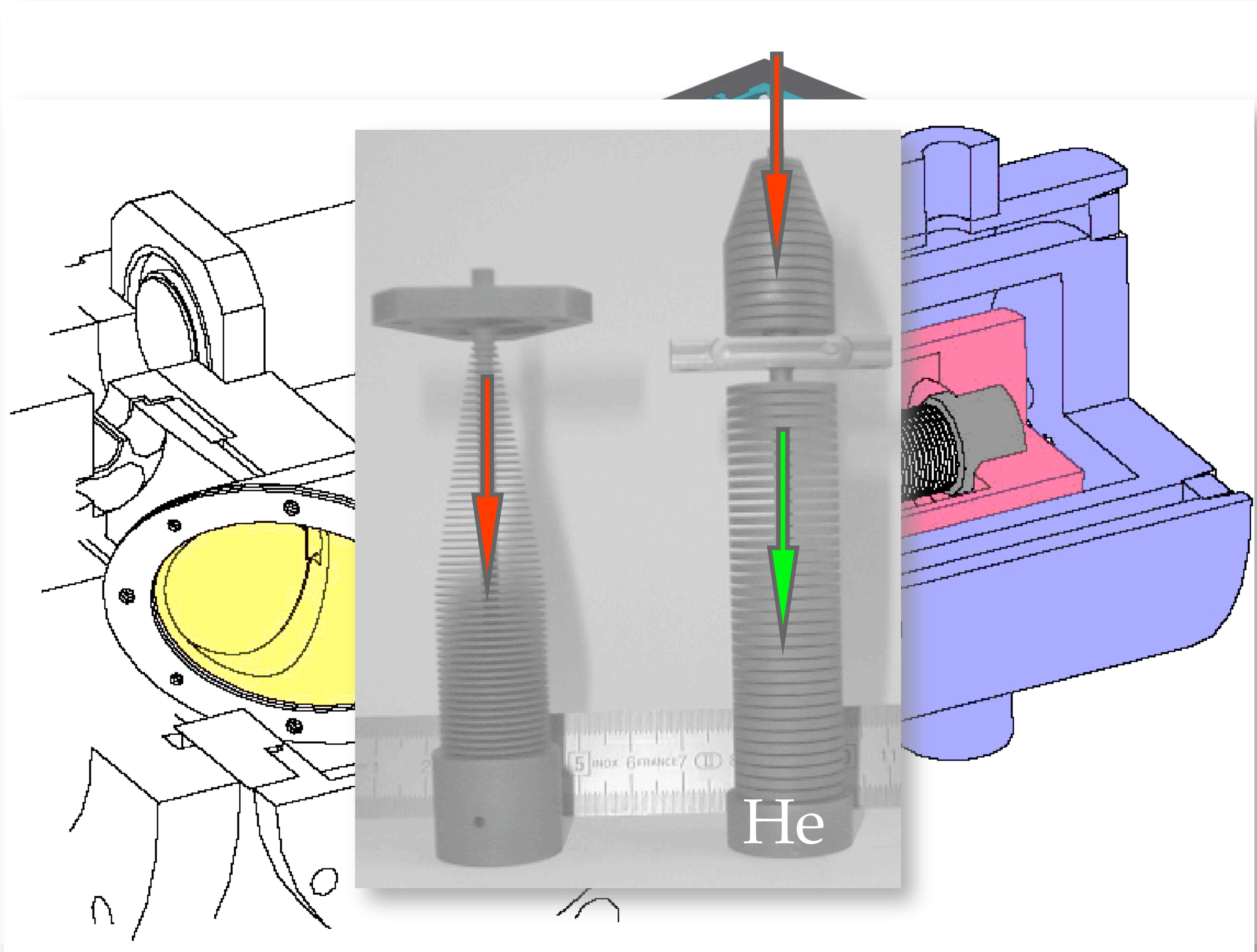

ACCV, Nucl.Phys. A693, 465 (2001)

Selected ISOL Facilities: SPIRAL - GANIL

http://www.ganil.fr/operation/available_beams/radioactive_beams.htm

Helium

update : 24 mars 2006

Radioactive Beam (halflife)	Charge State	Intensity (pps)		Min Energy (MeV/nucleon)	Max Energy (MeV/nucleon)	Primary Beam	Primary Beam Power on ECS Target (kW)	Primary Beam Energy (MeV/nucleon)
		LEB	Target*					
^{6}He (0.8s)	+1	$3\ 10^{7}$**				^{13}C	2.4	75
	+1		$1.7\ 10^{7}$	3.2	7.3		1.2	
	+1		$2.8\ 10^{7}$	3.8	7.3		2.5	
	+1		$3.2\ 10^{7}$	5	7.3		1.2	
	+2	$2.8\ 10^{7}$	$5.6\ 10^{6}$	6.8	22.8		1.4	
^{8}He (0.12s)	+1		$1.5\ 10^{5}$	2.5	4.1	^{13}C	2.5	75
	+1	$2.6\ 10^{5}$	$5.2\ 10^{4}$	3.5	4.1		0.9	
	+1		$1.8\ 10^{5}$	3.8	4.1		2.5	
	+2	1.3 to $1.5\ 10^{5}$	2 to $3\ 10^{4}$		15.4		1.4	

* Available intensity for the experiment.
** LIRAT figures

Color code :

$2.8\ 10^{7}$ = extrapolated figures from SIRA experiment from 400 W to 1.4 kW.

$2.8\ 10^{7}$ = measured figures with SPIRAL.

$2.8\ 10^{7}$ = expected figures after acceleration (not measured) with 20% transport efficiency.

Other ISOL facilities: CERN-ISOLDE

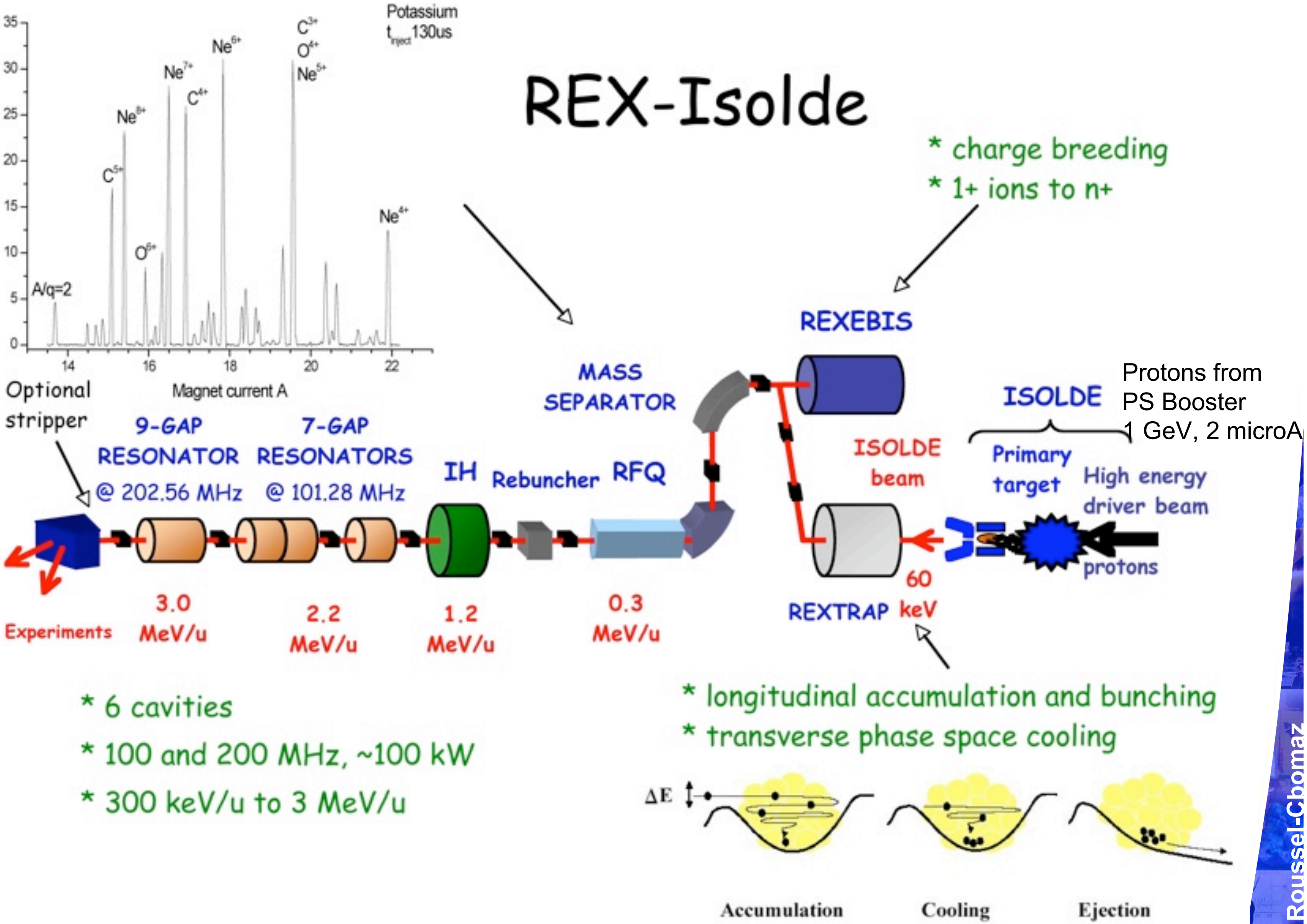

M. Lindroos courtesy

Other ISOL facilities

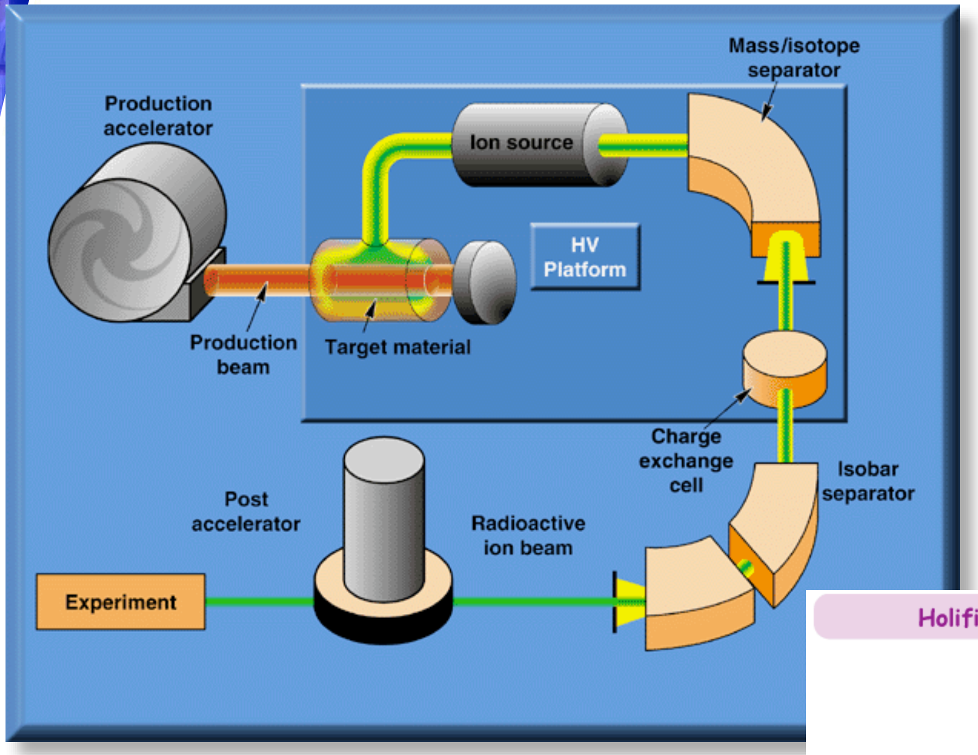

HRIBF

Injector: ORIC, light ions (protons 42 MeV, deutons 49 MeV, helium 85 MeV, Few microAmp.)
Production target: HfO_2, ZrO_2, UC_2
Postaccélération by Tandem
—>Charge exchange cell

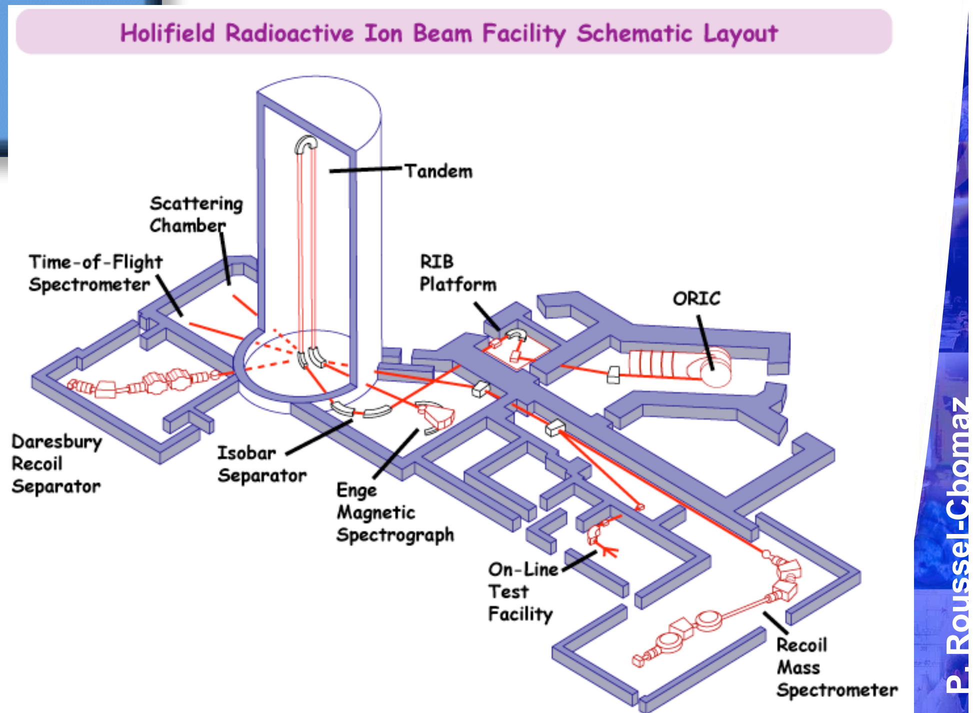

www.phy.ornl.gov/hribf

Other ISOL facilities

ISAC I and ISAC II

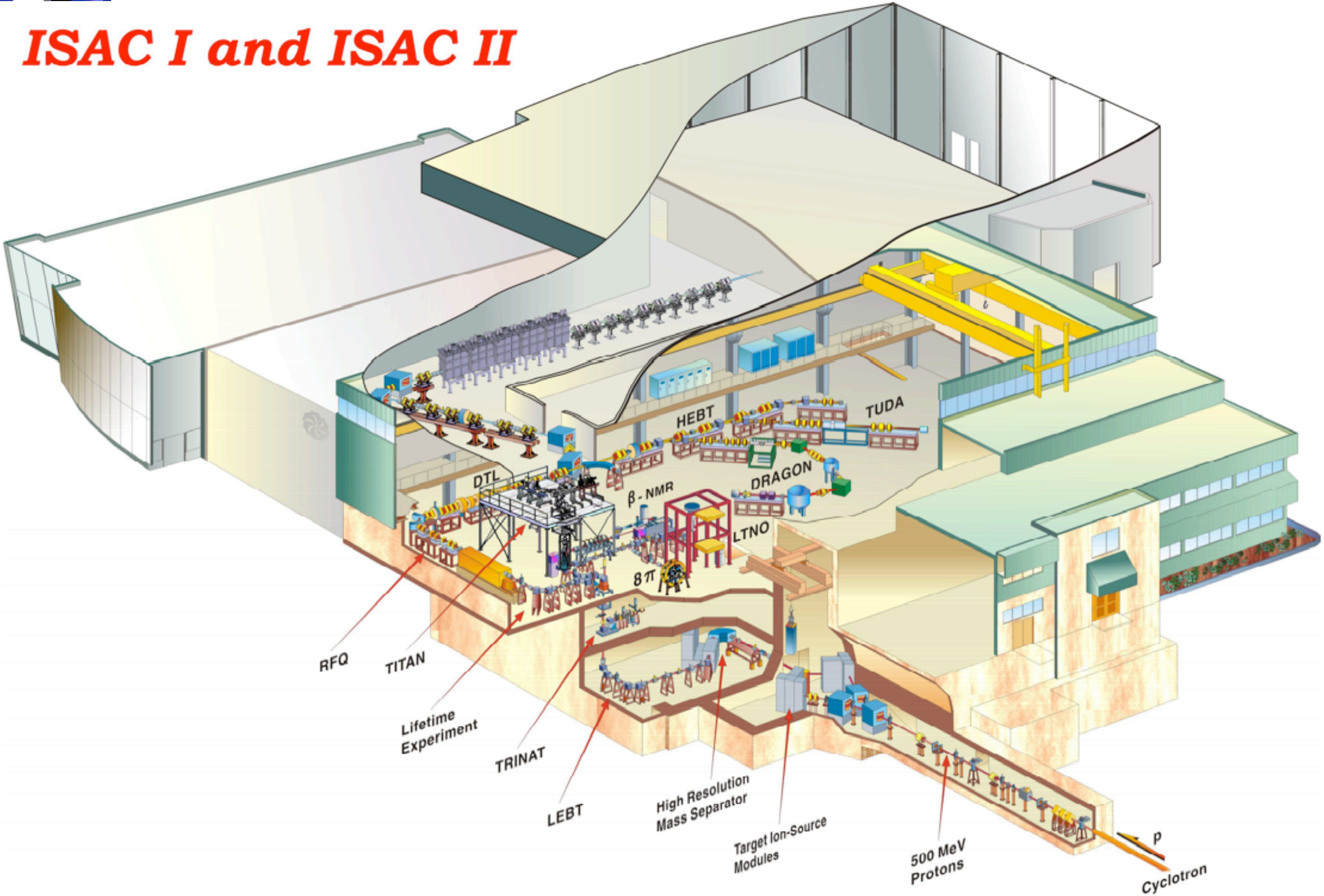

Other ISOL facilities

•EXCYT, Catania - delivered the first ^{8}Li beam

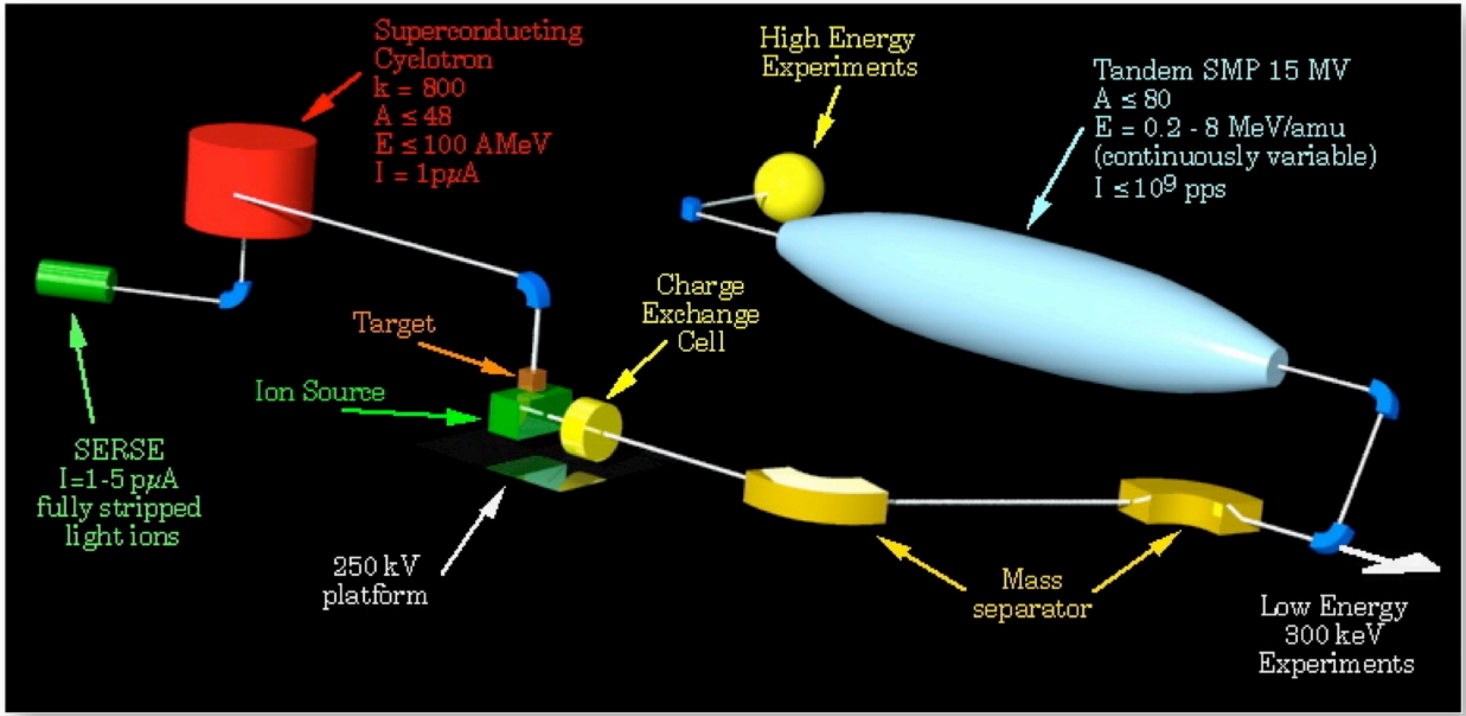

•DRIBS - Dubna

•TRIAC (KEK-JAERI) is also starting
(accelerator moved from former INS)

In Flight Facilities

In Europe

GSI

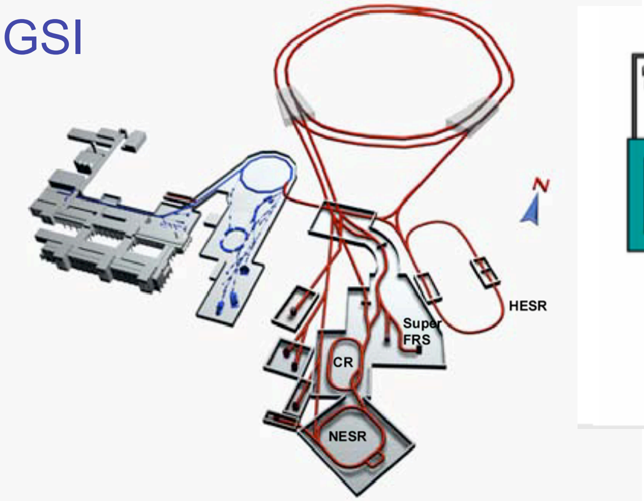

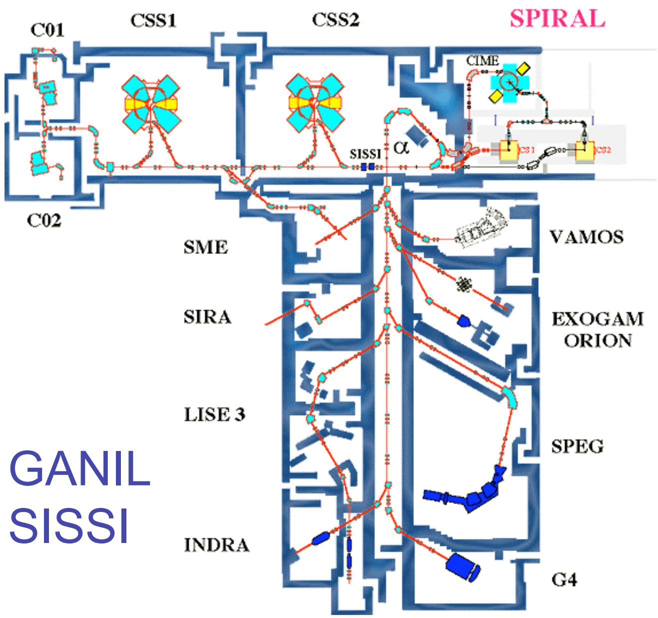

GANIL
SISSI

In USA MSU

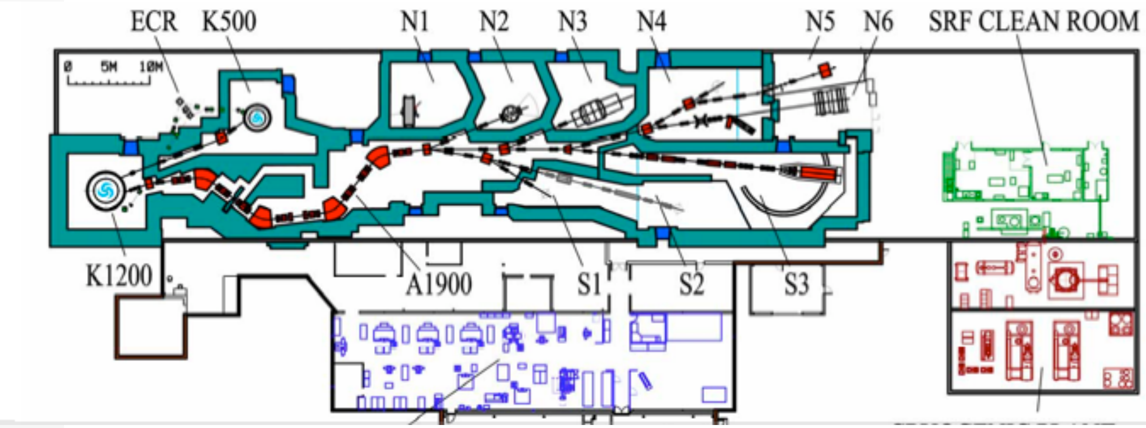

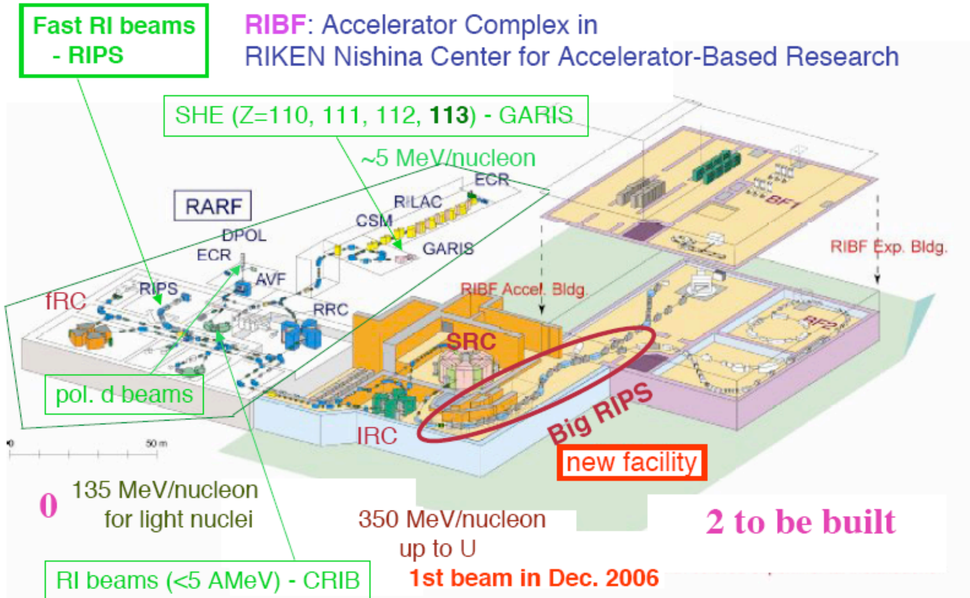

In Japan

In-flight production of rare isotopes

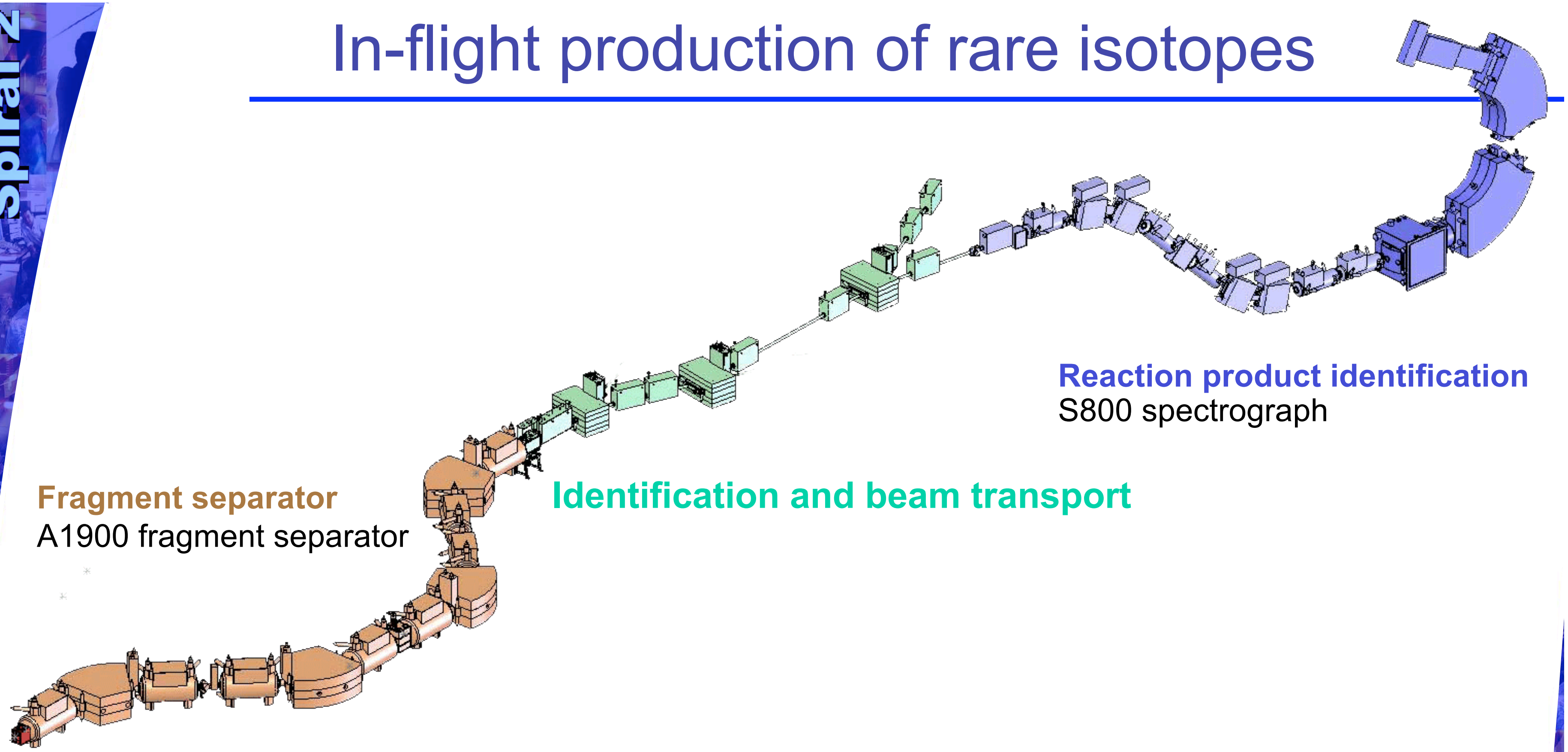

Driver accelerator (v = 0.25-0.6 c)

- Fragment separator (A1900 NSCL, FRS GSI, BigRIPS RIKEN, ALPHA spectrometer/LISE GANIL)
- Identification and beam transport
  - Stopped beam experiments, reaccelerated beam experiments
  - Fast beam experiments
    - Secondary reaction
    - Reaction product identification (S800 spectrograph, CATE/Aladin, Silicon telescopes/TOF wall, SPEG)

INPC 2007 Th. Glasmacher

In-flight production of rare isotopes
Example: ^{78}Ni from ^{86}Kr at NSCL

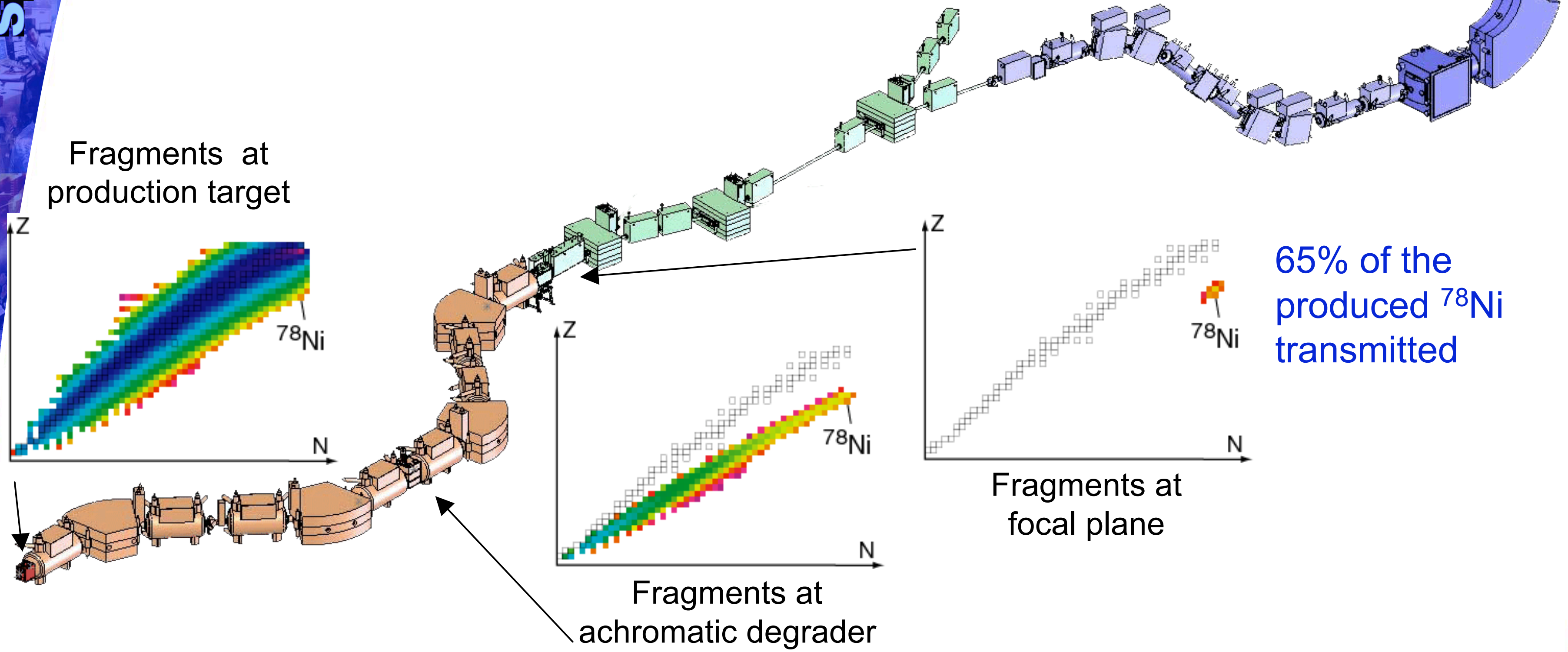

Driver accelerator (v = 0.25-0.6 c)

- Fragment separator (A1900 NSCL, FRS GSI, BigRIPS RIKEN, ALPHA spectrometer/LISE GANIL)
- Identification and beam transport
  - Stopped beam experiments, reaccelerated beam experiments
  - Fast beam experiments
    - Secondary reaction
    - Reaction product identification (S800 spectrograph, CATE/Aladin, Silicon telescopes/TOF wall, SPEG)

P. Roussel-Chomaz

Production of Secondary ^{30}S beam

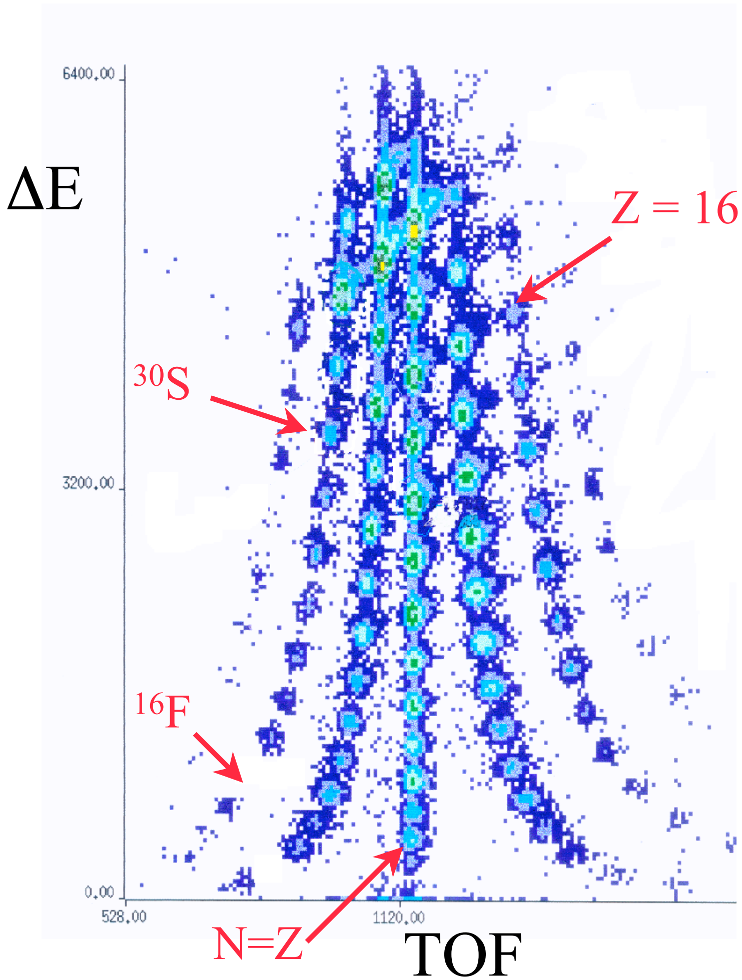

without degrader

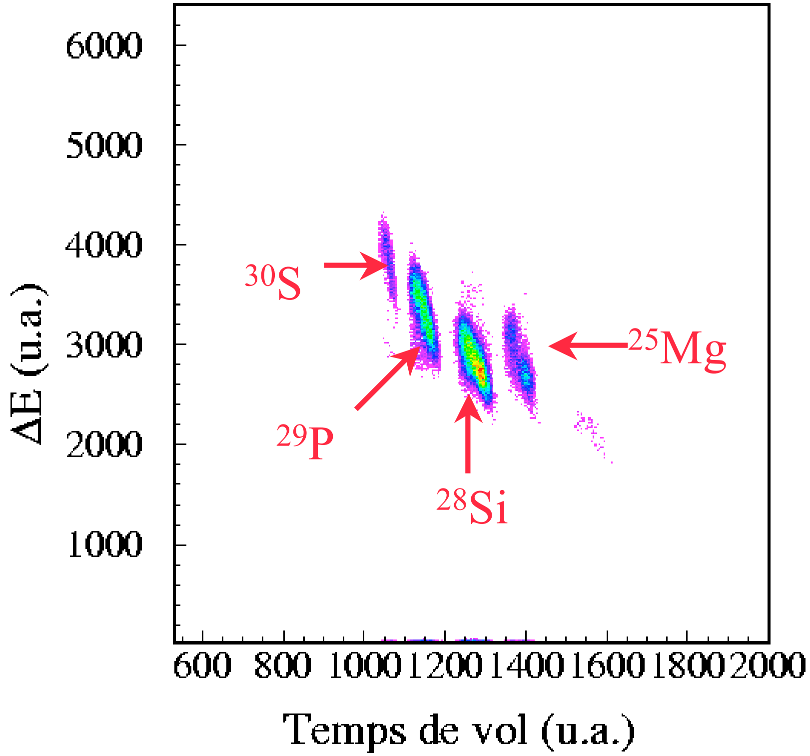

with degrader

Selection in A^3/Z^2

Intensity : 15000 ^{30}S /s

E. Khan, Thesis

P. Roussel-Chomaz

Experiments with RIBs: features to remember

Intensities are (typically 5) orders of magnitude lower than for stable beams:

- Highly efficient detection systems are needed
- Patience is required
- Results should be critically examined for lack of statistics

Intensity drops by 1 order of magnitude for each additional neutron (or proton).

Experiments with RIBs: some numbers

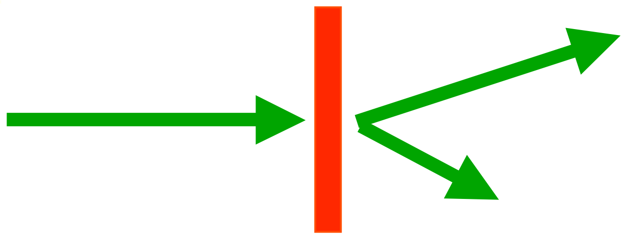

- $N_R = N_T \times N_B \times \sigma$
  - N_R reaction rate (yields observable)
  - N_T atomic density of target
  - N_B beam rate
  - σ cross section (given by nature)

- Example
  - σ = 10 mbarn
  - Target CH_2 1 mg/cm^2
  - $N_T = 10^{20}$ cm^{-2}
  - N_B = 3000 Hz
  - $N_R = 3\times10^{-3}$ Hz = 260/day

- Typical reactions
  - elastic scattering:
  - Inelastic scattering: 10 to few 10^3pps
  - Transfer reactions: 10^4pps
  - Knock-out reactions: few pps

P. Roussel-Chomaz

Experimental techniques

Part 3:

Targets

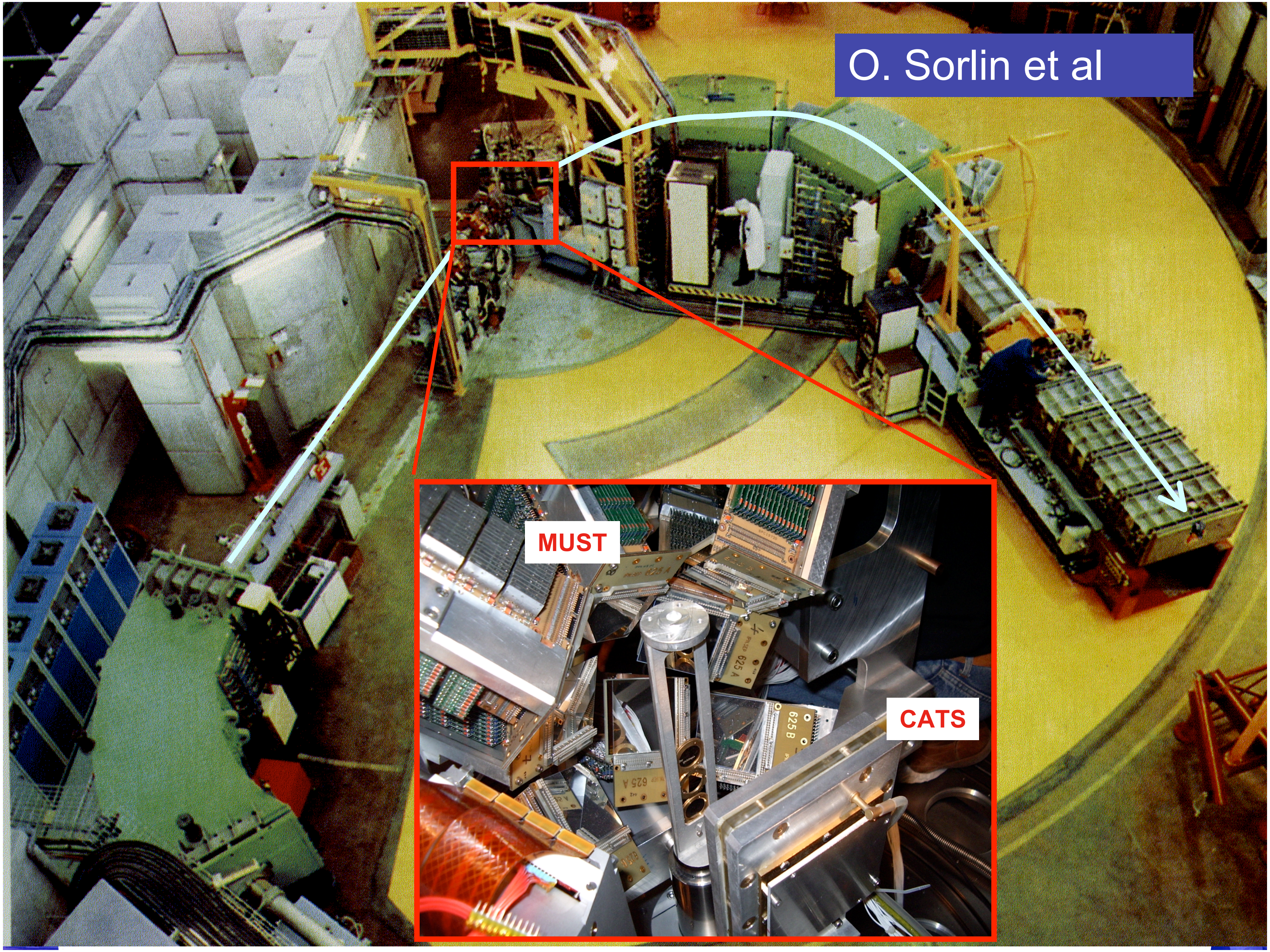
O. Sorlin et al
MUST
CATS

Targets for secondary beams

In high resolution spectrometer (SPEG) beam dispersed on target
If width of the beam in momentum is 1%
and dispersion on target 10 cm/%
⇒10 cm wide beam

CH_2, CD_2
⇒Need to measure background due to C

⇒for the same energy loss 3 times less atoms of H or D than in cryogenic Target with pure H_2/D_2

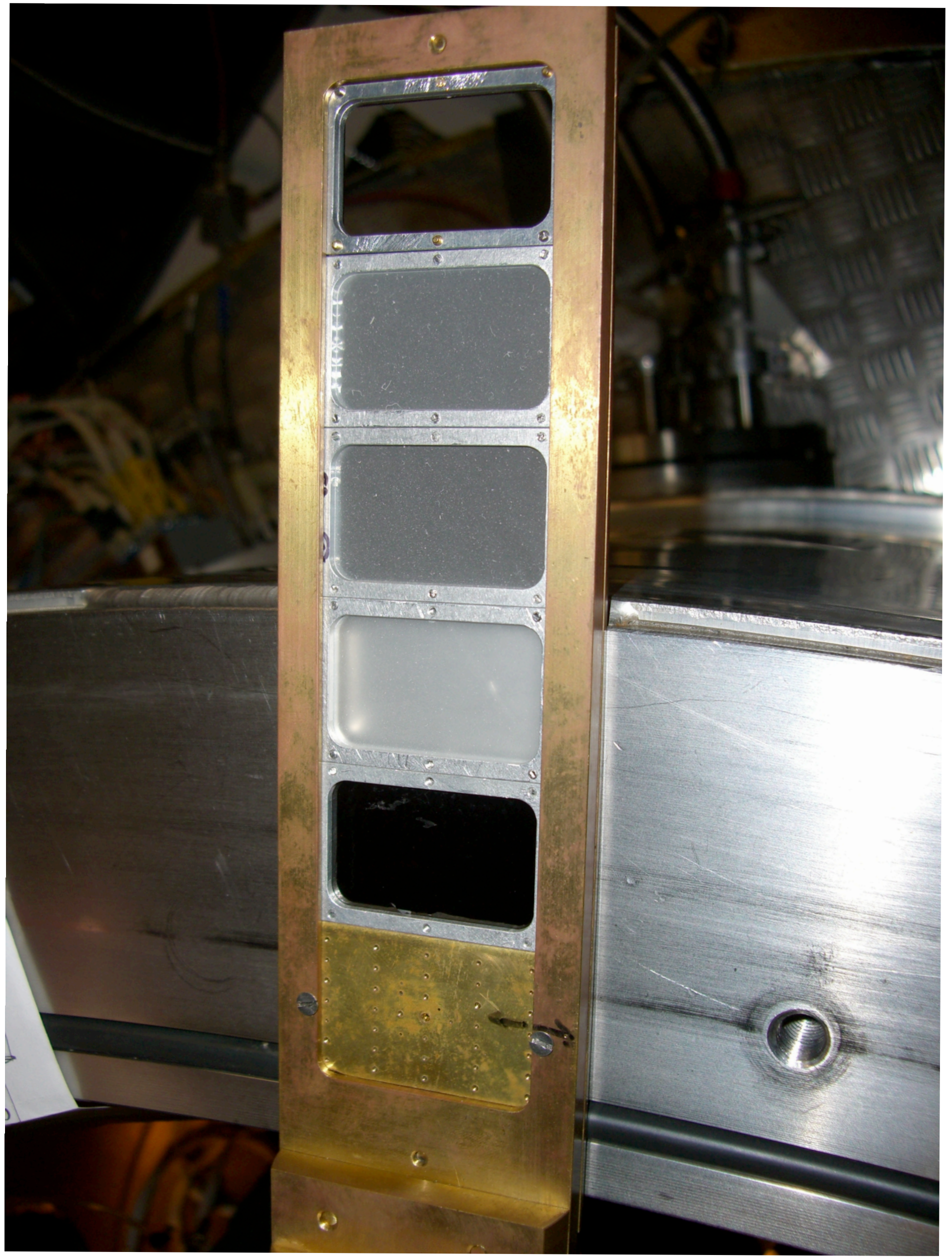

P. Roussel-Chomaz

Cryogenic targets

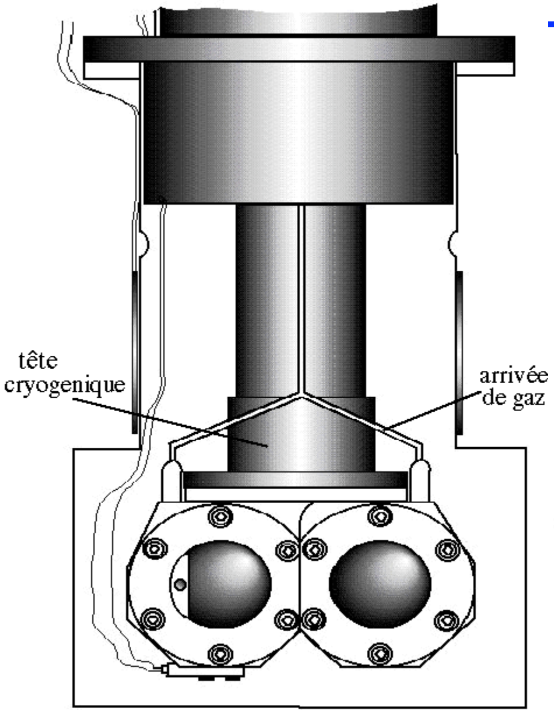

J.F. Libin, P.Gangnant
Rapport Ganil-Aires 01-97

Head of cryogenic pump + turbocompressor
T ≈ 15 K, thickness 1 cm et 0.5 cm, liquid hydrogen

Experiments:

GANIL	Proton reaction cross section measurements		
Dubna	$^{6}He(p,pp)^{5}H$	$^{6}He(d,p)^{7}He$	$^{8}He(p,t)^{6}He$
RIKEN	$^{8}He(p,pp)^{7}H$	$^{8}He(d,p)^{9}He$	

Cold finger + He
T ≈ 6K, 1-2 mm thick
Solid hydrogen

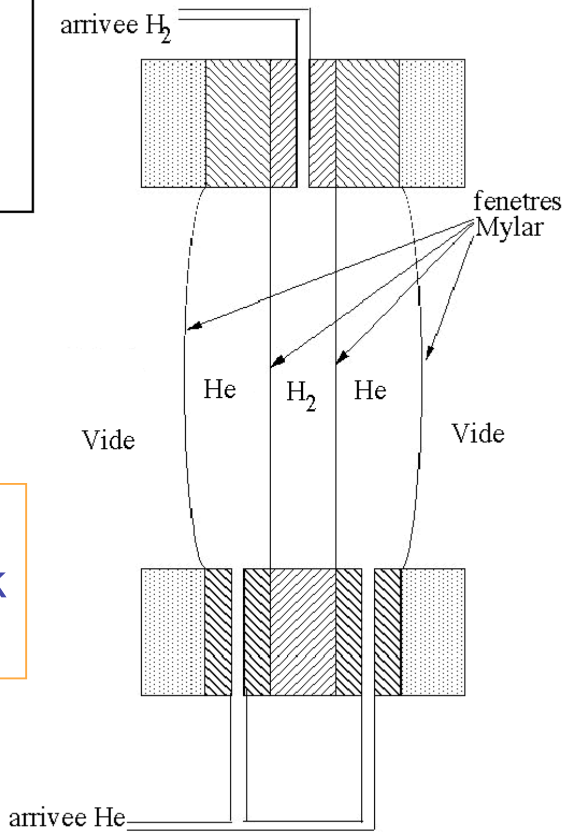

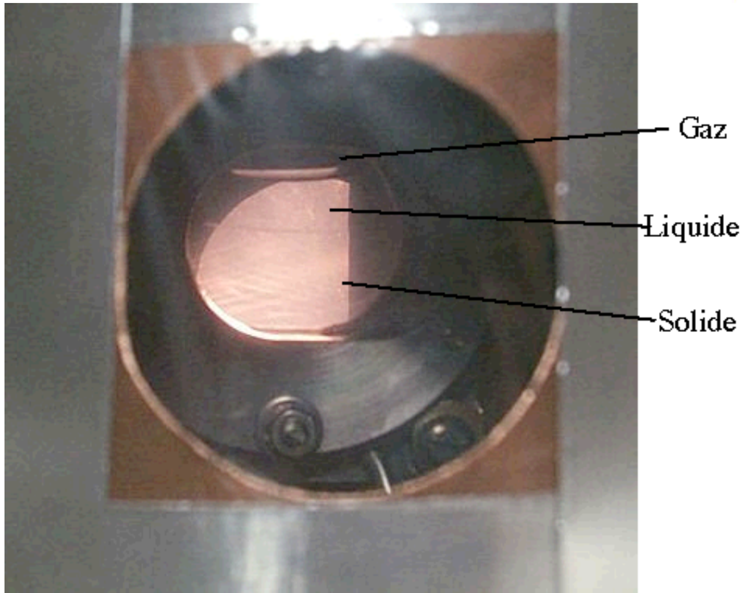

Cryogenic H_2/D_2 target

Thickness : 1 mm (17 mg.cm^{-2} ≡ 7. 10^{19} cm^{-2})
Windows : 4 × 6 mm Mylar (3. mg.cm^{-2})

Helium cooling (4 K)

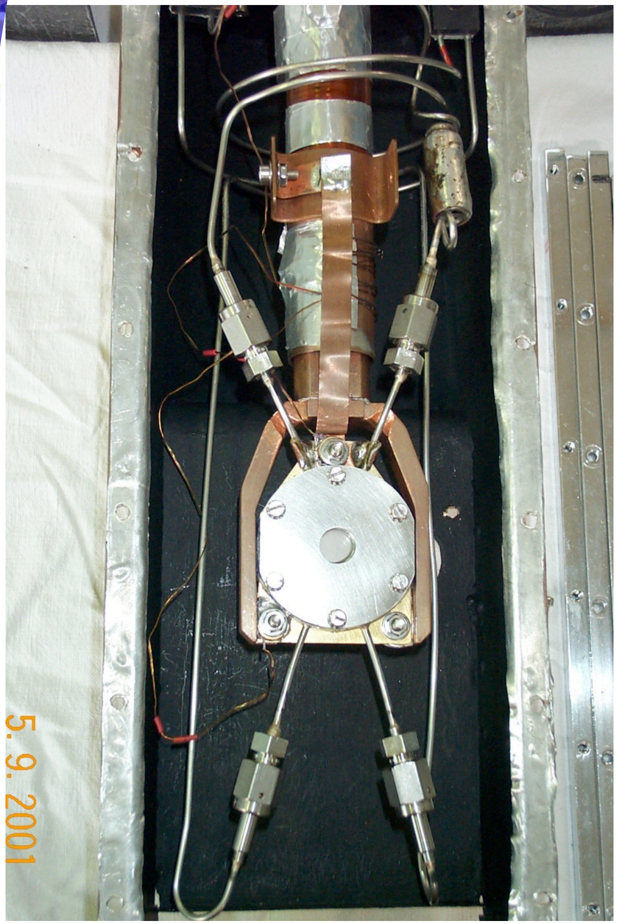

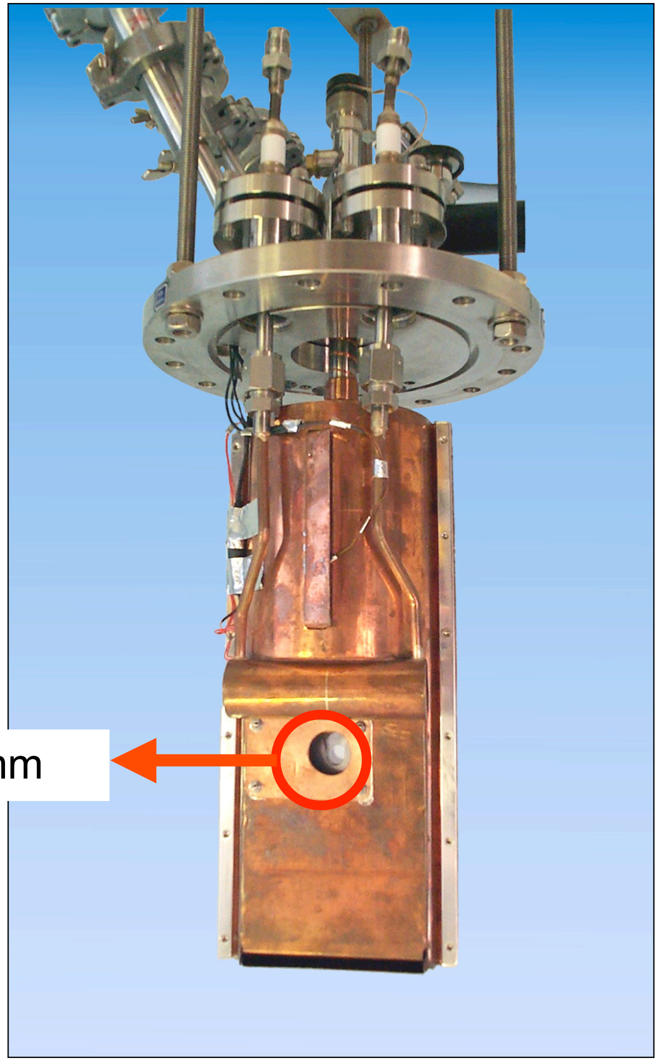

∅ = 10 mm

P.Dolégiéviez & al., Report GANIL A 00 01 (2000)
F. Santos de Oliveira & al., Eur. Phys. Jour. A, (2005)

Cryogenic H_2/D_2 target

34 P. Dolégiéviez et al. / Nuclear Instruments and Methods in Physics Research A 564 (2006) 32–37

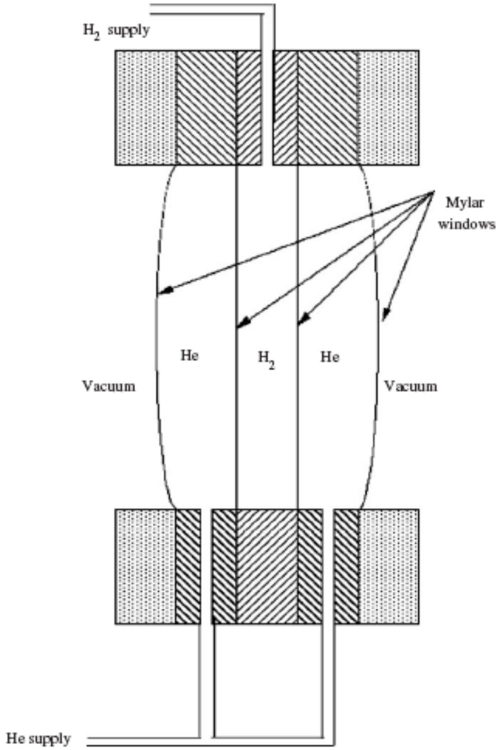

Fig. 1. Schematic view of the target that allows formation of homogeneous solid H_2 or D_2 without window deformation.

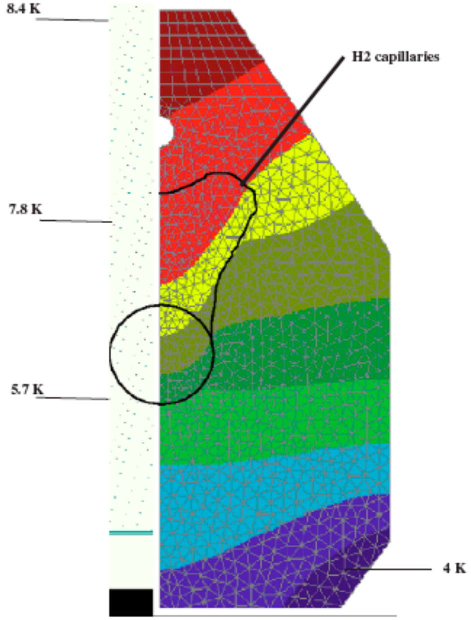

Fig. 3. Calculation of isotherms for a 1 mm thick target with brass frame.

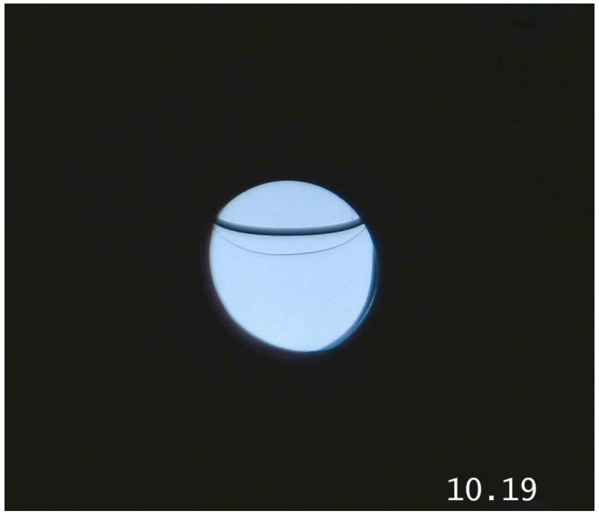

P.Dolégiéviez et al, NIM B 564(2006)32

Other cryogenic targets

RIKEN:
Windowless H_2 target

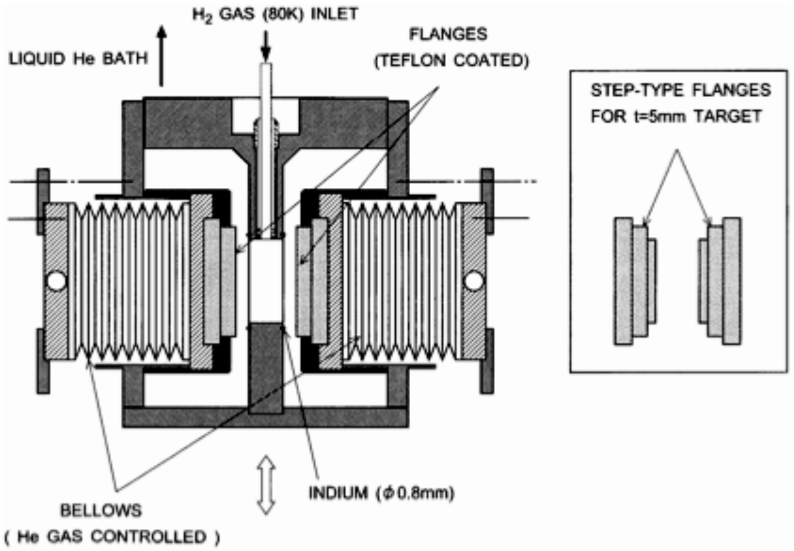

Diameter: 25 mm
Thickness: 5-10 mm (40-80 mg/cm^2)
T=4.2 K
Crystal formation from gas at 7K
Also possible from liquid at 3 MPa

S. Ishimoto, NIMA480 (2002) 304

Dubna:
Tritium target
(1kCi)

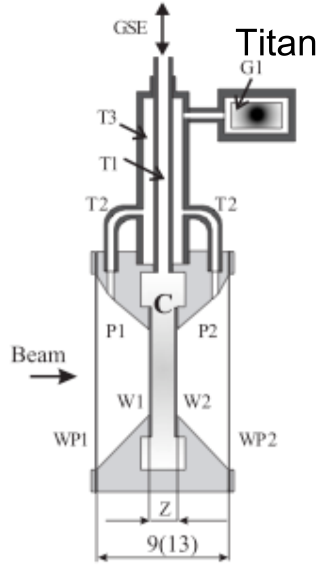

Thickness: 0.4 mm to 4mm (liq/gas)
12 μm stainless steel windows
+ two protection barriers
Operation pressure: 0.1 Mpa
Window destruction pressure: 2 Mpa
Storage in compound state with ^{238}U
(380 cm^3 of tritium)
Release by heating ≈700 K

A. Yukhimchuk et al., NIMA513 (2003) 439

Polarized target

CNS Polarized Proton Target

Unique pol. p target for RI-beam exp. !

- **Strong point**
  - Operation in modest conditions
    - Low magnetic field: 0.1 T
    - High temperature: 100 K

⇔ Conventional pol. p target (2.5 T, 0.5 K)

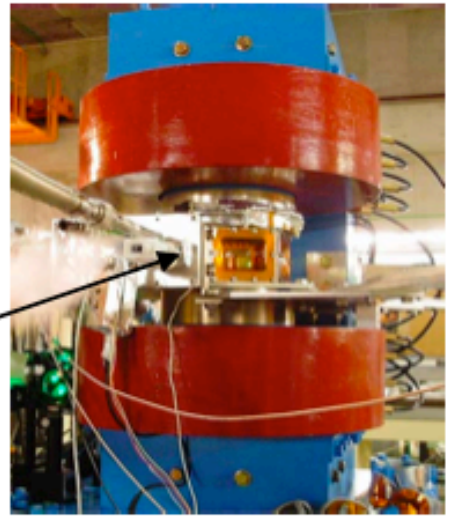

- **Target material**

Single crystal of naphthalene 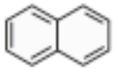

+ pentacene 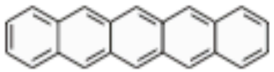

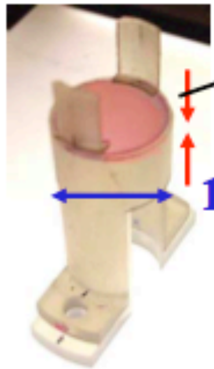

1 mm^t

14 mmφ

- **Polarizing method**
  - Laser excitation

→ Electron pol. in aromatic molecules

A. Henstra et al., Phys. Lett. A **134** (1988) 134.
T. Wakui et al., NIM A **526** (2004) 182.

Study of unstable nuclei with polarized proton

Thickness: 4 10^{21} at/cm^2 Polarisation 14%
T. Uesaka, NIMA526 (2004) 186

Polarised Targets

J^π dependence

- Which experiments?
  - Elastic Scattering (p,p) (d,d)
    spin-orbit potential
  - (p,p'), (p,n): spin-isospin response
  - (d, p), (p,d) , (d, t): J^π of single particle-hole states from analyzing power

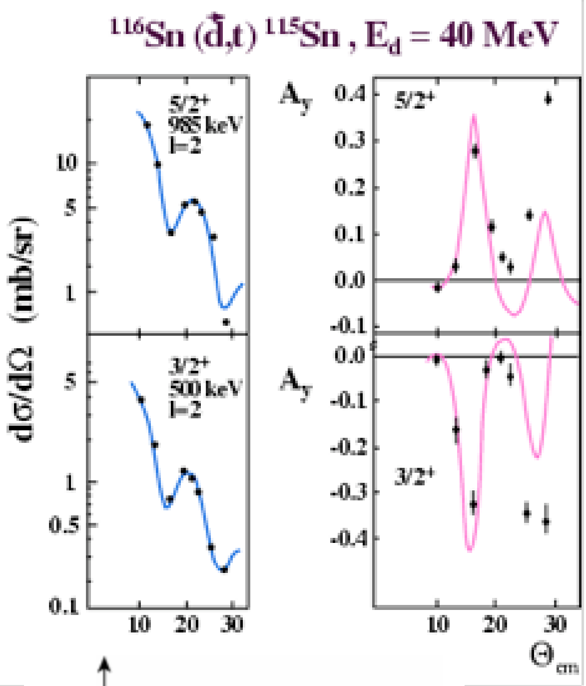

- Spin-orbit potential
  localized on nuclear surface

$$V_{LS} \approx \frac{1}{r}\frac{d}{dr}\rho$$

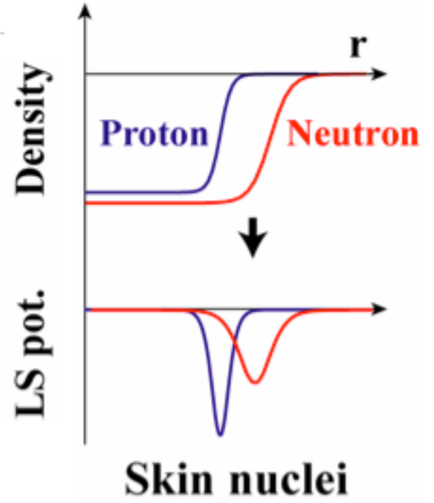

Neutron halo/skin nuclei: difference between Proton and neutrons densities
How does spin-orbit potential behave???

Active target: MAYA

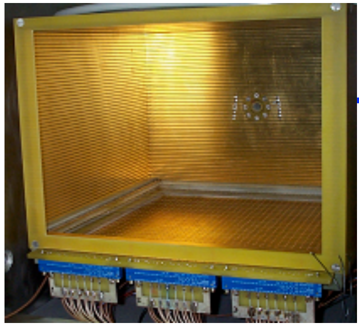

MAYA is essentially an ionization chamber, where the gas plays also the role of reaction target.

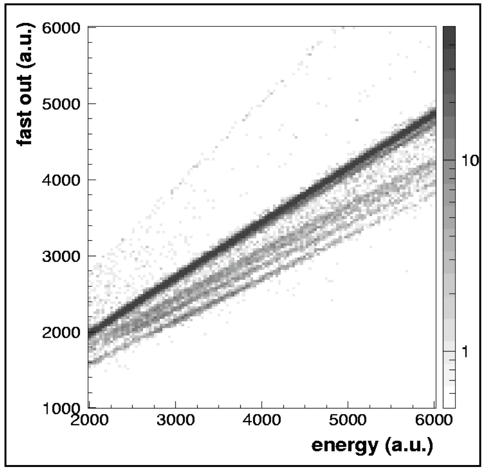

the light scattered particles escape the gas volume. They are stopped, and identified in the CsI wall.

two drift chambers before MAYA, to monitor the beam.

the projectile reacts with a nucleus of the gas.

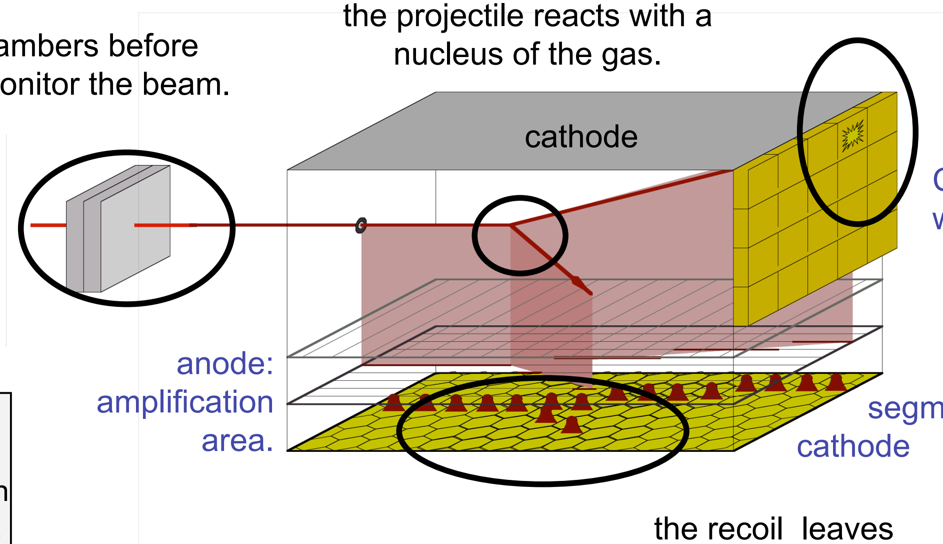

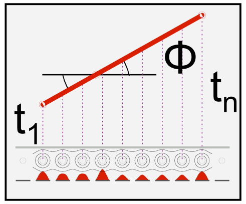

the drift time to the amplification wires allows the determination of the reaction plane.

the recoil leaves enough energy to induce an image of its trajectory in the segmented cathode.

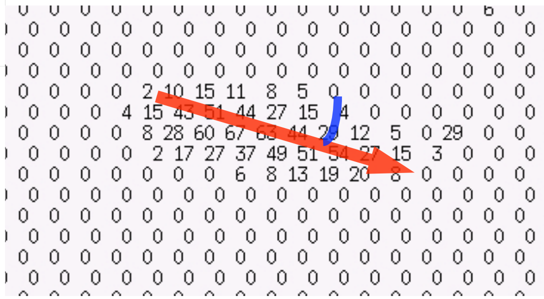

P. Roussel-Chomaz

Part 4:

Beam tracking detectors

Beam Tracking Detectors

Why do we need beam tracking detectors?

— Count the incoming particles
— Identify them : TOF, ΔE-TOF
— reconstruct trajectories and impact point on target

At high energy:

- plastic scintillators
- diamond detectors

At low energy:

- gas detectors
- microchannel plates

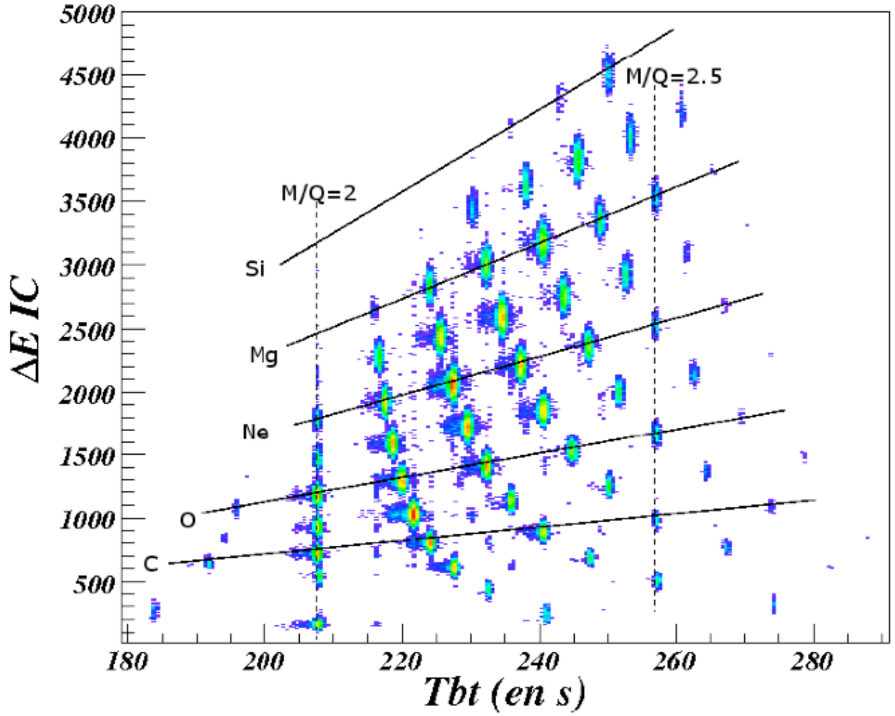

Beam tracking detectors

Beam detectors :

As low interception of the beam as possible (1 mg/cm^2)
Efficiency ≈ 100 %
Counting rate ≈ 10^5 - 10^6 pps
Position resolution ≈ 1mm
Angular resolution ≈ 1 mrad

- Drift chamber
- CATS: Low pressure multiwire chambers

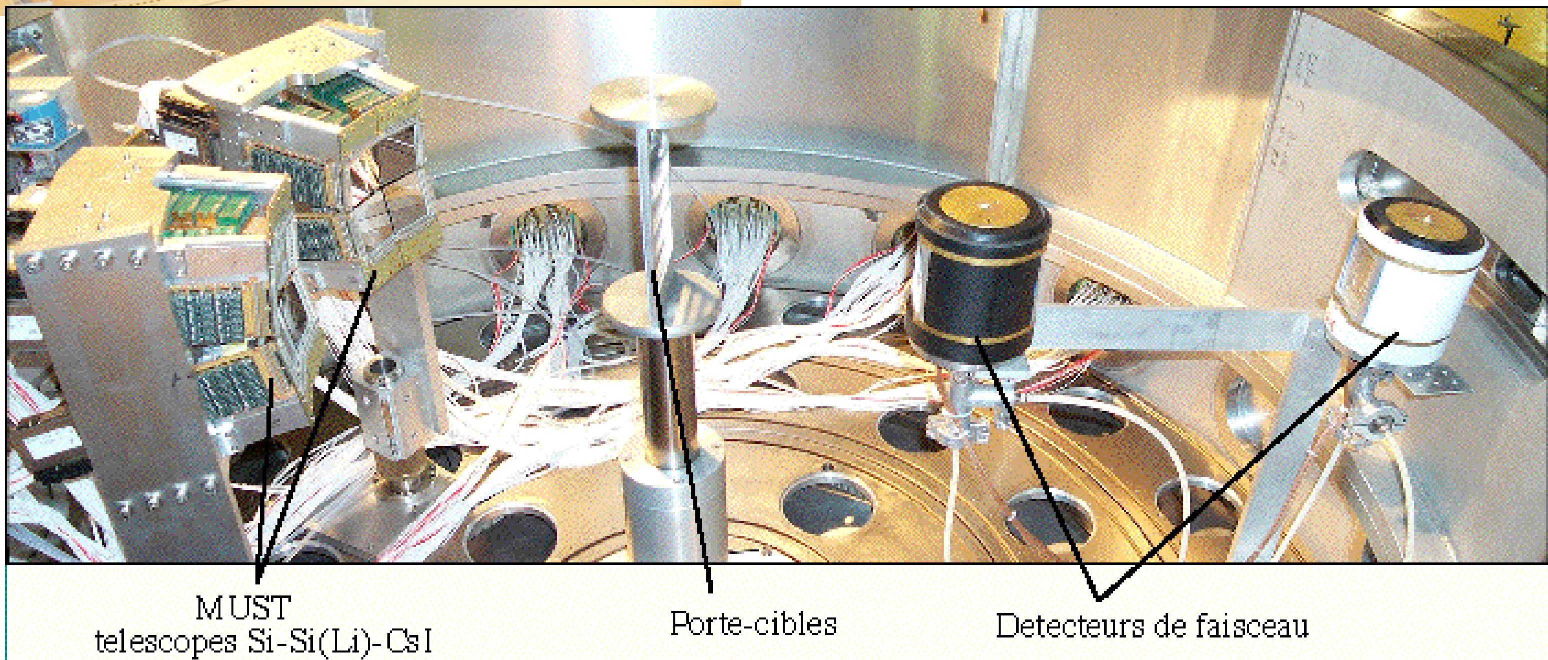

Beam tracking detectors: CATS

CATS: Chambre à trajectoires de Saclay

S. Ottini-Hustache et al., NIMA431 (1999)476

MWPC, isobutane 6-15 torr

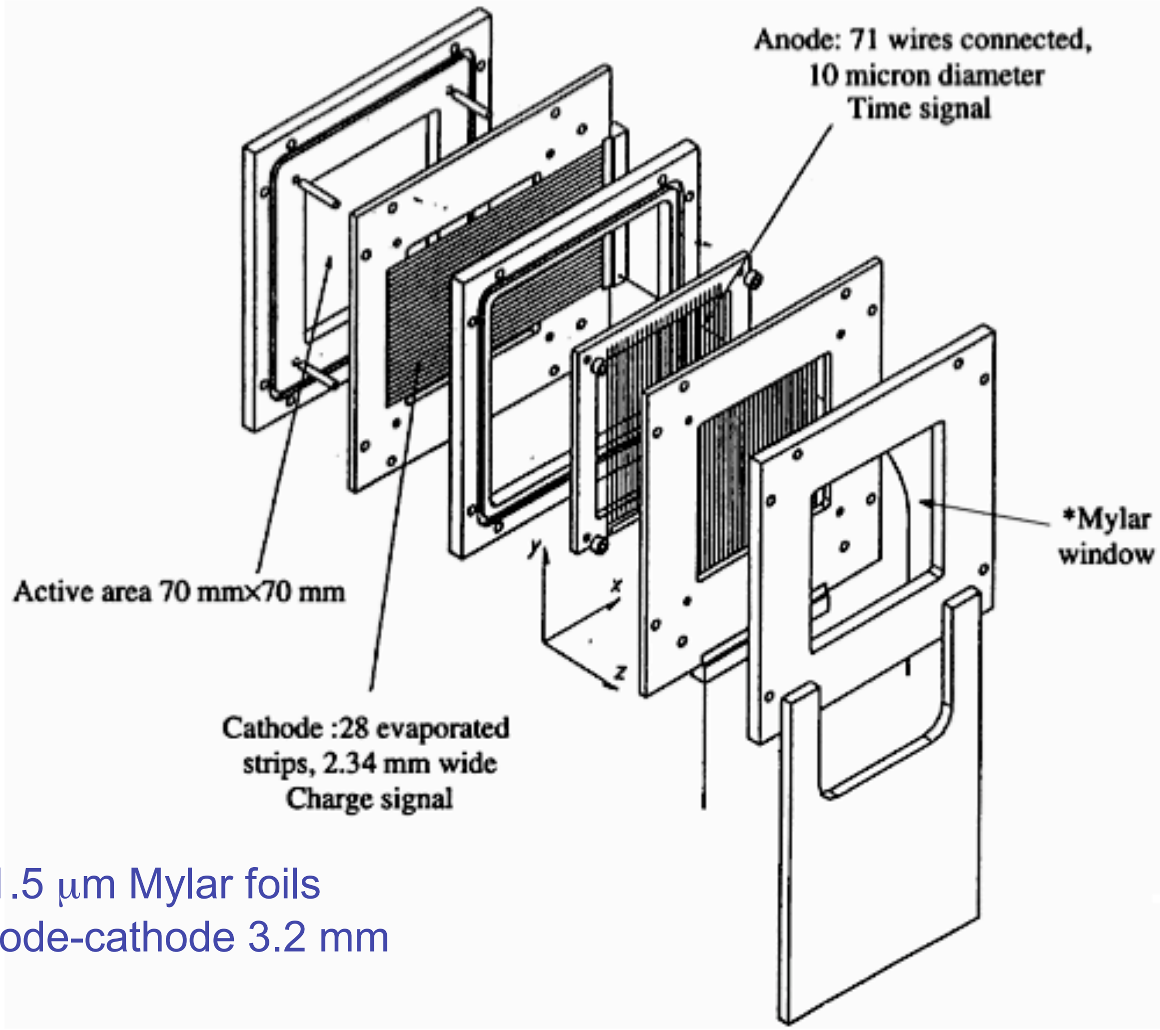

4 windows 1.5 μm Mylar foils

Distance anode-cathode 3.2 mm

Beam detectors: CATS

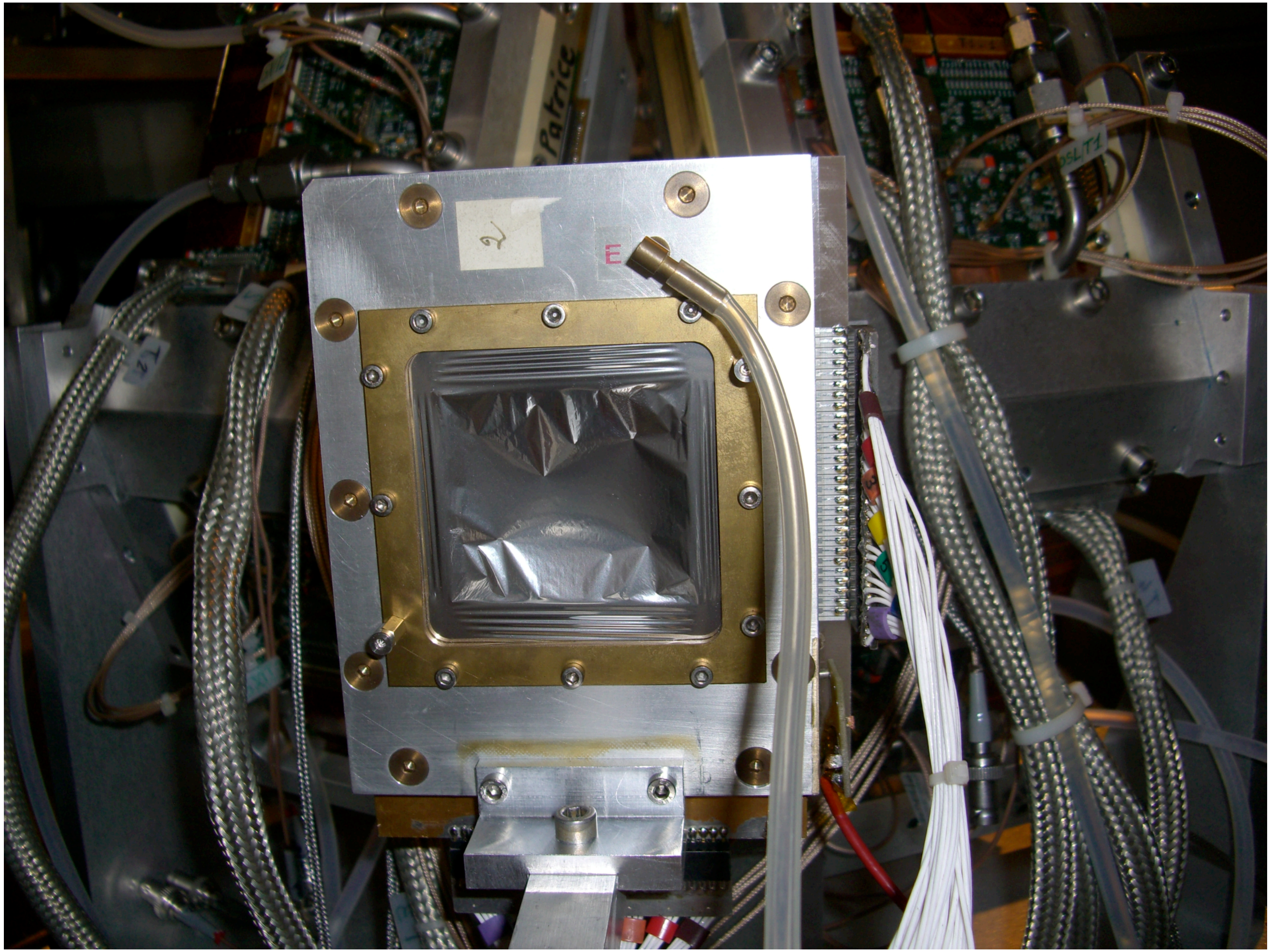

Beam tracking detectors

Reconstruction of beam impact on target (angle and position)

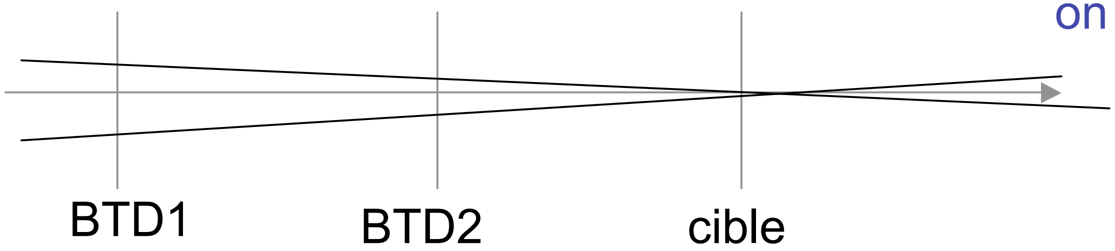

Calibration with grid at the target position

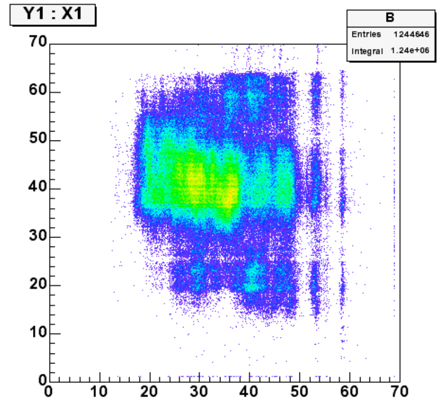

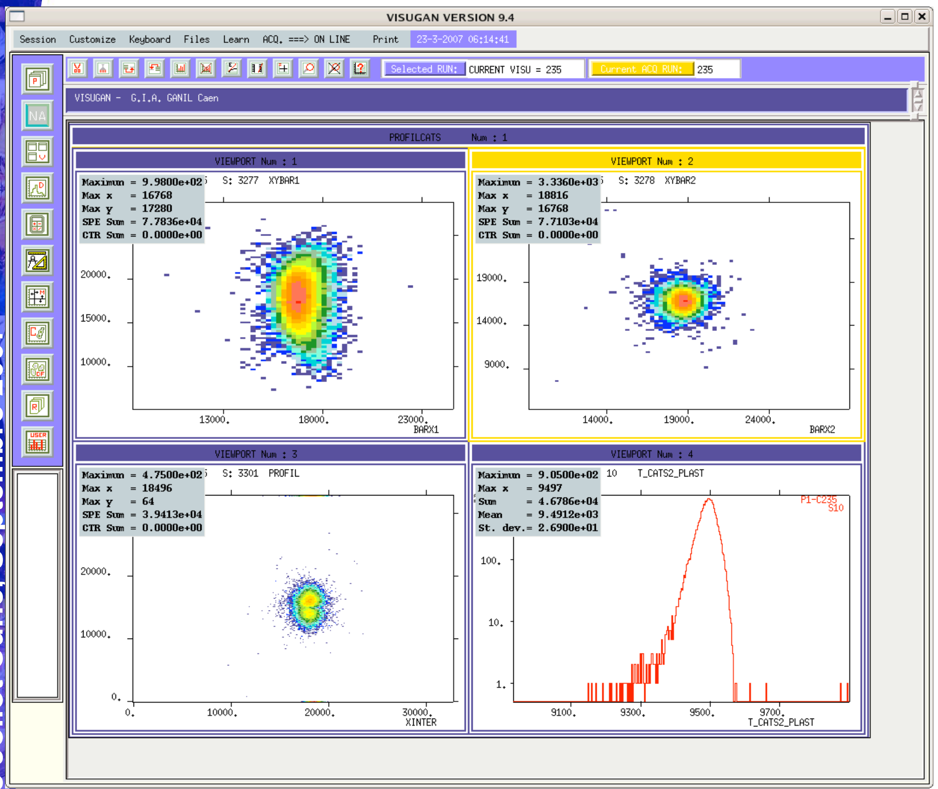

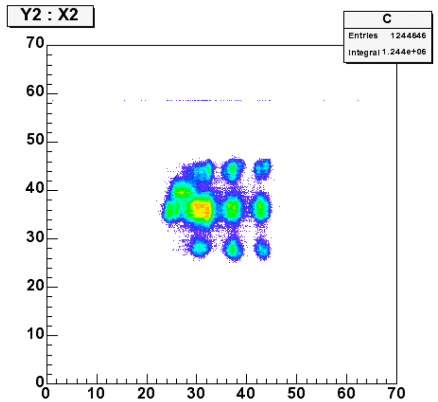

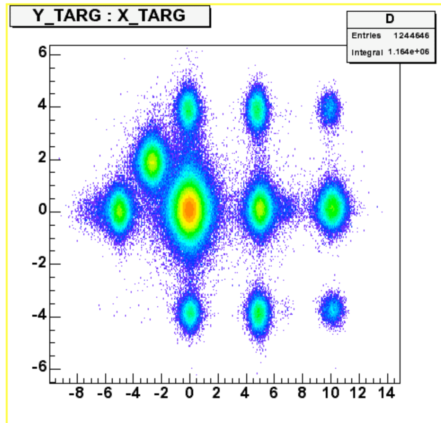

Courtesy of L. Gaudefroy

Effect of beam tracking detectors...

…in the focal plane of SPEG

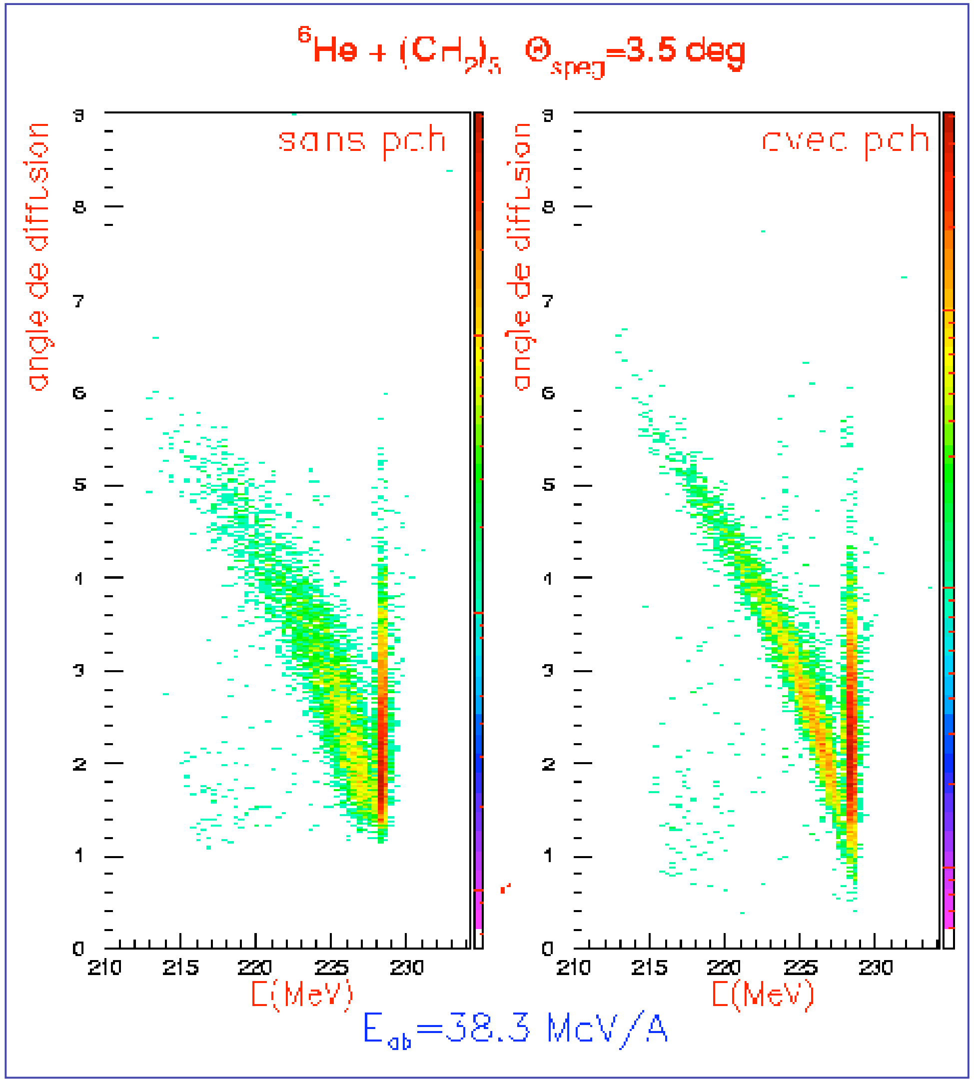

Thèse V. Lapoux

…and for the recoil nucleus detected with MUST/MUST2

P. Roussel-Chomaz

Effect of beam tracking detectors

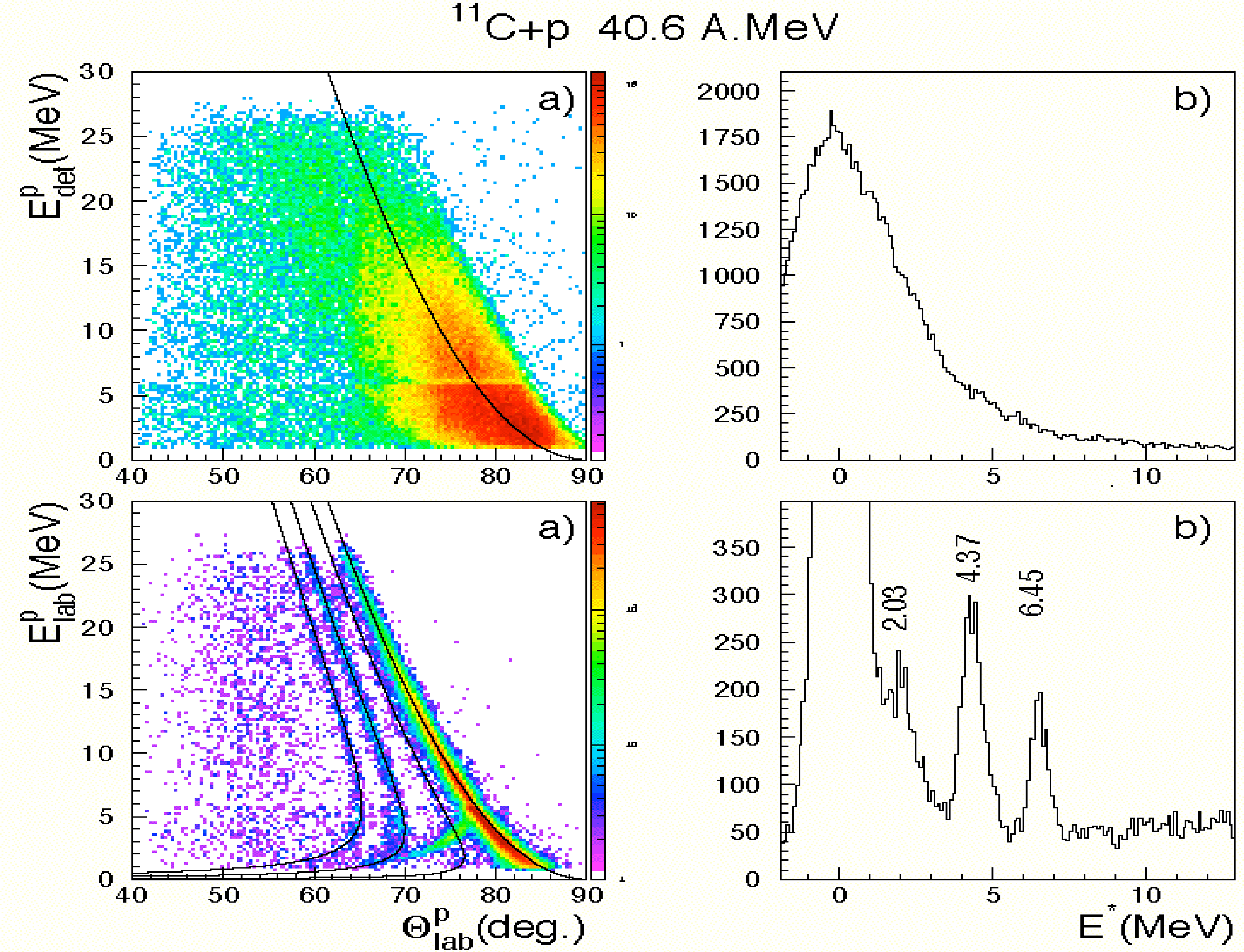

Thèse C. Jouanne, Saclay

End of first lecture

Part 5

Detection systems and selected examples of experiments

a) Missing mass method: Detection of recoil nucleus
Application to elastic & inelastic scattering, transfer reactions
MUST, MUST2, TIARA, HIRA, ORRUBA, MAYA

b) Invariant mass method: Detection of all outgoing particles
Application to giant resonances

c) And the contrary:
Transfer via invariant mass method
Giant resonances via missing mass method

P. Roussel-Chomaz

Part 5

Detection systems and selected examples of experiments

Experimental techniques

In a nuclear reaction a(A,b)B we need to characterize the particles by their:

M mass

Z atomic number

Q charge state

E energy (or v velocity)

Experimental techniques

Variable	Detector	Resolution typically	Domain
E	semiconductor scintillatorr gas	qq.10^{-3} qq.10^{-2} qq.10^{-2}	range < 1 cm E≥ some MeV/n range < 1 m.atm
ΔE	semiconductor scintillator gas	qq.10^{-2}	E≥ some MeV/n
Bρ	spectrometer	10^{-3} - ~10^{-5}	E ≥ some keV/n
t_{flight}	scintillator gas semiconductors	(0.1-0.5) ns Δt/t dependant on d typically : 10^{-2} - ~10^{-4}	E ≥ qq keV/n E ≥ ~ MeV/nucl

P. Roussel-Chomaz

Experimental techniques

In a nuclear reaction a(A,b)B we need to characterize the particles by their:

M mass

Z atomic number

Q charge state

E energy (or v velocity)

Very often B (projectile residue) is not bound.

Two ways to obtain information on its structure:

— missing mass method: due to the 2-body character of the reaction, all the information on B can be inferred from the kinematical characteristics of b

— invariant mass method: all the outgoing particles resulting from the decay of B are measured.

Part 5

Detection systems and selected examples of experiments

a) *Missing mass method: Detection of recoil nucleus*
Application to elastic & inelastic scattering, transfer reactions

Missing mass method

^{16}C incident on ^{2}H at 35 MeV/u

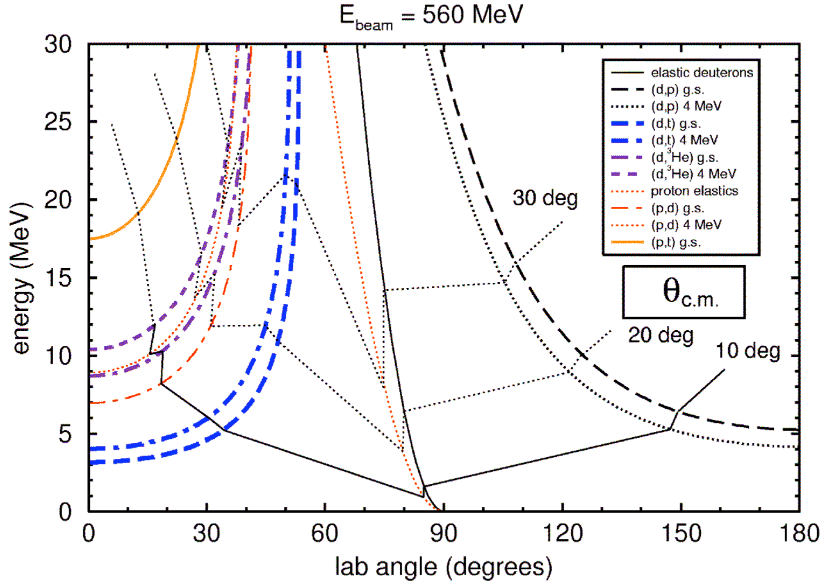

(p,d) and (d,t) and (d,p) on ^{74}Kr in inverse kinematics

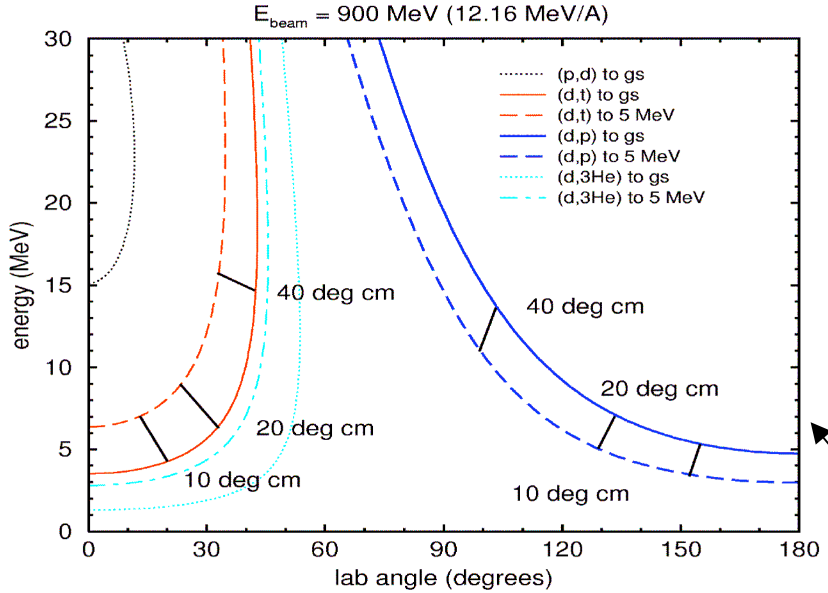

« Catford » plots

Reaction a(A,b)B

Detection of b

— forward center of mass angles (large cross sections) correspond to very low energy recoil particles

—elastic scattering at 90 °

—pick-up at 0°

—stripping at 180°

Detection set up must have

— low threshold

— large dynamic range

— a large angular coverage

— modularity

Experimental setup : MUST

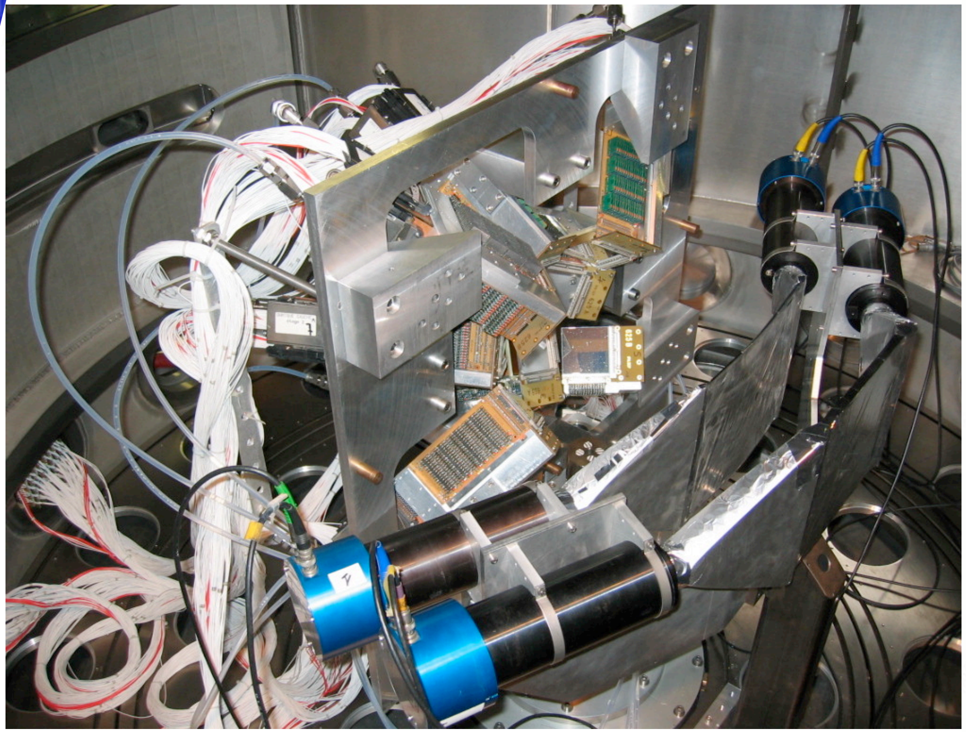

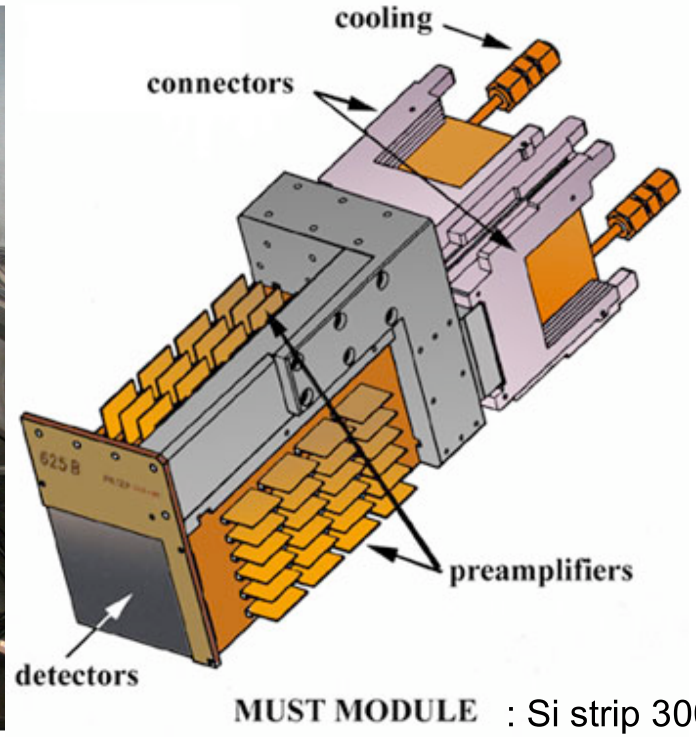

: Si strip 300 μm
(ΔE+ToF+X+Y)
\+ Si(Li) 3 mm
(ΔE or E)
\+ CsI (E)

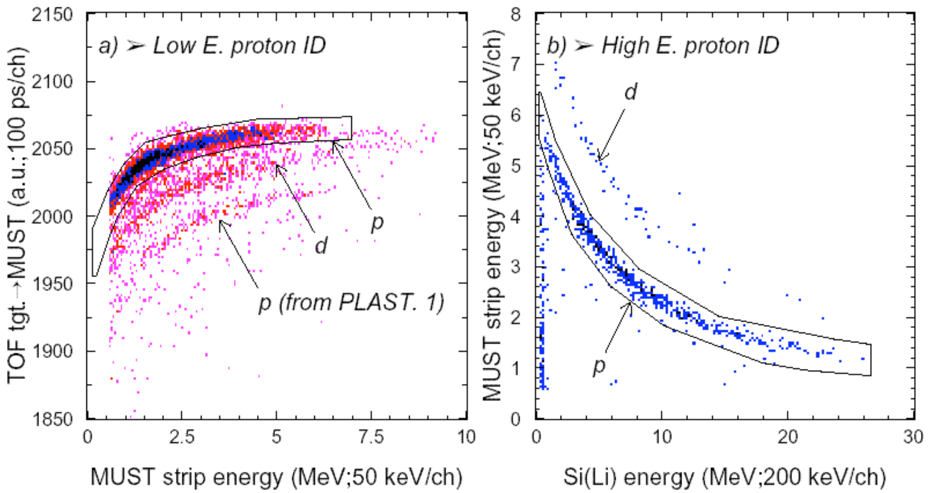

P. Roussel-Chomaz

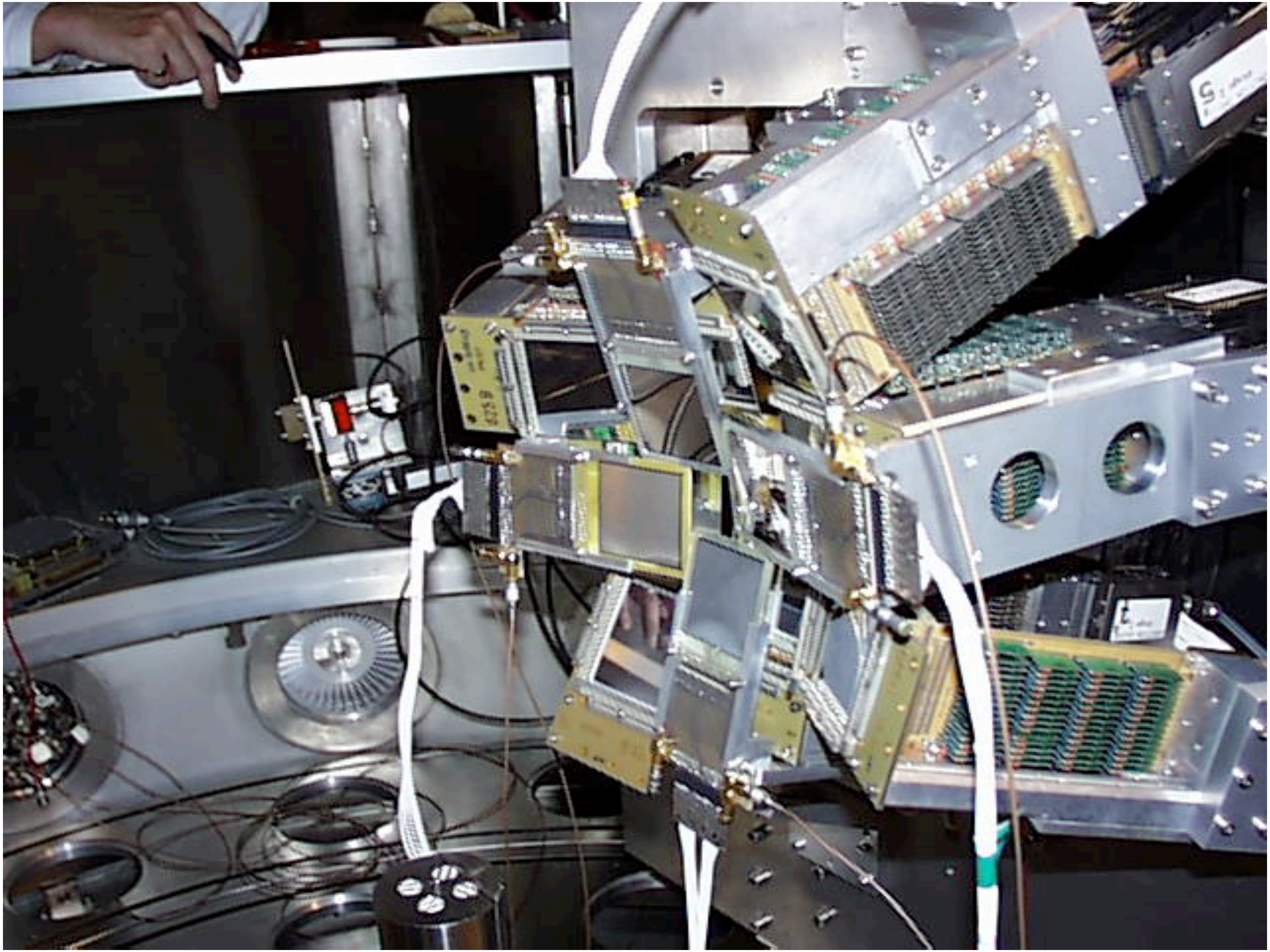

Structure of the ^{8}He nucleus via direct reactions on proton target

2+	3.62 ± 0.14 MeV	Γ = 0.3 ± 0.2 MeV
?	5.4 ± 0.5 MeV	Γ = 0.3 ± 0.5 MeV

2n Transfer ^{8}He(p,t)^{6}He

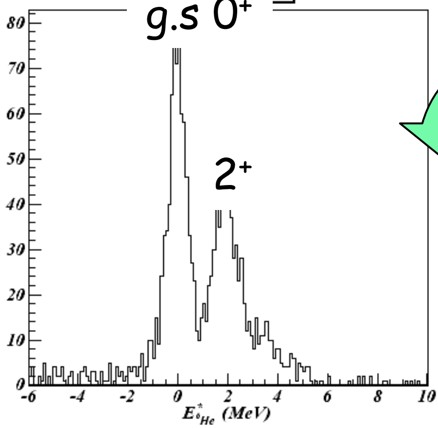

^{8}He excitation energy spectrum

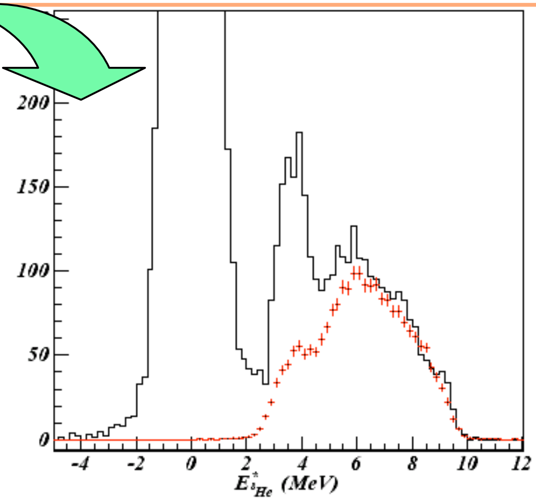

^{8}He +p @ 15.6 MeV/n

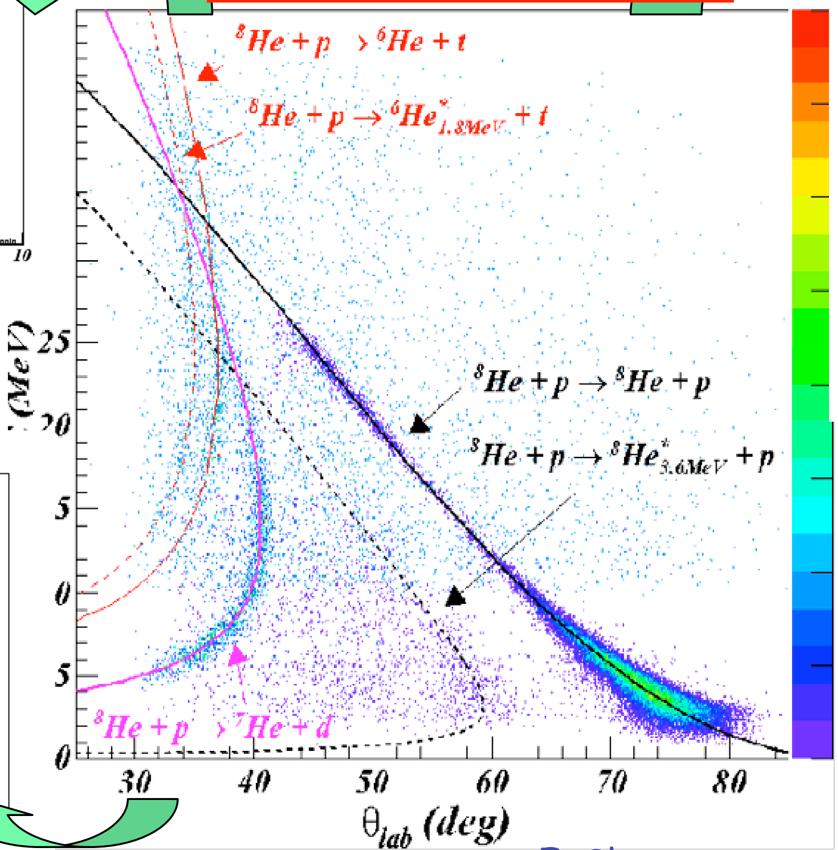

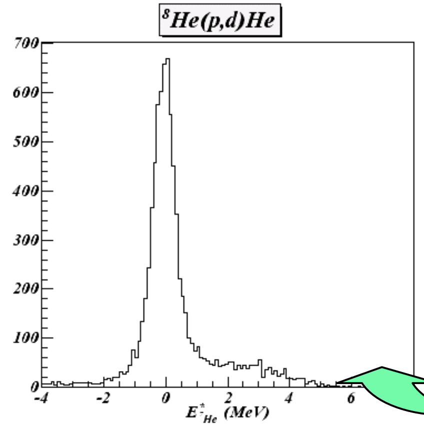

1n transfer : ^{8}He(p,d)^{7}He

* Large (p,d), (p,t) cross sections
• DWBA not valid
GENERAL framework :
Coupled Reactions calc. *needed*, PLB619, 82 ('05)

F. Skaza,
PhD thesis SPhN
V.Lapoux et al

(d,p) reactions with ^{40,44,46}Ar beams

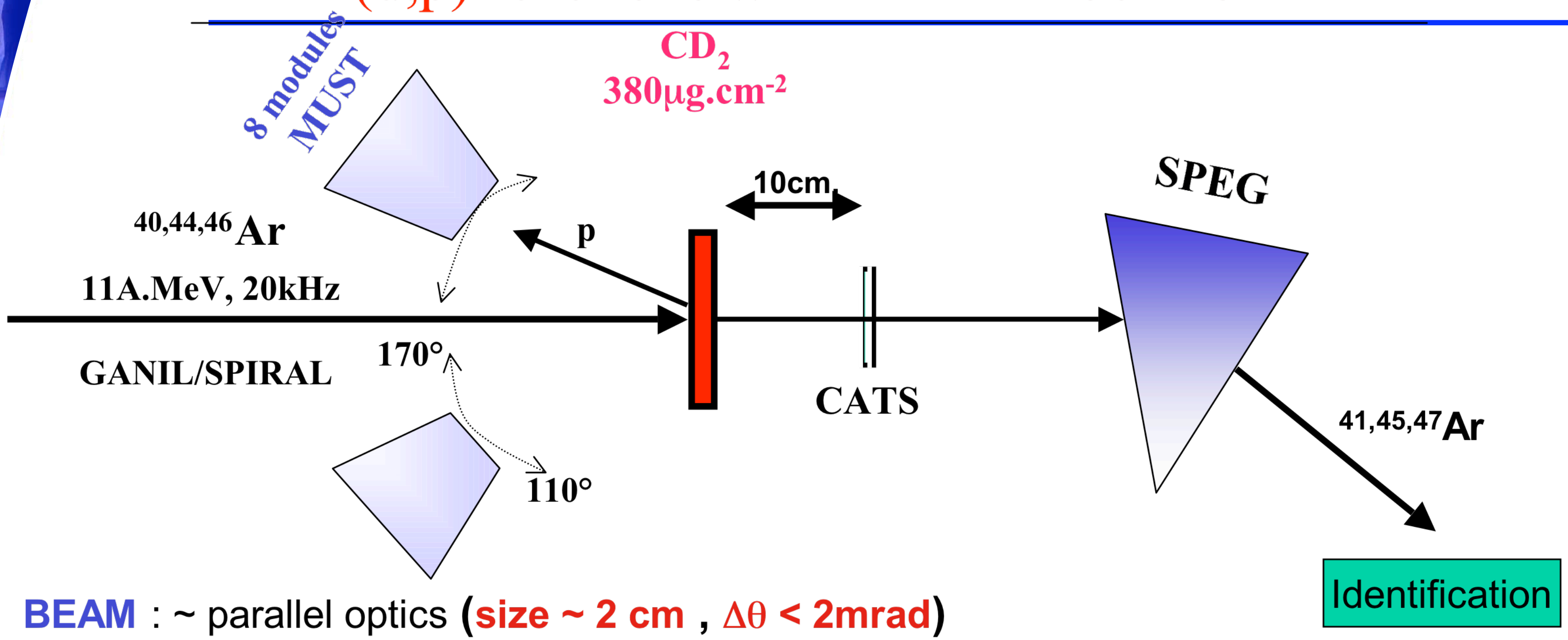

BEAM : ~ parallel optics (**size ~ 2 cm , Δθ < 2mrad**)

CATS : -**beam**-tracking detector

- Proton **emission point**.
  resolution : ~0.6 mm

MUST : -**Si Strip** detector

-Proton **impact localisation**
 resolution : 1 mm

-Proton **energy** measurement.
 resolution : 50 KeV

SPEG : Energy loss spectrometer : **recoil ion** identification→transfert-like products

L. Gaudefroy PhD Thesis

$^{44,46}Ar(d,p)^{45,47}Ar$, 10 MeV/u, SPIRAL

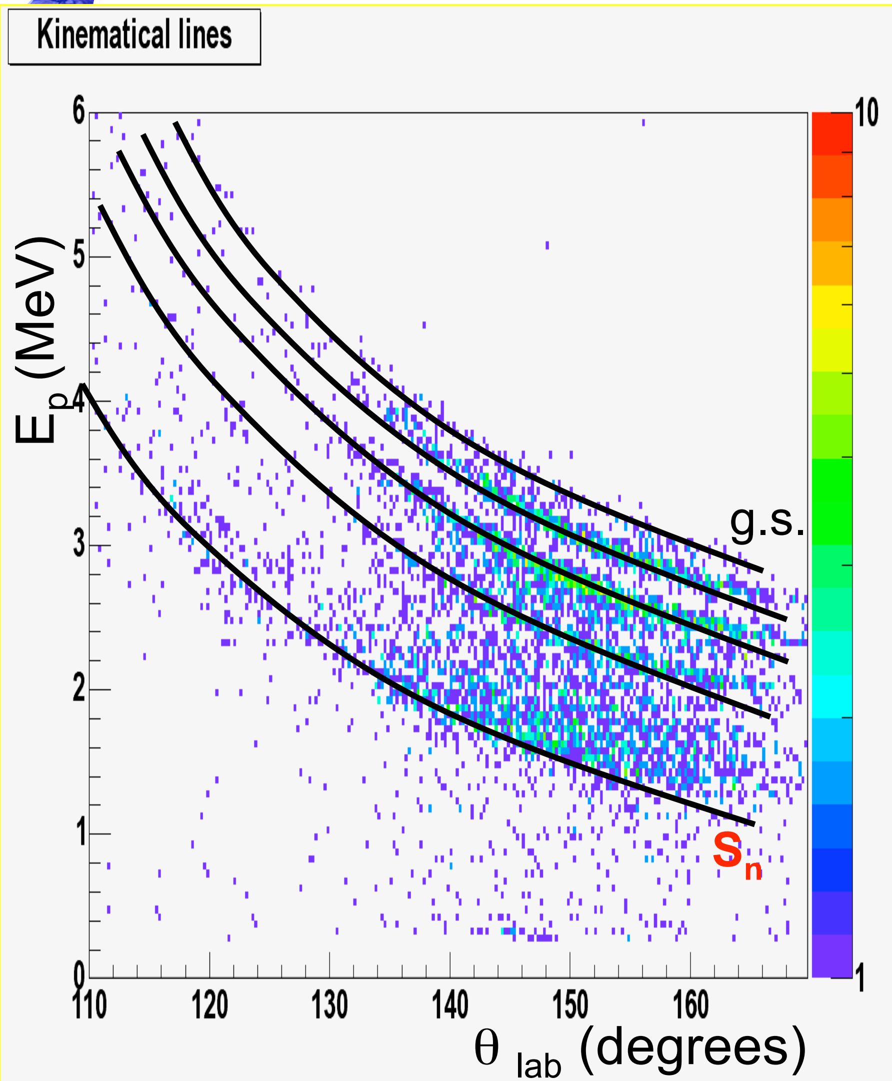

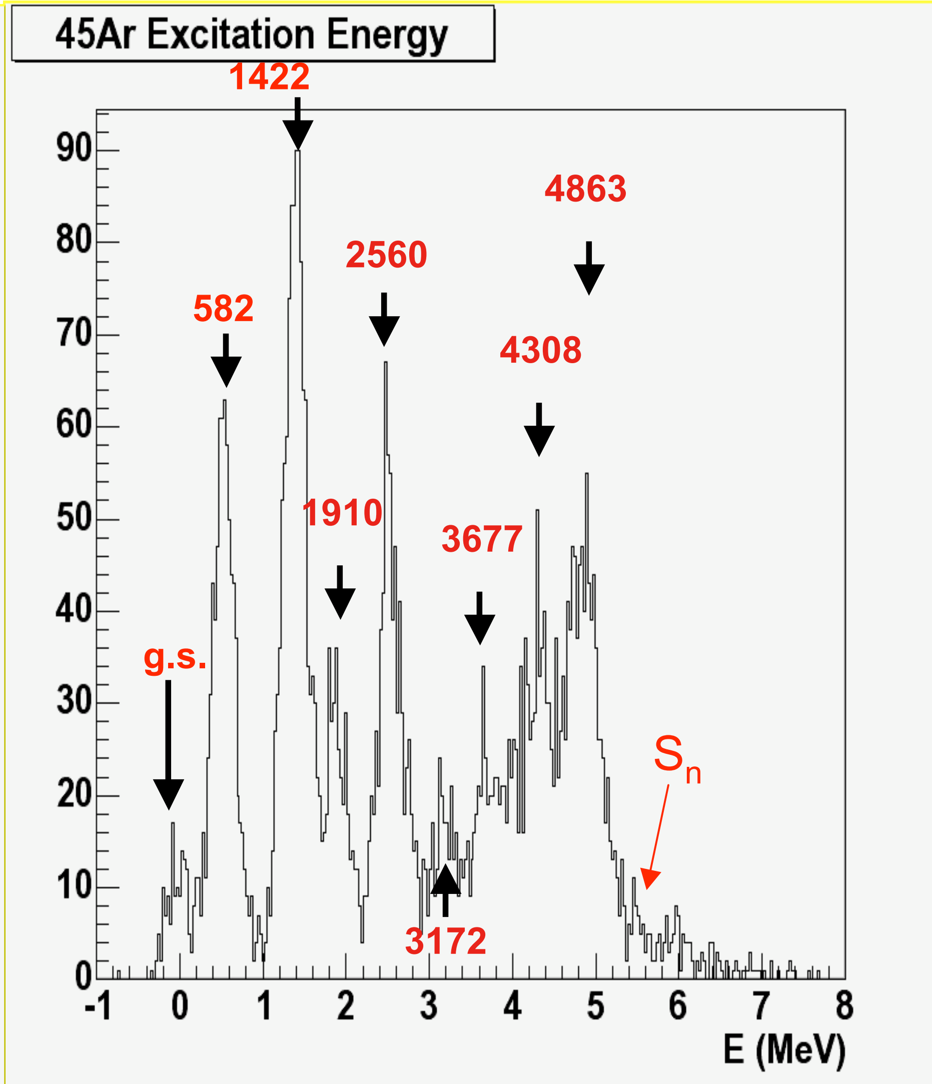

PRL 97, 092501 (2006) PHYSICAL REVIEW LETTERS week ending 1 SEPTEMBER 2006

Reduction of the Spin-Orbit Splittings at the $N = 28$ Shell Closure

L. Gaudefroy,[1,2] O. Sorlin,[2,1] D. Beaumel,[1] Y. Blumenfeld,[1] Z. Dombrádi,[3] S. Fortier,[1] S. Franchoo,[1] M. Gélin,[2] J. Gibelin,[1] S. Grévy,[2] F. Hammache,[1] F. Ibrahim,[1] K. W. Kemper,[4] K.-L. Kratz,[5,6] S. M. Lukyanov,[7] C. Monrozeau,[1] L. Nalpas,[8] F. Nowacki,[9] A. N. Ostrowski,[5,6] T. Otsuka,[10] Yu.-E. Penionzhkevich,[7] J. Piekarewicz,[4] E. C. Pollacco,[8] P. Roussel-Chomaz,[2] E. Rich,[1] J. A. Scarpaci,[1] M. G. St. Laurent,[2] D. Sohler,[11] M. Stanoiu,[12] T. Suzuki,[13] E. Tryggestad,[1] and D. Verney[1]

$^{46}Ar(d,p)^{47}Ar$

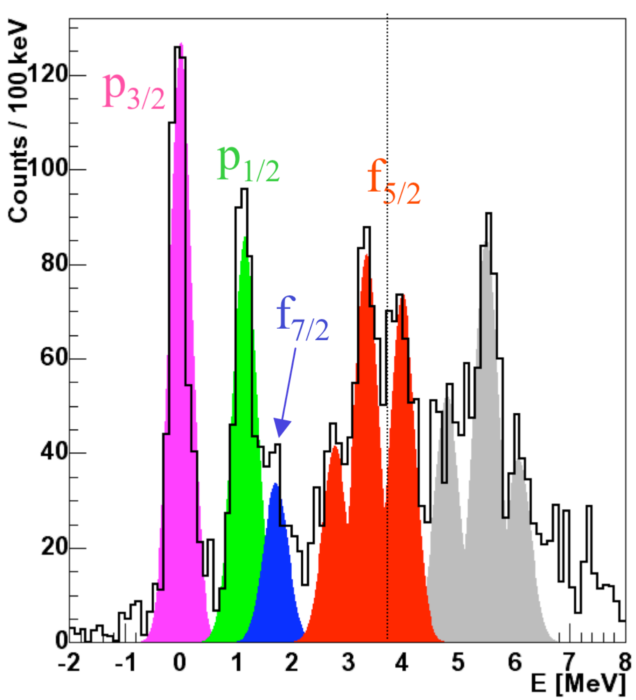

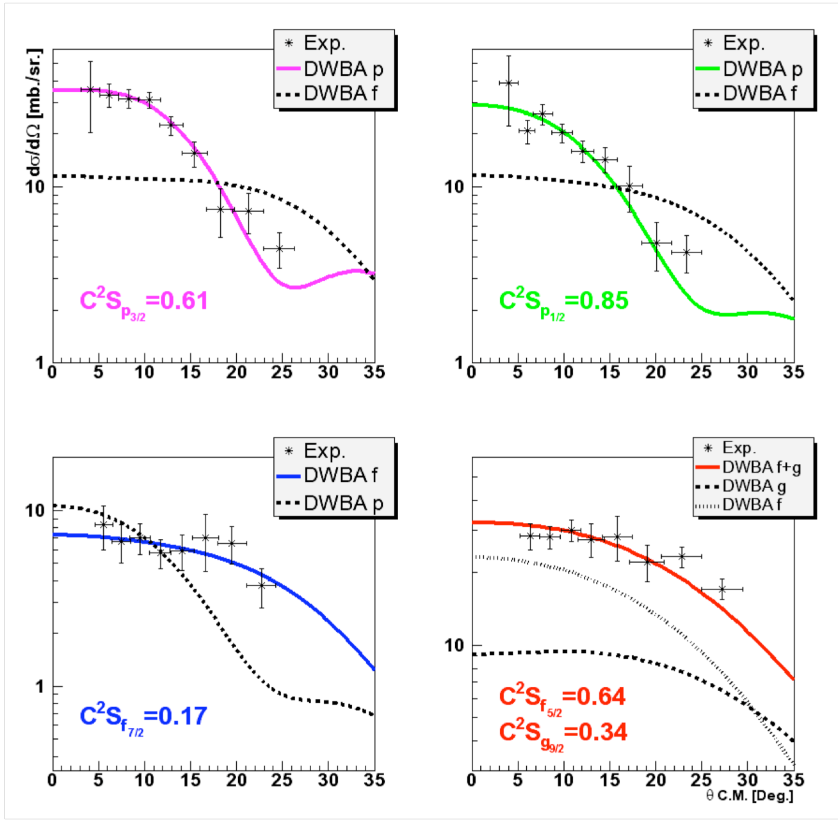

S_n (^{47}Ar) determined from Q value

N=28 gap reduced by 330(80)keV

EVOLUTION OF THE LEVELS AT N=29

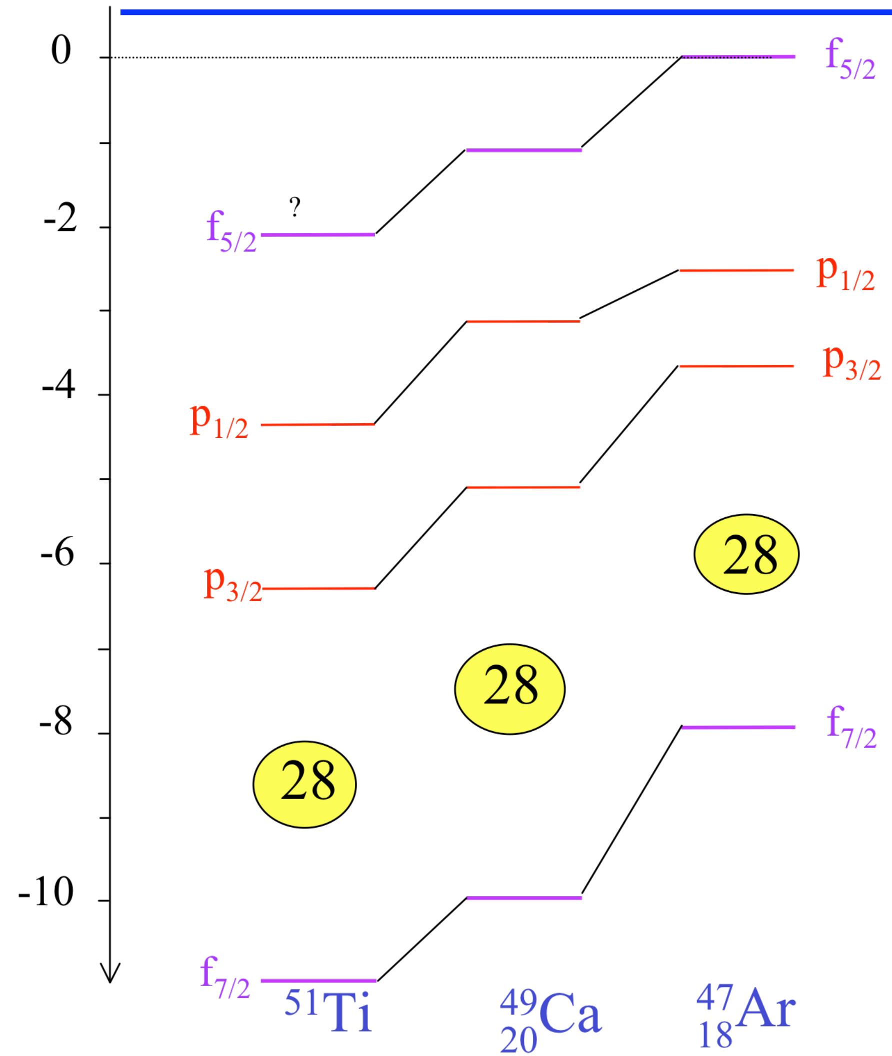

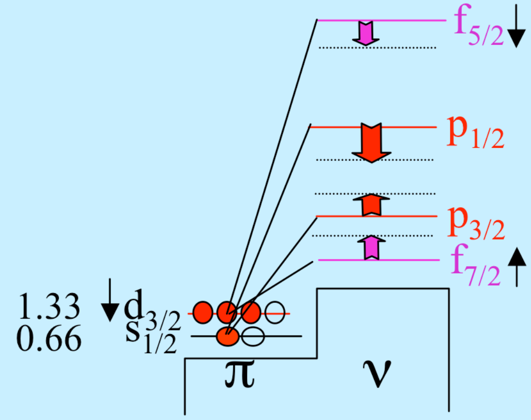

Tensor interaction (*T. Otsuka)*

$\pi d_{3/2} - \nu(f_{7/2}\text{-}f_{5/2})$

or/and

Density dependence (*J. Piekarewicz)*

$\pi s_{1/2} - \nu(p_{1/2}\text{-}p_{3/2})$

Role of specific n-p interactions

N=28 gap has decreased by **330(80) keV** between Ca and Ar

Decrease of the *f* and *p* spin-orbit splittings by **800keV** and **900keV**, respectively

O. Sorlin courtesy

The MUST2 Array

Collaboration: IPNO,SPhN/Saclay,GANIL

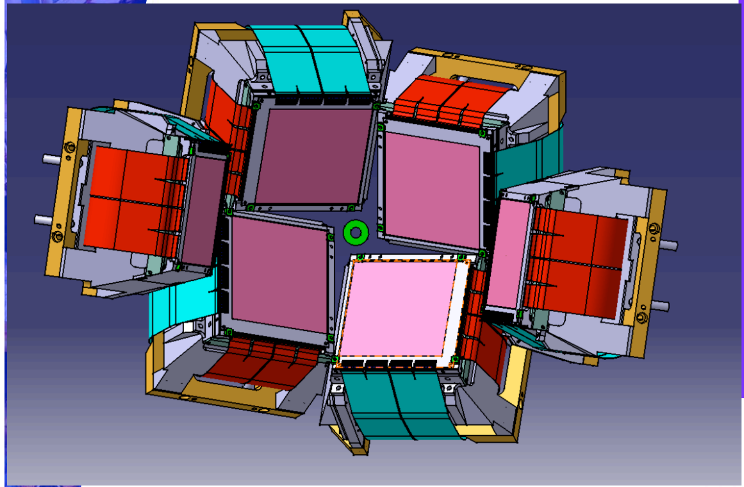

MUST2 : a major upgrade of MUST

- Increased angular coverage
  - Better efficiency
  - Measure several reactions in one shot
- Increased granularity (multiparticle events)
- New ASIC based electronics : more compact

-Si strips: 128 X
+128 Y
(Energy and time)
-2 Si(Li) segmented in 8
-16 CsI

Each telescope =
576 electronics channels
6 telescopes in 2007
10 telescopes in 2009

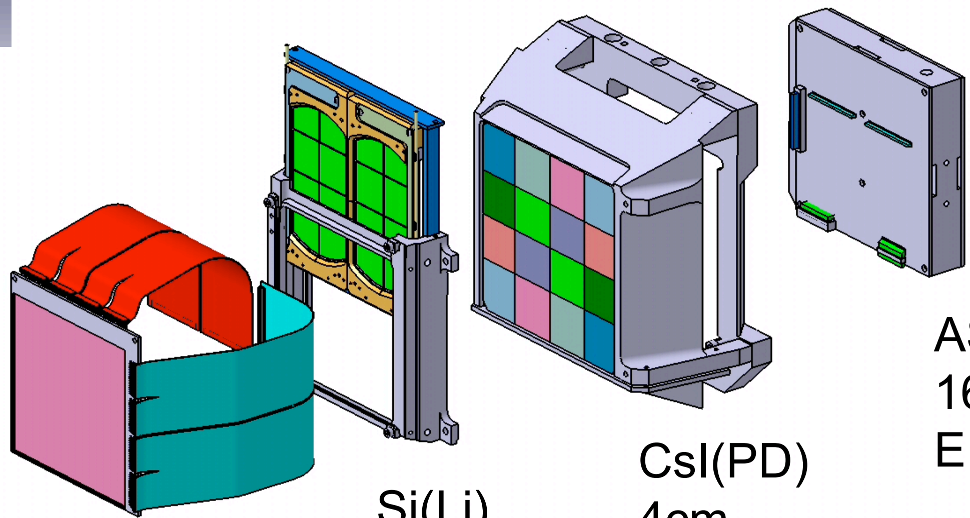

P. Roussel-Chomaz

MATE for Si, Si(Li) & CsI

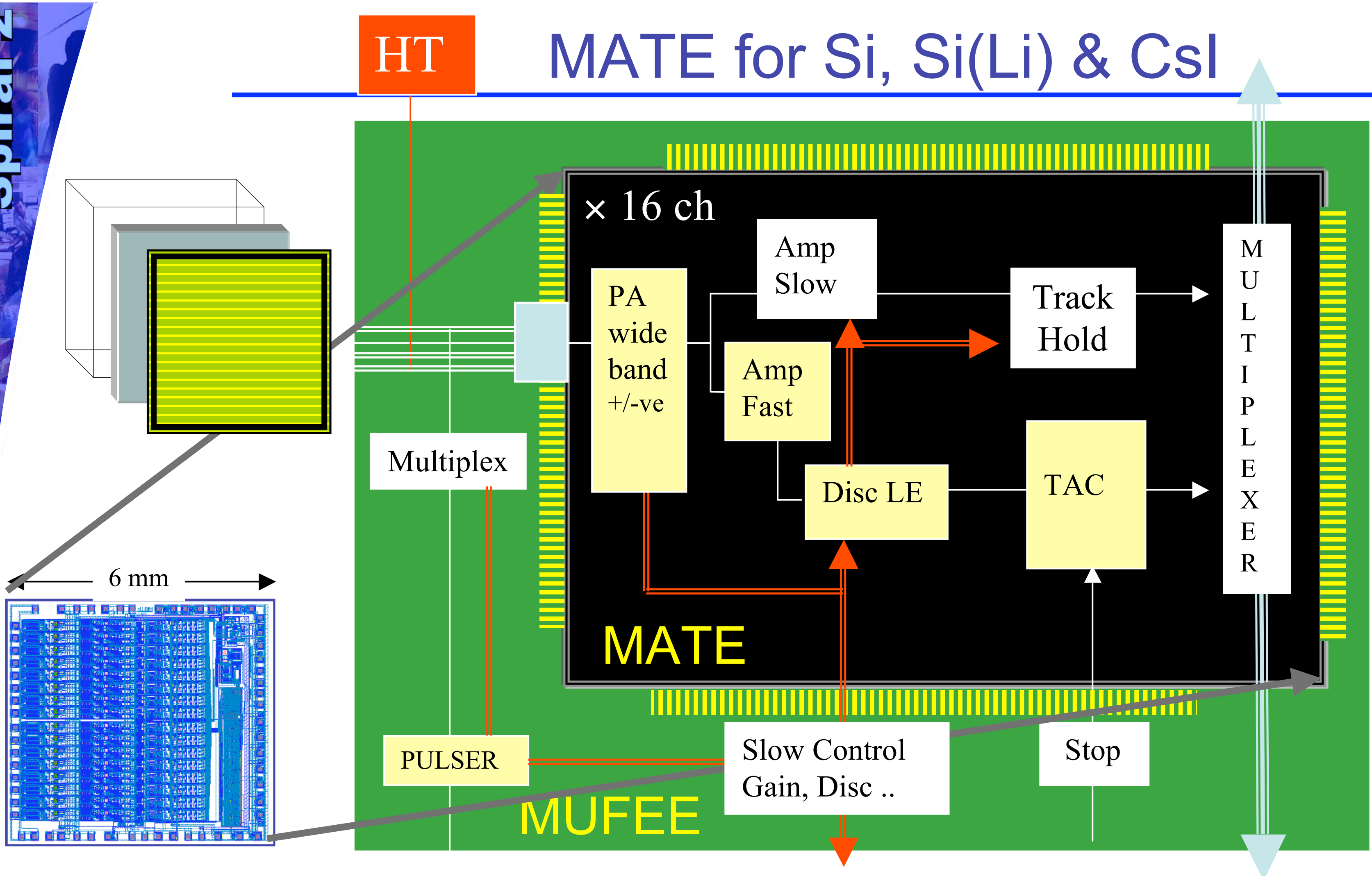

16 Channels (Fast & Slow)
Chip 36mm²
BCMOS 0.8 µ
16000 transistors
35 mWatt/channel
Serial output 2 MHz

Energy
Bipolar (slow & fast)
Slow Control
Energy (Track & Hold)
1µs/3µs RC-CR
0.3 - 50/250MeV
20/90 KeV

Time
Disc Leading Edge
TAC (300/600nsec)
240 psec jitter

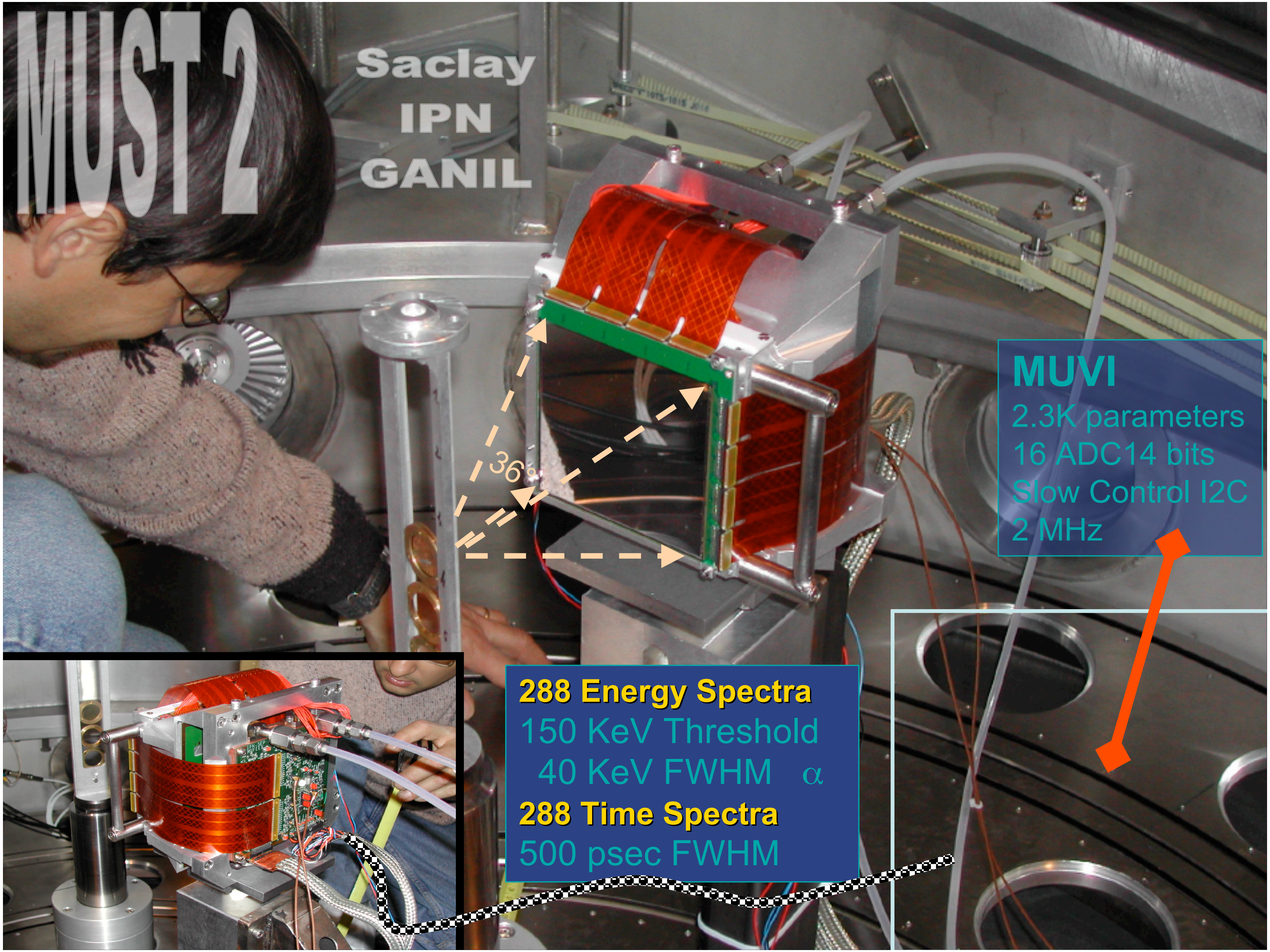
MUST 2
Saclay
IPN
GANIL
36°
MUVI
2.3K parameters
16 ADC14 bits
Slow Control I2C
2 MHz
288 Energy Spectra
150 KeV Threshold
40 KeV FWHM α
288 Time Spectra
500 psec FWHM

MUST2

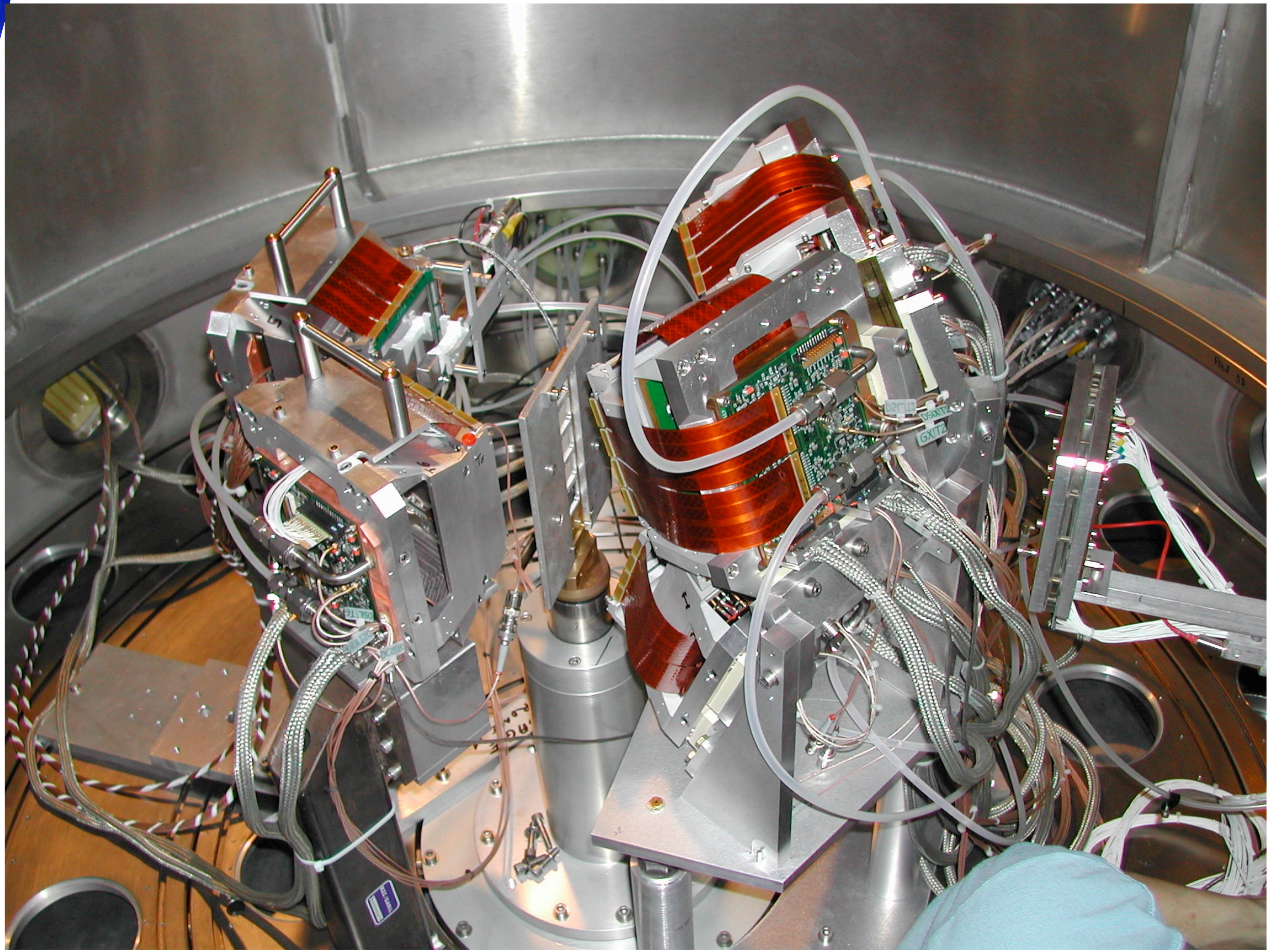

P. Roussel-Chomaz

MUST2

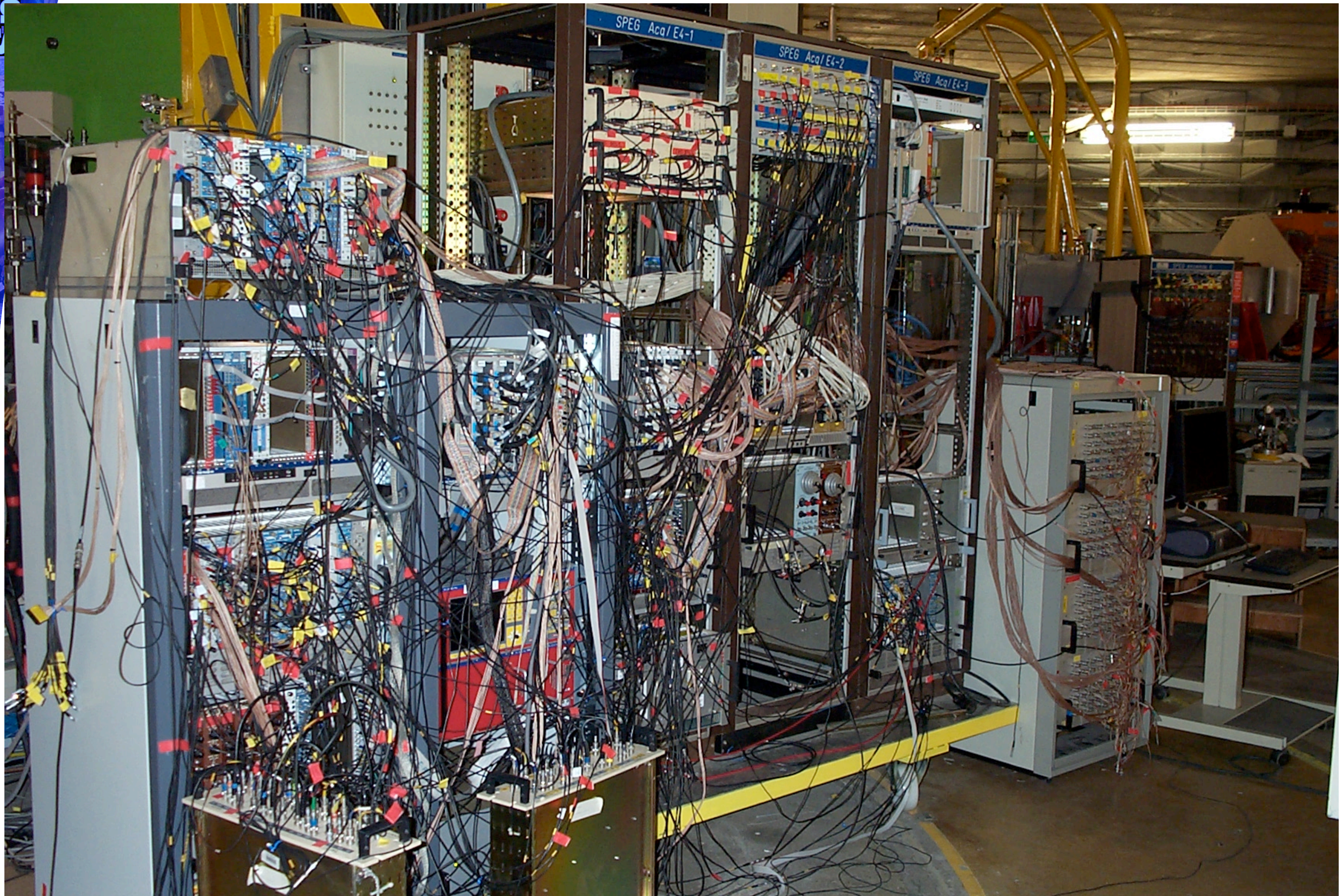

VAMOS + EXOGAM +Tiara + MUST2

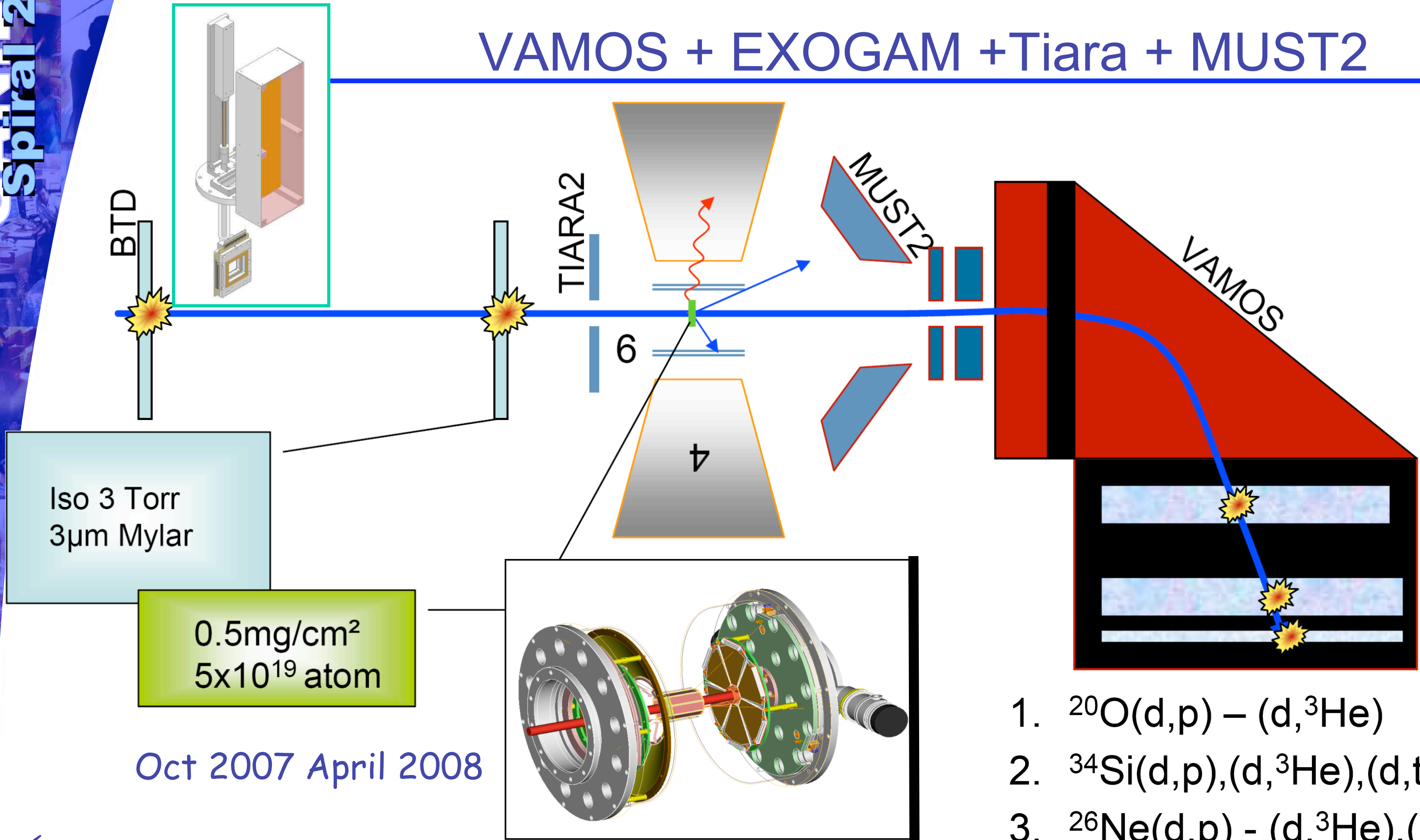

Oct 2007 April 2008

1. $^{20}O(d,p)$ – $(d,^{3}He)$
2. $^{34}Si(d,p),(d,^{3}He),(d,t)$
3. $^{26}Ne(d,p)$ - $(d,^{3}He),(d,t)$
4. $^{56}Ni,^{48}Cr(d,a),(p,^{3}He),(p,t)$

- ✓ Transfer angular distributions
- ✓ Evolution of single particle levels
- ✓ Spin orbit splitting, np pairing

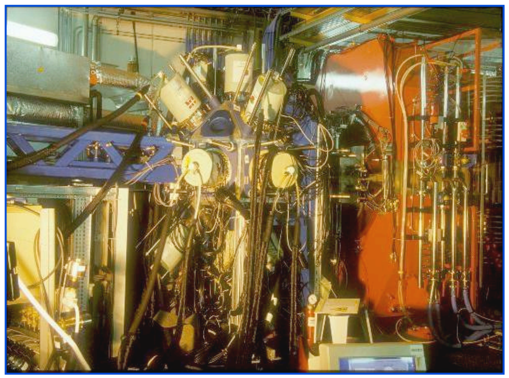

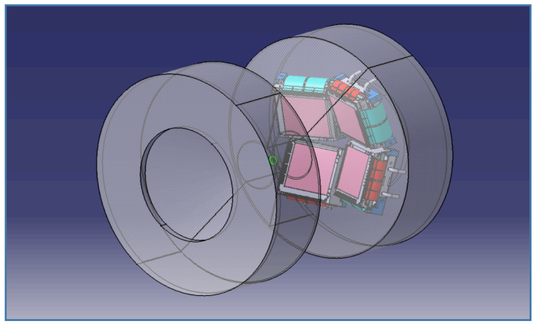

Other detection systems: HIRA@ MSU/NSCL

Collab: MSU/NSCL-IUCF-Washington Un.-Milano-Illinois Un.

- **20 Telescopes**
- **62.3 x 62.3 mm² Active Area**
- **strip pitch 1.8 mm**
- **1024 Pixels per telescope**

HiRA High Resolution Array

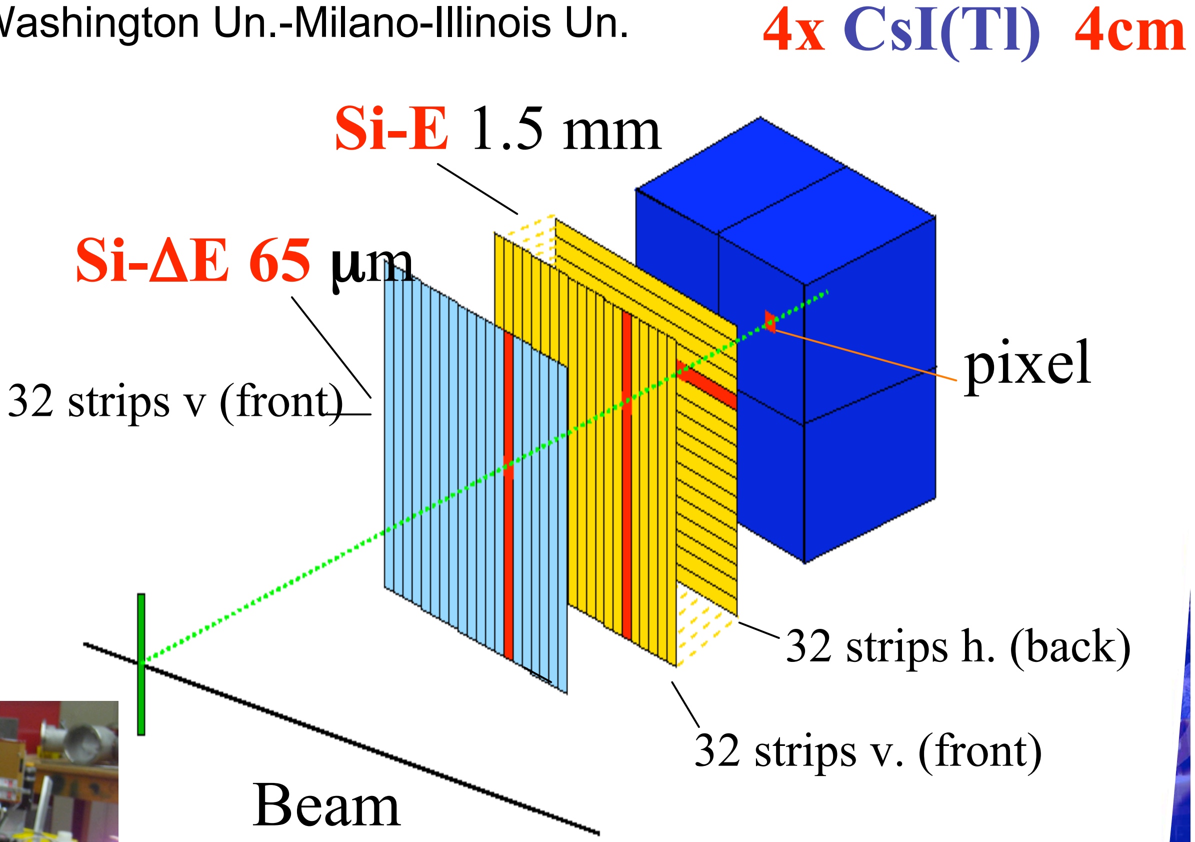

ASIC chip (16ch):
Multiple preamps
Shapers
Discriminator
TAC

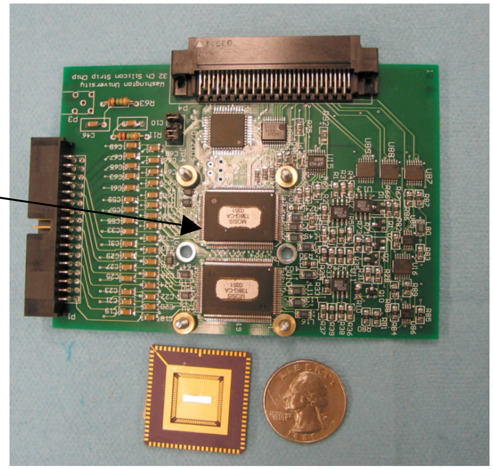

Other detection systems : ORRUBA @ Oak Ridge

ORRUBA: Oak Ridge Rutgers University Barrel Array

- Flexible design for measuring ejectiles from transfer reactions in inverse kinematics
- Resistive and non-resistive Si detectors (1000µm, 500µm and 65µm)
- ORRUBA gives ~80% ϕ coverage over the range 47° →132°
- 288 electronics channels (conventionally instrumented)

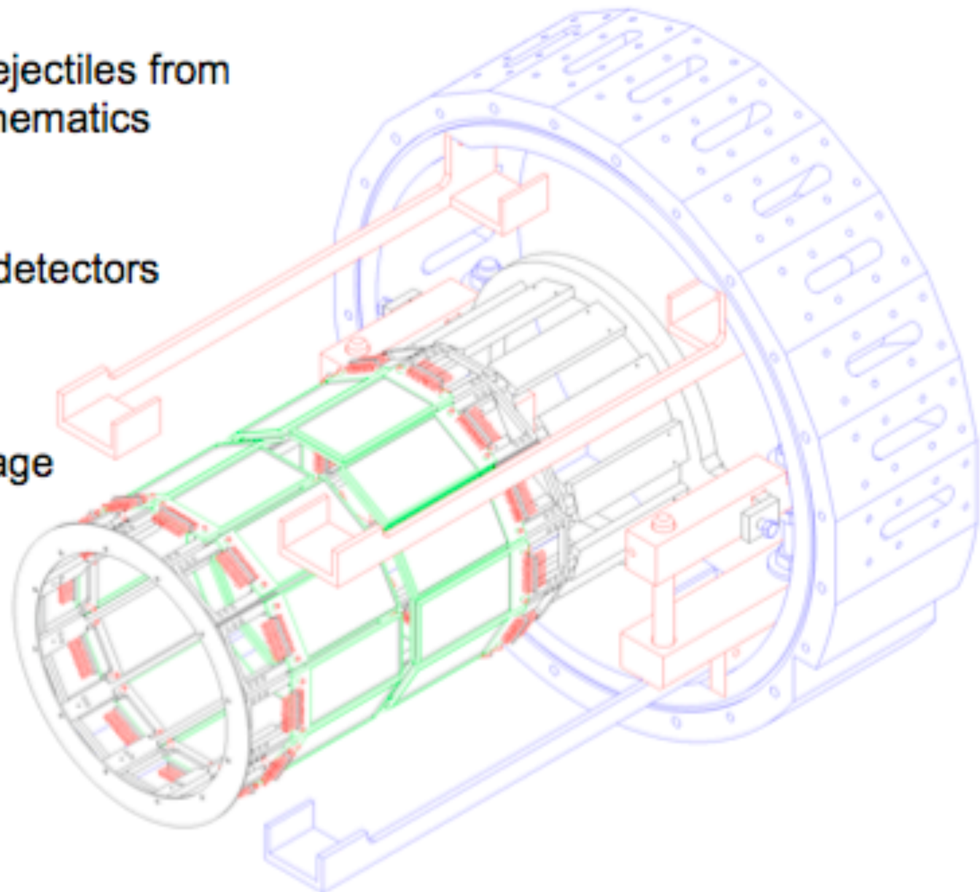

J. Cizewski, DREB 2007

Other detection systems : ORRUBA @ Oak Ridge

$^{132}Sn(d,p)$ Courtesy of K. Jones

ORRUBA detectors
(back angles)

SIDAR detectors
(back angles)

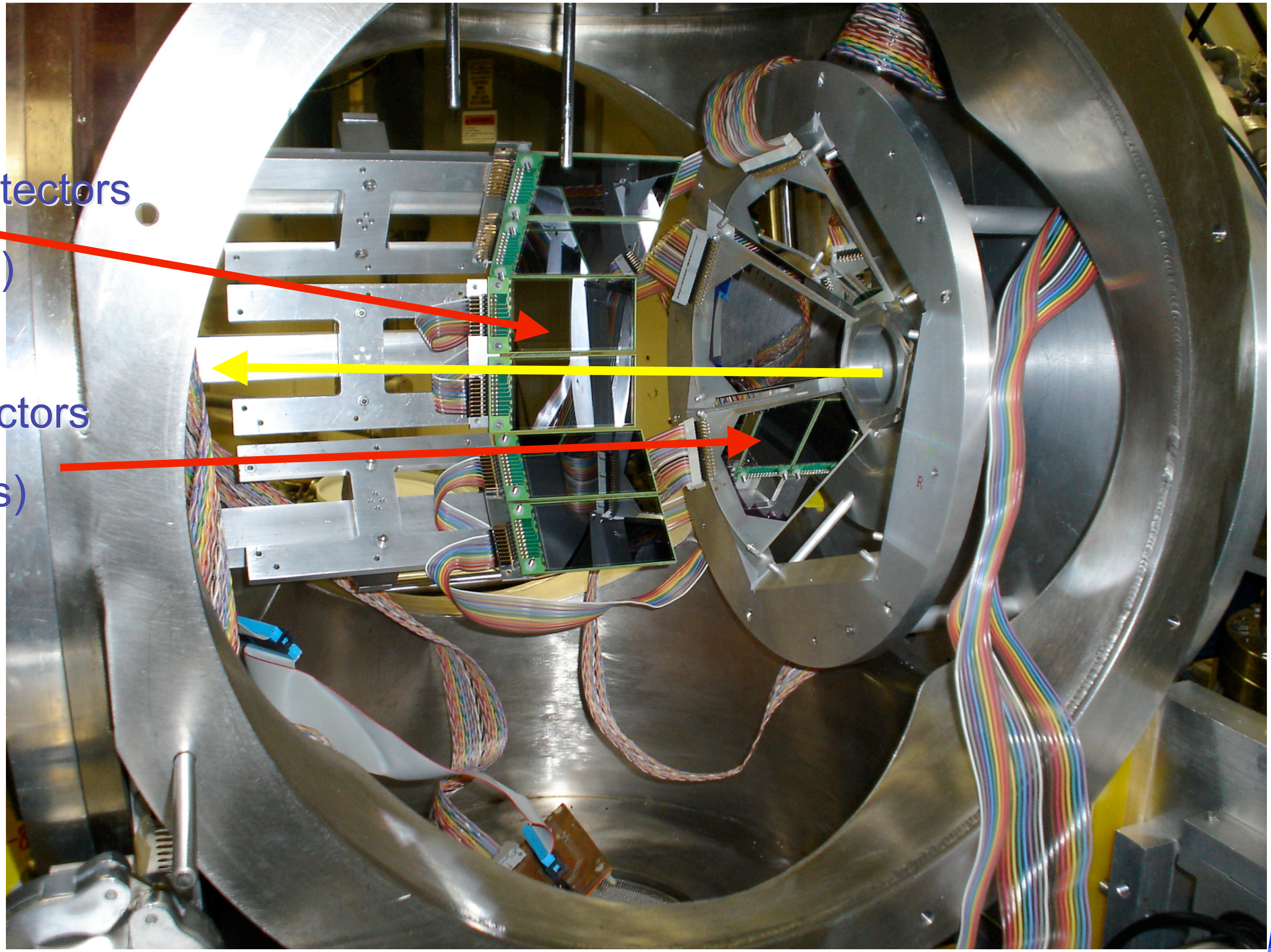

Active Target concept

- ❍ The most exotic nuclei are usually the most interesting ones.
- ❍ The production rate for exotic nuclei decreases basically exponentially with the increase of proton-neutron imbalance

  – High efficiency set-up
  – Thick targets : loose of energy resolution
  – Low energy of light-ion recoil

➠ **New concept : Target becomes a good resolution detector**

Detector gas : H_2, D_2, ^3He, ^4He, C_4H_{10} ...
3-D tracking, Range & Energy losses of particles

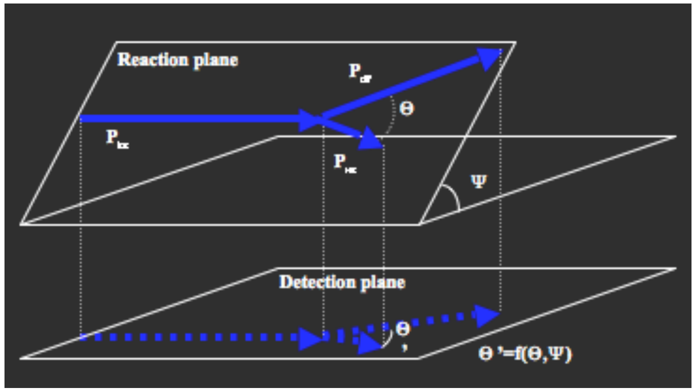

✓ *Very high efficiency*
✓ *Thick target*
✓ *Low particle thresholds*
✓ *Large range of center of mass angles*
✓ *Excitation function*
✓ *10^4 Hz*

MAYA Active Target

there is a beam detector before MAYA, to start the DAQ.

the projectile makes reaction with a nucleus of the gas.

the light scattered particles do not stop inside, and go forward to a wall made of 20 Si detectors, where they are stopped, and identified.

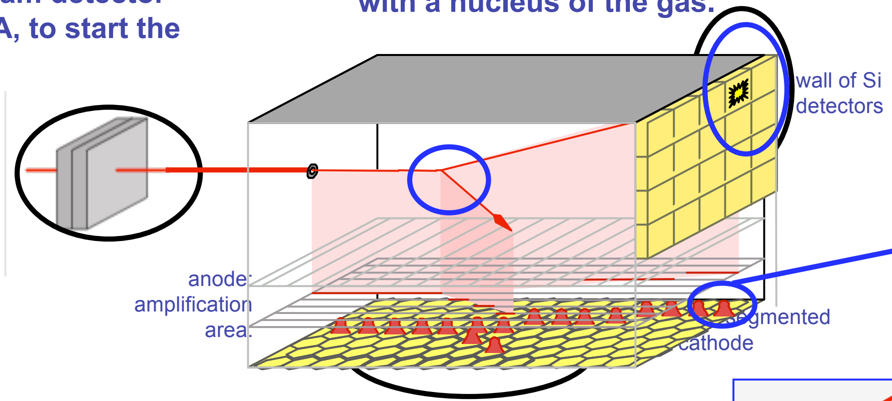

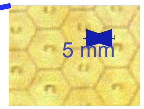

COG over 3 axes

the product leaves enough energy to induce an image of its trajectory in the plane of the segmented cathode.

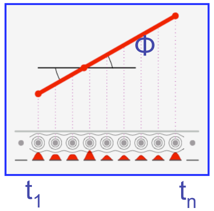

we measure the drift time up to each amplification wire. The angle of the reaction plane is calculated with these times.

➠ **Si-wall (20 Si), CsI-array (20 csi)**

Pulse height (~energy loss)

➠ **Anode wires**

Pulse height,

drift time (time from incident beam by PPAC) provide y-coordinate

➠ **Pads (32 x32)**

Pulse height, provide x-z coordinates

➠ **Three dimensional track of a charged particle is determined from wires and pads data.**

W. Mittig *et al*. **European Physical Journal A 25 (2005) 263**

C. E. Demonchy *et al*. **Journal of Physics G 31 (2005) S1831**

MAYA active target

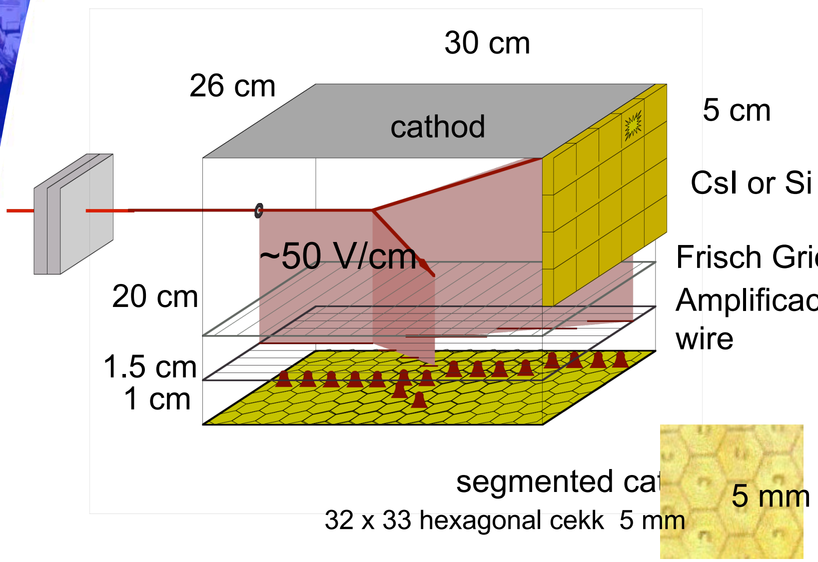

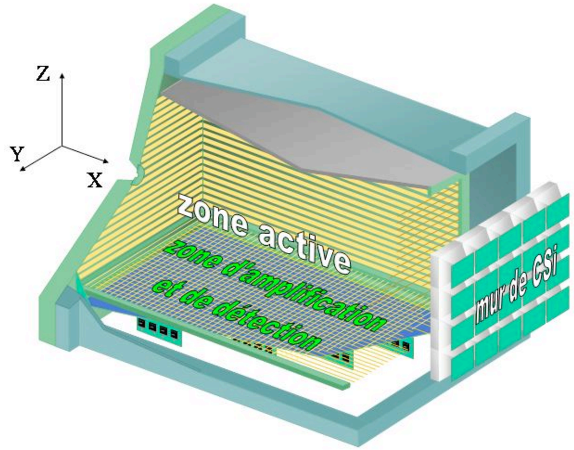

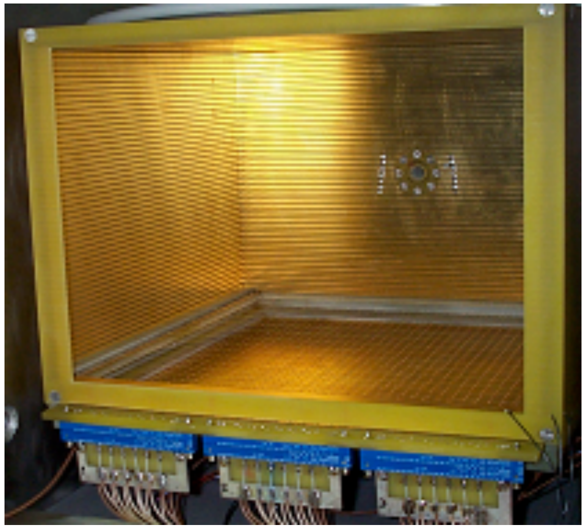

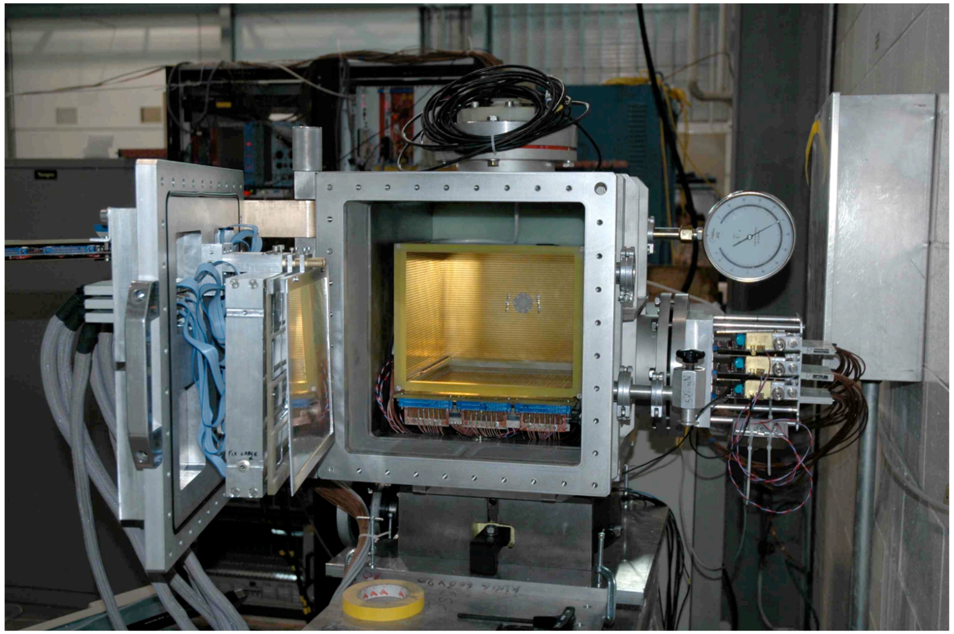

MAYA active target

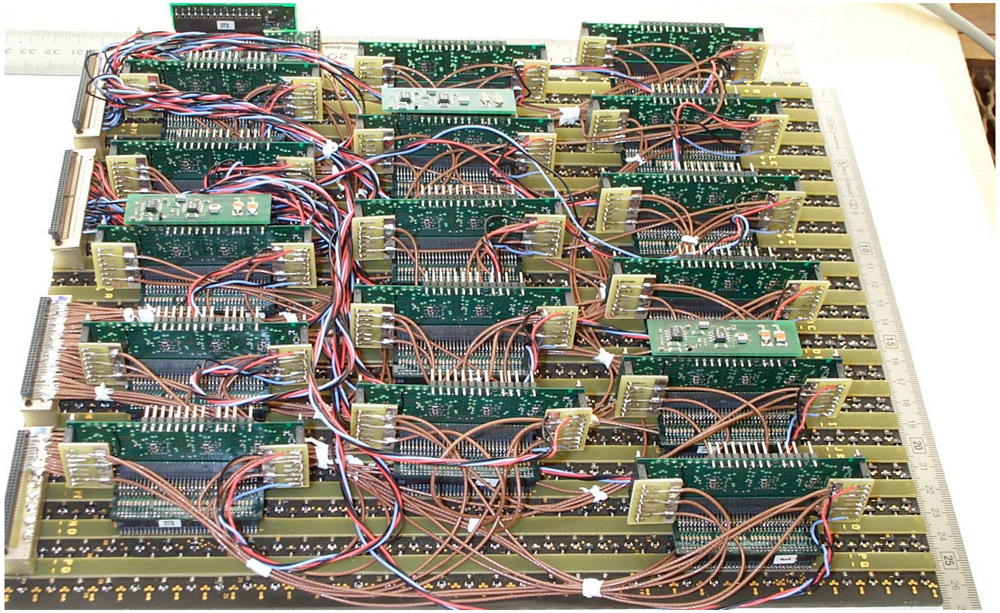

ASIC technology : Gassiplex (GAS64)

- ≈thousand channels
- Multiplexed serial readout
- Dynamic fixed
- Common track & hold

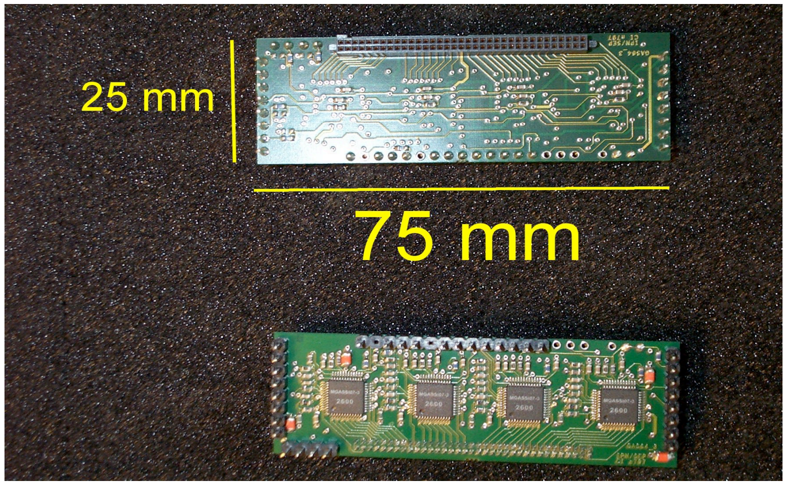

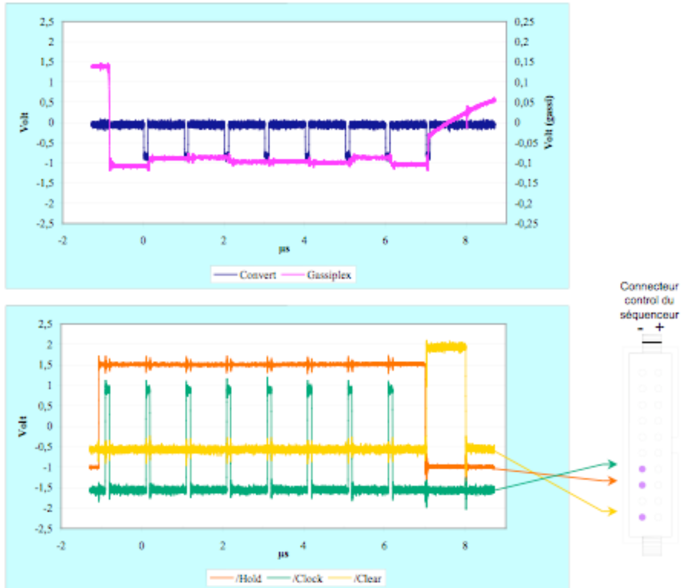

P. Roussel-Chomaz

Specificity of MAYA data analysis

Principle :

- Energies (Ranges) and scattering of all charges particles are determine inside MAYA

Quantities used for data analysis are :

- Energy deposited in Si and CsI wall
- Scattering angle of particles (heavy and light partners)
- Totally and partially integrated energy loss in MAYA
- Vertex of the reaction ➠ Excitation function

Limitations :

- Vertex determination at small angle
- Resolution depends on the length of tracks
- Tracking cannot be made near Φ=90° and 270° (reaction plane is vertical and drift time can not be measured)

Maya identification

❍ For particle stopping inside MAYA, identification is given by the energy of the particle and its range :

Range ∝ E^2/MZ^2

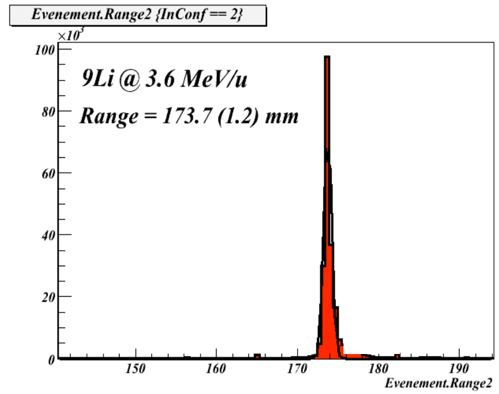

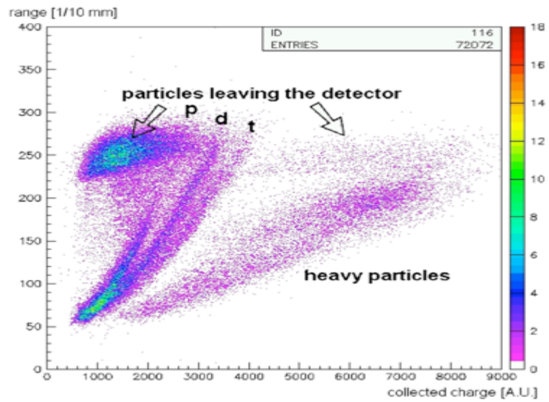

❍ For particle leaving MAYA at forward angles, identification is given by the energy loss in MAYA, energy deposit in Si and CsI wall

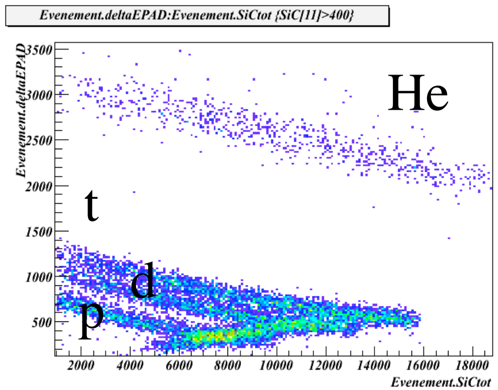

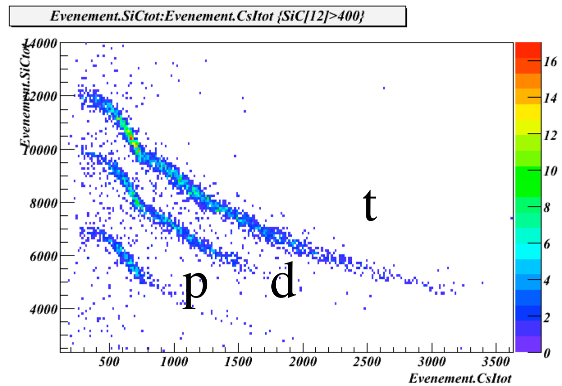

❍Reconstruction of the reaction kinematics

Event analysis

Event display of pads signals.
Each dot shows the pulse height of the pad

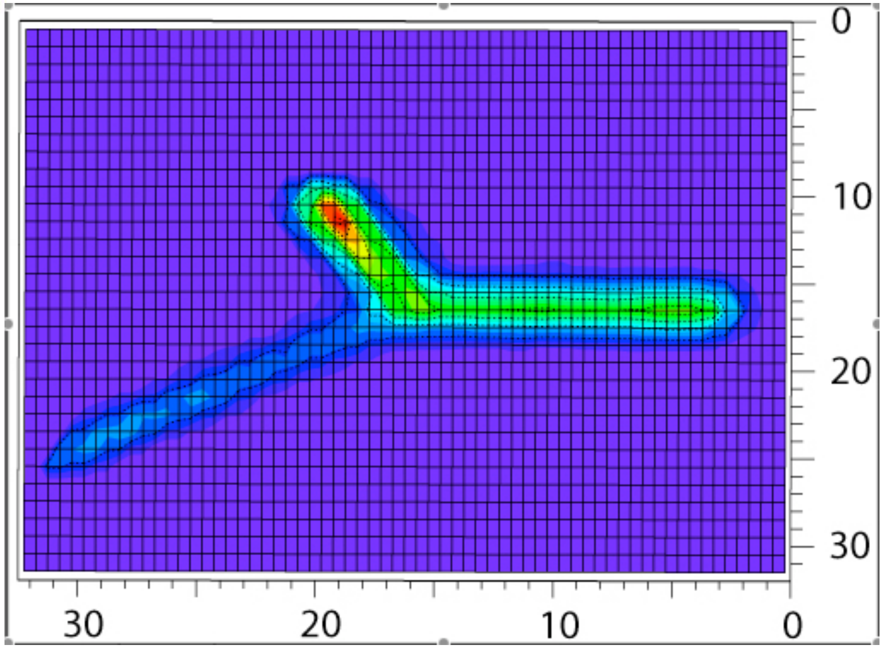

Drift time
distribution

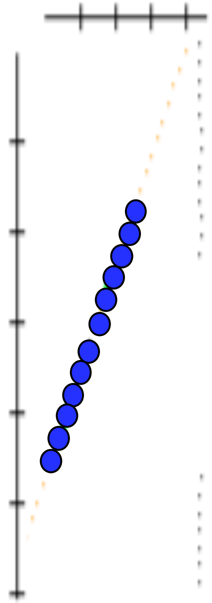

- Selection of the particle in Si
- Projected trajectectory reconstruction Theta2D and Range2D
- Vertex (target depth)
- Reaction plane angle

❍ Energy resolution
Range resolution ≈ 1mm
$\Delta R/R \approx$ 1mm/R (≈ 1% for Range = 10cm)
$\Delta E/E$ = 0.5*1/R (≈ 0.5% for Range = 10cm)

❍ Angular resolution
$\Delta\theta \approx \Delta x/R$ (0.6 deg for R=10cm)

❍ Charge resolution ~ 10 %

❍ Vertex resolution ~ 3 mm

P. Roussel-Chomaz

MAYA random selected events

MAYA@TRIUMF ^{11}Li campaign
(H. Savajols and I. Tanihata spokepersons,
thèse Th. Roger)

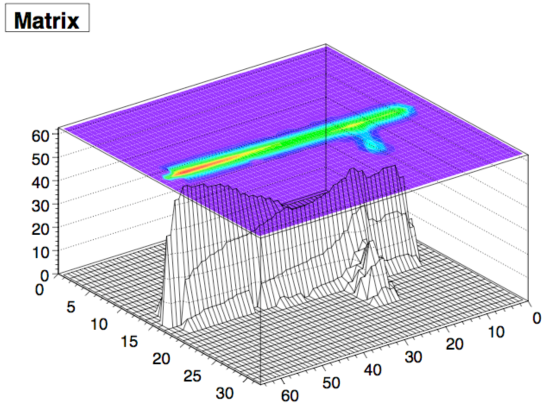

(p,t) & (p,d) reactions

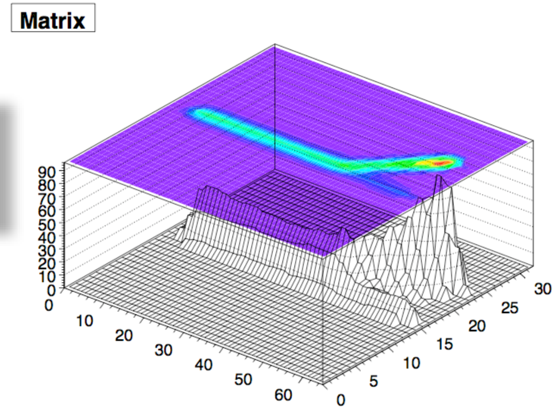

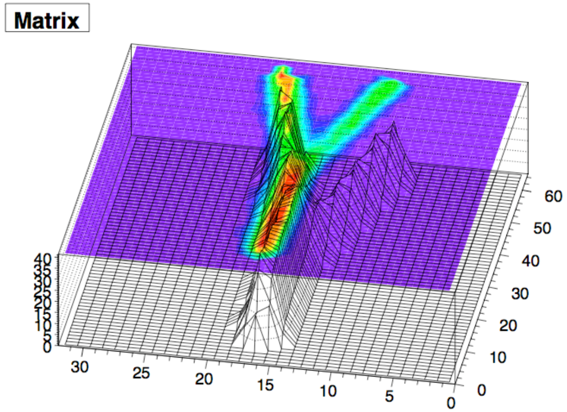

Scattering on Carbon

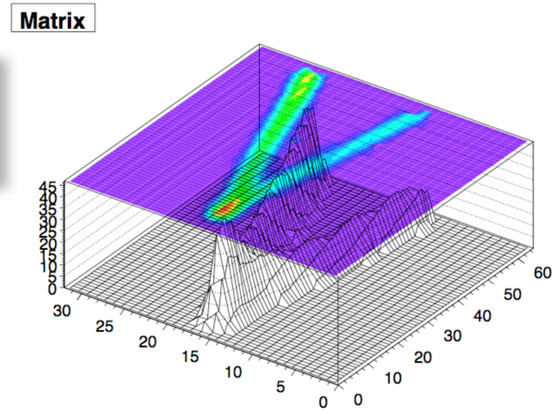

The quest of ^{7}H

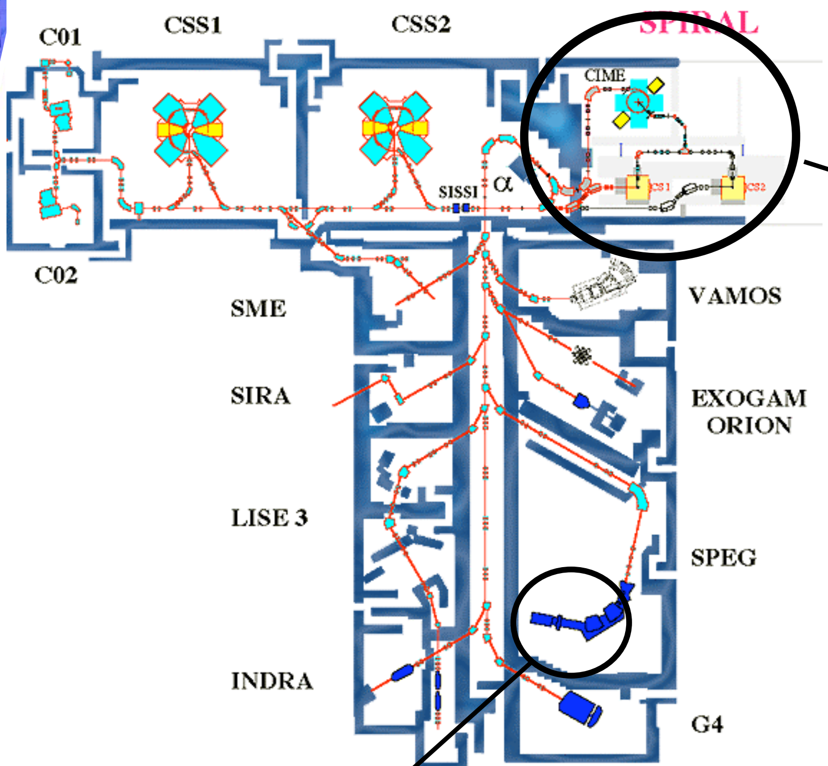

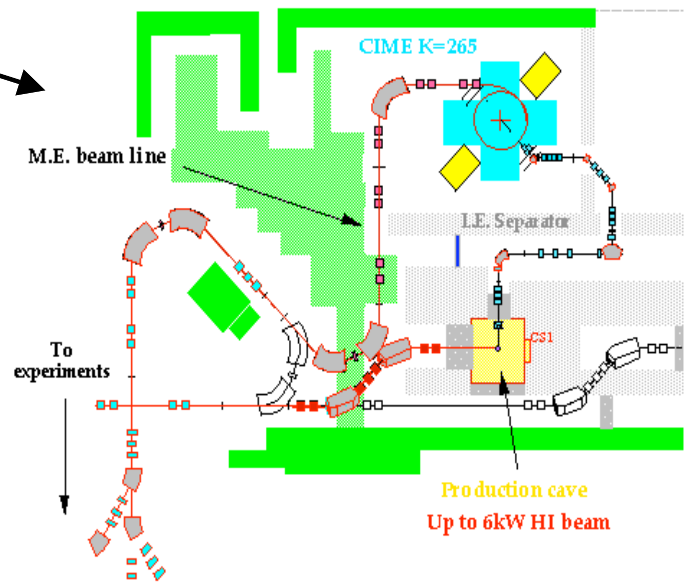

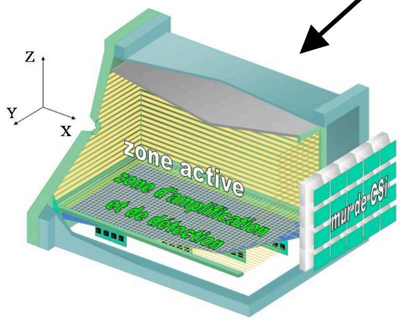

^{8}He 15.4 MeV/nucleon

~**20** MHz

C_4H_{10}, at 25, and 30 mbar
10^{20} atoms/cm^2 of ^{12}C

^{8}He(^{12}C,^{13}N)^{7}H → ^{3}H+4n

M. Caamano PhD Thesis
L. Cortina, H. Savajols

MAYA and the quest of ^{7}H

$^{8}He(^{12}C,^{13}N)^{7}H \rightarrow {}^{3}H+4n$

MAYA filled with C_4H_{10}, at 30 mbar
10^{20} atoms/cm^2 of ^{12}C

$^{13}N \approx$ 10MeV stopped in 1.3 mg/cm^2 of Carbon
6 10^{19} atoms/cm^2 of ^{12}C

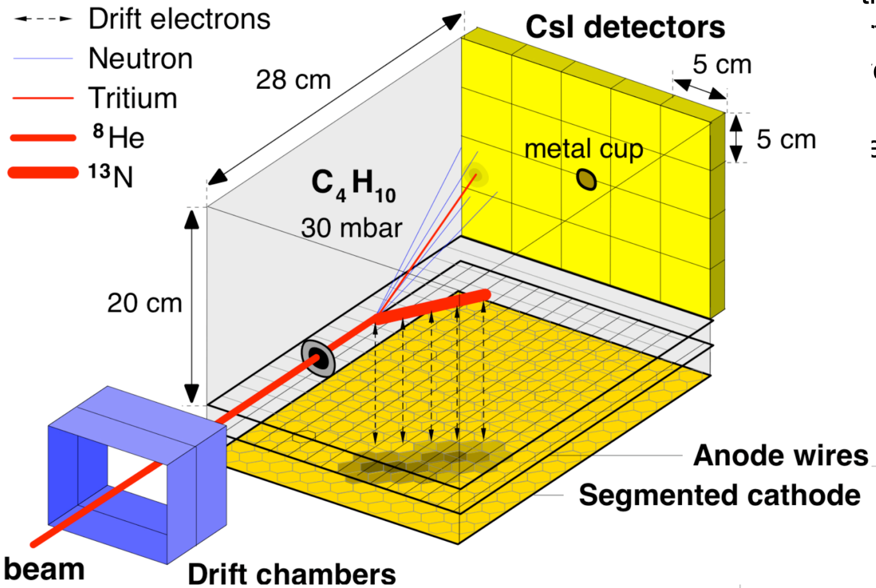

the light scattered
ticles escape the
olume. They are
stopped, and
entified in the CsI
wall.

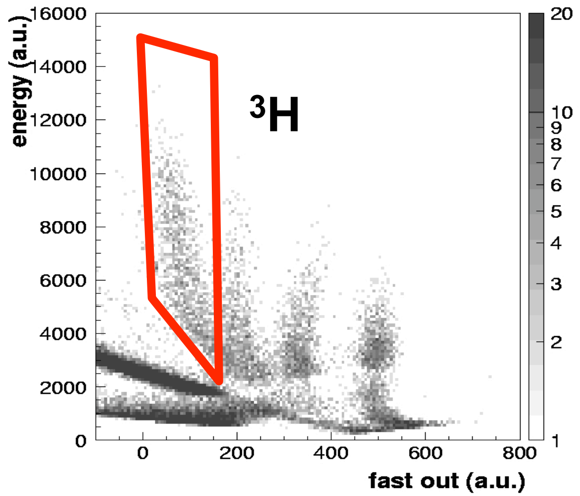

3D trajectory reconstruction

the recoil leaves enough energy to induce an image of its trajectory in the segmented cathode.

the drift time to the amplification wires allows the determination of the reaction plane.

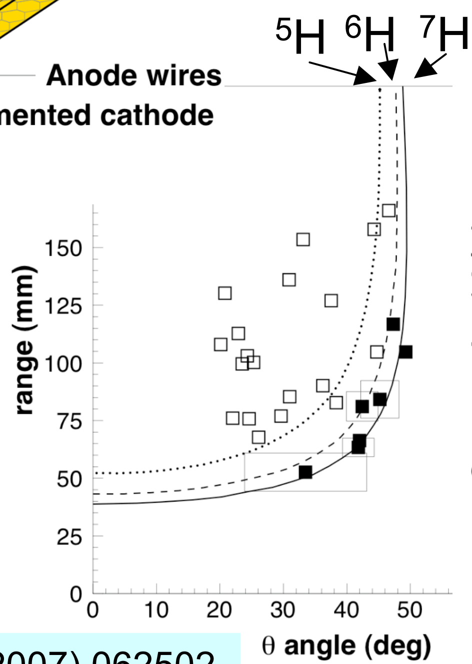

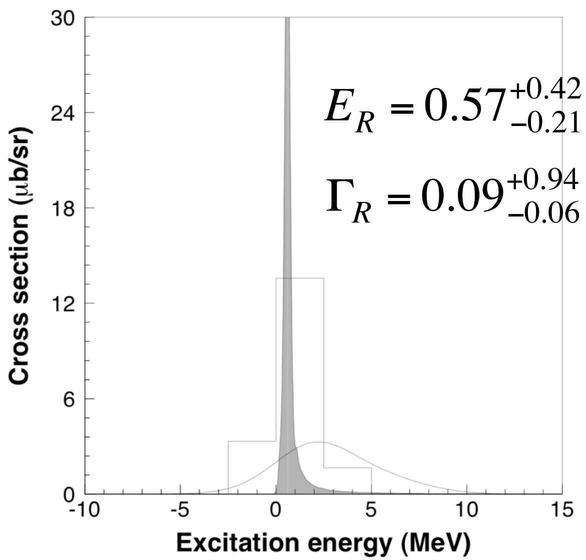

$$E_R = 0.57^{+0.42}_{-0.21}$$

$$\Gamma_R = 0.09^{+0.94}_{-0.06}$$

M. Caamaño PhD thesis 2006 and PRL99 (2007) 062502

Definition of geometry for the next generation active target

Cylindrical geometry: symmetry around beam axis
E // beam axis, uniform
Projection on the endcap of the cylinder
B // beam axis

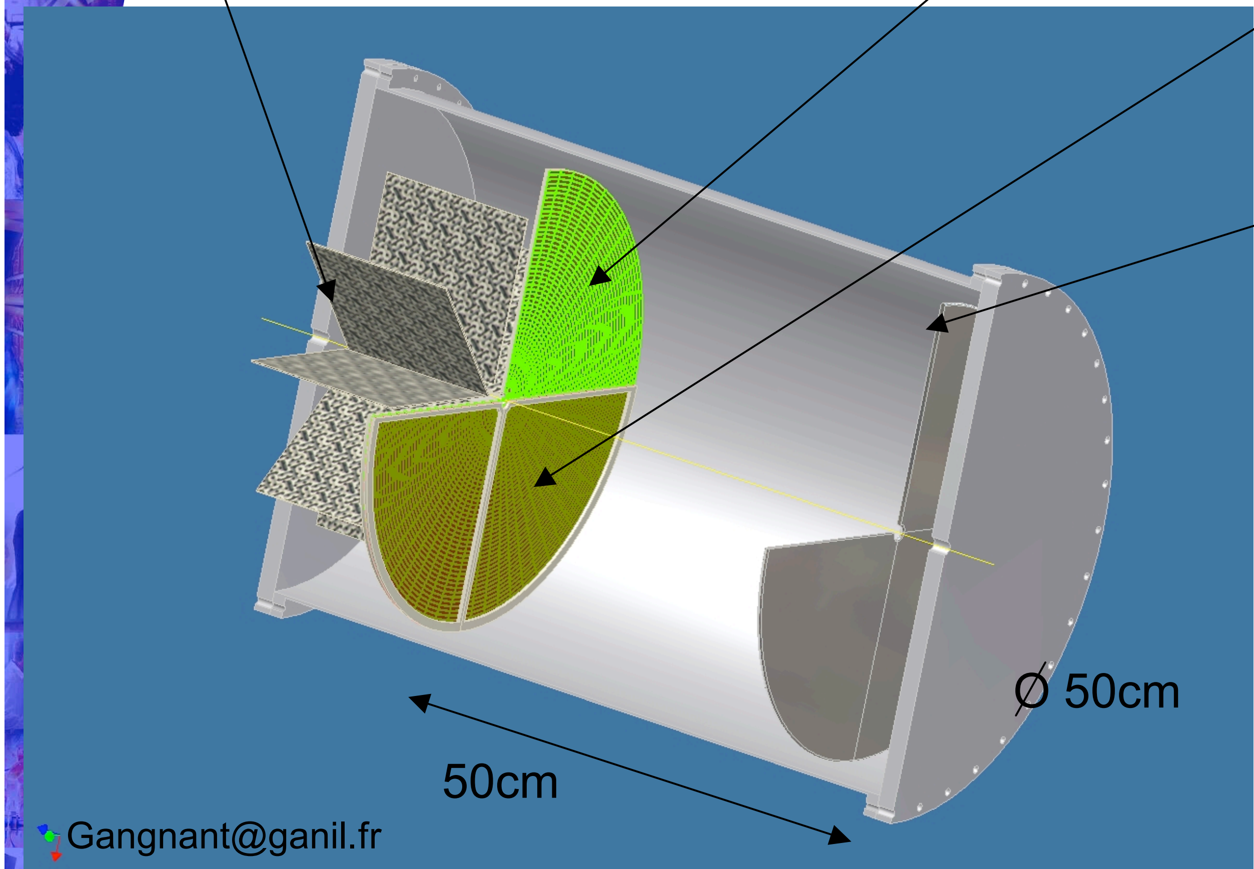

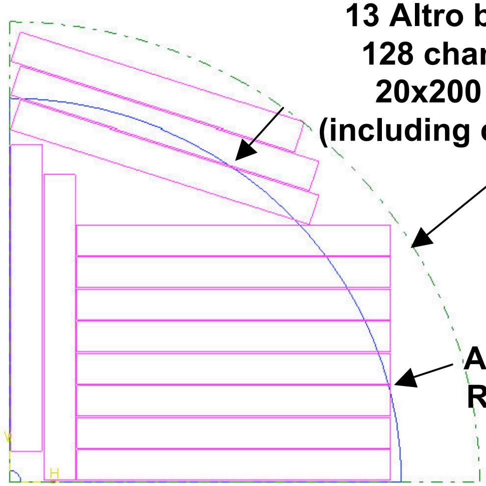

Quantities to be measured: curvature radius, collected charge, range, angles
For 0.5 mm position resolution, $\Delta E/E=2\Delta R/R$, expected energy resolution≈100 keV for $\theta_{cm}>20°$

Simulations : $^{78}Ni(d,p)^{79}Ni$ $\theta_{cm}=20°$ $E_x=0,1.5,3$ MeV

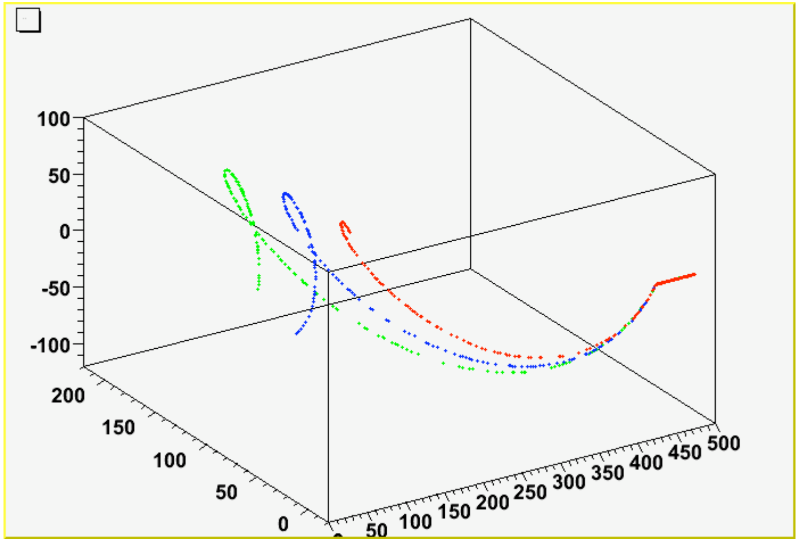

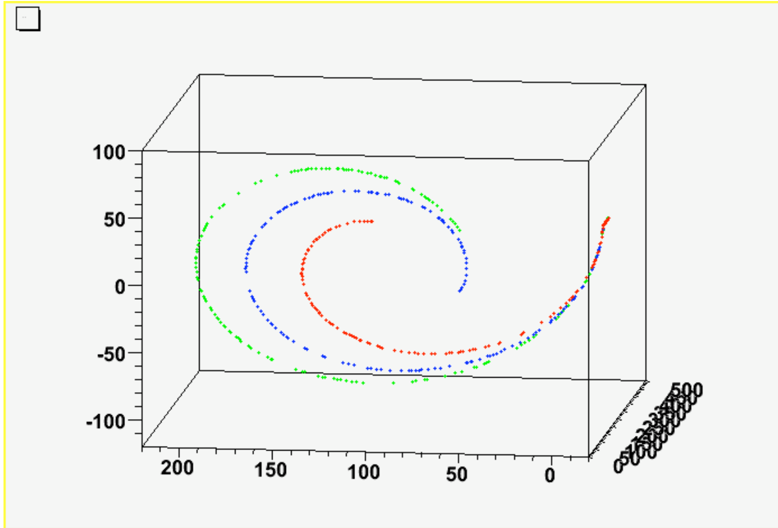

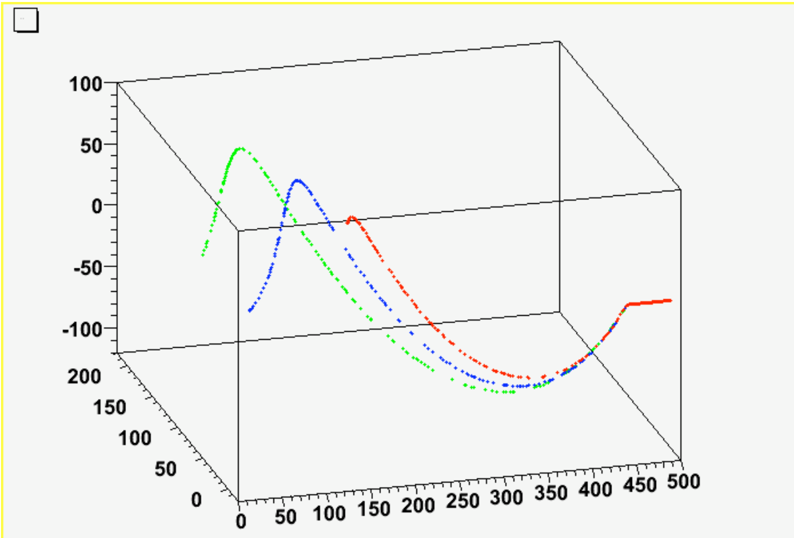

E_{inc}= 8.5 A.MeV
D_2 at 1atm
X_{reac}= 5 cm
B=2 T

E_x = 0, g.s.
E_x = 1.5 MeV
E_x = 3 MeV

Hector Alvarez-Pol, Esther Estevez-Aguado, USC

Amplification in the gas detector: GEMS

THIN METAL-COATED POLYMER FOIL CHEMICALLY ETCHED WITH 5-100 HOLES mm^2

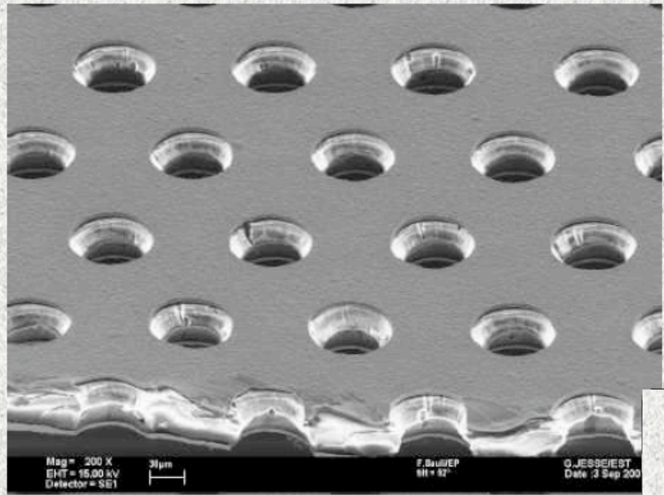

Typically:
50 µm Kapton
5 µm Copper
70 µm holes at 140 µm pitch

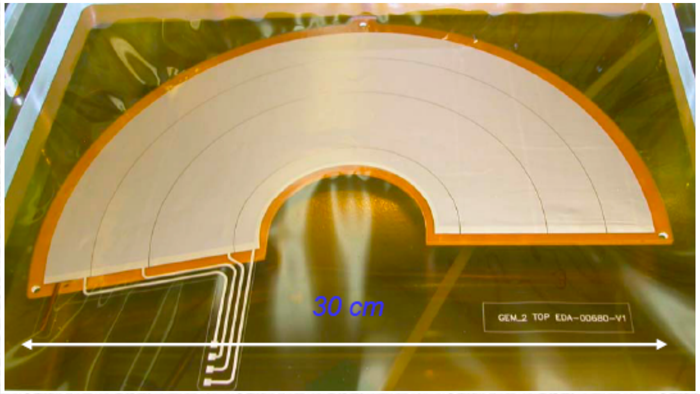

MANUFACTURED BY CERN-TS-DEM
(Rui De Oliveira)

F. Sauli, NIMA 386(1997)531

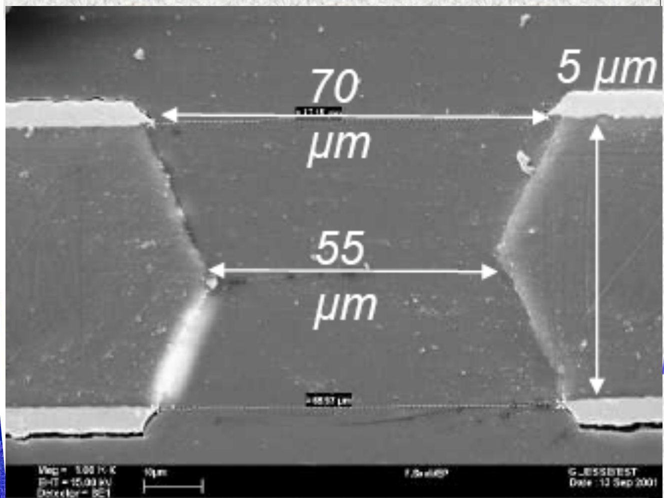

AMPLIFICATION AND TRANSFER
SINGLE GEM DETECTOR:

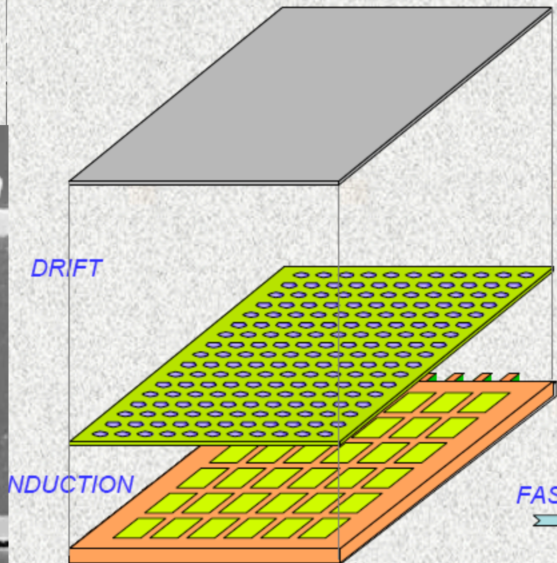

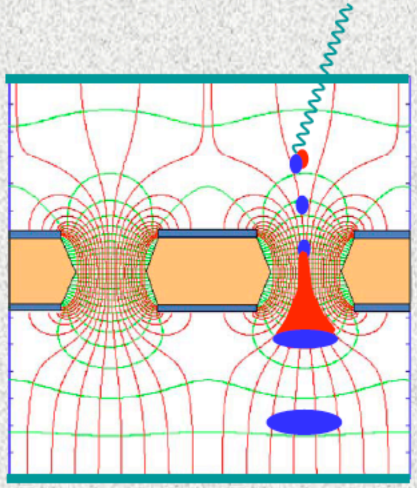

INDEPENDENT PROPORTIONAL COUNTERS
(~ 50/mm^2) ⟹ HIGH RATE CAPABILITY

HIGH VOLTAGE ELECTRODE SEPARATED
FROM READOUT ⟹ ROBUSTNESS

FAST ELECTRON SIGNAL ONLY
⟹ HIGH RATES, GOOD TWO-TRACK RESOLUTION

READOUT ELECTRODE: ARBITRARY PATTERN

Amplification in the gas detector: MICROMEGAS

Micromegas : Micro Mesh Gaseous Detector

Y. Giomataris et al, NIMA376 (1996) 29

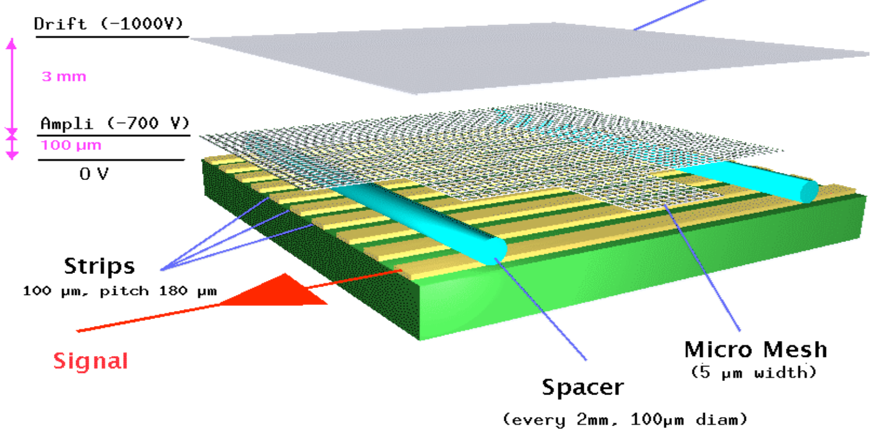

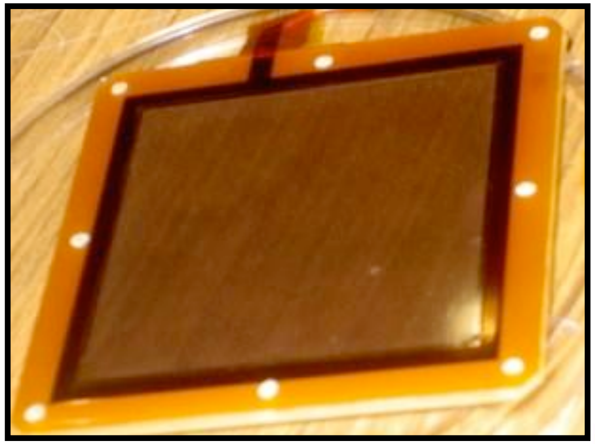

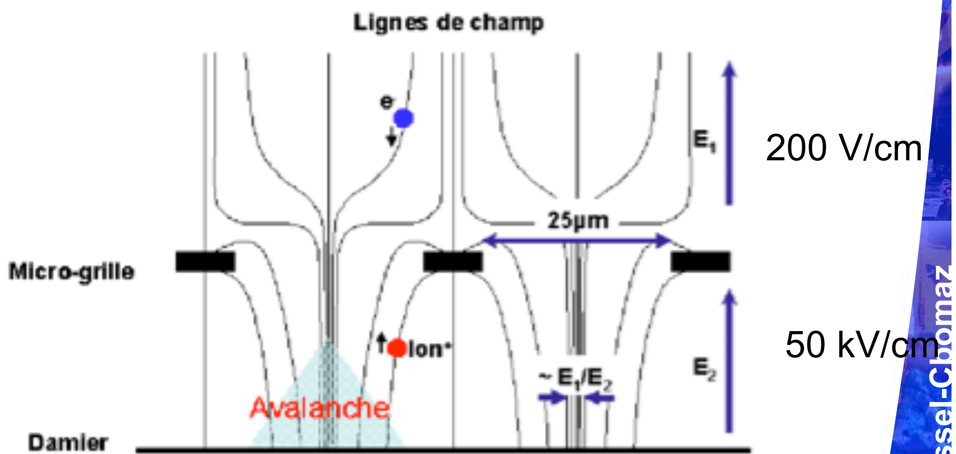

Part 5

Detection systems and selected examples of experiments

b) Invariant mass method: Detection of all outgoing particles Application to giant resonances

The collective response of the nucleus: Giant Resonances

Electric giant resonances: Hydrodynamic Picture

Isoscalar | Isovector

Monopole (GMR)

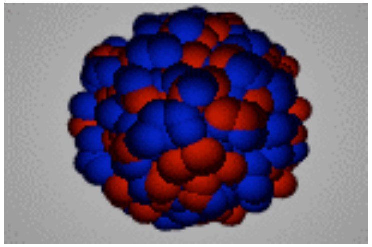

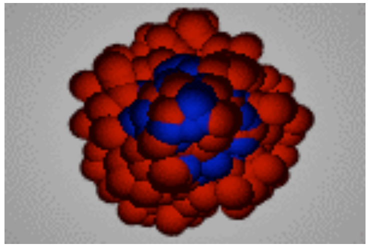

Dipole (GDR)

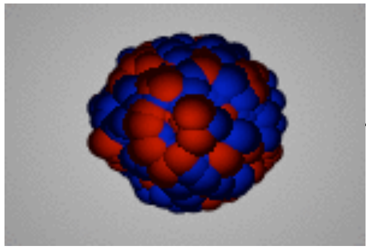

Quadrupole (GQR)

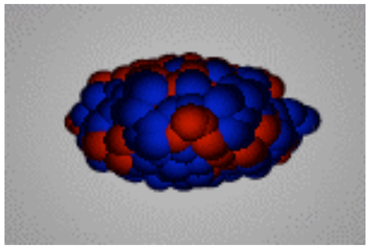

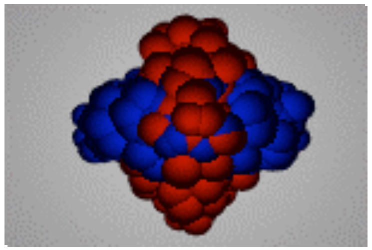

From T. Aumann

Photo-neutron cross sections

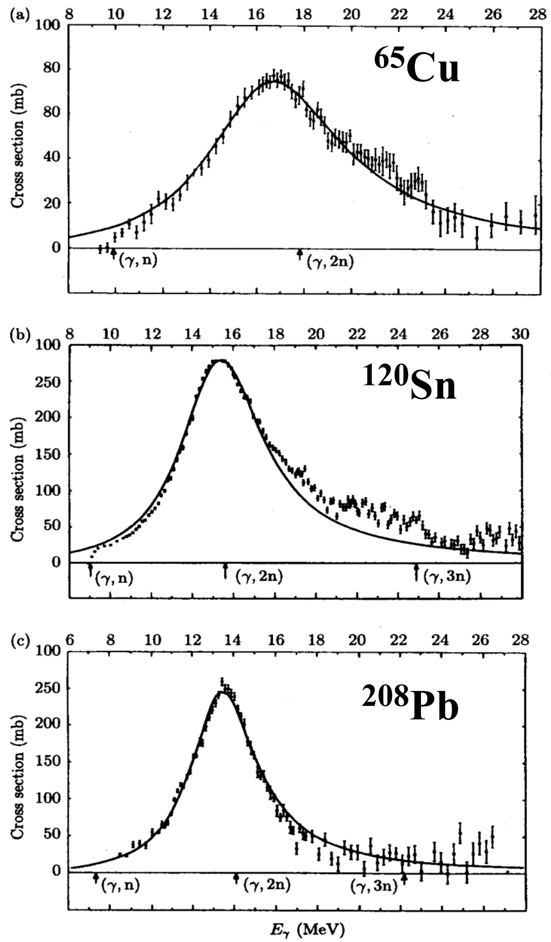

Berman and Fulz, Rev. Mod. Phys. 47 (1975) 47

The dipole response of neutron-rich nuclei

Stable nuclei:

100% of the E1 strength absorbed into the **Giant Dipole Resonance** (GDR)

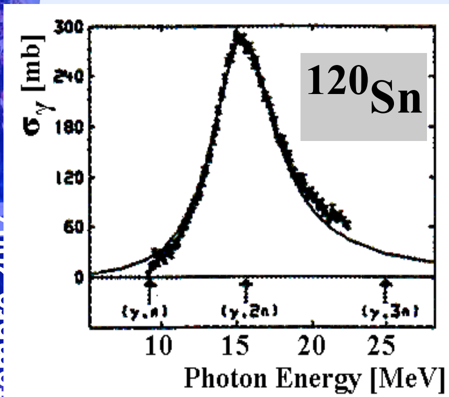

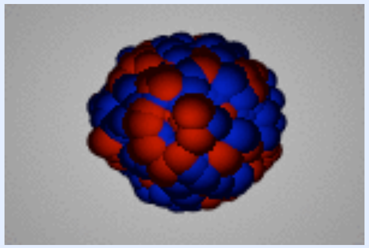

From T. Aumann

Neutron-Proton asymmetric nuclei: low-lying dipole strength

! threshold strength

non-resonant transitions

The one-neutron Halo ^{11}Be

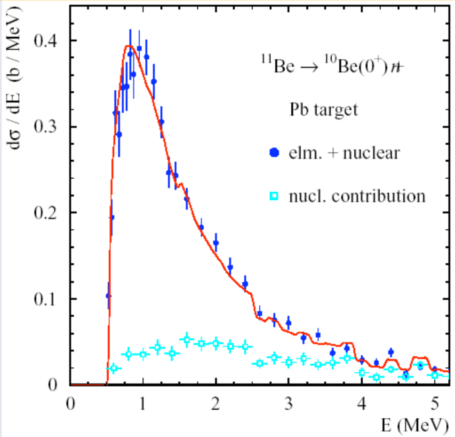

! strong fragmentation

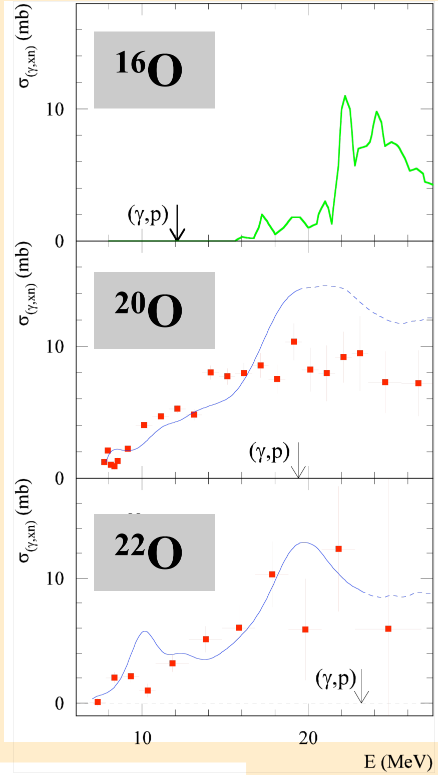

? new collective soft dipole mode

(Pygmy resonance)

Prediction: RMF
(N. Paar et al.)

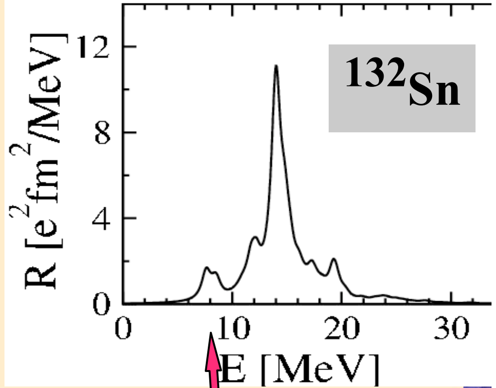

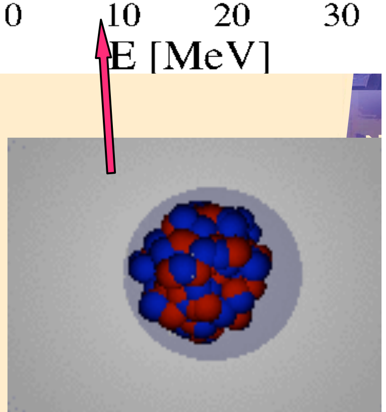

spectroscopic tool:

$$\frac{d\sigma}{dE^*}(I_c^\pi) = \left(\frac{16\pi^3}{9\hbar c}\right) N_{E1}(E^*) \sum_{n\ell j} C^2 S(I_c^\pi, n\ell j) \times \sum_m |\langle \boldsymbol{q}|(Ze/A) r Y_m^1|\phi_{n\ell j}(r)\rangle|^2.$$

Electromagnetic excitation at high energies

From T. Aumann

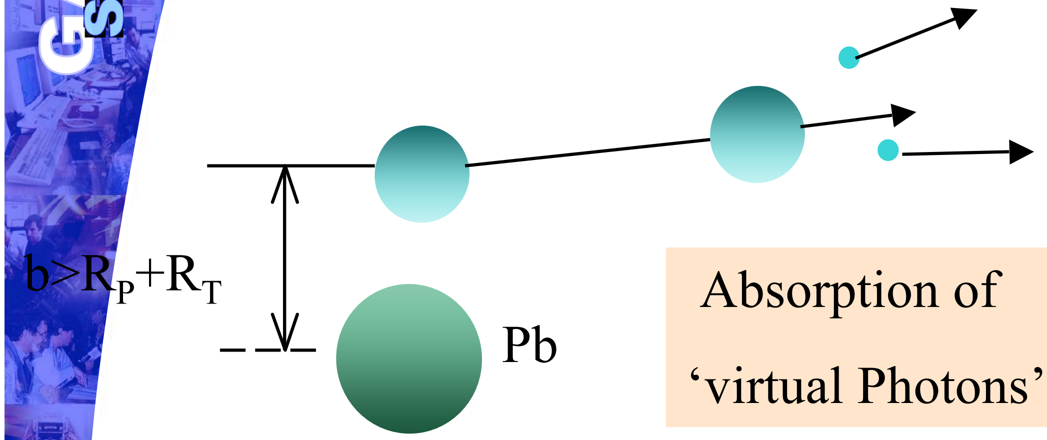

Semi-classical theory:

$$d\sigma_{elm} / dE = N_{\gamma}(E)\, \sigma_{\gamma}(E)$$

Absorption of 'virtual Photons'

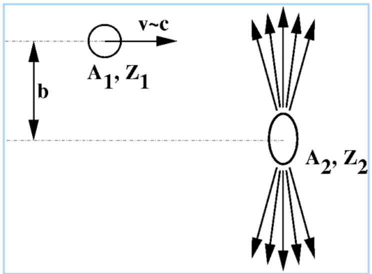

$\sigma_{elm} \sim Z^2$

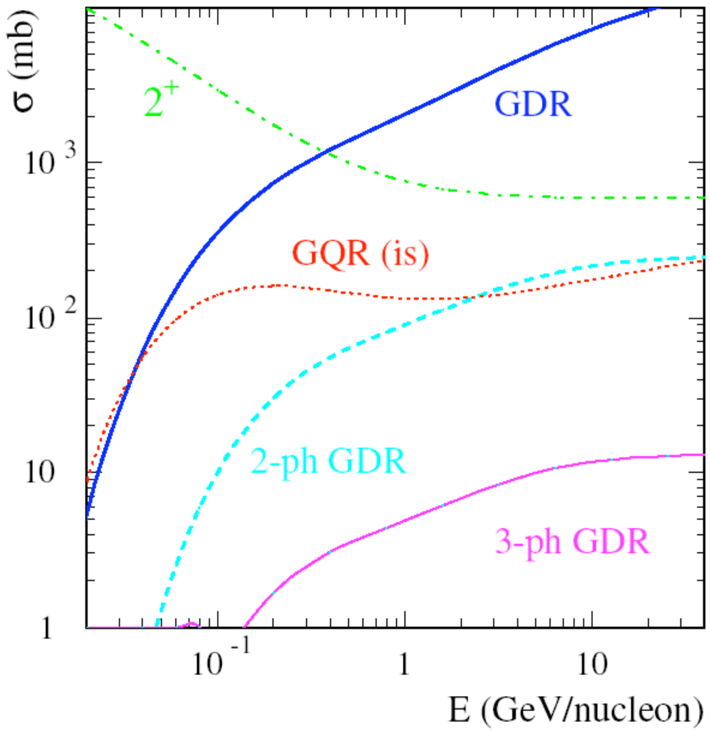

High velocities $v/c \approx 0.6$-0.9

$\Rightarrow$ High-frequency Fourier components

$E_{\gamma,max} \approx 25$ MeV (@ 1 GeV/u)

Determination of 'photon energy' (excitation energy) via a kinematically complete measurement of the momenta of all outgoing particles (invariant mass)

Experimental Approach: Production of (fission-)fragment beams

- Primary: $3 \cdot 10^{8}$ ^{238}U/spill @550MeV/u
- Secondary (mixed): 50 ions ^{132}Sn/spill (~10/sec @500 MeV/u)

$$\frac{A}{Z} = \frac{e}{m_u c}\frac{B\rho}{\beta\gamma}$$

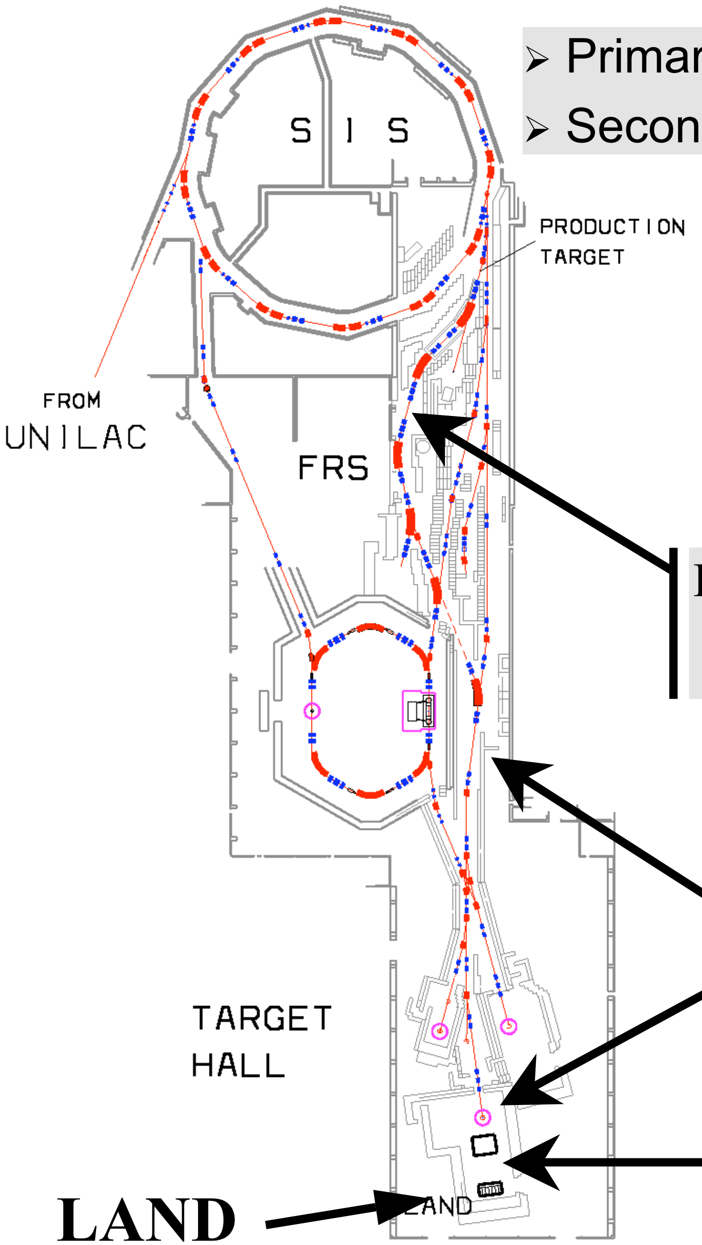

Bρ – from position at middle focal plane of the FRS

β – from TOF

Z – from ΔE

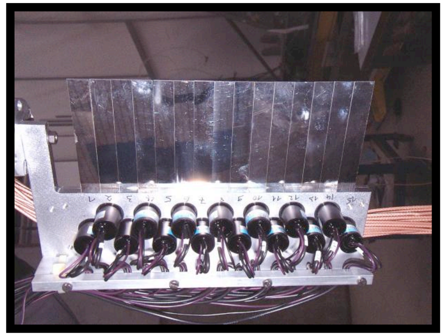

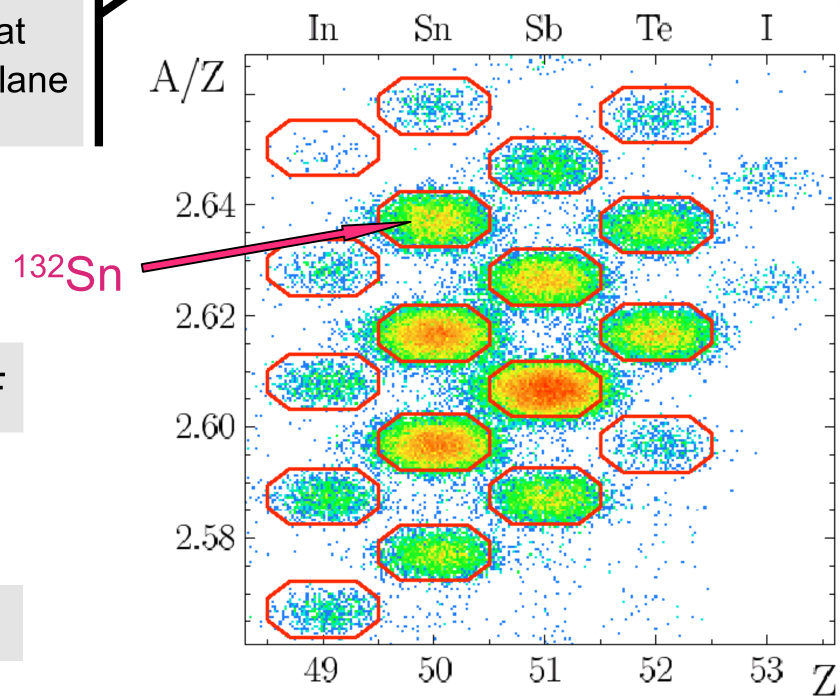

Experimental Scheme: The LAND reaction setup @GSI

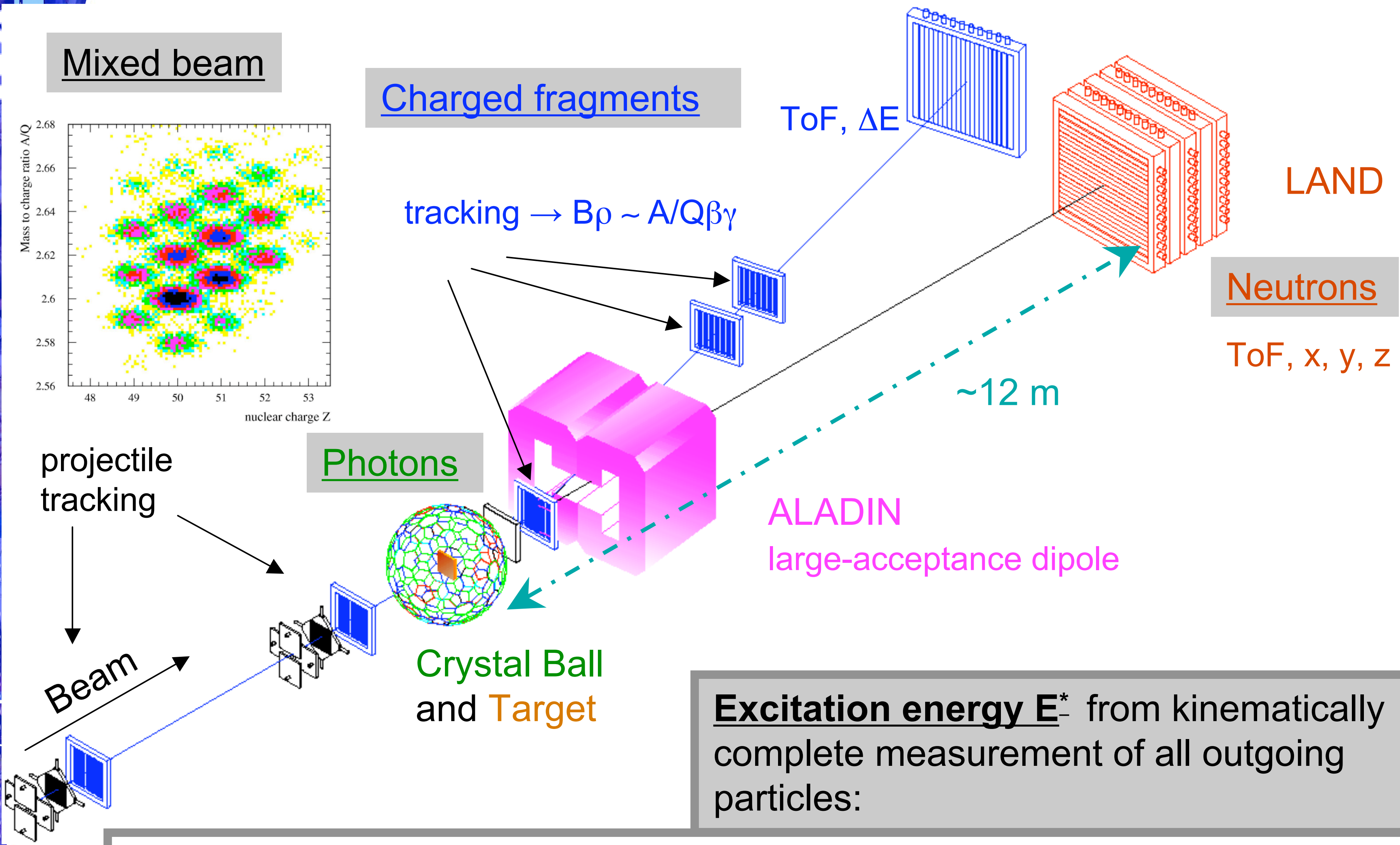

Excitation energy E* from kinematically complete measurement of all outgoing particles:

$$E^* = \left(\sqrt{\sum_i m_i^2 + \sum_{i\neq j} m_i m_j \gamma_i \gamma_j (1-\beta_i\beta_j\cos\theta_{ij})} - m_{proj}\right)c^2 + E_\gamma$$

Dipole-strength distributions in neutron-rich Sn isotopes

Electromagnetic-excitation cross section

Photo-neutron cross section

Comparison with theoretical predictions

RMF (N. Paar et al.)

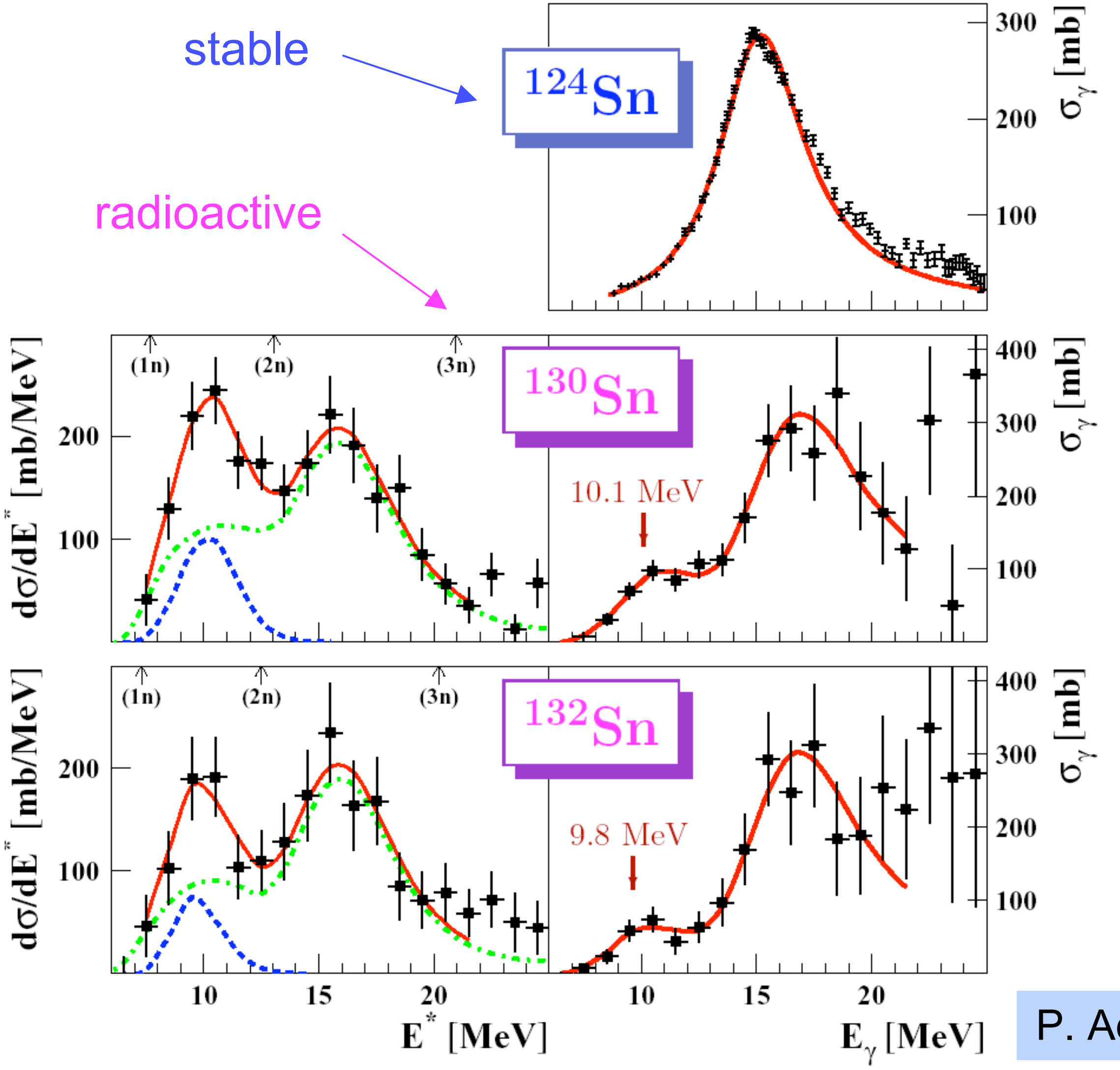

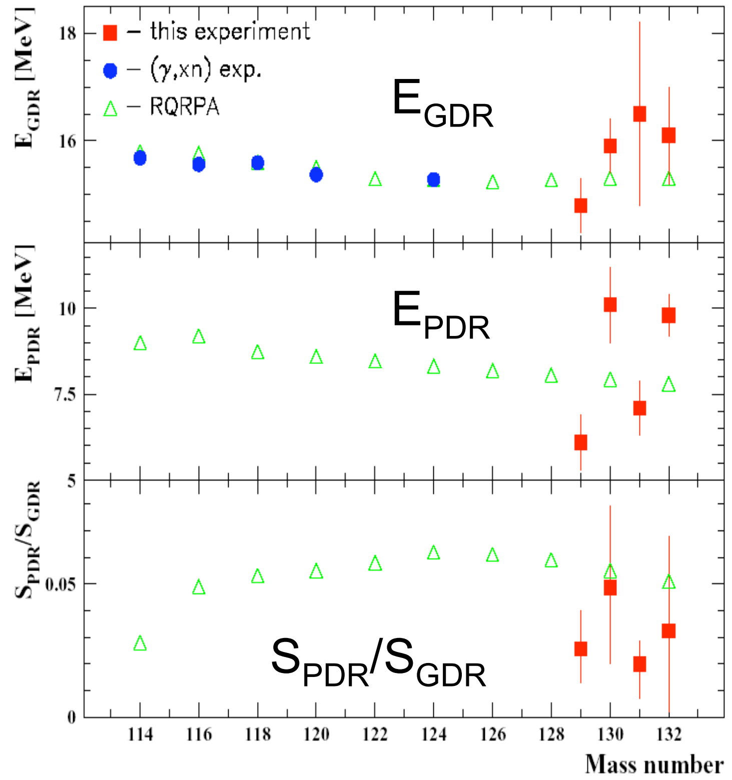

P. Adrich et al., PRL 95 (2005) 132501

P. Roussel-Chomaz

Part 5

Detection systems and selected examples of experiments

c) And the contrary:

Giant resonances via missing mass method

Transfer via invariant mass method

ISGMR : experimental probe

Inelastic scattering (d,d') (α,α') @ E ≥ 25 A.MeV

^{58}Ni (α,α') E_α=240 MeV

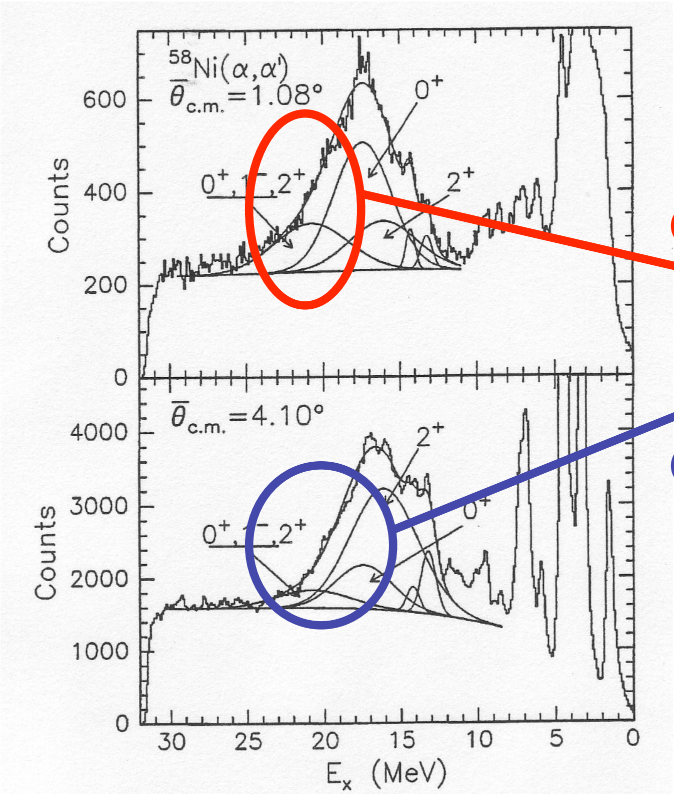

GMR

GQR

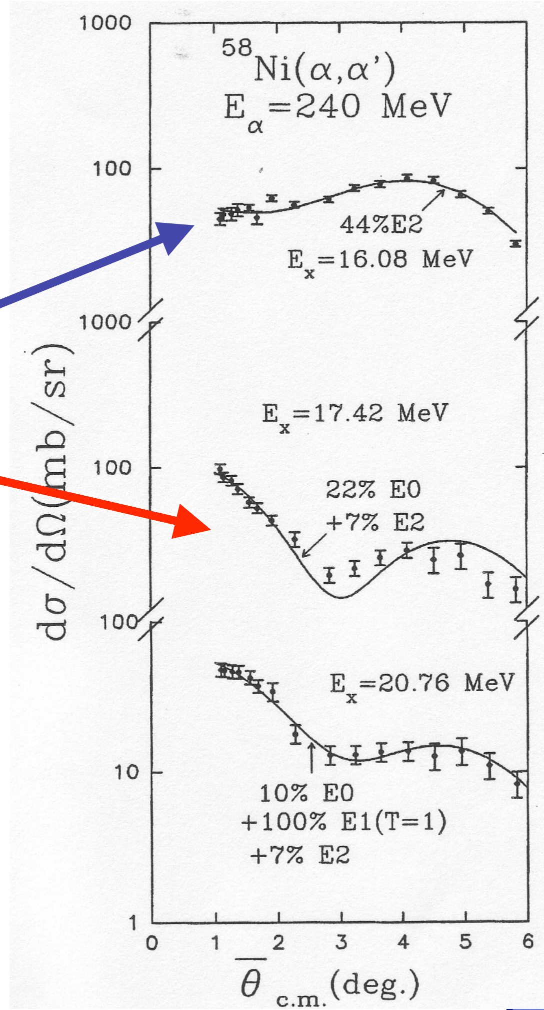

GR in ^{58}Ni :
analysis
mixing 0^+ and 2^+

D.H. Younblood *et al*, Phys. Rev. Lett **76**, 1429 (1996)

ISGMR in unstable nuclei …

unstable nuclei → reverse kinematics → low energy threshold; thin target; large solid angular coverage

unstable nuclei → low intensity beam → good detection efficiency; thick target

^{58}Ni (α,α') $E_α$=240 MeV

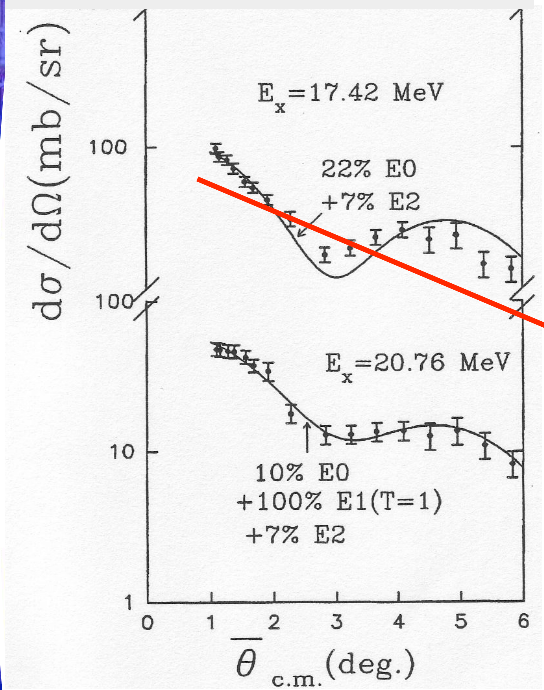

0° ≤ $θ_{CM}$ ≤ 5°

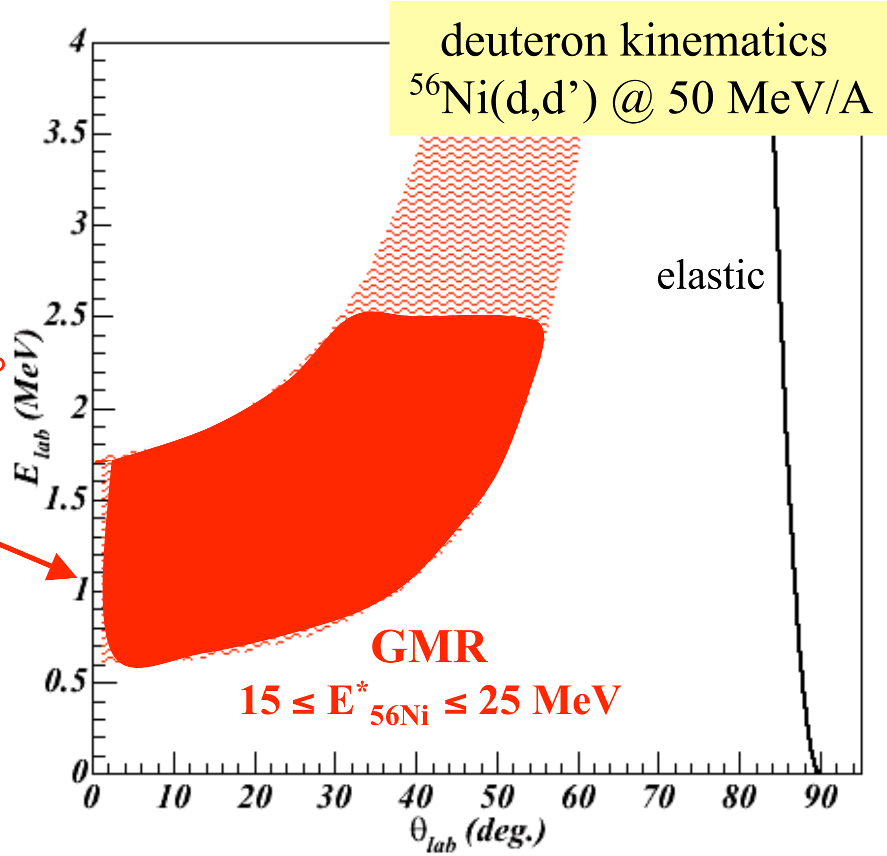

P. Roussel-Chomaz

Experimental setup

^{56}Ni @ 50 MeV/A
5.10^{4} pps

- July 2005, GANIL
- SISSI beam

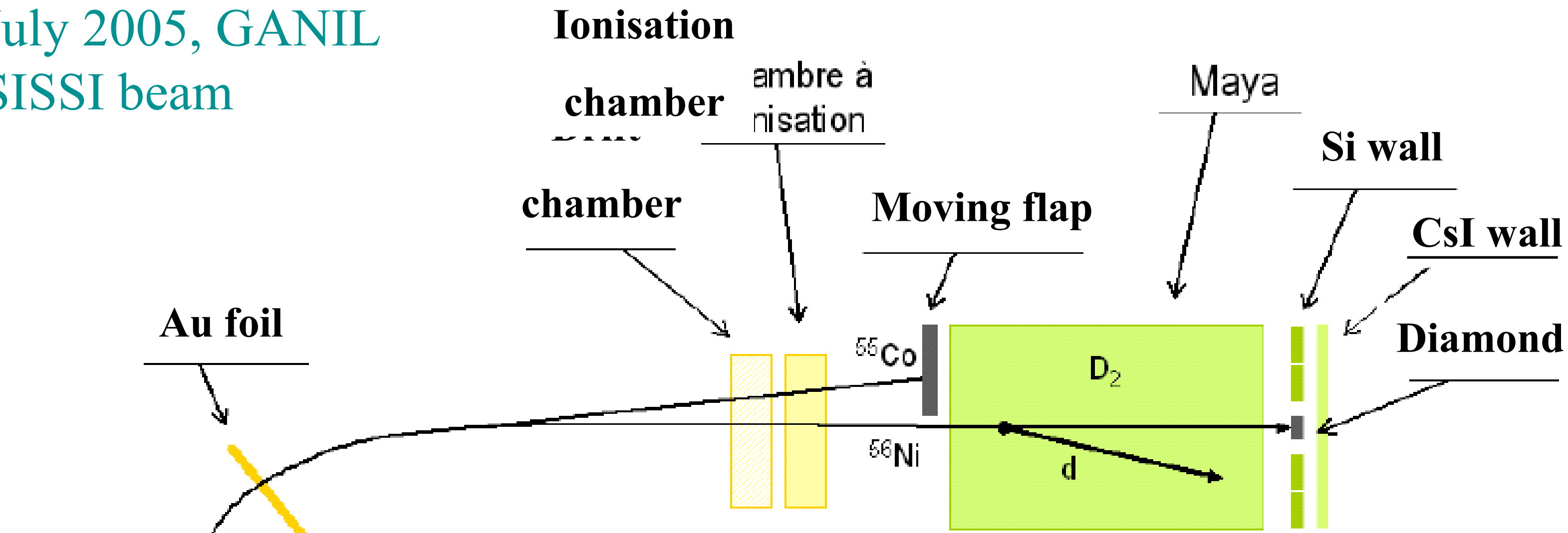

MAYA

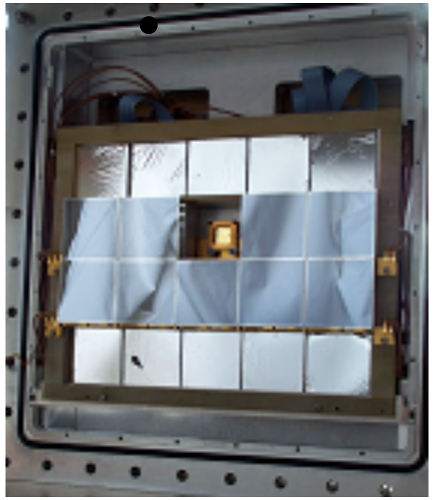

E. Khan et al IPNO
Thesis Ch. Monrozeau

Analysis with gaussian fit

Ch. Monrozeau

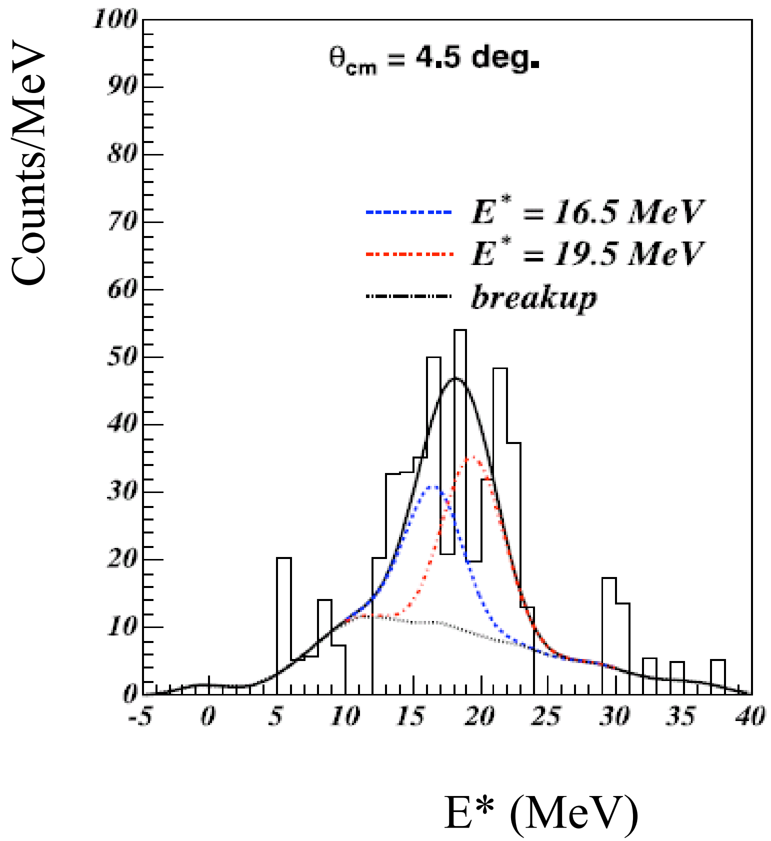

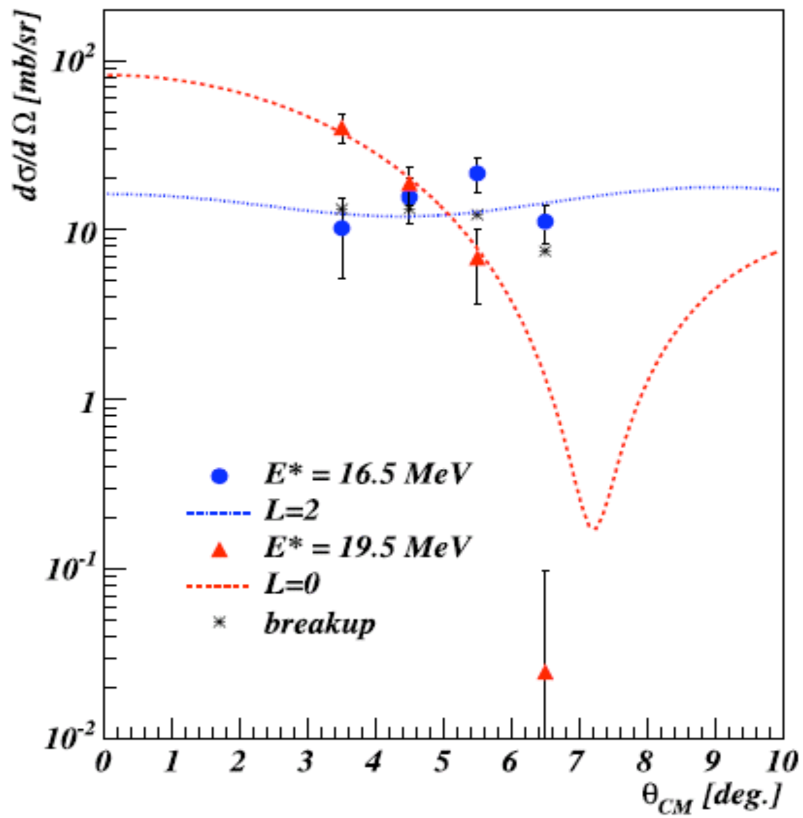

Reaction : DWBA with double folding using HF and RPA ^{56}Ni gs and transition densities

Multipole Decomposition Analysis

Ch. Monrozeau

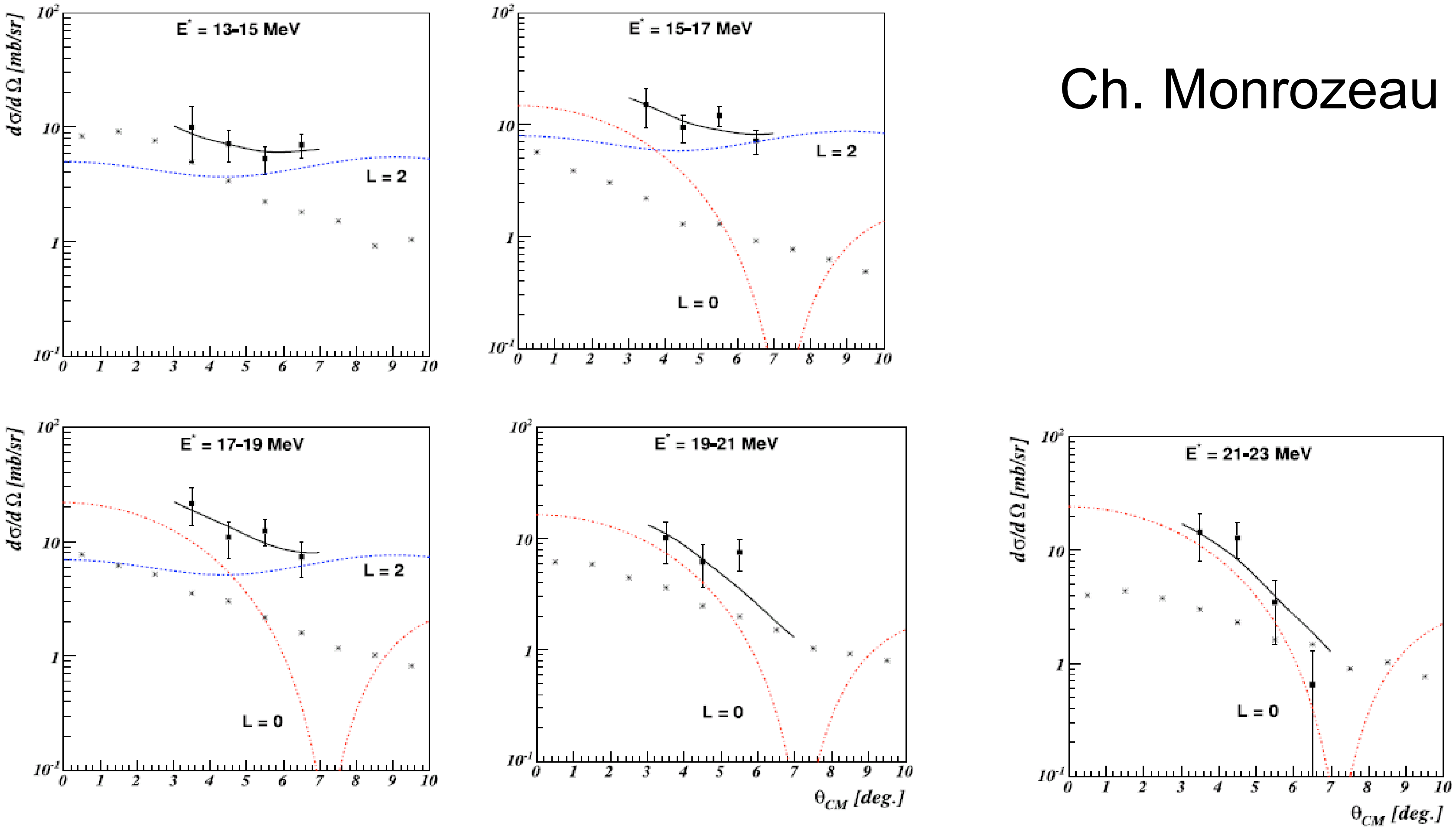

MDA	m_1/m_0 [MeV]	rms [MeV]	% EWSR
L=0	19.3	2.3	136 ± 27
L=2	16.2	1.7	76 ± 13

Summary & outlooks

- Isoscalar GMR and GQR measured in the ^{56}Ni unstable nucleus
- Use of MAYA active target with d gas
- 16h of 10^4 pps beam
- Results compatible with the ^{58}Ni (stable) data
- The method works !

•Improvements : identification & d breakup, reaction model

• Next : neutron rich Ni isotopes, ^{132}Sn
ACTAR active target

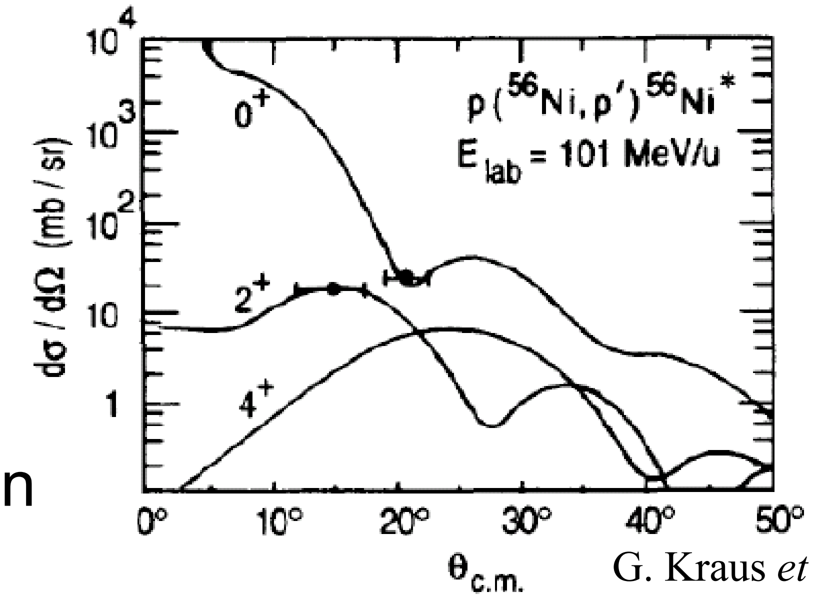

first (p,p') experiment in inverse kinematics !

G. Kraus *et al.* Phys Rev. Lett. **73** (1994) 1773

From E. Khan DREB 2007

$^{22}O(d,p)^{23}O$

RIKEN RIPS 34AMeV ^{22}O 600pps
CD_2 target 30mg/cm^2
Si telescope 96cm down the target: identification of scattered particles, x and y
156 CsI(Tl) array: Backward emitted protons
80 NaI(Tl) scintillators: γ rays
Neutron wall: neutrons from decaying ^{23}O above threshold

$$E^* = \left(\sqrt{\sum_i m_i^2 + \sum_{i\neq j} m_i m_j \gamma_i \gamma_j (1-\beta_i\beta_j\cos\theta_{ij})} - m_{proj}\right)c^2 + E_\gamma$$

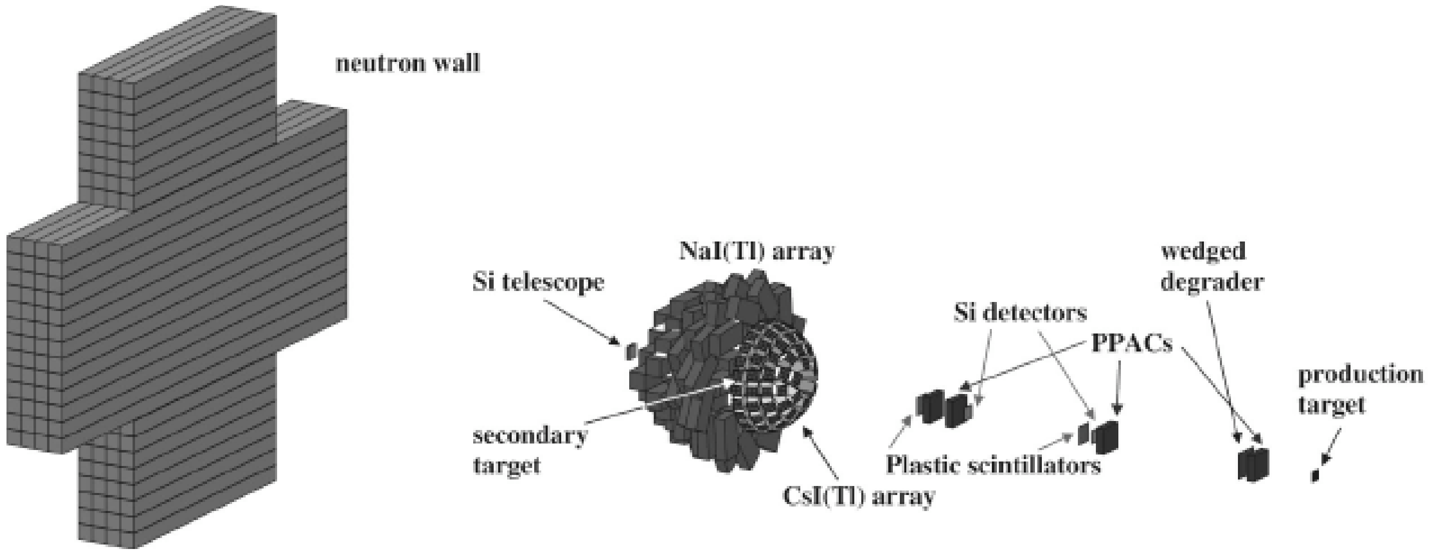

Z. Elekes et al. PRL98 (2007) 102502

$^{22}O(d,p)^{23}O$

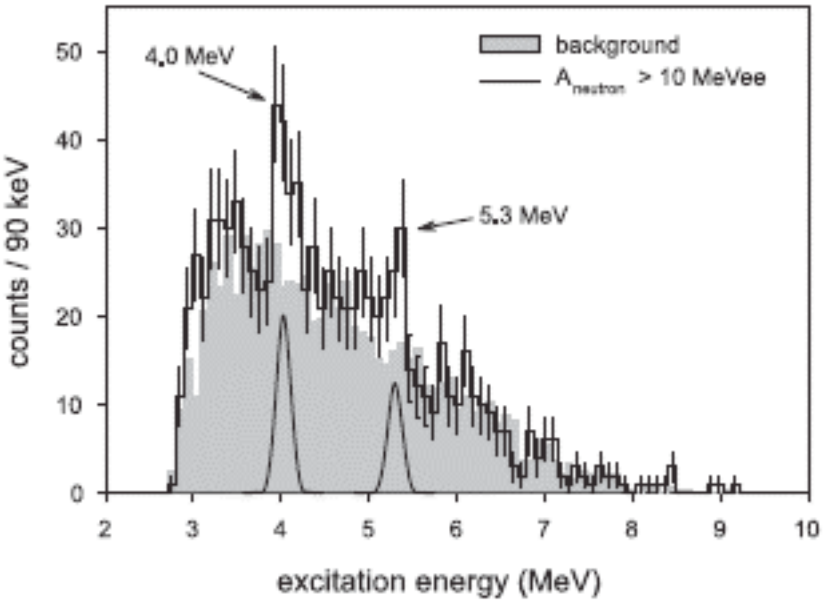

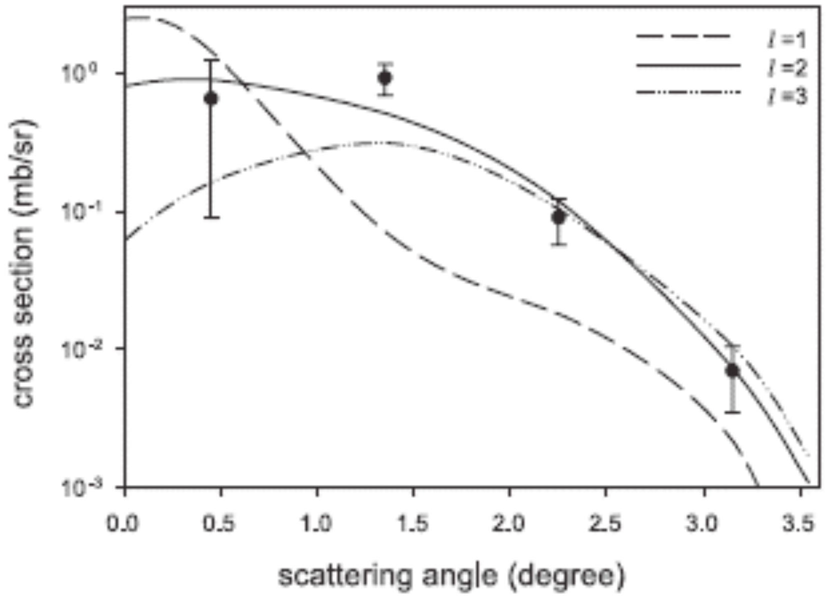

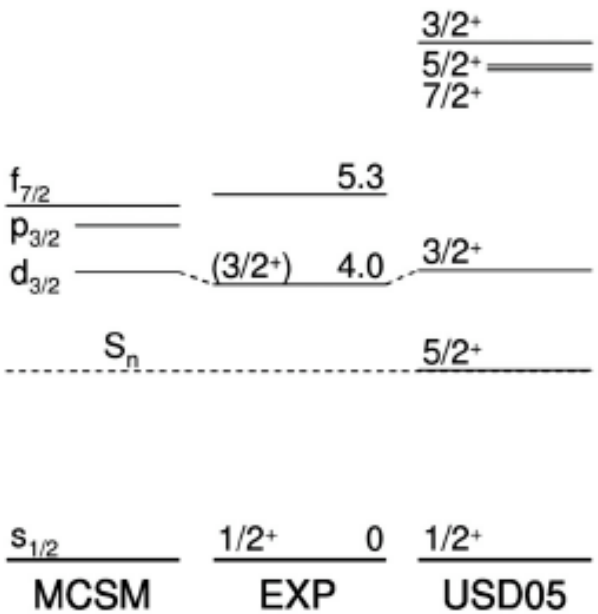

Confirmation of N=16 shell closure (gap=4 MeV)

Second excited state not present in USD shell model: fp shell

N=20 shell gap ≈ 1.3 MeV in good agreement with MCSM

Disappearance of N=20 at Z=8

End of second lecture

Part 5 (continued)

Detection systems and selected examples of experiments

d) Magnetic spectrometers

- *i) angular distributions*
- *ii)momentum distributions*

e) Magnetic spectrometers in coincidence with γ-detection

- *i) momentum distributions*
- *ii) in beam γ spectroscopy*
- *iii) direct reactions: inelastic scattering, transfers*
- *iv) deep inelastic*

Part 6

Future facilities

P. Roussel-Chomaz

Part 5

Detection systems and selected examples of experiments

d) Magnetic spectrometers

Some notions on magnetic optics

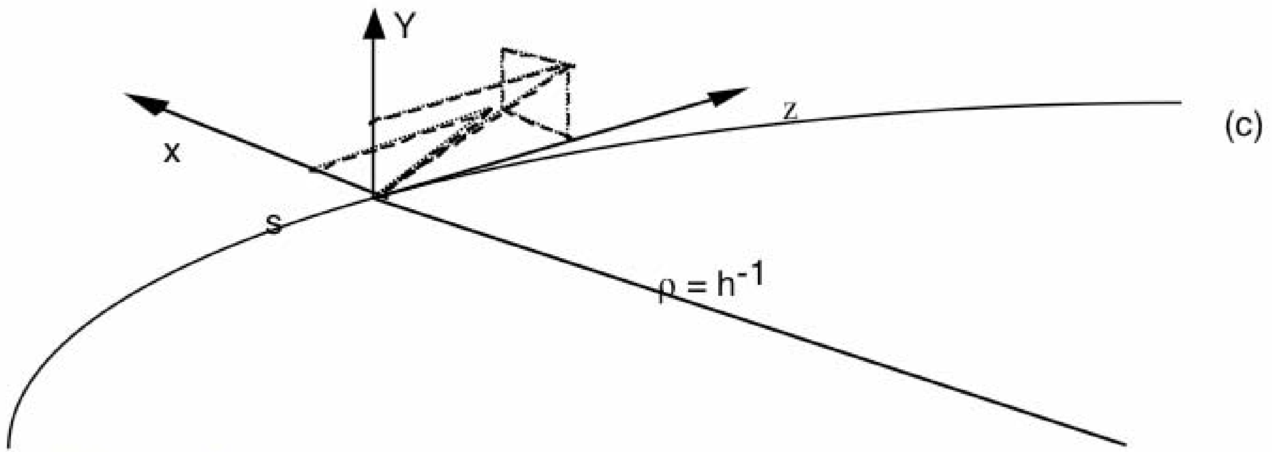

particle coordinates

x distance in the horizontal plan of the z axis

θ angle in the plane x, z

y distance in the vertical plane of the z axis

φ angle in the plane y, z

l difference of length of the trajectory considered and the central trajectoire

δ difference of momentum of the particle with respect to the reference particle $\delta = (p - p_0)/p_0$.

formalism of particle transport to 1st order

example

$$x_f = f_x(x_i, \theta_i, y_i, \varphi_i, l_i, \delta_i)$$

with i=initial, f=final

Taylor expansion, for example for x, θ to 1st order

$$x_f = \frac{\partial f_x}{\partial x} x_i + \frac{\partial f_x}{\partial \theta} \theta_i + \frac{\partial f_x}{\partial y} y_i + \frac{\partial f_x}{\partial \varphi} \varphi_i + \frac{\partial f_x}{\partial l} l_i + \frac{\partial f_x}{\partial \delta} \delta$$

$$\theta_f = \frac{\partial f_\theta}{\partial x} x_i + \frac{\partial f_\theta}{\partial \theta} \theta_i + \ldots$$

In matrix formalism, this is :

$$\begin{pmatrix} x_f \\ \theta_f \\ y_f \\ \varphi_f \\ l_f \\ \delta_f \end{pmatrix} = \begin{pmatrix} R_{11} & R_{12} & R_{13} & R_{14} & R_{15} & R_{16} \\ R_{21} & R_{22} & . & & & \\ & & \vdots & & & \\ & & \vdots & & & \\ R_{61} & & & & & R_{66} \end{pmatrix} \begin{pmatrix} x_i \\ \theta_i \\ y_i \\ \varphi_i \\ l_i \\ \delta_i \end{pmatrix}$$

R_{16}=0 système non dispersif
R_{16}=R_{26}=0 système achromatique
⟹ R52=0 isochronisme
R_{12}=0 focalisation point-point
R_{22}=0 foc. point parallèle

Use of this matrix formalism:

$$\vec{x}_1 = R_1 \vec{x}_0$$

$$\vec{x}_2 = R_2 \vec{x}_1 = R_2 R_1 \vec{x}_0$$

The final result is formally described as a product of matrices, representing the different elements of the optical system

See Ecole Joliot Curie 1994:
« Physique Nucléaire expérimentale: des éléments pour un bon choix »
Cours W. Mittig

Standard detection system for a spectrometer

At the focal plane of a spectrometer, we need to:
-identify the particles
-reconstruct their trajectory to determine their momentum and (eventually) their angle of emission

For that purposes, the focal plane of a spectrometer is usually equiped with gas detectors (drift chambers) to measure the position of the particles, and a set of detectors to obtain ΔE-E or TOF-E identification: ionisation chamber, Si detector array, plastic scintillator, secondary emission detectors.

Spectrometer description

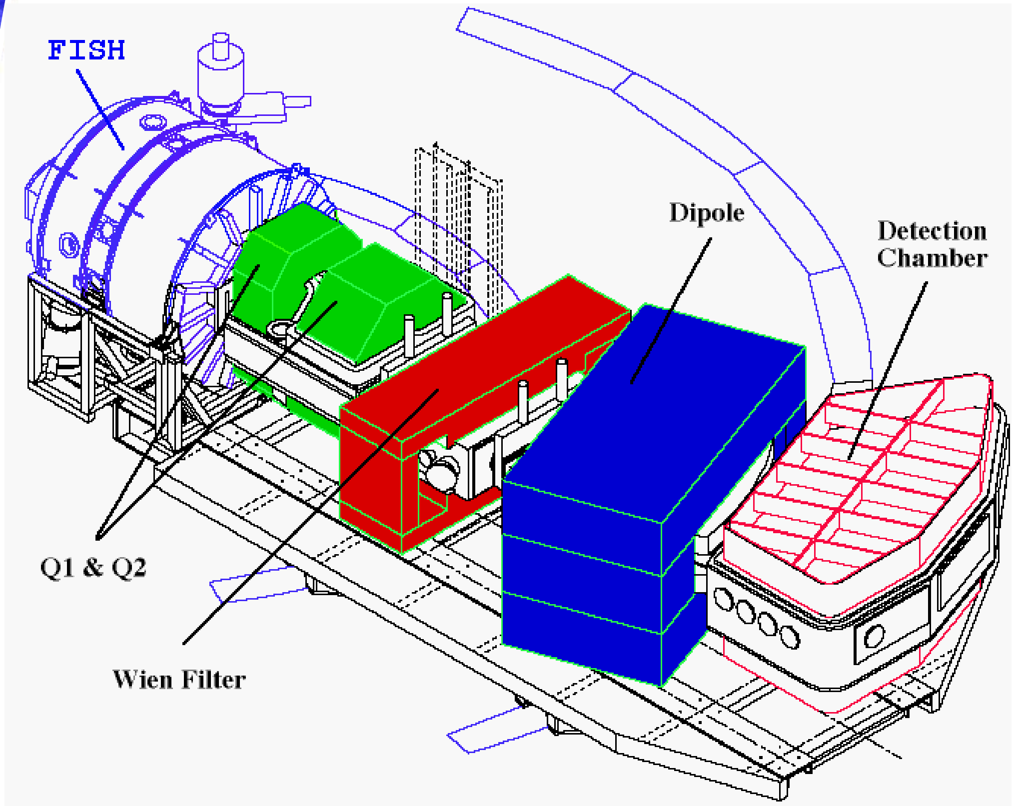

VAMOS
VARIABLE MODE SPECTROMETER

- A doublet of quadrupoles
  - wide aperture gap for large acceptance
- A Wien filter
  - velocity selection
- A variable angle dipole
  - dispersion
- A focal plane detection
- A variable distance between the target and the first lens
  - d = 40 cm   Bρ = 1.6 T.m
  - d = 1m   Bρ = 2.3 T.m
- Acceptance
  - ± 6% in momentum

P. Roussel-Chomaz

Focal Plane Setup

beam

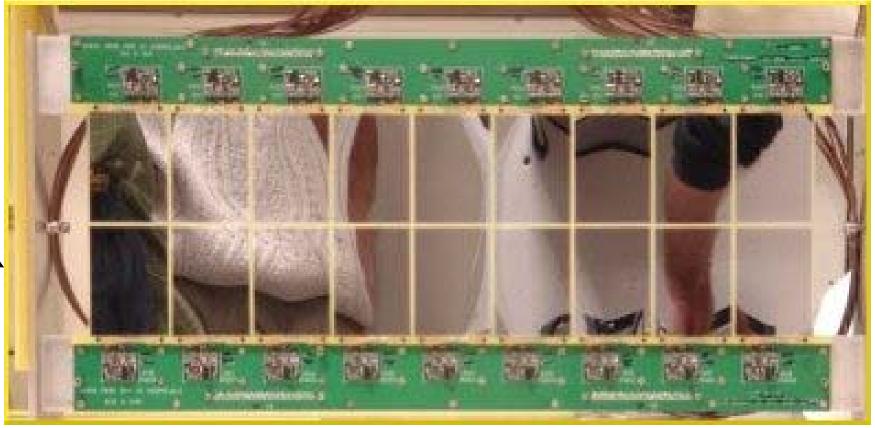

Si Wall

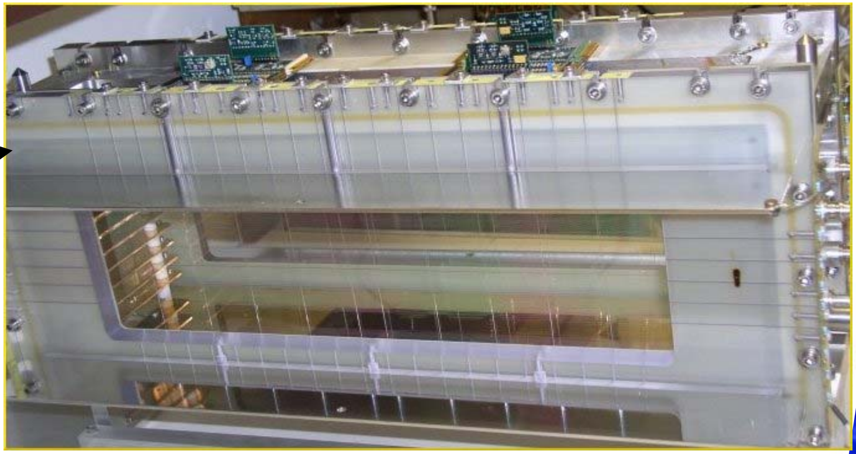

Drift Chamber

Position measurement

C_4H_{10}

P ≈ 20 mb

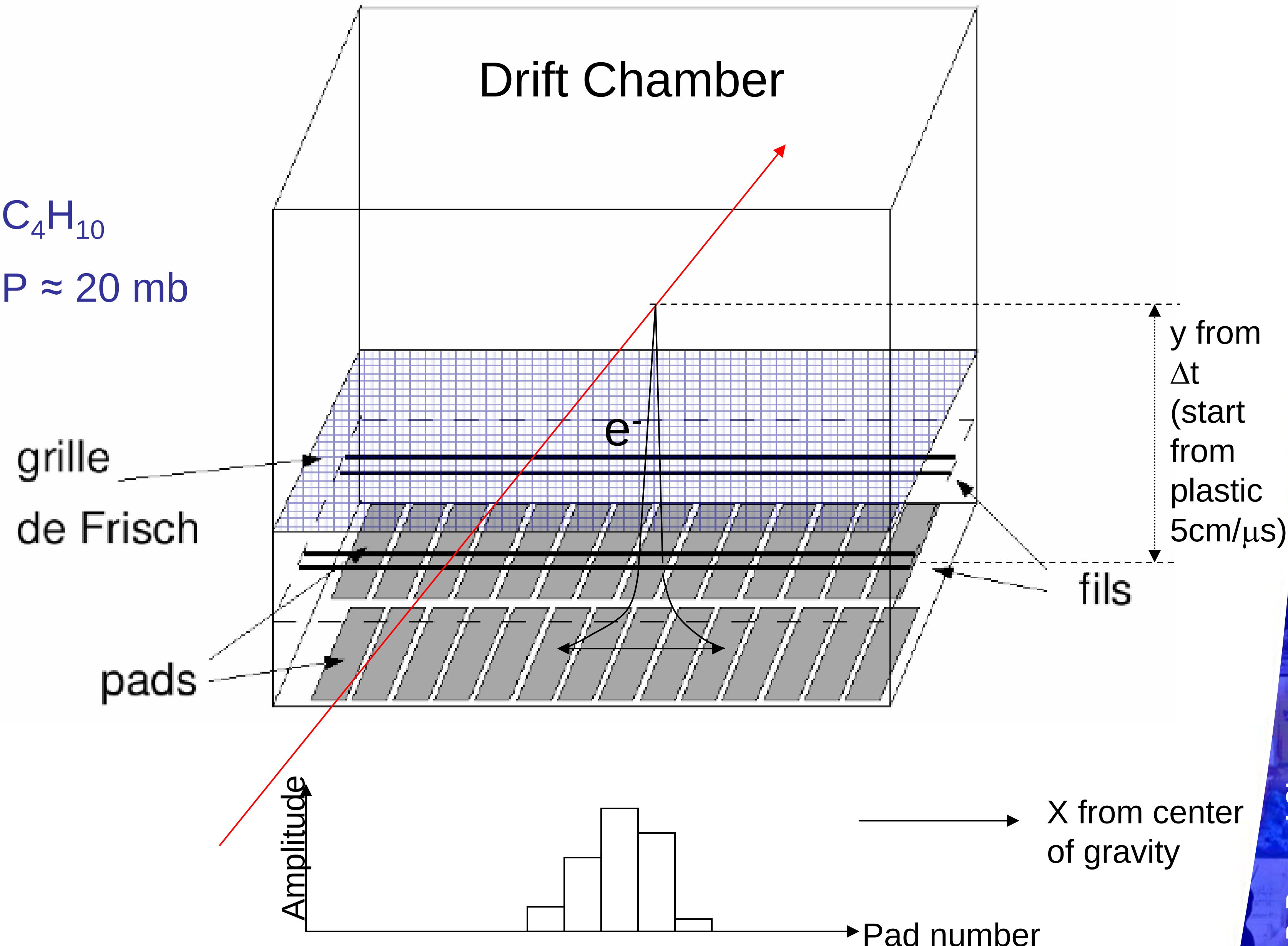

Heavy/Slow Ion Detection

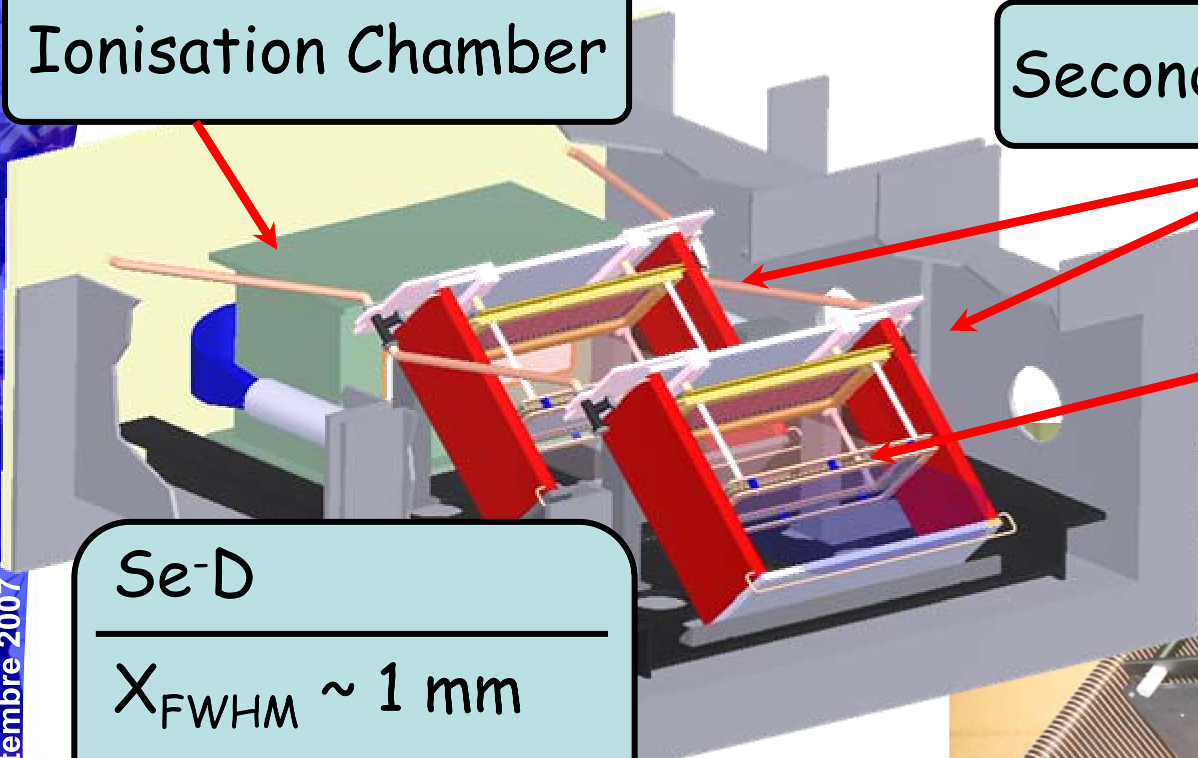

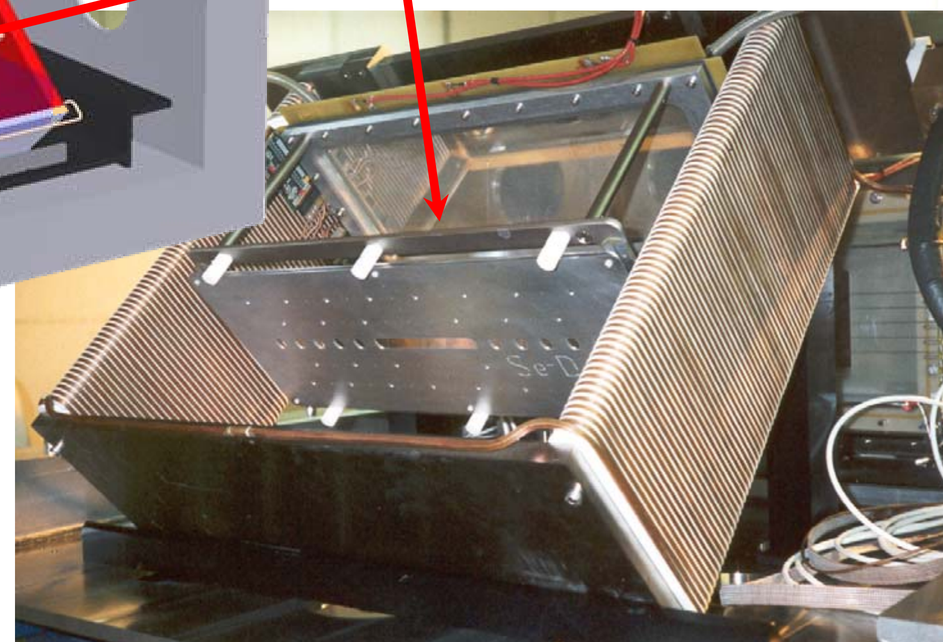

Se-D

X_{FWHM} ~ 1 mm

Y_{FWHM} ~ 2 mm

T_{FWHM} ~ 300 ps

Emittance of object
~100*100πmm mrad

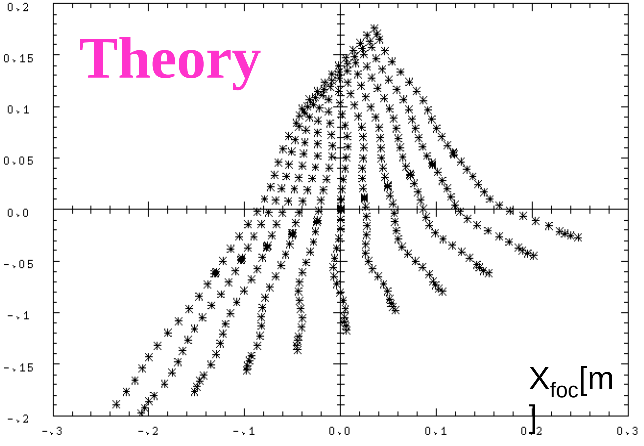

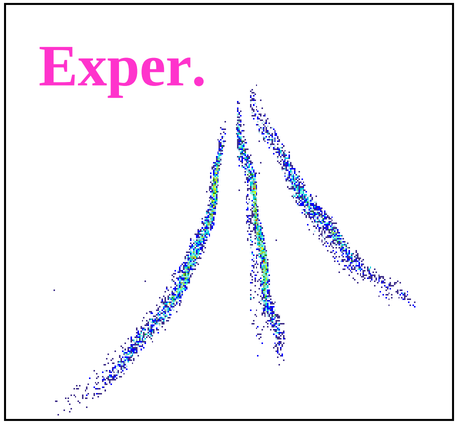

VAMOS
VARIABLE MODE SPECTROMETER

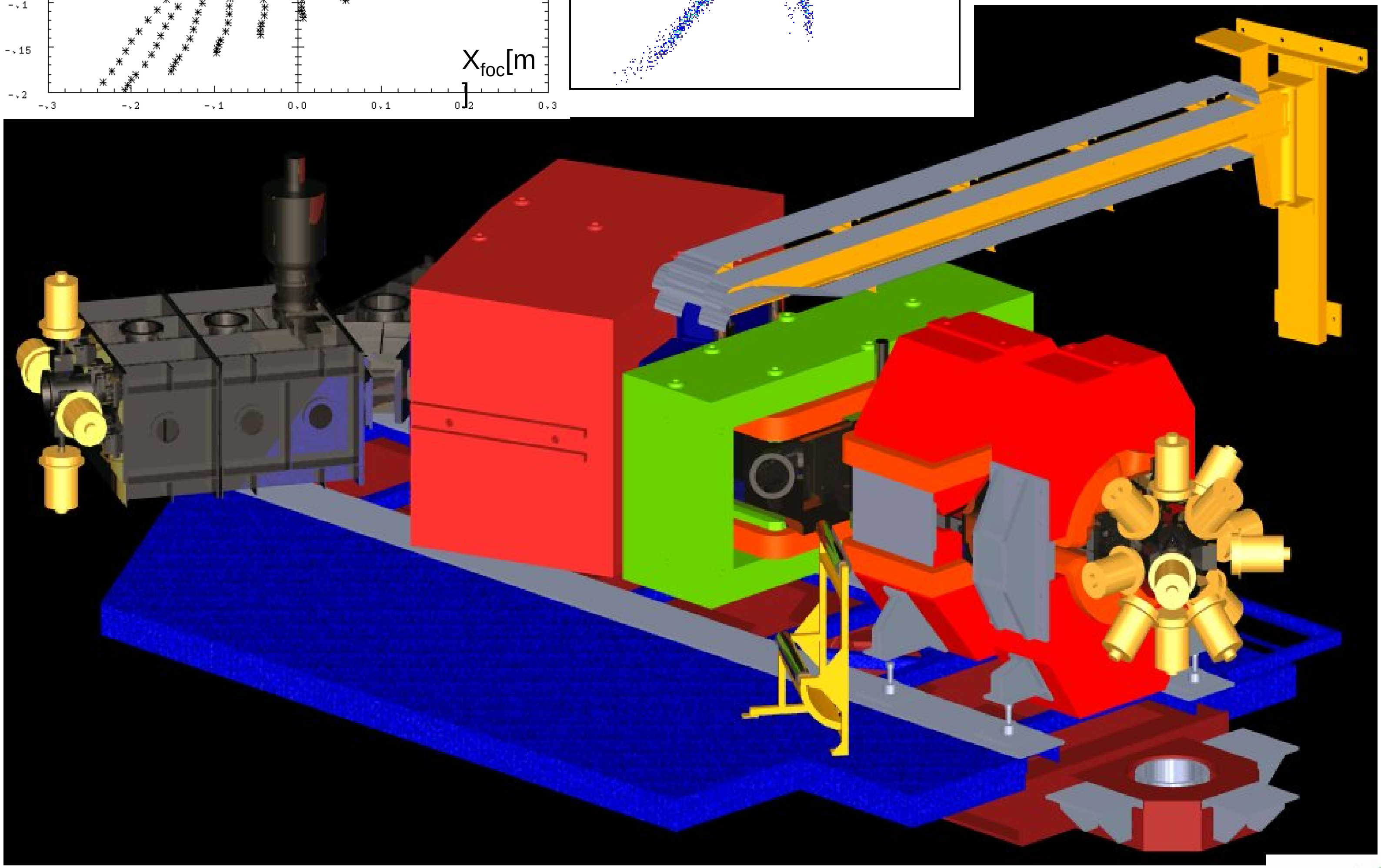

Focal plane of VAMOS

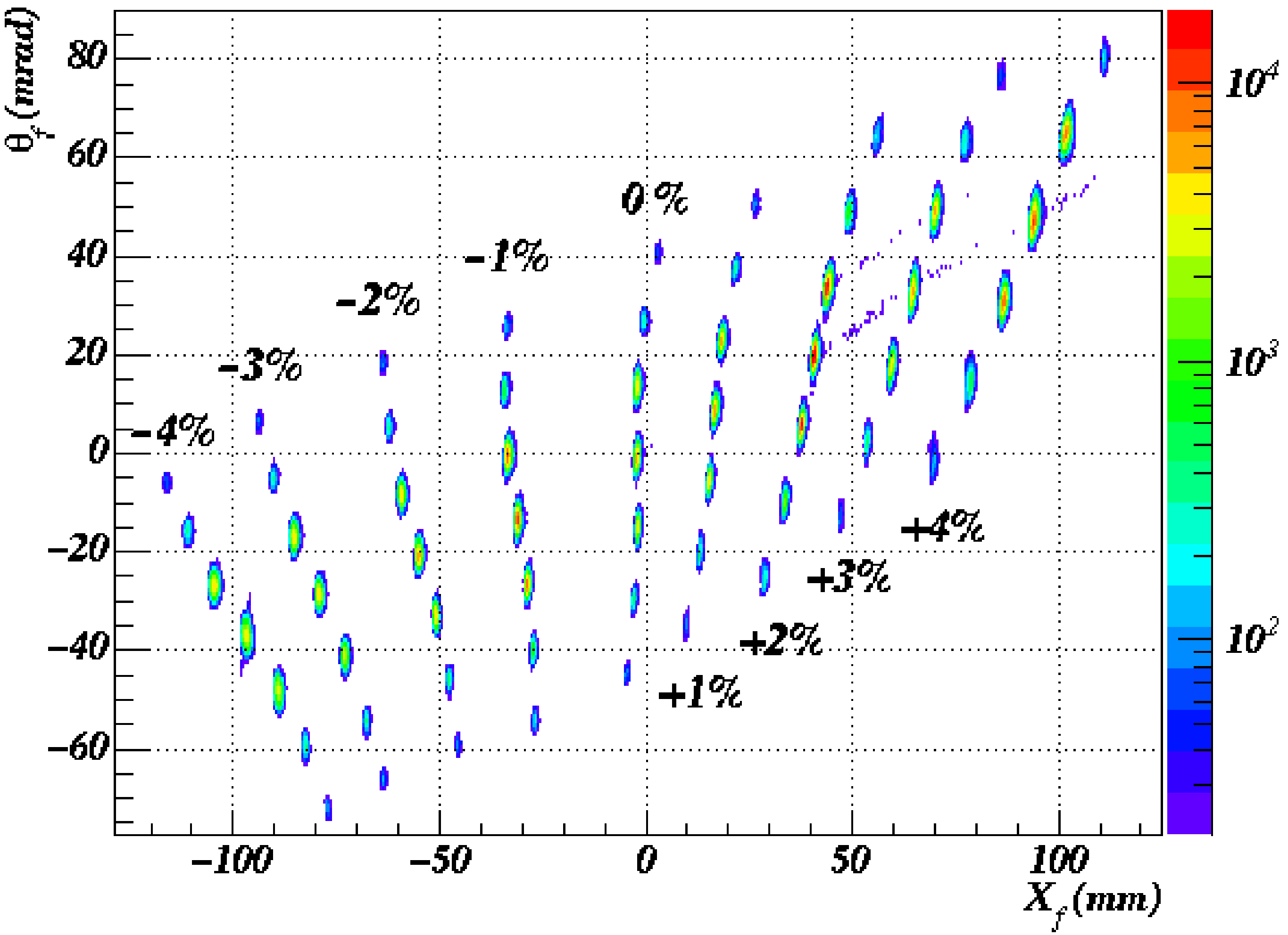

P. Roussel-Chomaz

Angular calibration of VAMOS

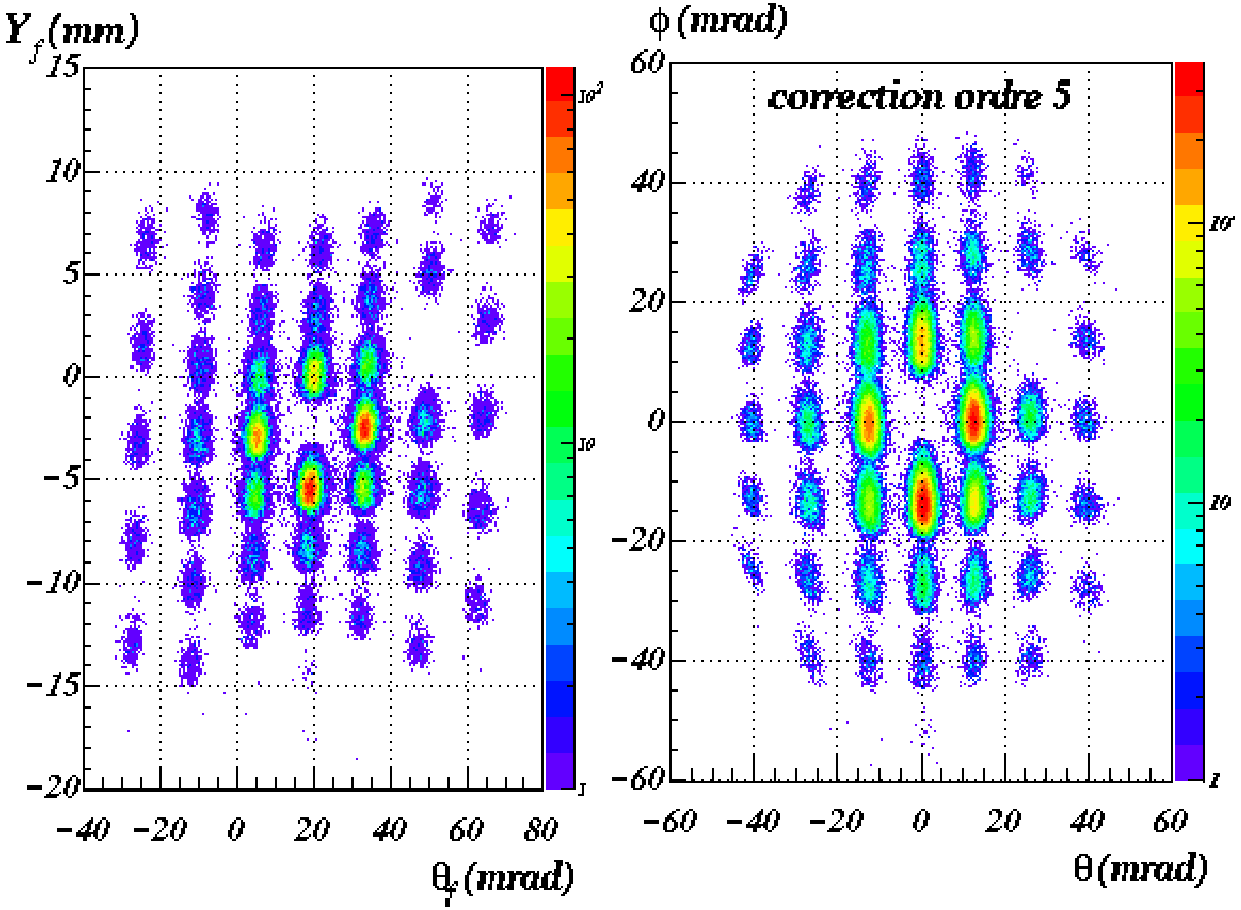

$B\rho = B\rho_0 + 3\%$

Part 5

Detection systems and selected examples of experiments

d) Magnetic spectrometers

i) angular distribution

P. Roussel-Chomaz

Examples: elastic/inelastic sattering, charge exchange reaction

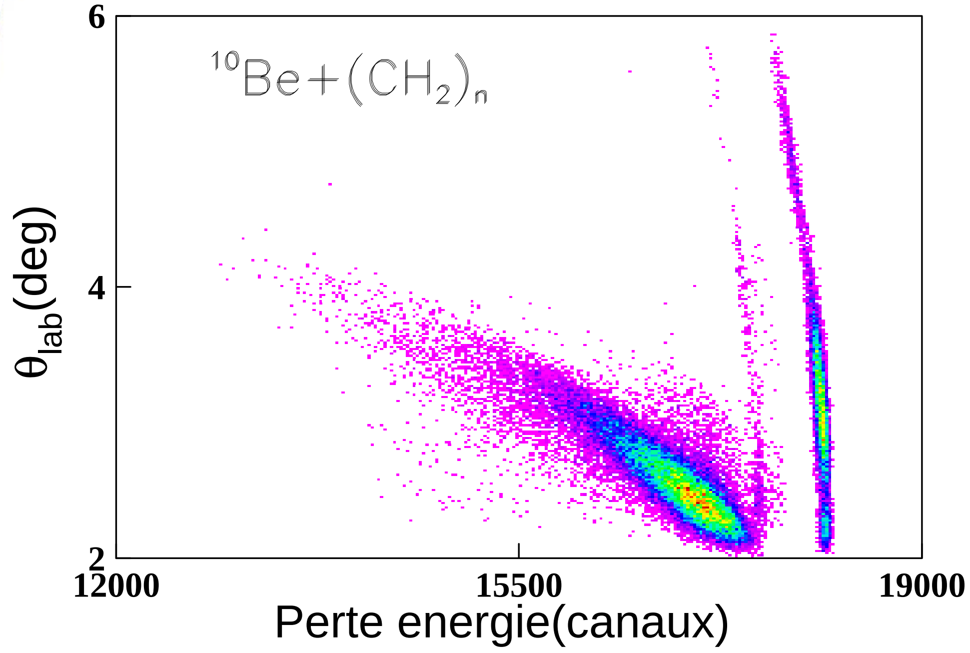

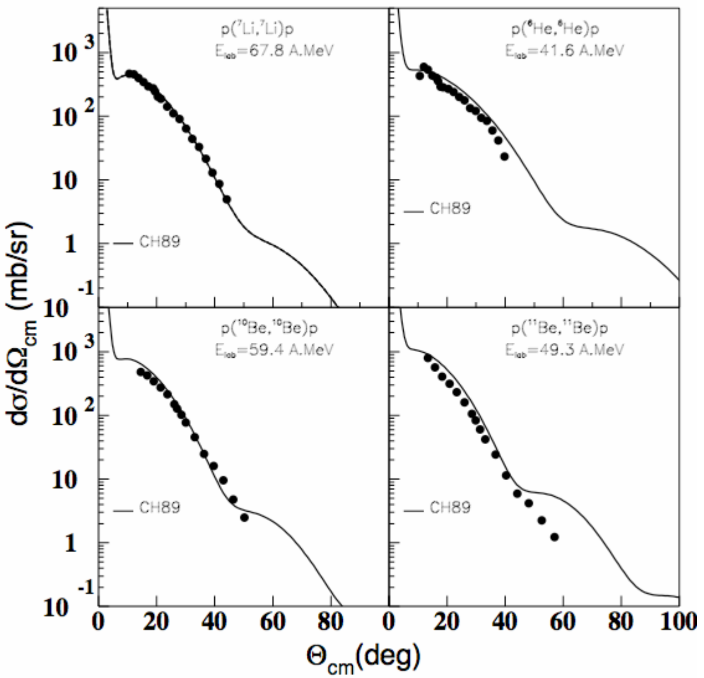

Données:
M.D. Cortina-Gil et al,
Phys. Lett. B401 (97) 9
V. Lapoux et al.,
Phys. Lett. B 517 (01) 18
A. Lagoyannis et al,
Phys. Lett. B 518 (01) 27

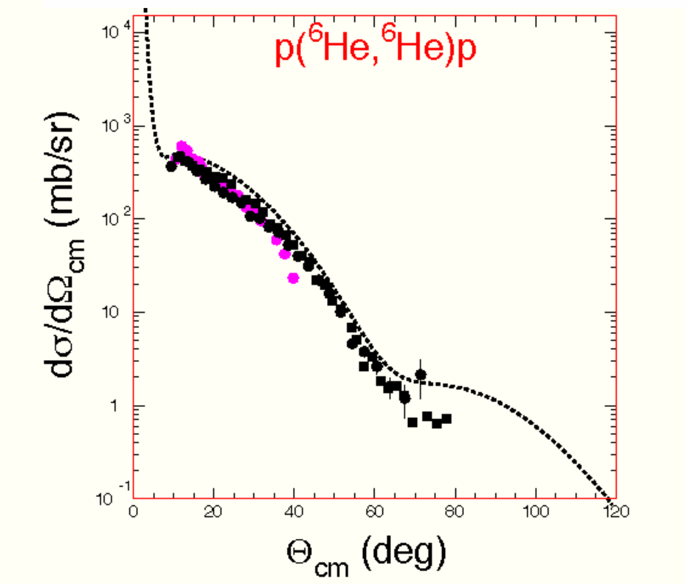

P. Roussel-Chomaz

Réaction d 'échange de charge p(^{6}He,^{6}Li)n

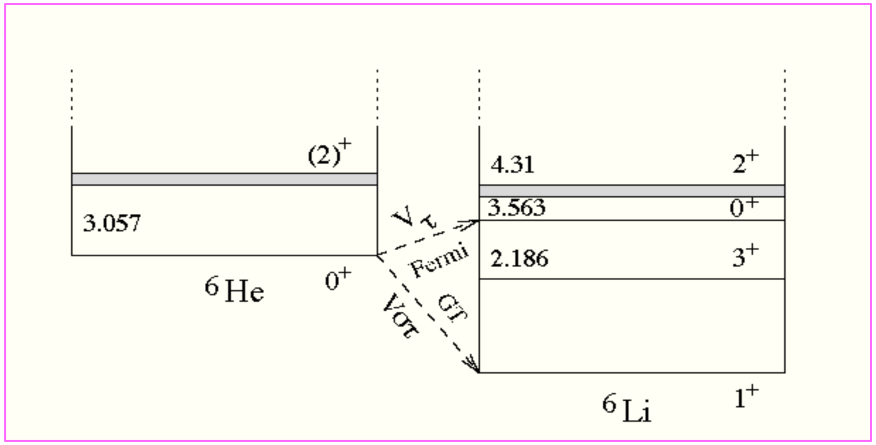

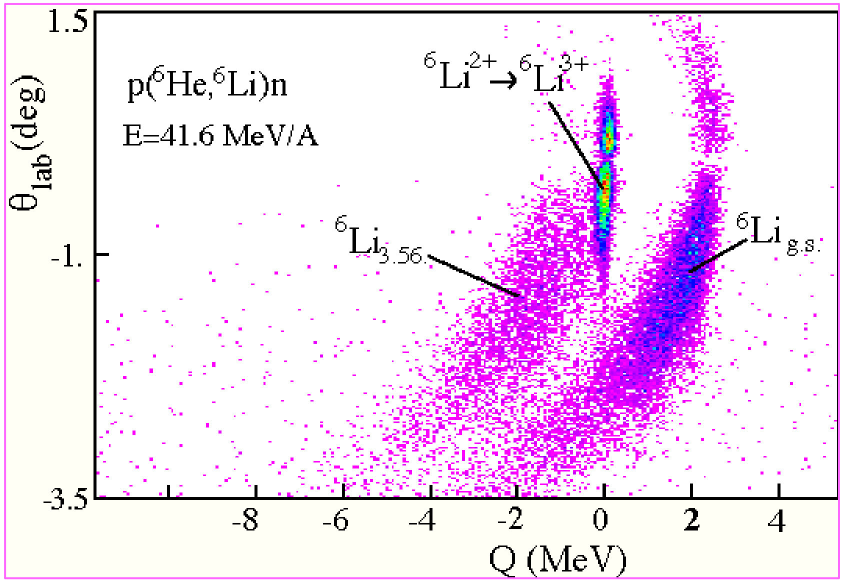

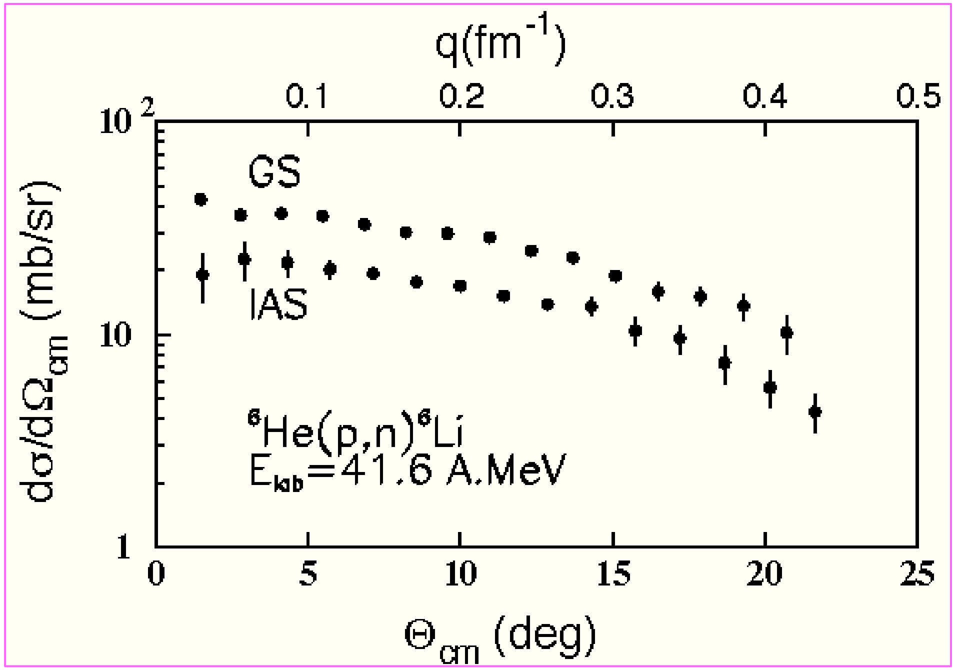

M.D. Cortina-Gil et al., Phys. Lett. B 371 (96) 14
M.D. Cortina-Gil et al., Nucl. Phys. A 641 (98) 263

Angular distributions of the heavy residue

Rather restricted range of possibilities

— angular resolution difficult to achieve for A>10 in reverse kinematics

— not possible for unbound ejectile

— not very efficient beam use: several (many) Bρ values necessary for a complete angular distribution.

Part 5

Detection systems and selected examples of experiments

d) Magnetic spectrometers

ii) momentum distribution

Fragment Momentum Distributions

Neutron in a potential well

Particle in a square well (s state):

For $r>R_0$ the wave function is a Hankel function:

$\varphi(r) \;\alpha\; e^{-\kappa r}/\kappa r$ with

$\kappa^2=2\mu E_s/h^2$

By Fourier transform:

$\phi(\mathbf{p}) = 1/(\Gamma^2/4 + \mathbf{p}^2)^2$

With $\Gamma=2\kappa$

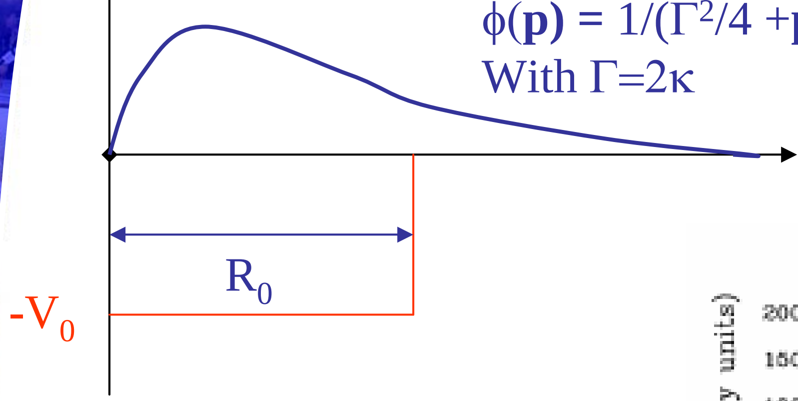

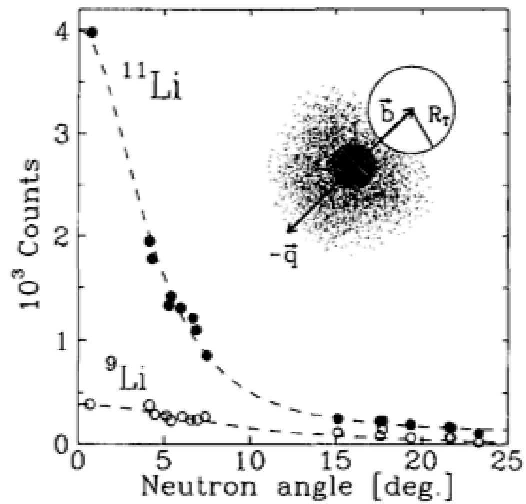

R. Anne et al, Phys. Lett. B250 (1990)

Parallel Momentum distributions :

^{11}Be + X at 63 MeV/A

Fit with $2s_{1/2}$ neutron

with S_n = 500 keV

$\sigma_{//} \approx$ 45 MeV/c

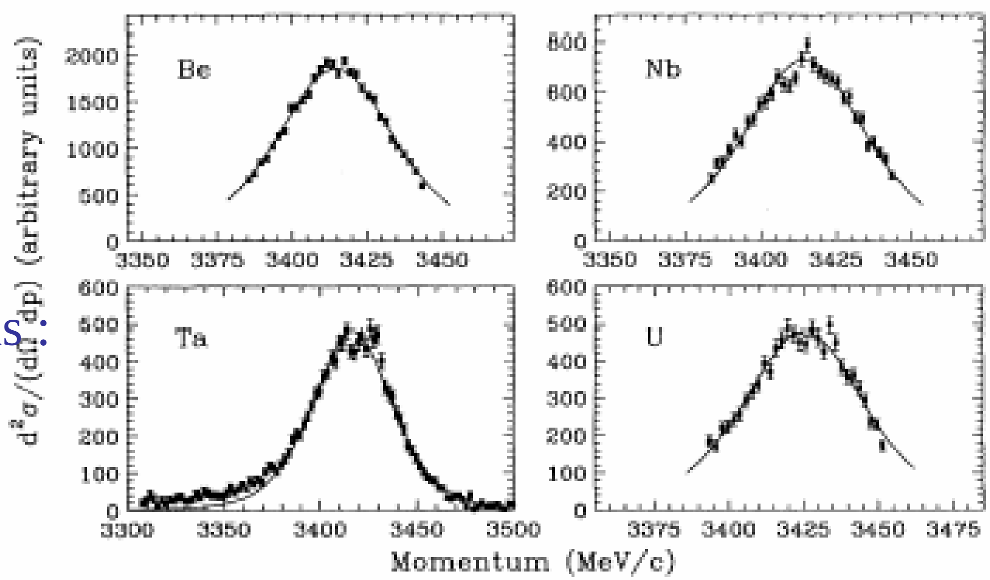

J.H. Kelley et al. PRL 74 (1995) 30

Fragment Momentum Distributions

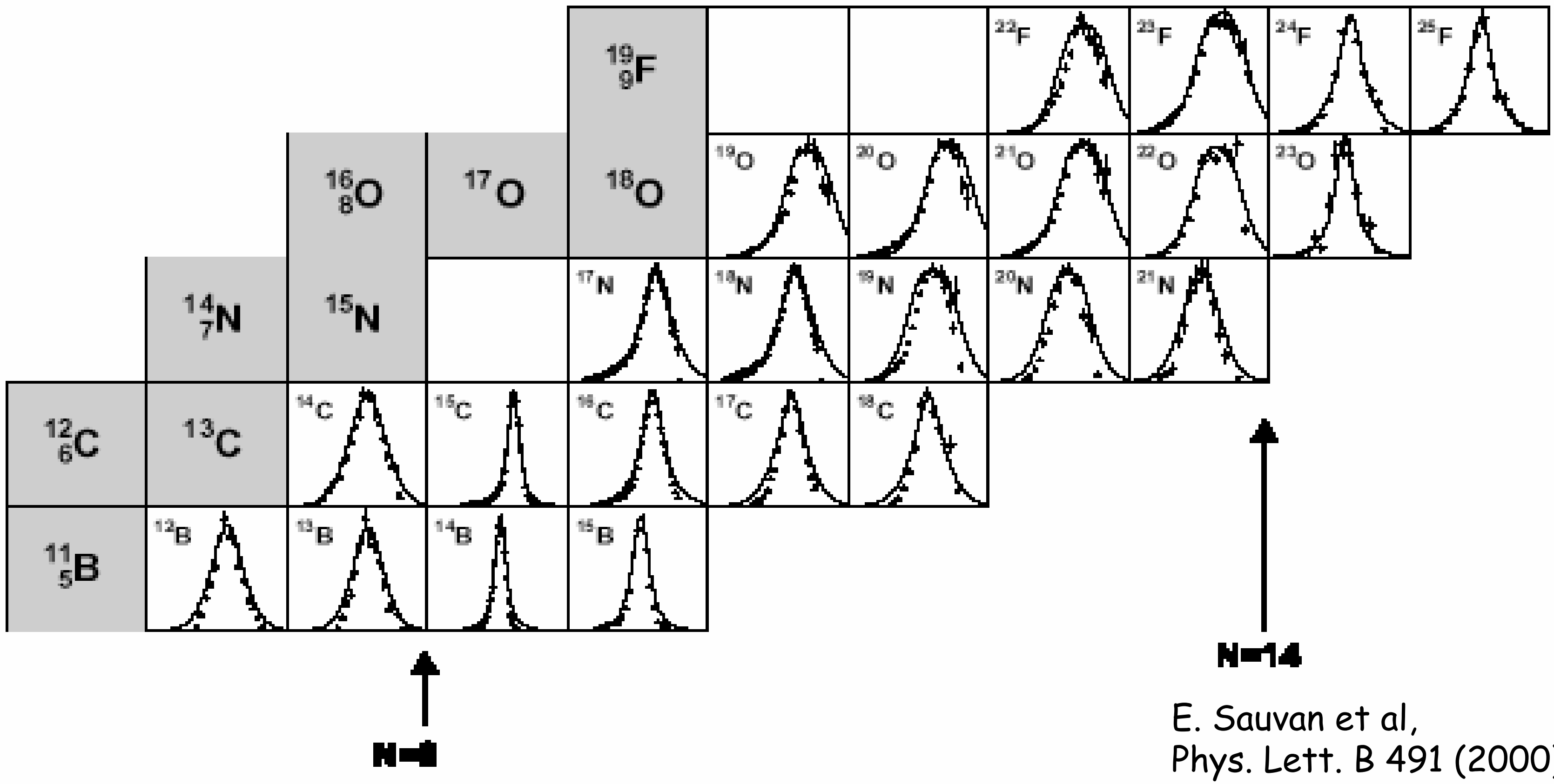

E. Sauvan et al,
Phys. Lett. B 491 (2000)1

Part 5

Detection systems and selected examples of experiments

e) Magnetic spectrometers in coincidence with γ-detection

Some examples of γ-detection arrays

Château de cristal: 74 BaF2

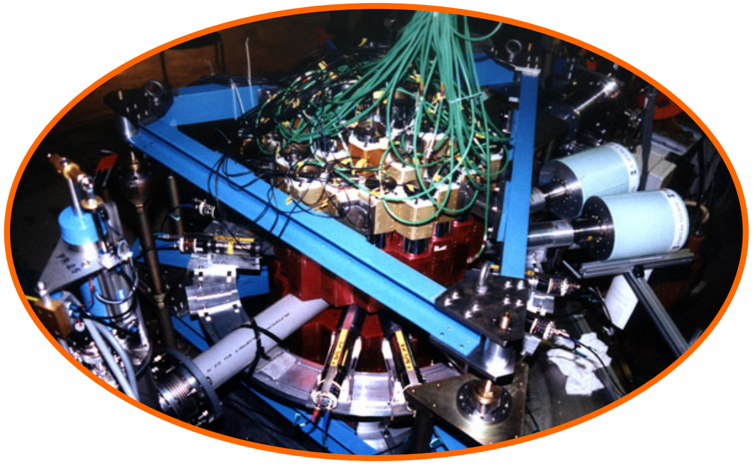

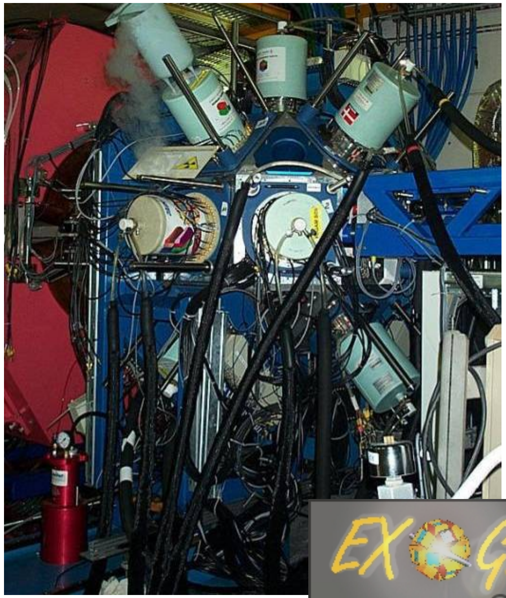

RIKEN:
CNS GRAPE: planar Ge detectors (18) with PSA analysis
DALI2: 160 NaI(Tl) detectors →

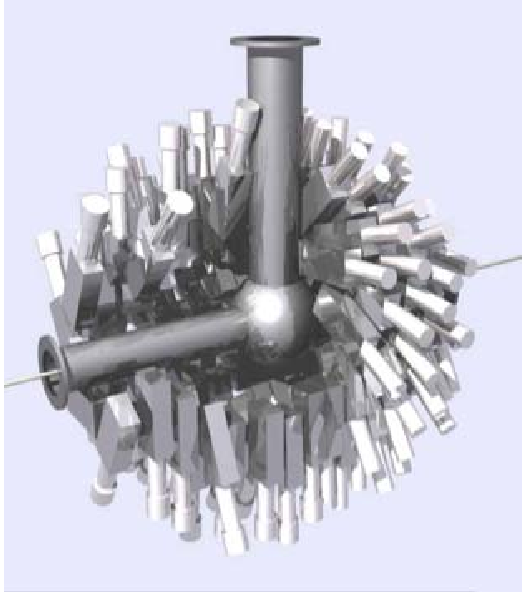

MSU/NSCL: SeGA

TRIUMF: TIGRESS

Gamma-ray energy spectrum

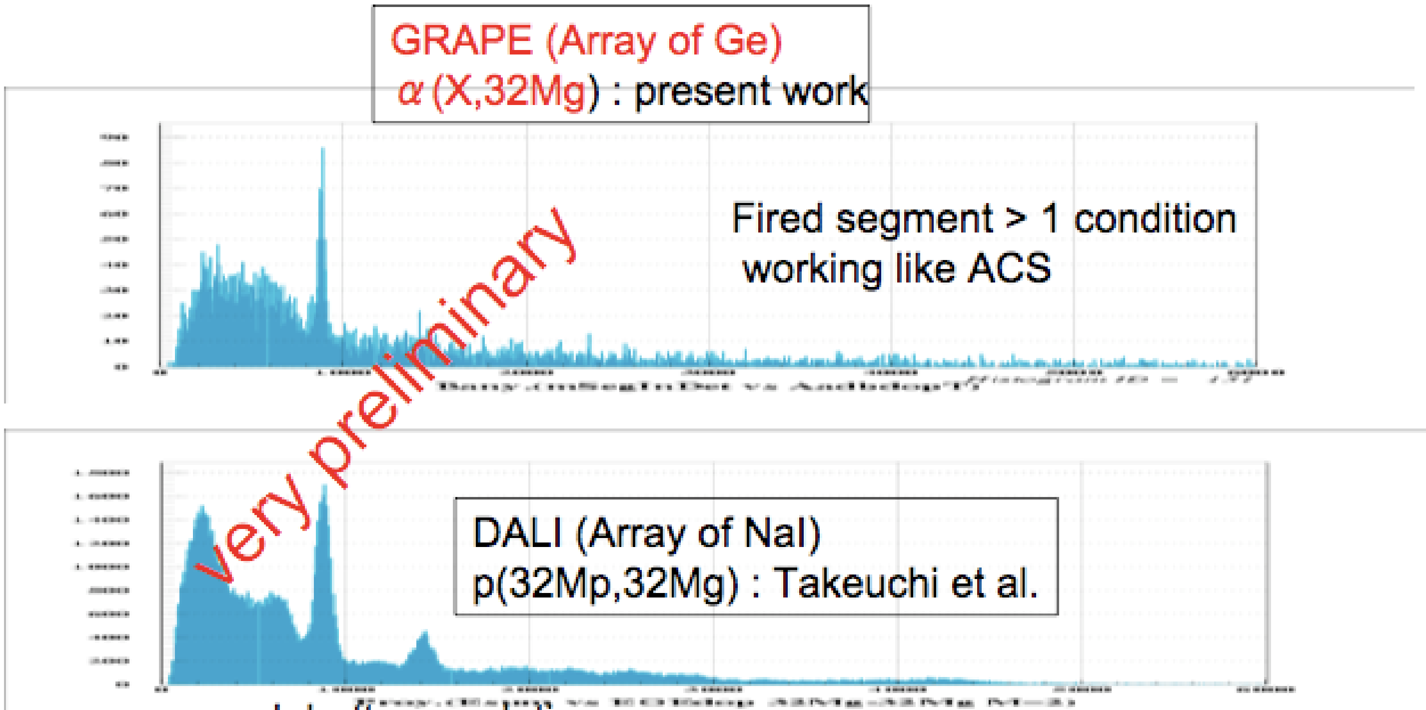

much better resolution,
and can be improved

2007/06/02 DREB2007@RIKEN

Doppler corrections

VAMOS :
Recoil velocity (v ~ 6.8 cm/ns)

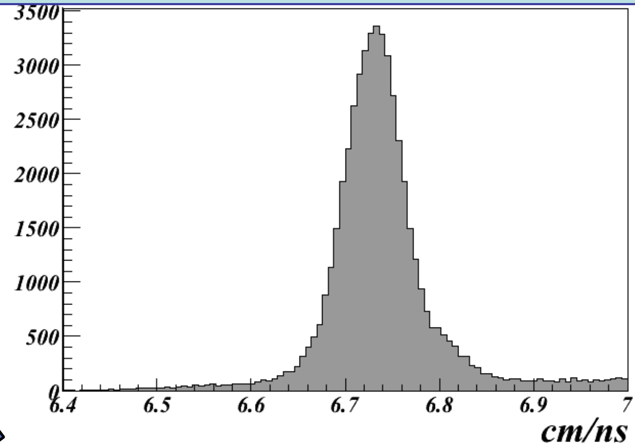

- Energy from crystal
- Angle from GOCCE
  - * Doppler correction
  - *Angular distribution

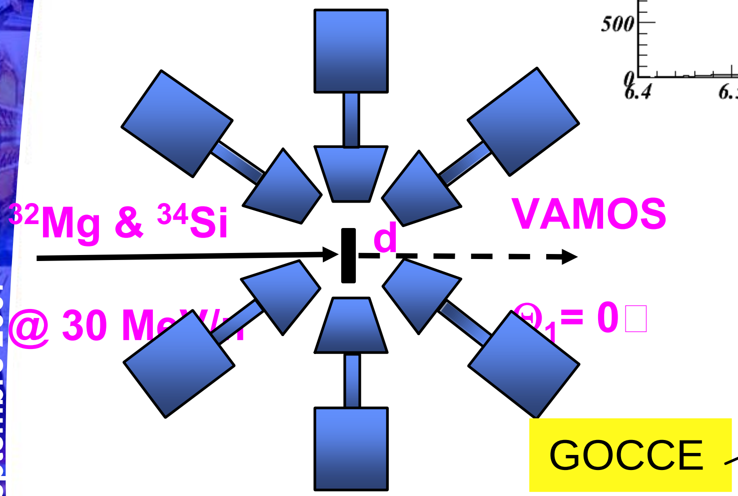

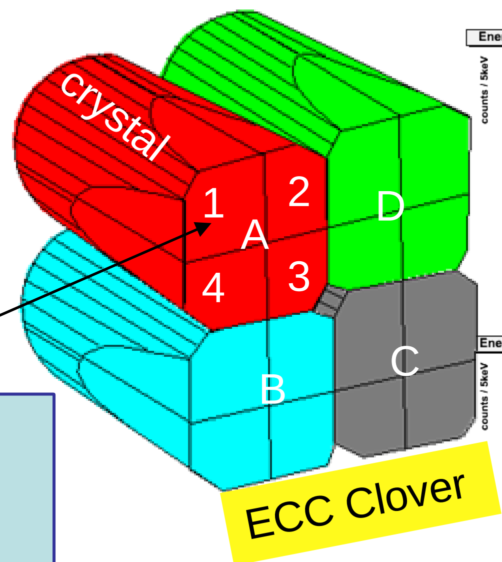

Doppler correction for 885 keV γ-ray in ^{32}Mg

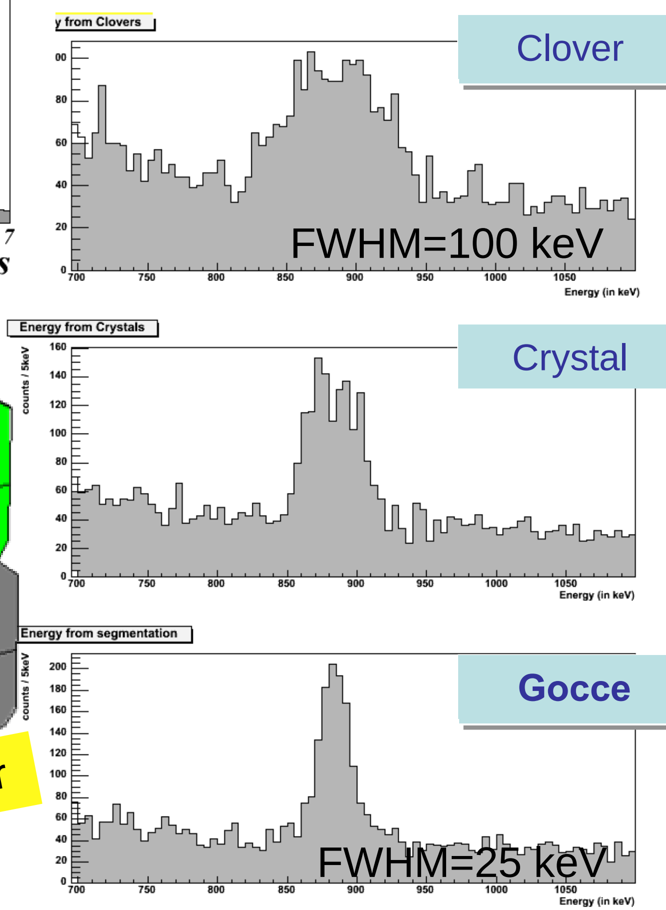

12 GOCCE rings:
Forward: 30^0, 40^0, 50^0, 60^0
Middle: 75^0, 85^0, 95^0, 105^0
Backward: 120^0, 130^0, 140^0, 150^0

Part 5

Detection systems and selected examples of experiments

e) Magnetic spectrometers in coincidence with γ-detection
i) momentum distribution

Exclusive 1-n removal reaction: Experimental procedure

- ^{11}Be beam, ^{9}Be target
- Ascertain 1n stripping (identify ^{10}Be)
- Final state of ^{10}Be (measure γ)
- l of emitted nucleon (measure ^{10}Be momentum distribution)

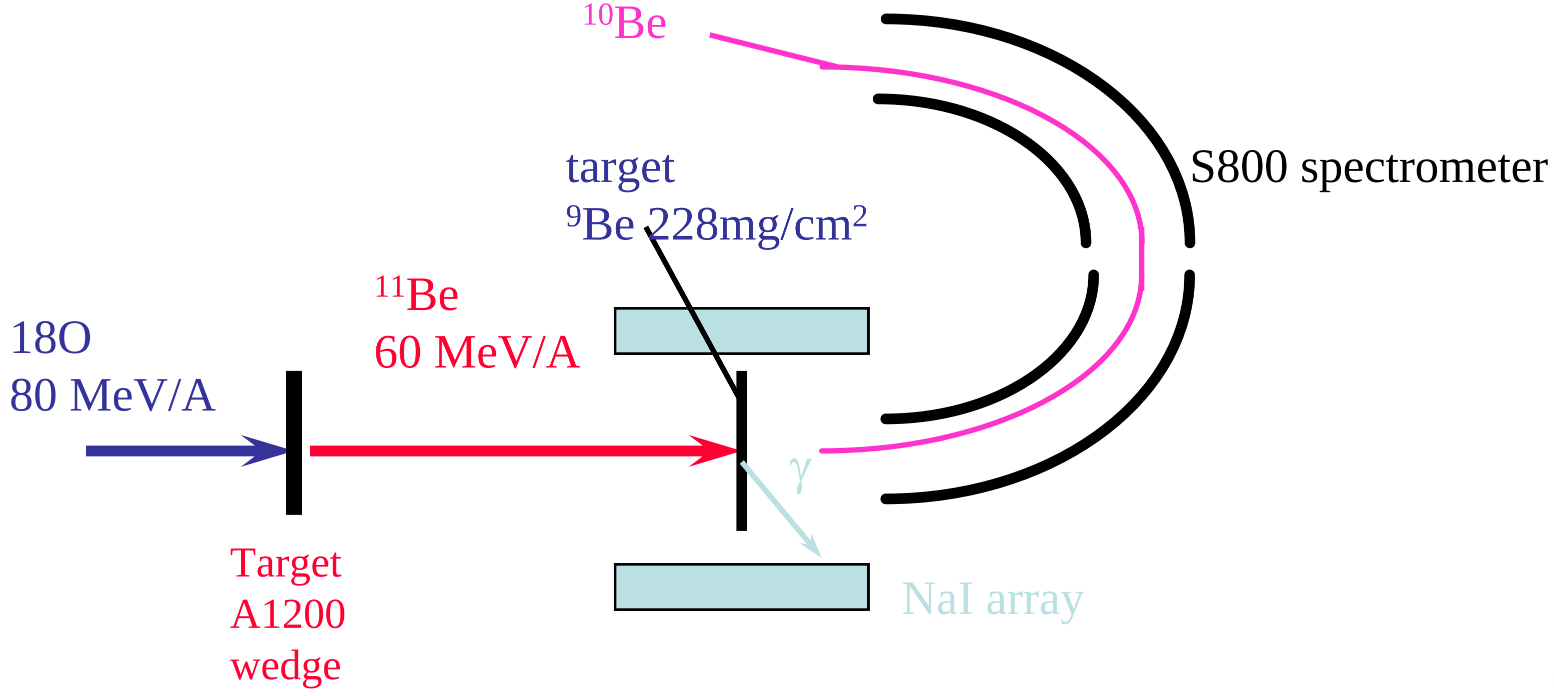

P. Roussel-Chomaz

Is ^{11}Be a pure s-wave halo state?

$$\left|{}^{11}_{4}Be_{g.s.}\right\rangle = S^{1/2}(0^+)\left|{}^{10}Be_{0+}\otimes 2s\right\rangle + S^{1/2}(2^+)\left|{}^{10}Be_{2+}\otimes 1d\right\rangle + \ldots$$

γ spectrum (from ^{10}Be)

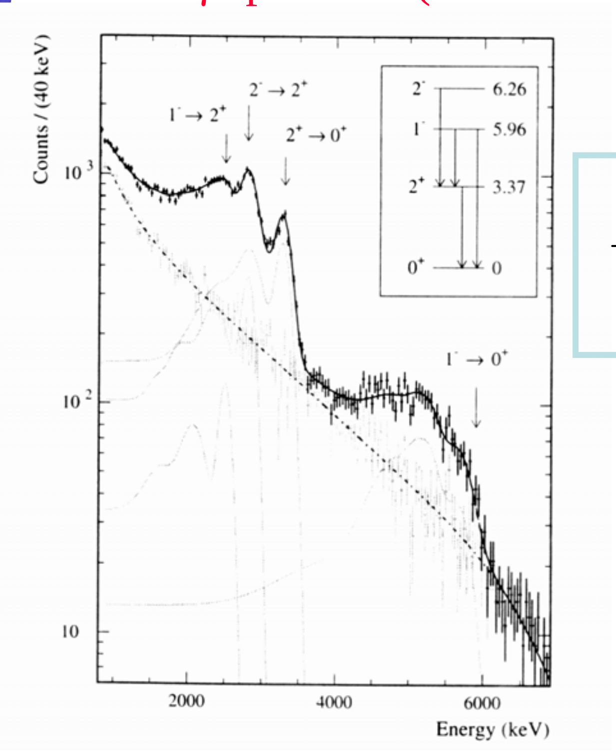

$$\frac{S(2+)}{S(2+) + S(0+)} = 0.2$$

ground state momentum distribution

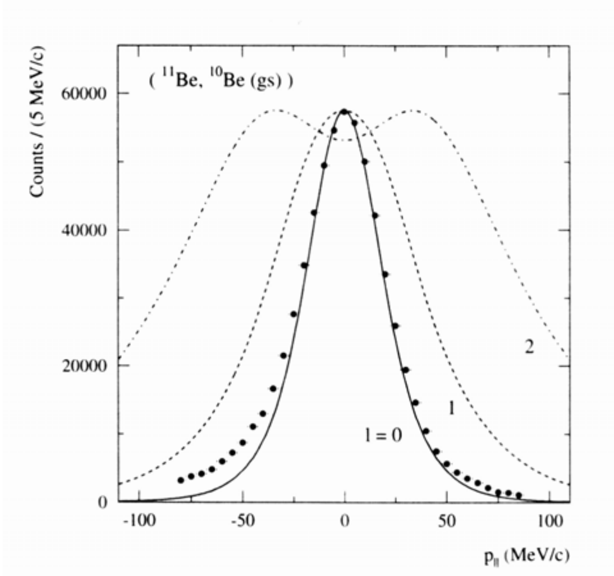

Eikonal model

I^π	l	S	σ_{sp}^{knock}	σ_{sp}^{diff}	σ^{other}	σ^{theo}	σ^{expt}
0^+	0	0.74	125	98	10[a]	172	203(31)
2^+	2	0.18	36	14	11[b]	17	16(4)
1^-	1	0.69	25	9		23	17(4)
2^-	1	0.58	25	9		20	23(6)
Σ						224	259(39)

T. Aumann et al. PRL 84 (2000) 35

P. Roussel-Chomaz

Microscopic structure of ^{11}Be through (p,d) reaction

$$\left|{}^{11}_{4}Be_{g.s.}\right\rangle = S^{1/2}\left(0^+\right)\left|{}^{10}Be_{0+}\otimes 2s\right\rangle + S^{1/2}\left(2^+\right)\left|{}^{10}Be_{2+}\otimes 1d\right\rangle + ...$$

$$(d\sigma/d\Omega)_{exp} = S(d\sigma/d\Omega)_{calc}$$

$$\frac{S(2+)}{S(2+) + S(0+)} = 0.2$$

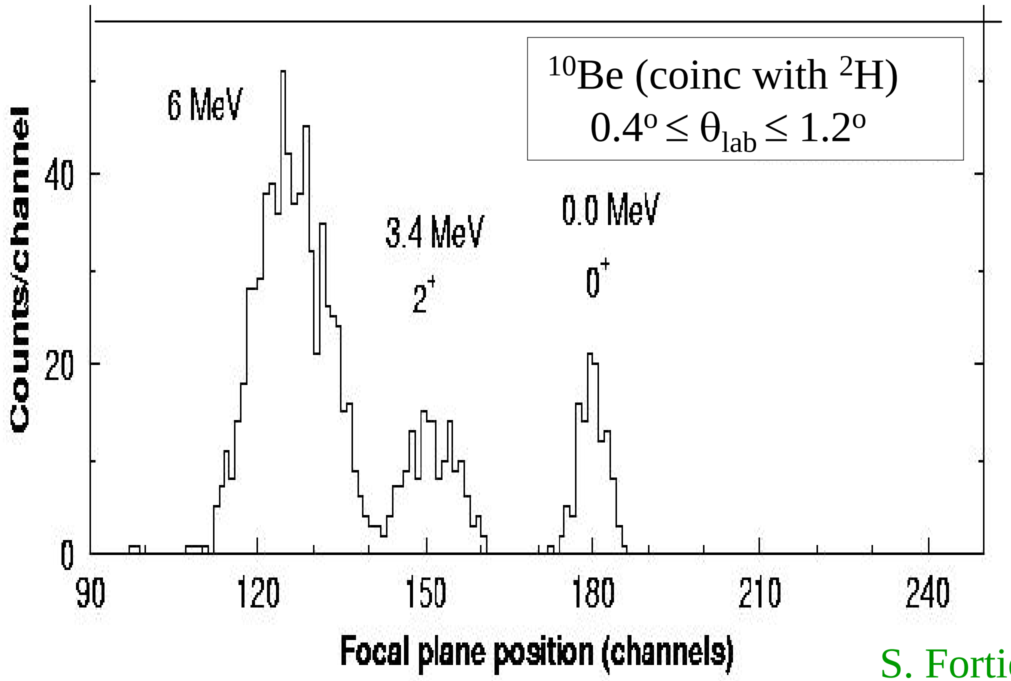

H(^{11}Be,^{10}Be)^{2}H
E = 35 A.MeV

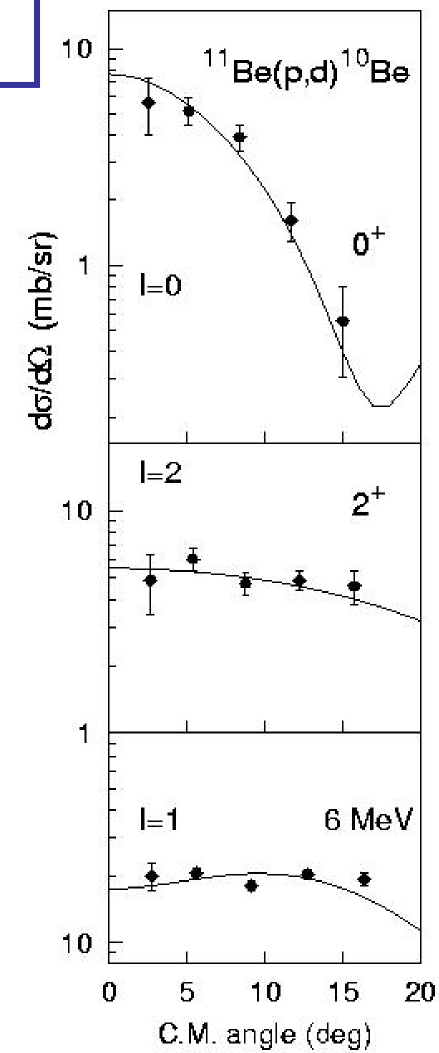

S. Fortier et al. PLB 461 (1999) 22
J.S. Winfield et al. NPA 683 (2001) 48

Ecole Joliot Curie, Septembre 2007

P. Roussel-Chomaz

An Example: The Ground State of ^{12}Be

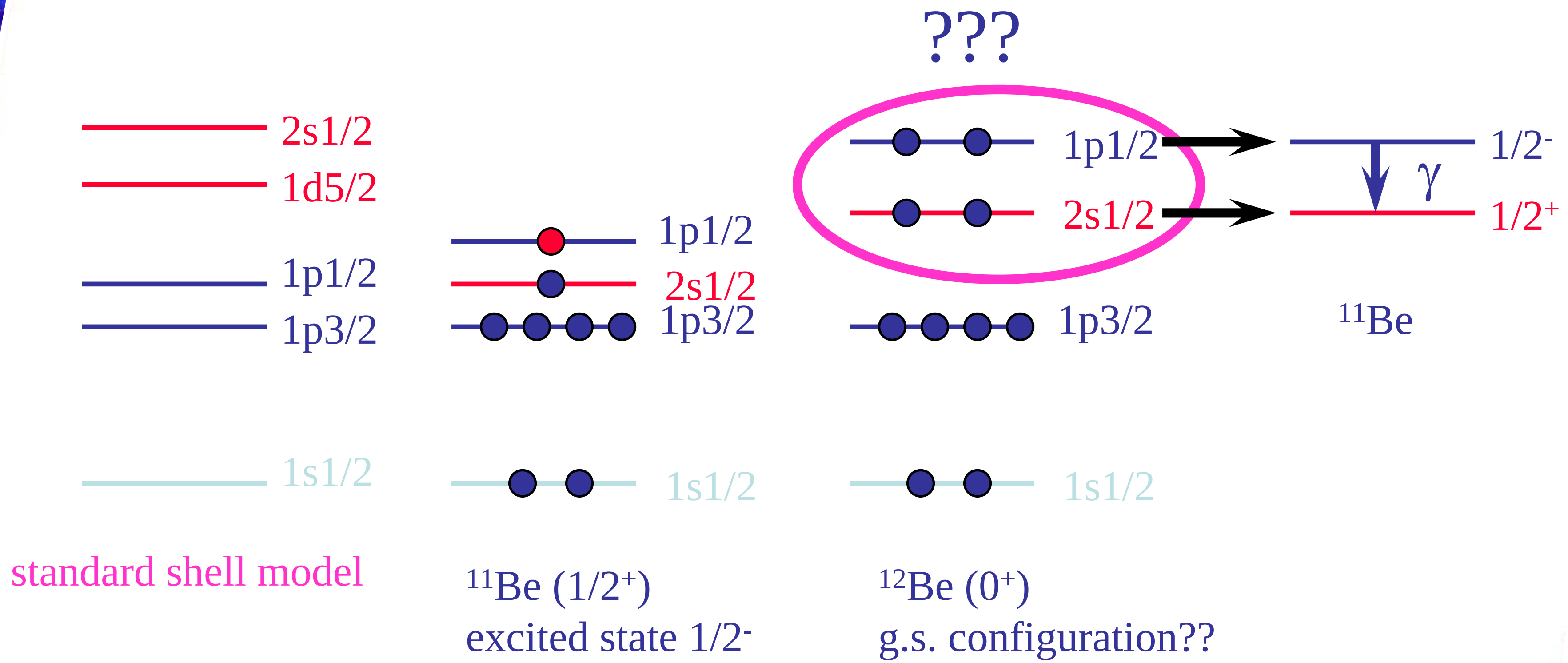

P. Roussel-Chomaz

Exclusive Momentum Distributions

Breakdown of the *N*=8 shell gap in ^{12}Be

^{12}Be ground state only 32% $\nu(1s1p)^8$ and 68% $\nu(1s1p)^6$-$(2s,1d)^2$

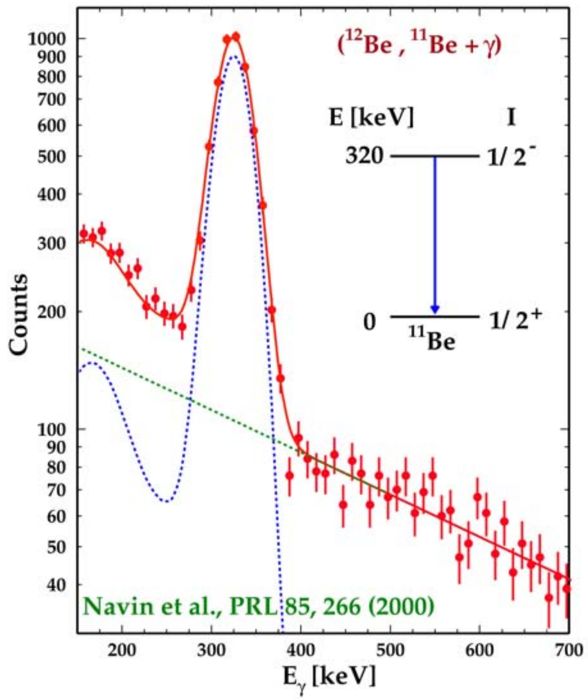

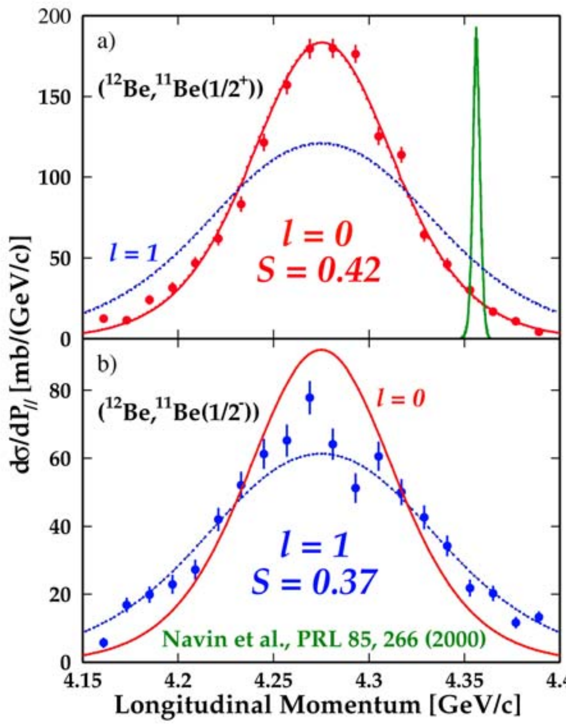

^{11}Be ground state (inclusive - coincidence)

^{11}Be excited state (coincidence with 320 keV γ)

$$^{12}Be \rightarrow {}^{11}Be + n + \gamma$$

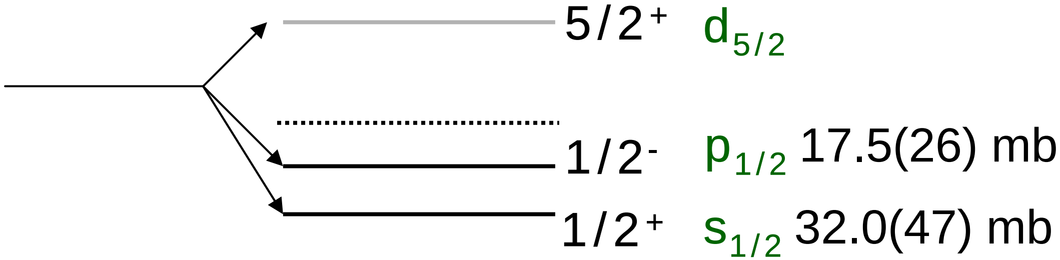

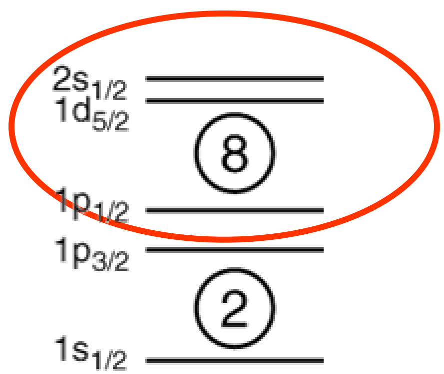

From T. Glasmacher INPC 2007

Part 5

Detection systems and selected examples of experiments

e) Magnetic spectrometers in coincidence with γ-detection
ii) in beam spectroscopy

In beam spectroscopy

γ Détection :

BaF2

Ge

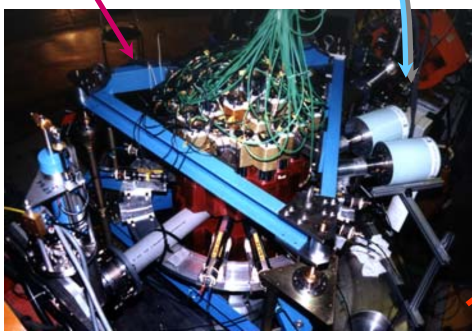

Fragment identification

S.P.E.G. (G.A.N.I.L.)

Dipôles

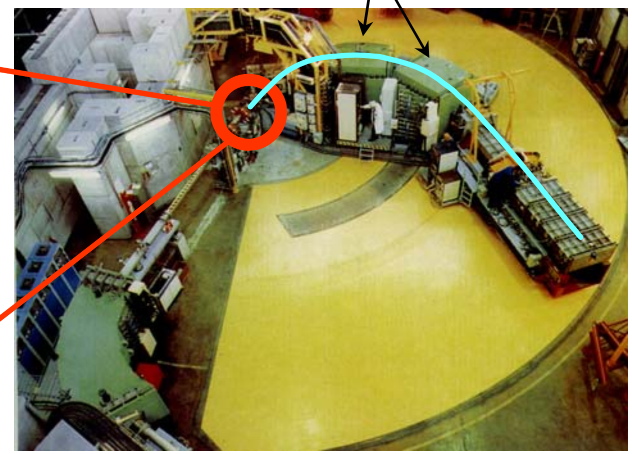

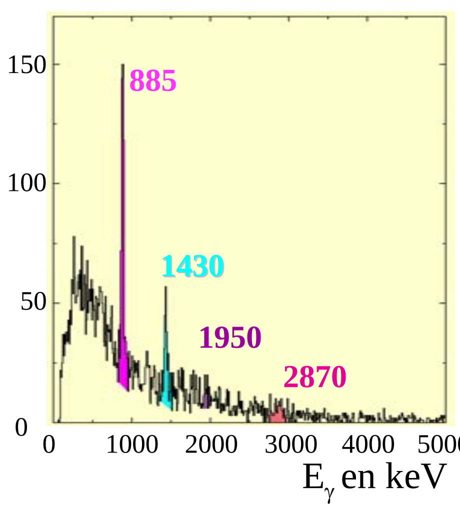

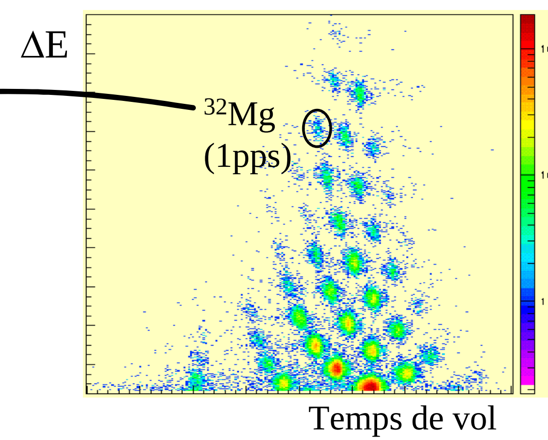

F. Azaiez et al.

P. Roussel-Chomaz

In-beam spectroscopy at N=28, ^{42}Si

B. Bastin PhD Thesis
S. Grévy et al, PRL99 (2007) 022503

^{48}Ca (>10^{12} pps) → ^{44}S (100-150 pps) → ^{42}Si* (8/day) → ^{42}Si + γ

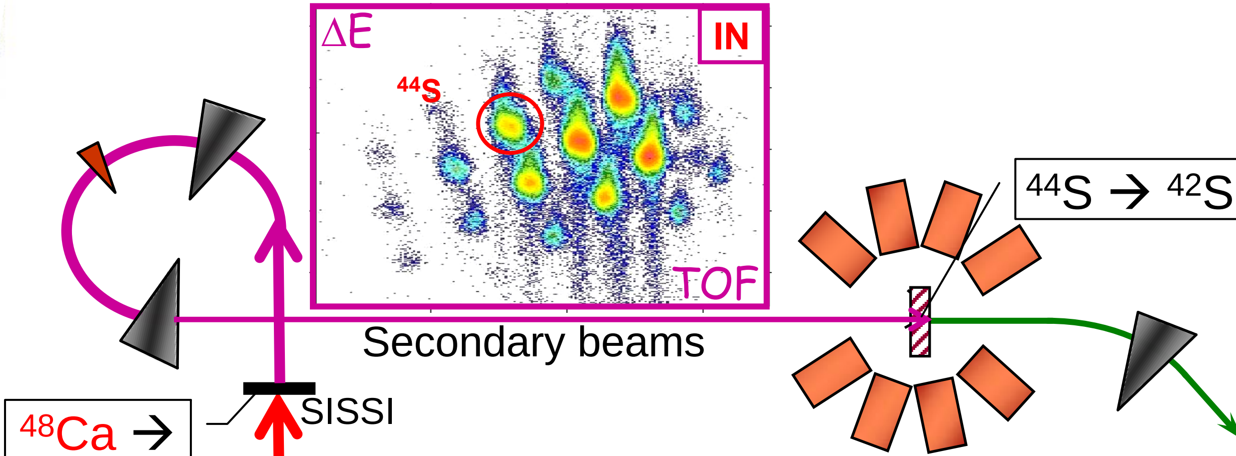

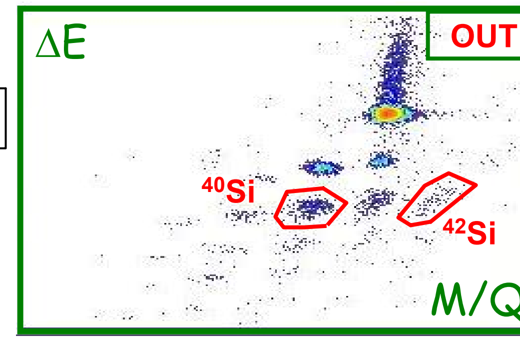

SPEG (ε~100%)

- **I(^{48}Ca) ~ 4 μAe - 60 A.MeV**
- **C and Ta production targets (~180 mg/cm²)**
- **^{44}S ~ 100-150 pps**

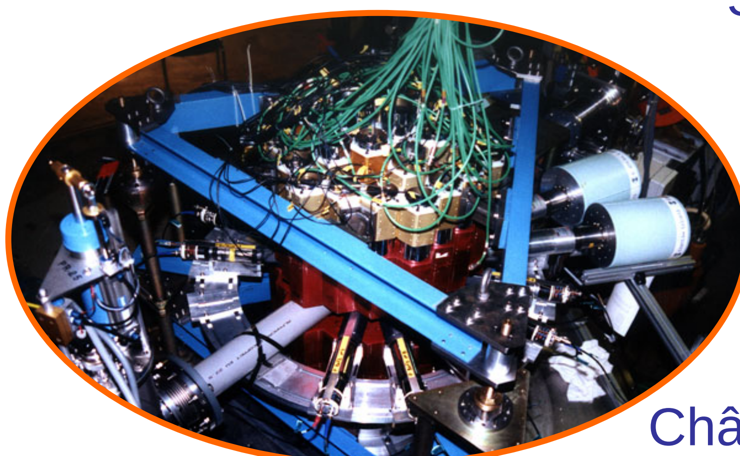

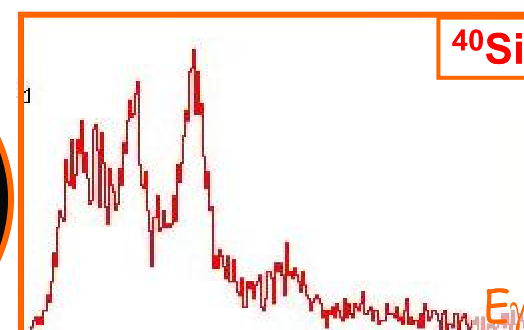

Château de Cristal (ε~40%)

In-beam spectroscopy at N=28, ^{42}Si

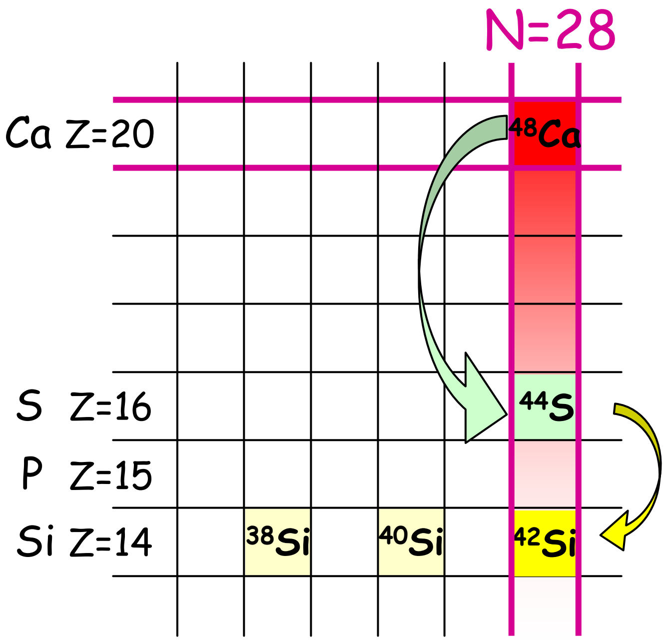

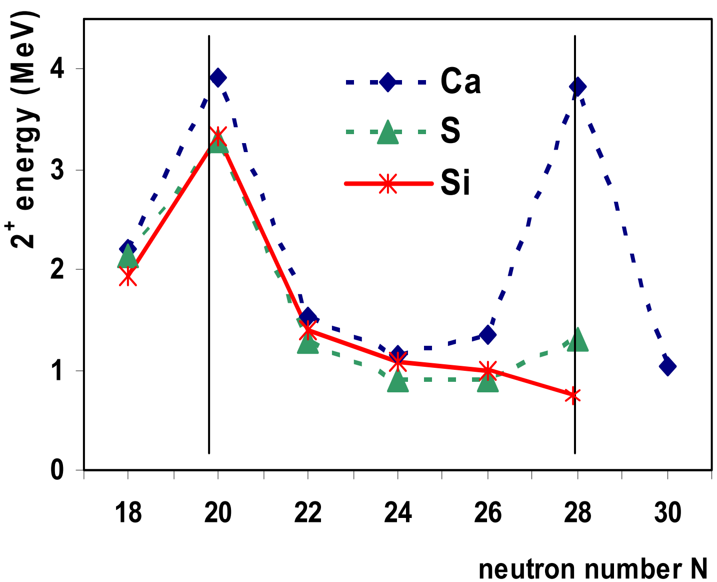

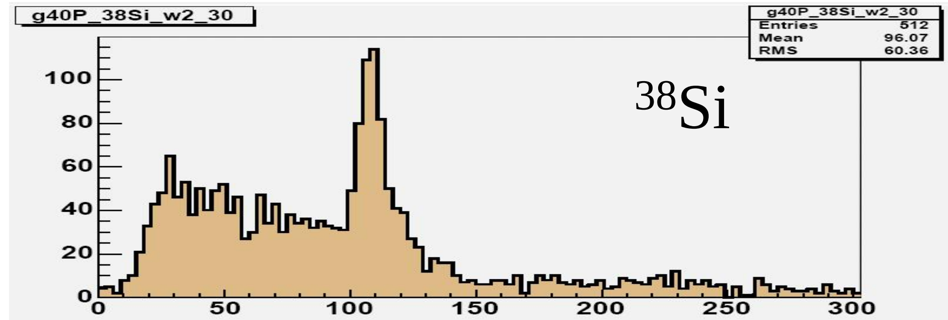

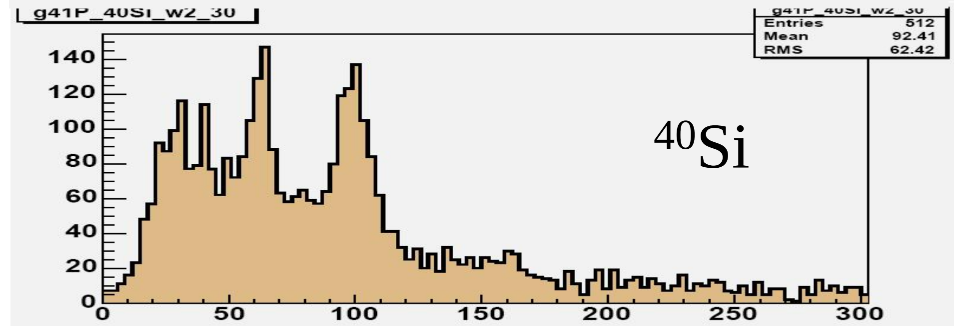

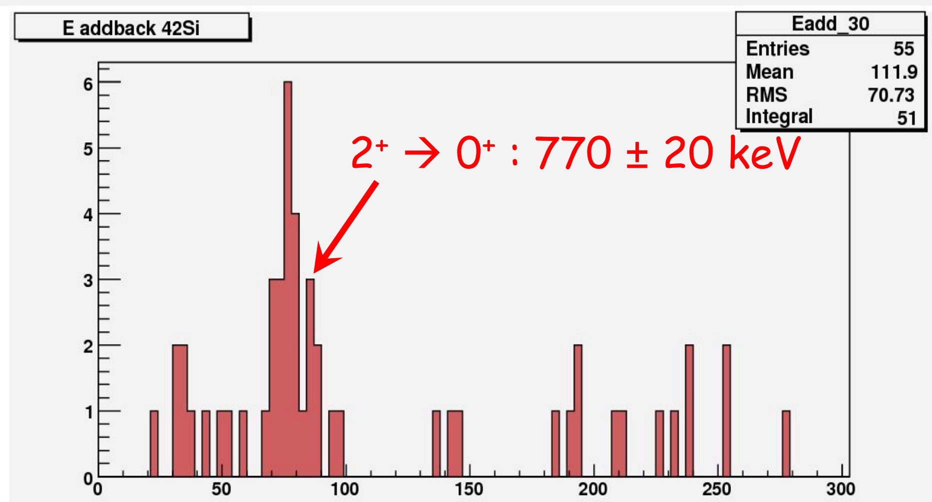

S. Grévy et al. PRL99 (2007)

Part 5

Detection systems and selected examples of experiments

Magnetic spectrometers in coincidence with γ-detection
iii) direct reactions: inelastic scattering, transfers

Study of N=20 region

Experimental details

❍ **VAMOS spectrometer**
⇩ Efficiency = 100%
⇩ Momentum acceptance ± 10%
⇩ Unambiguous identification : M/Q, M, Z
⇩ Event by event reconstruction of :
Bρ, velocity, angular distribution

❍ **γ-ray spectrometer EXOGAM**
⇩ **11 clovers**
(4 @ 45° , 3 @ 90°, 4 @ 135°)

❍ **Sissi Cocktail beams**
^{34}Si (10^4pps), ^{32}Mg (100pps)....
⇩ Ebeam ≈ 30 AMeV (β~0.24)
⇩ Identification
ΔE (Ionisation chamber)
TOF

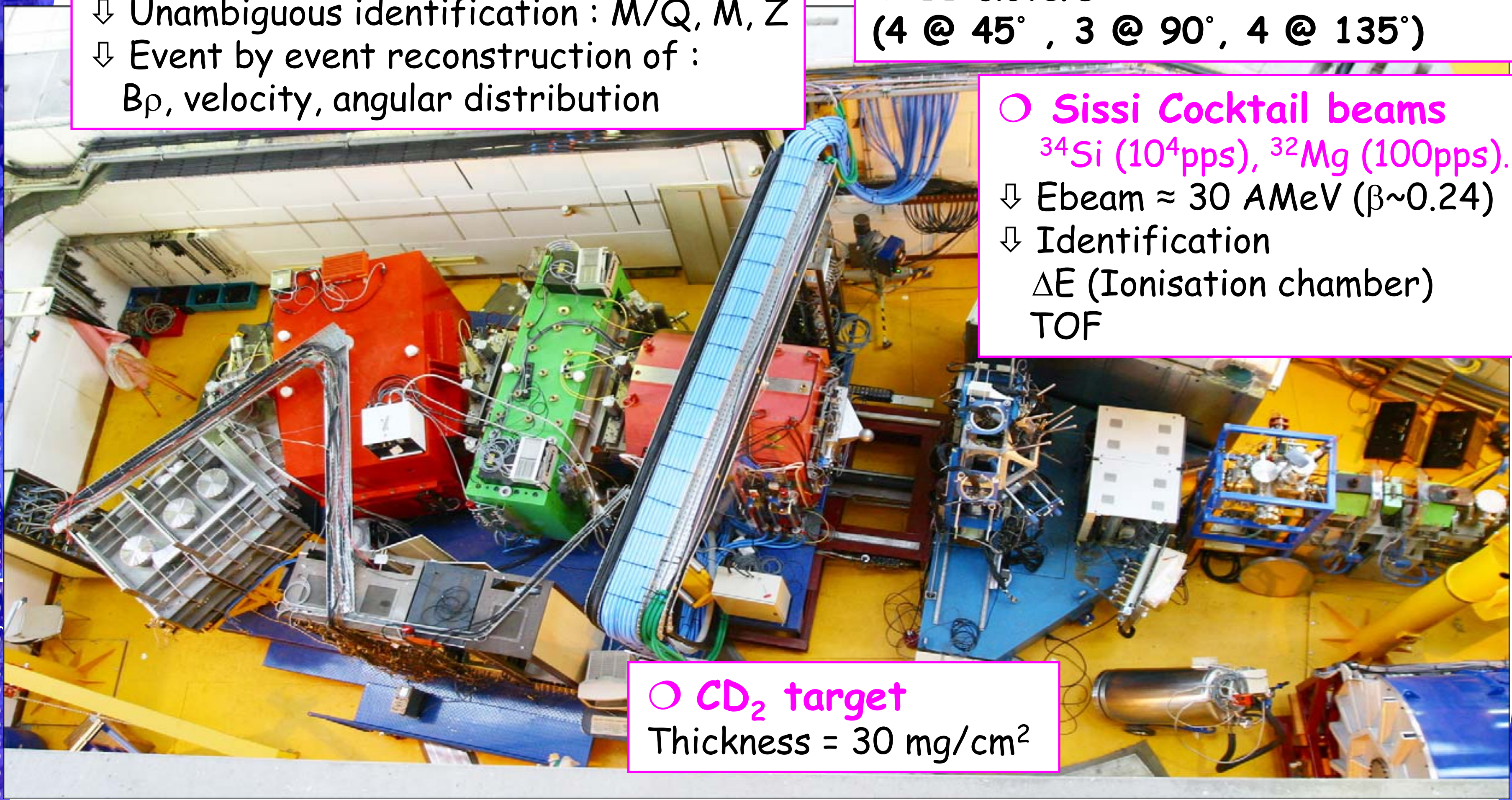

❍ **CD_2 target**
Thickness = 30 mg/cm^2

W. Mittig, H. Savajols, P. Roussel-Chomaz et al.

M. Gelin PhD Thesis

Study of N=20 region

Experimental details

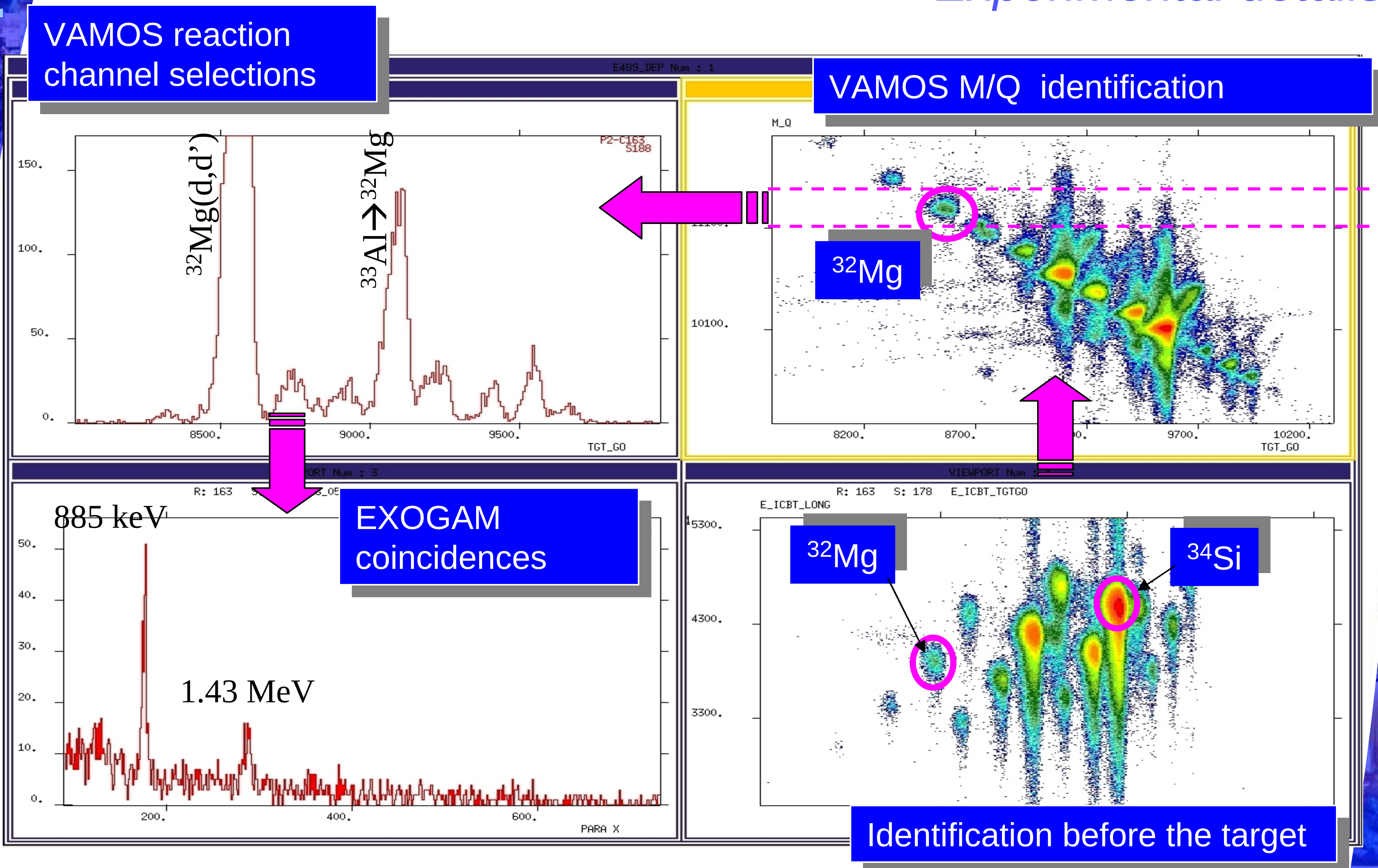

P. Roussel-Chomaz

The case of ^{32}Mg

- → Several nuclei
- → Several reaction channels at the same time

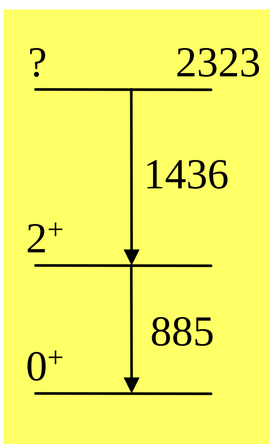

M.Gelin, PhD Thesis

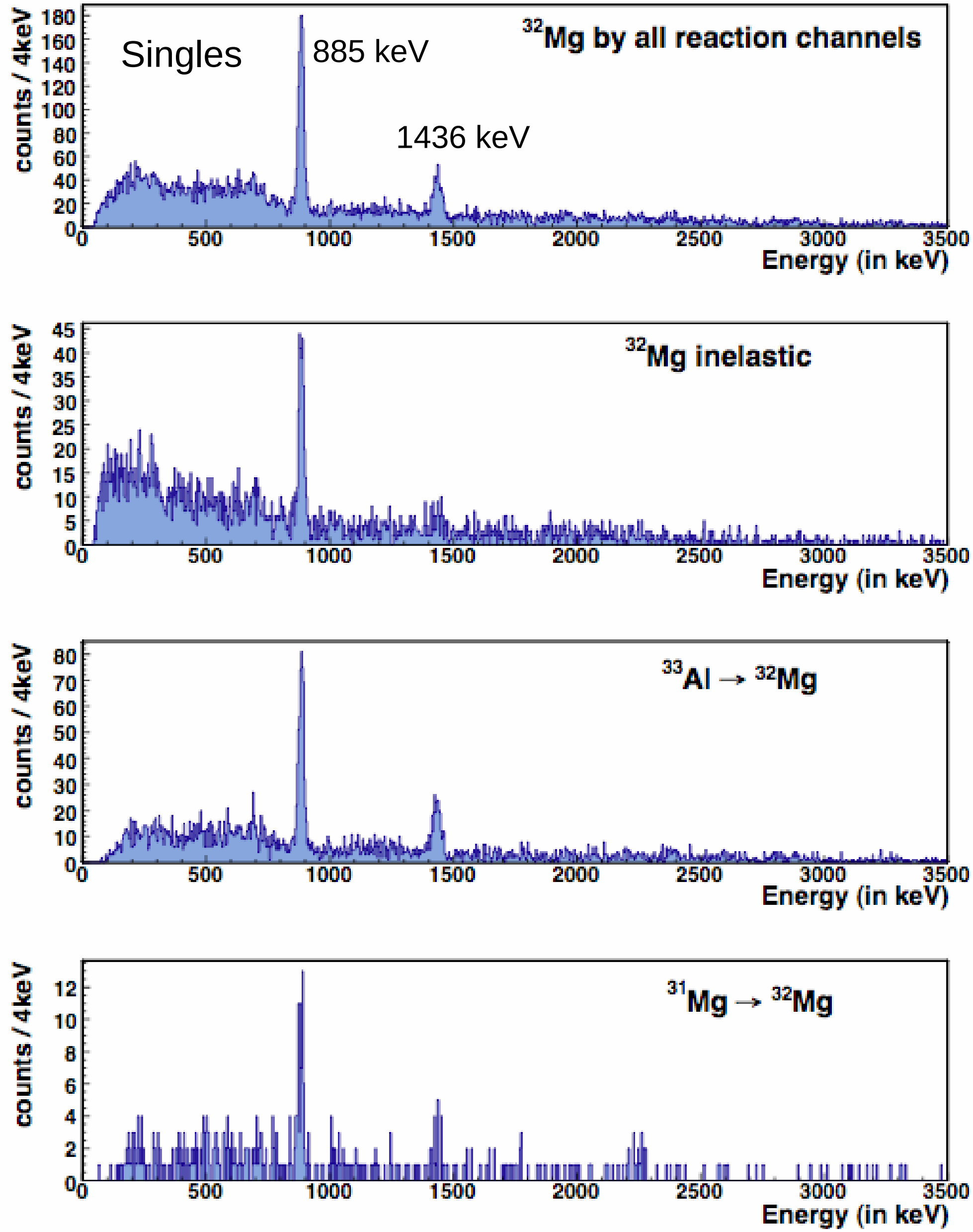

γ–γ coincidences for ^{32}Mg

Channel $^{33}Al \longrightarrow {}^{32}Mg$

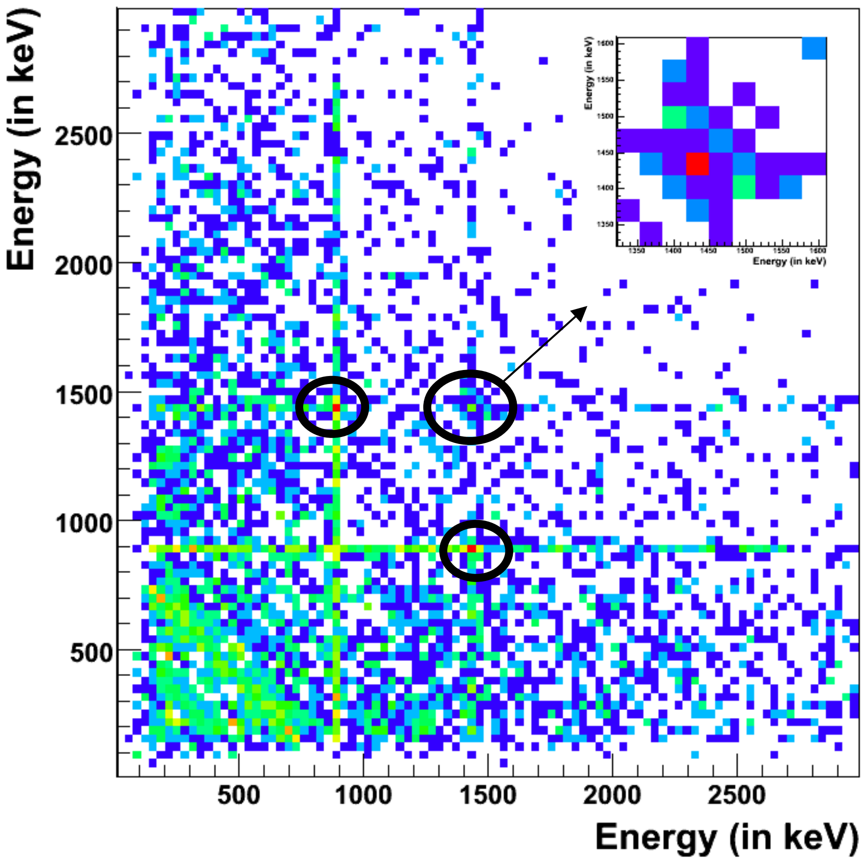

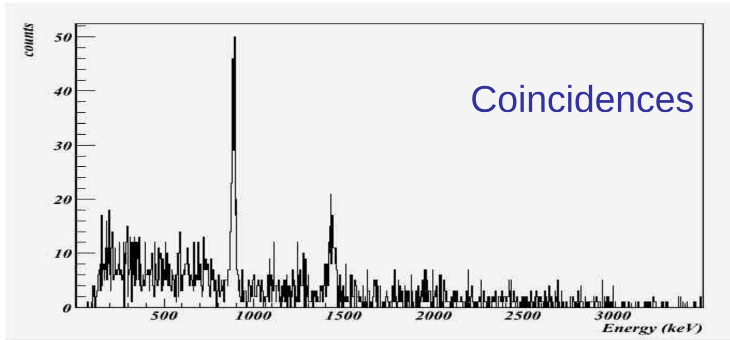

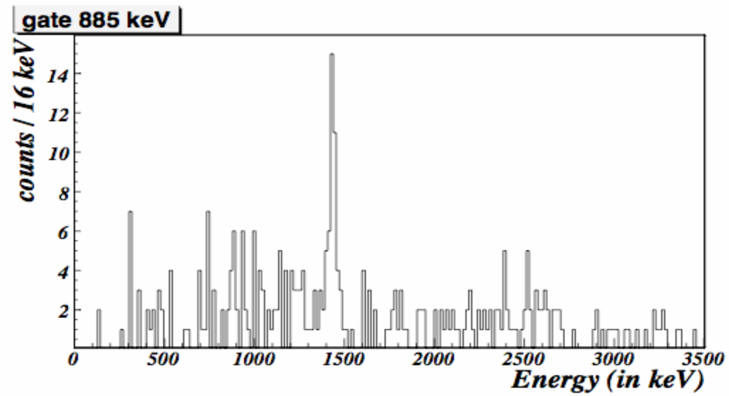

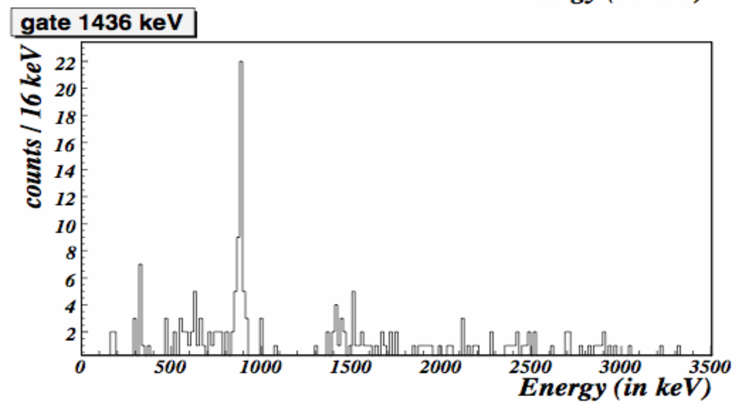

NEW: 2 transitions around 1430 keV

P. Roussel-Chomaz

Angular distributions for ^{34}Si and ^{32}Mg

$$W(\theta) = Const[1+a_2P_2\cos(\theta)]$$

^{34}Si inelastic scattering

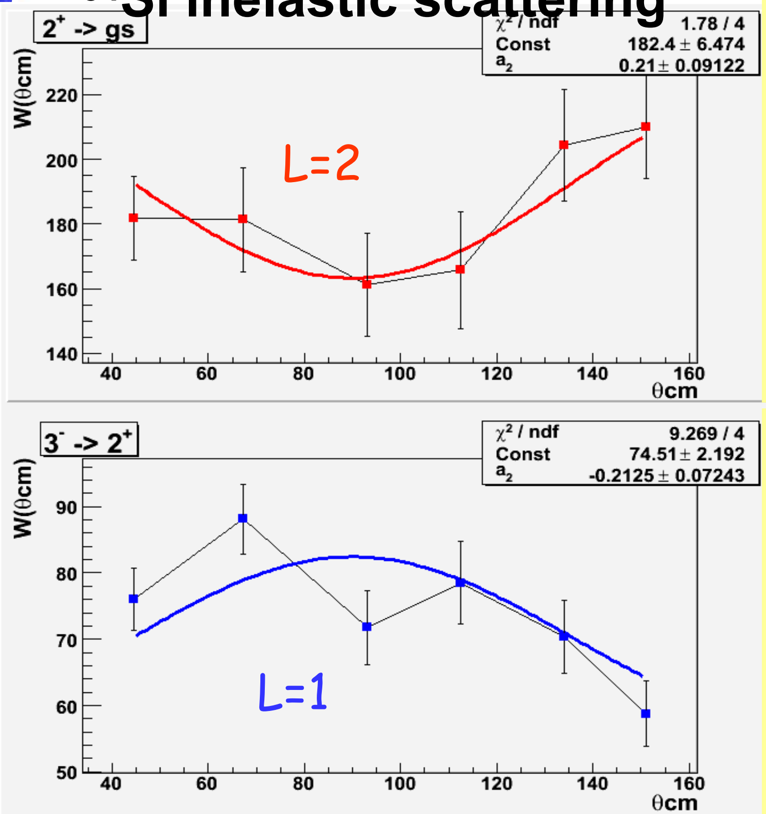

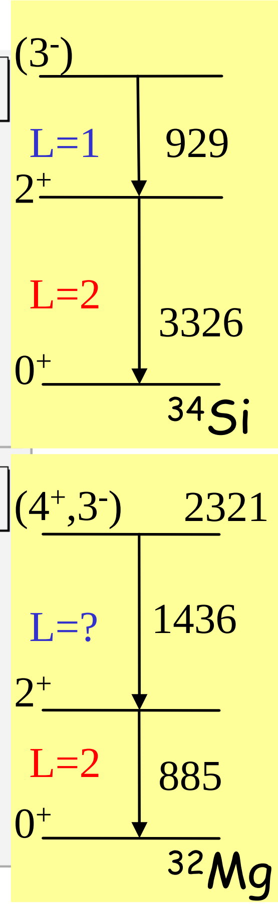

^{32}Mg inelastic scattering

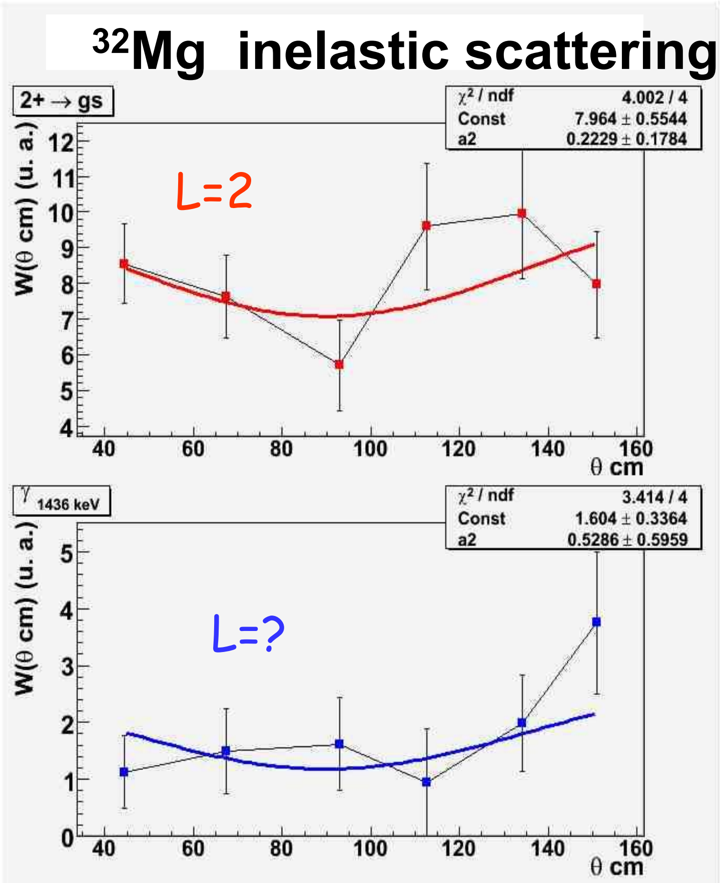

Firm assignment of 3^- in ^{34}Si at 4.2 MeV

P. Roussel-Chomaz

Structure of ^{23}F: Multiple reactions in one experiment

~35 MeV/nucl,100 mg/cm^2 liquid helium target at RIKEN

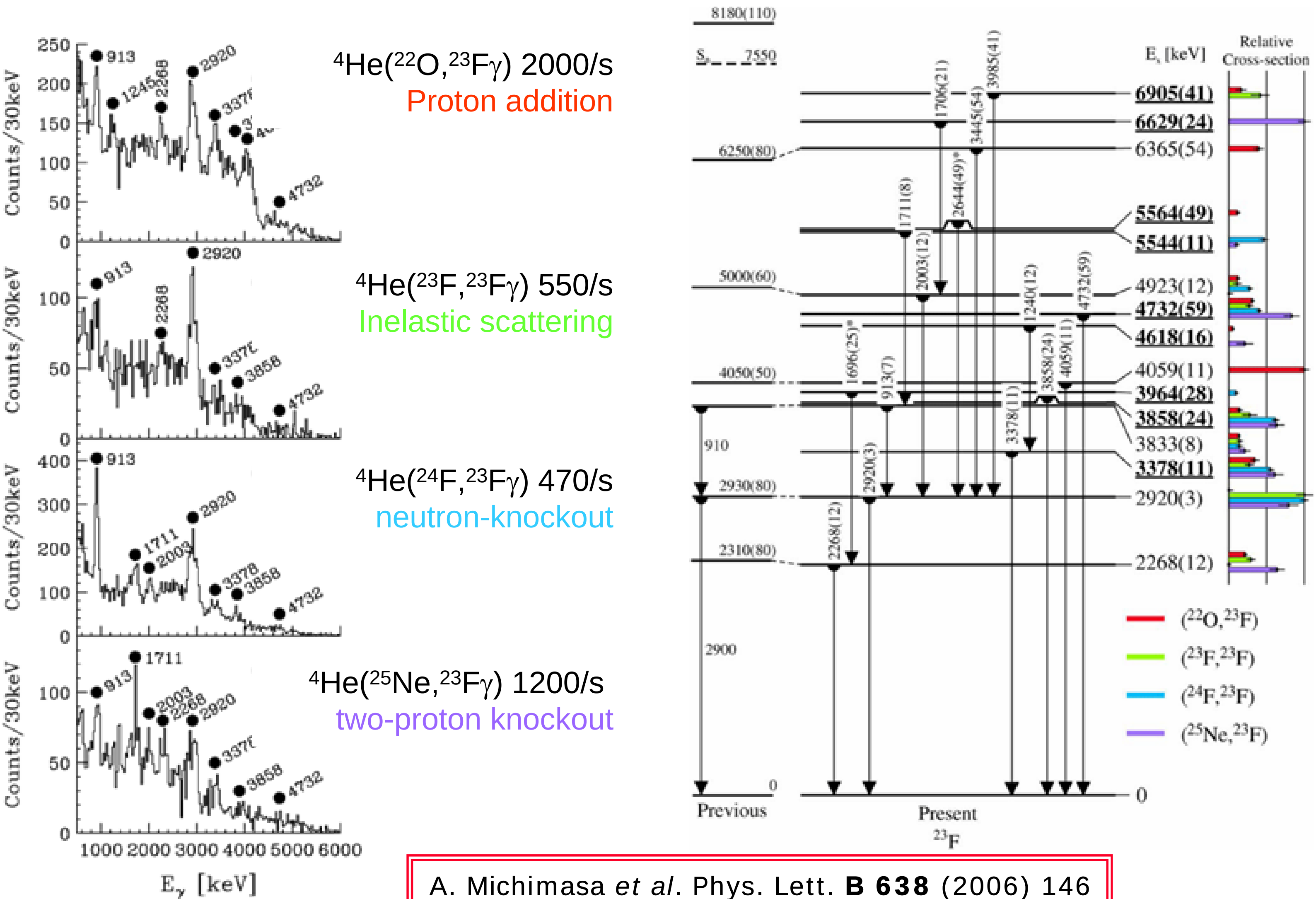

A. Michimasa *et al*. Phys. Lett. **B 638** (2006) 146

Part 5

Detection systems and selected examples of experiments

Magnetic spectrometers in coincidence with γ-detection
iv) deep inelastic

Gamma spectroscopy using deep inelastic reactions

Deep inelastic reactions

- populate neutron rich nuclei
- single particle and collective states
- many nuclei at the same time
- Excitation energy

For small cross sections

- selectivity
- sensitivity

VAMOS

EXOGAM - GANIL -

- beam - ^{238}U at 5.5 MeV/u
- target – ^{48}Ca
- inverse kinematics

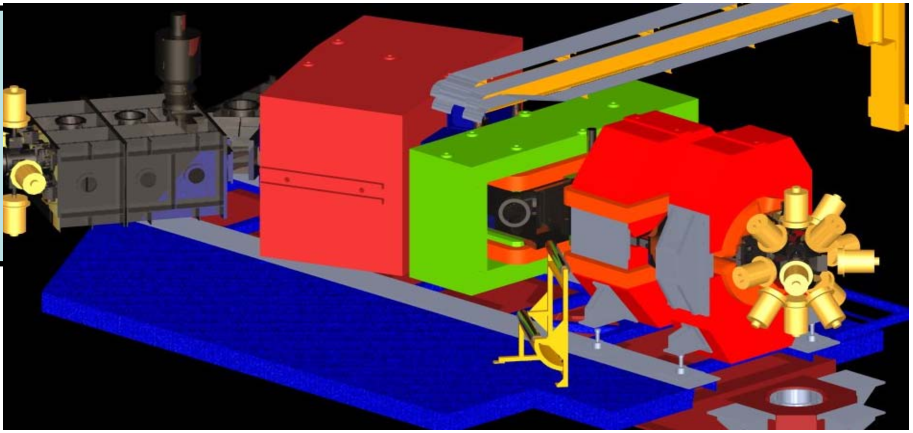

P. Roussel-Chomaz

Identification spectra

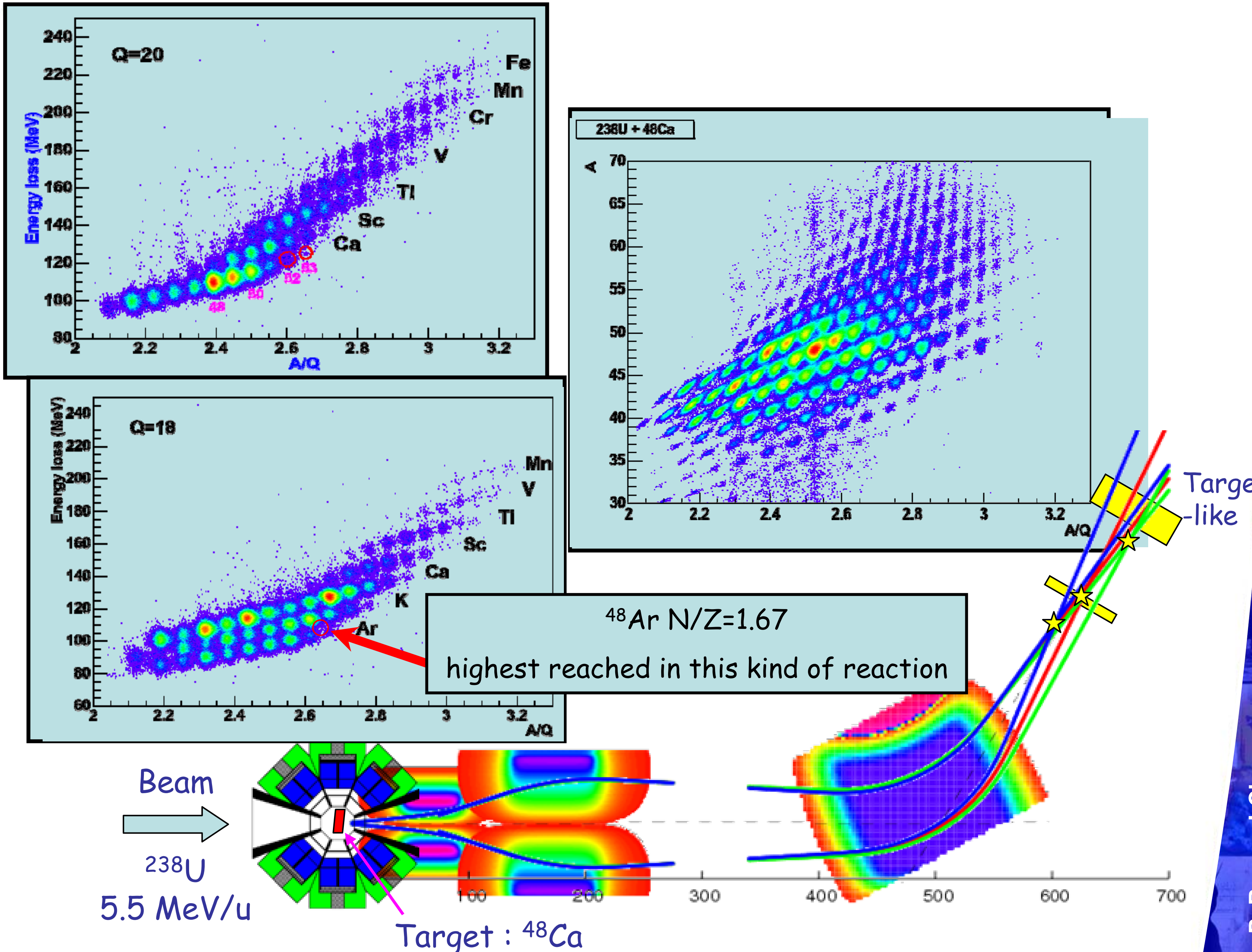

P. Roussel-Chomaz

Neutron rich Calcium isotopes

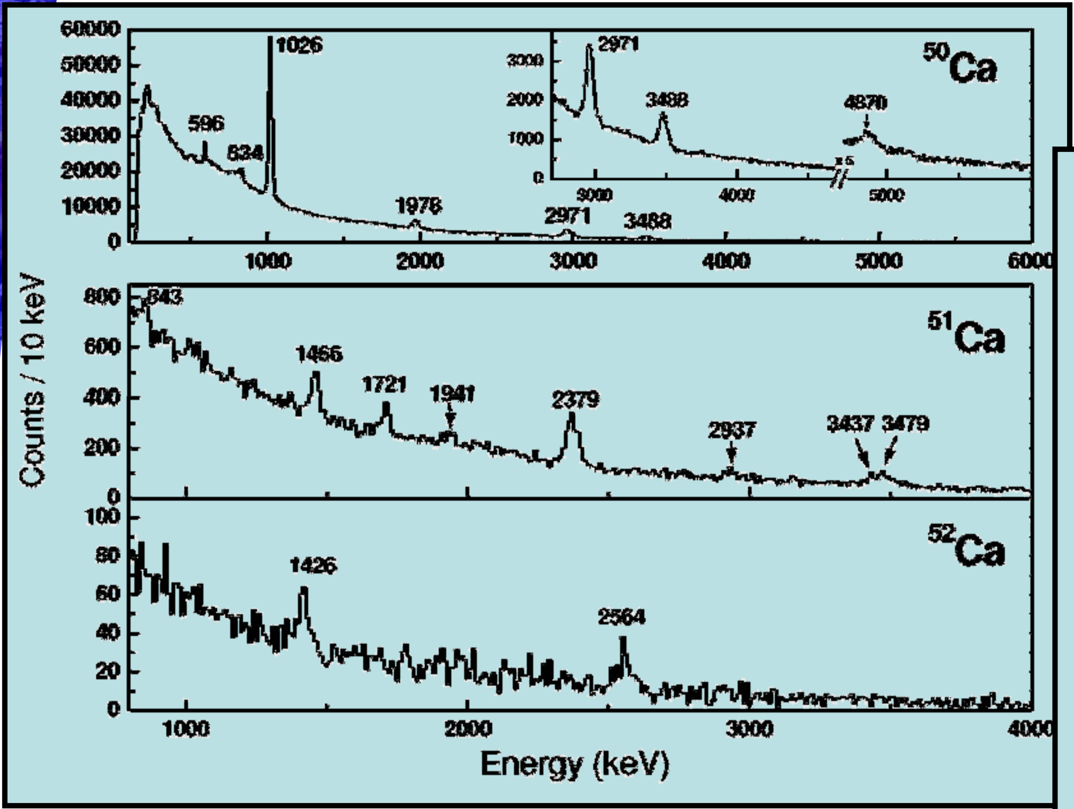

Doppler corrected using $\vec{V}$ from VAMOS

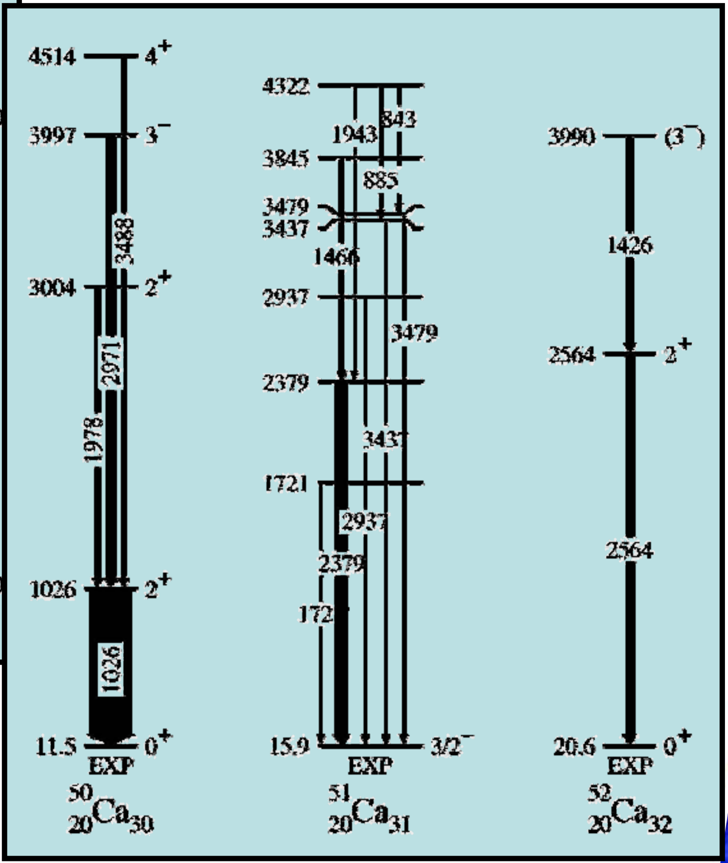

M. Rejmund et al Phy Rev C76 (2007) 021304

No gap at N=34

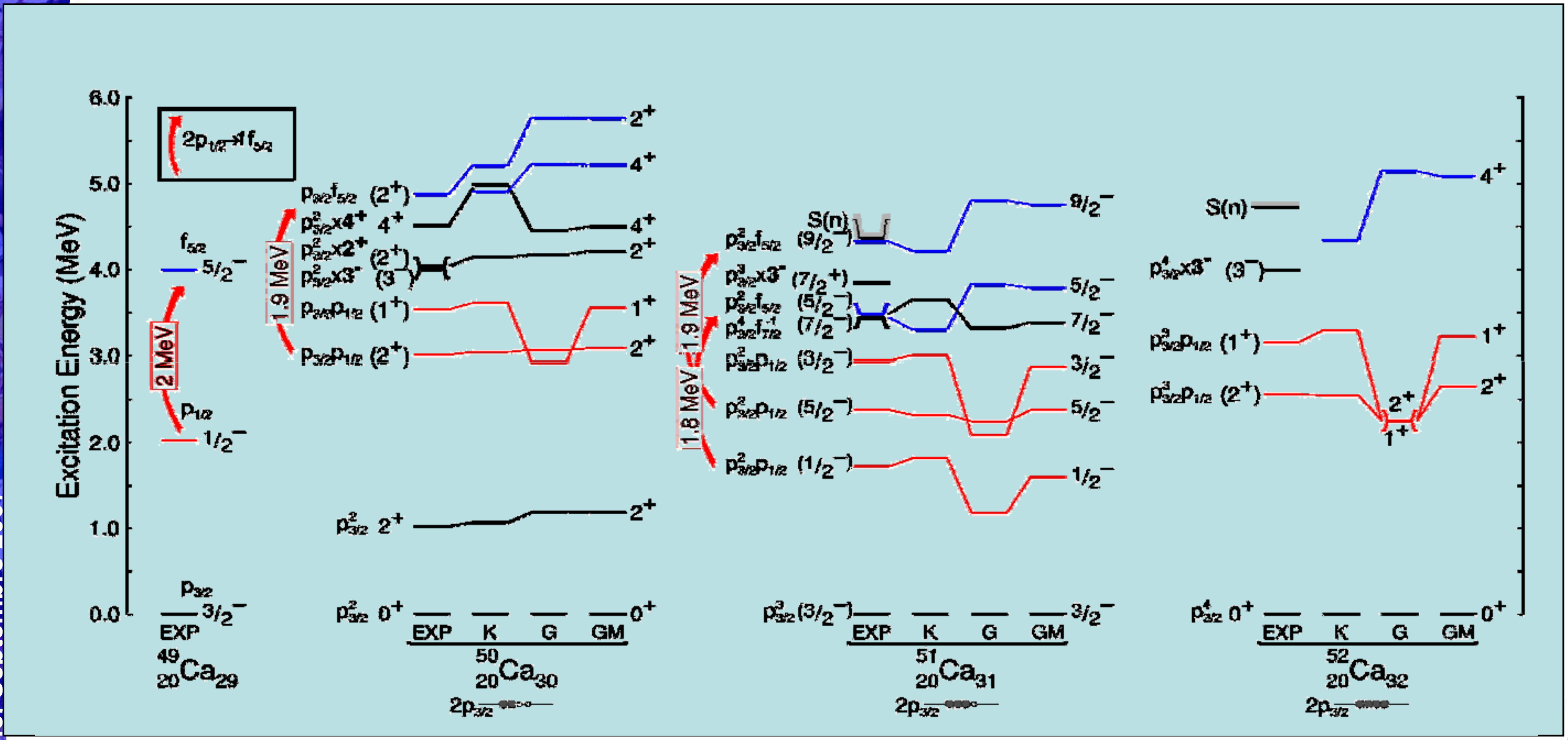

P. Roussel-Chomaz

Limits of the method

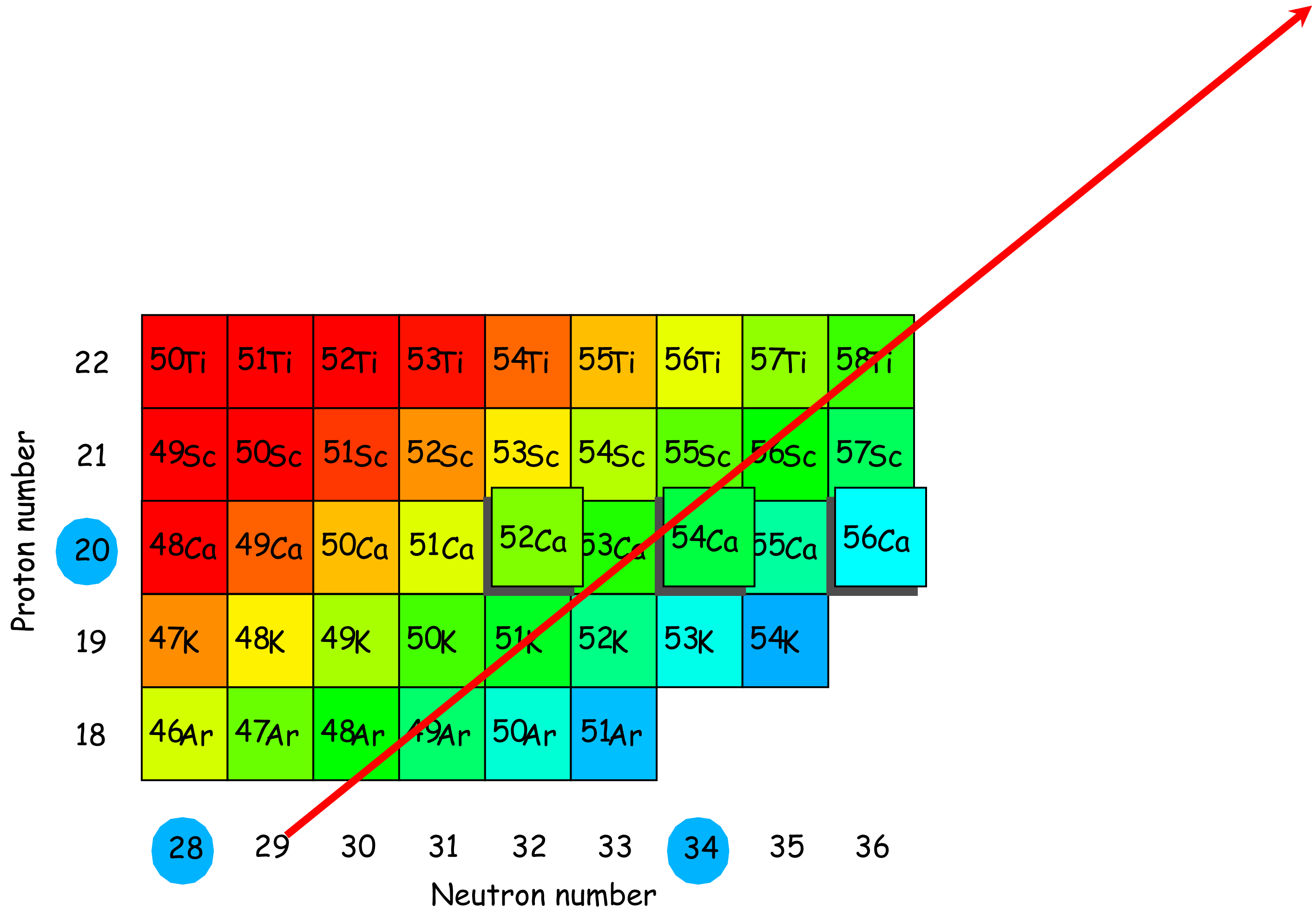

P. Roussel-Chomaz

Part 6

Future facilities

RIBF: Accelerator Complex in RIKEN Nishina Center for Accelerator-Based Research

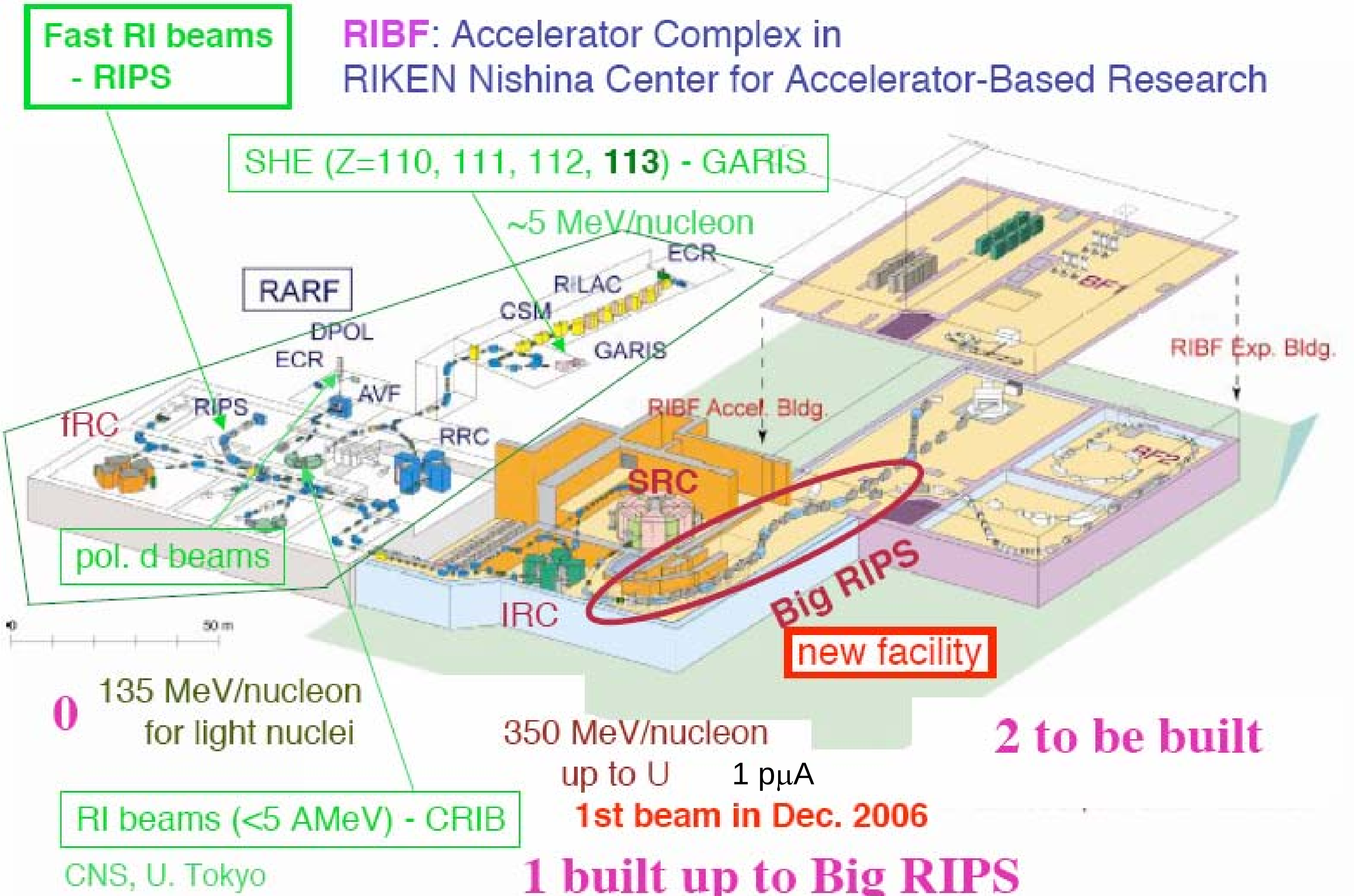

RIA – Light @ NSCL-MSU

E>200 AMeV

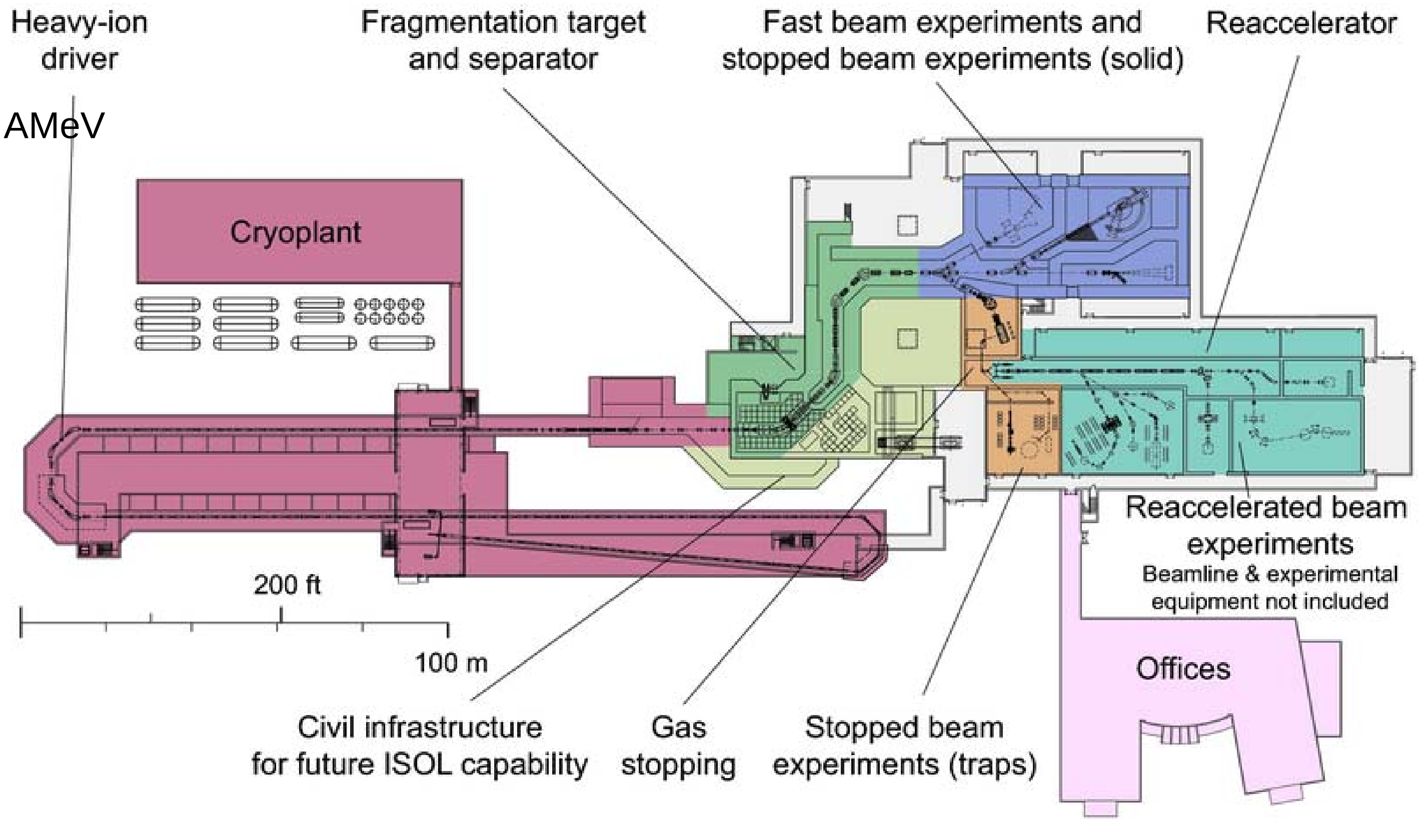

Instruments for the future :

The radioactive beam roadmap in Europe

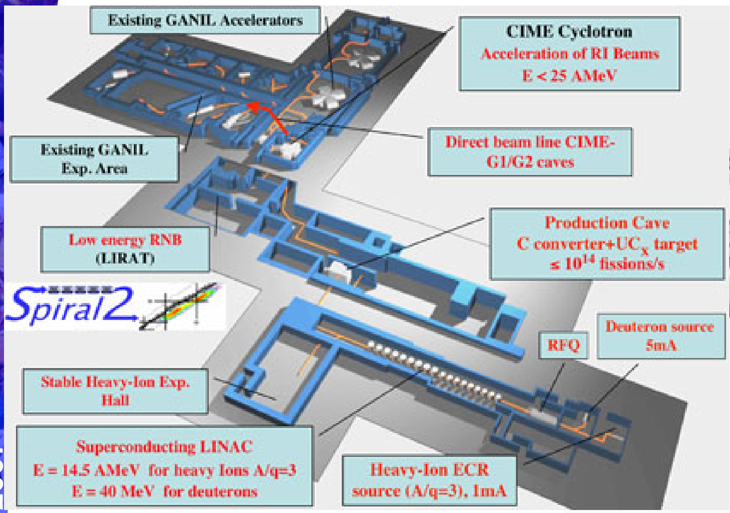

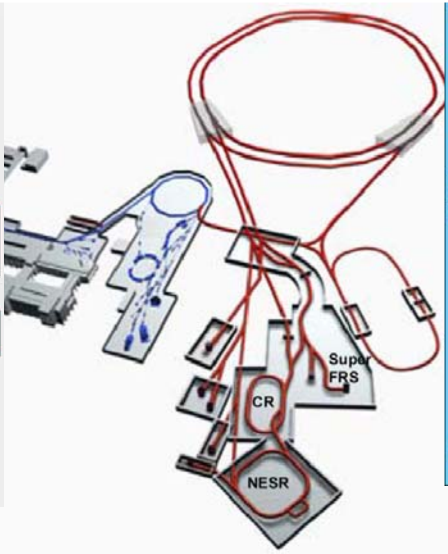

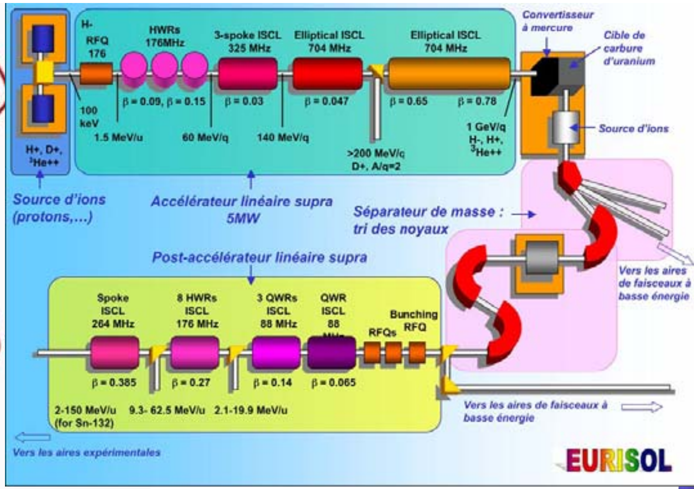

Spiral2 GSI EURISOL

The FAIR project(GSI)

Green light from German authorities
Staged construction 2008 – 2012 (?)

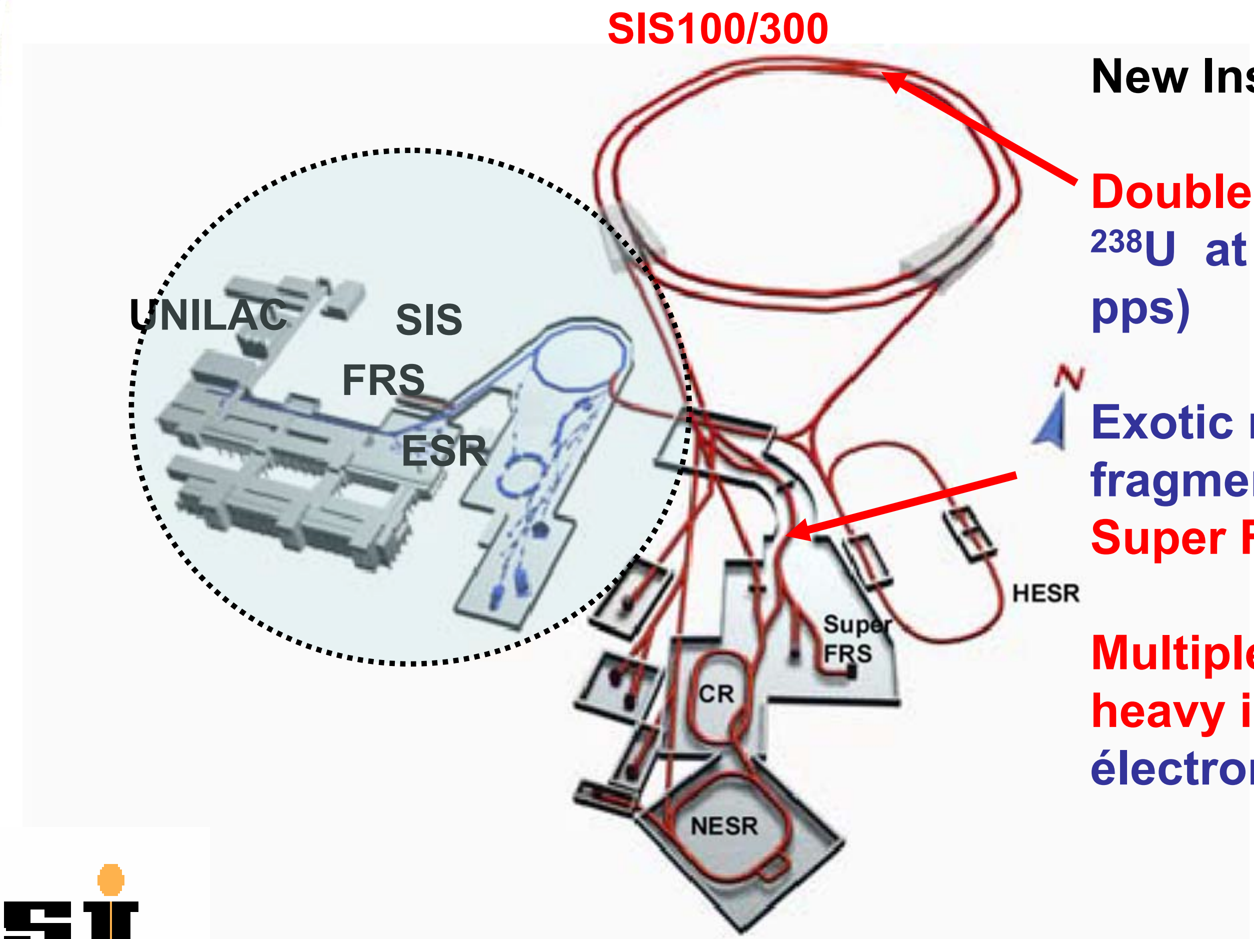

New Installations :

Double Synchrotron
^{238}U at 1 - 2.5 GeV/u (10^{12} pps)

Exotic nuclei produced by fragmentation and fission
Super FRS (intensity x10^3)

Multiple storage rings for heavy ions, anti-protons and électrons

The New Accelerator Facility for Beams of Ions and Antiprotons FAIR

High-Intensity Synchrotron
Fast cycling superconducting magnets
60 GeV protons, 23 GeV/u U^{92+}
30 GeV/u Ne10+, **1 GeV/u U^{28+}**

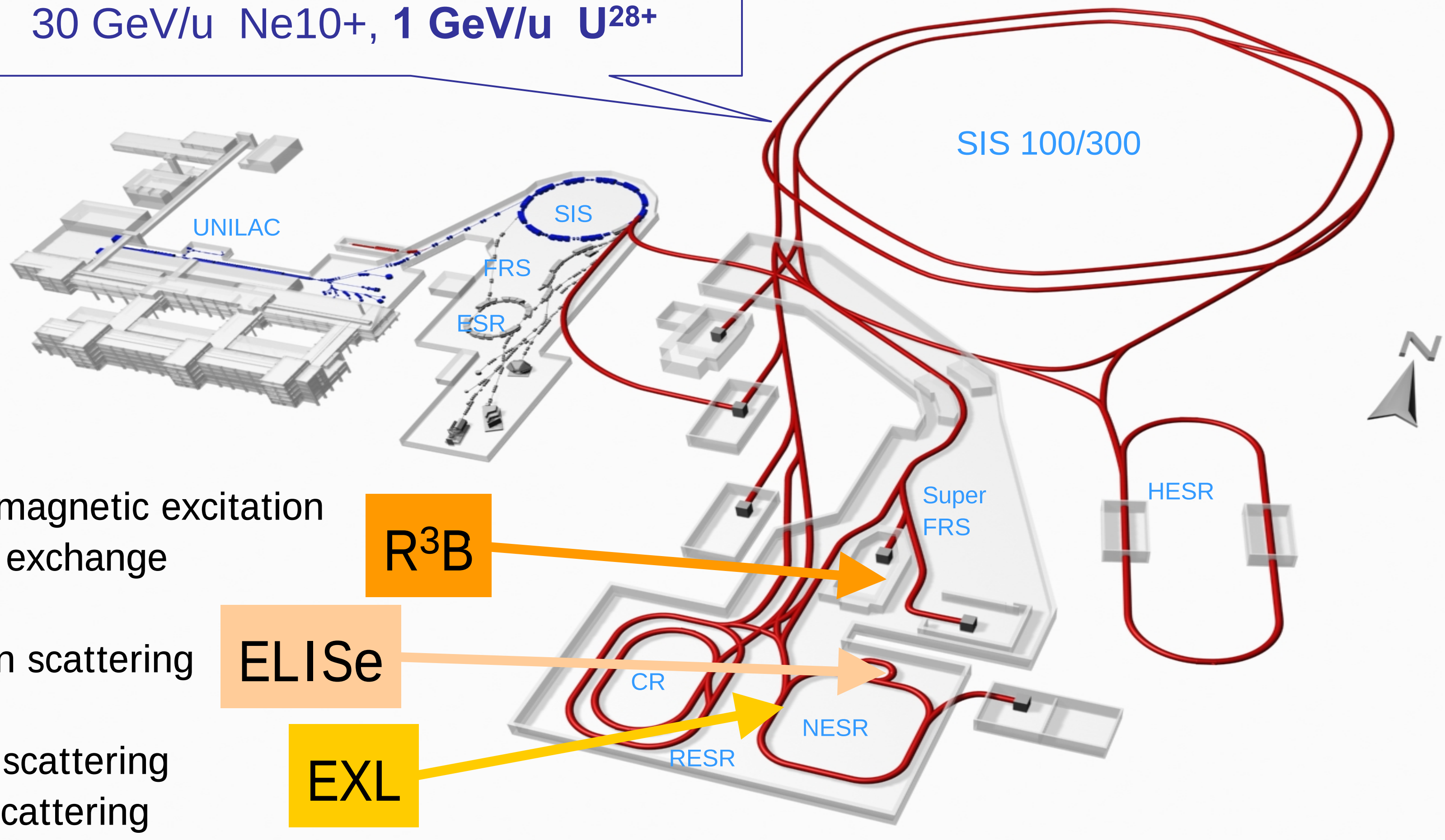

electromagnetic excitation
charge exchange — R^{3}B

electron scattering — ELISe

proton scattering
alpha scattering — EXL

A New In-Flight Exotic Nuclear Beam Facility

I High intensity primary beams from SIS 200 (e.g. 10^{12} ^{238}U / sec at 1 GeV/u)

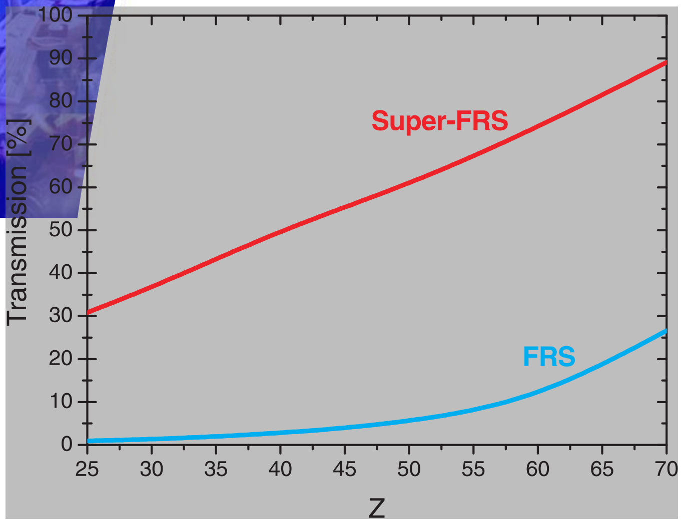

II Superconducting large acceptance Fragmentseparator

Optimized for efficient transport of fission products

III Three experimental areas

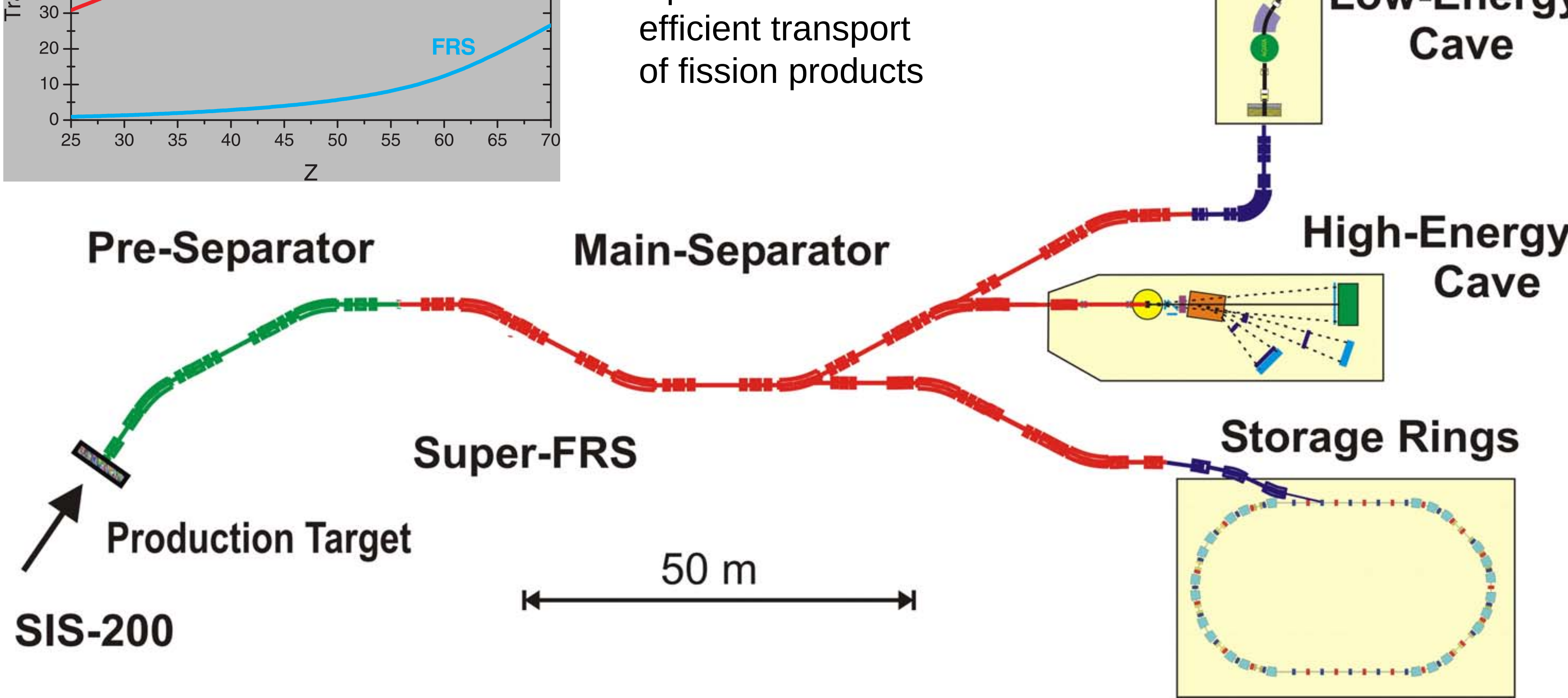

Production rates at FAIR

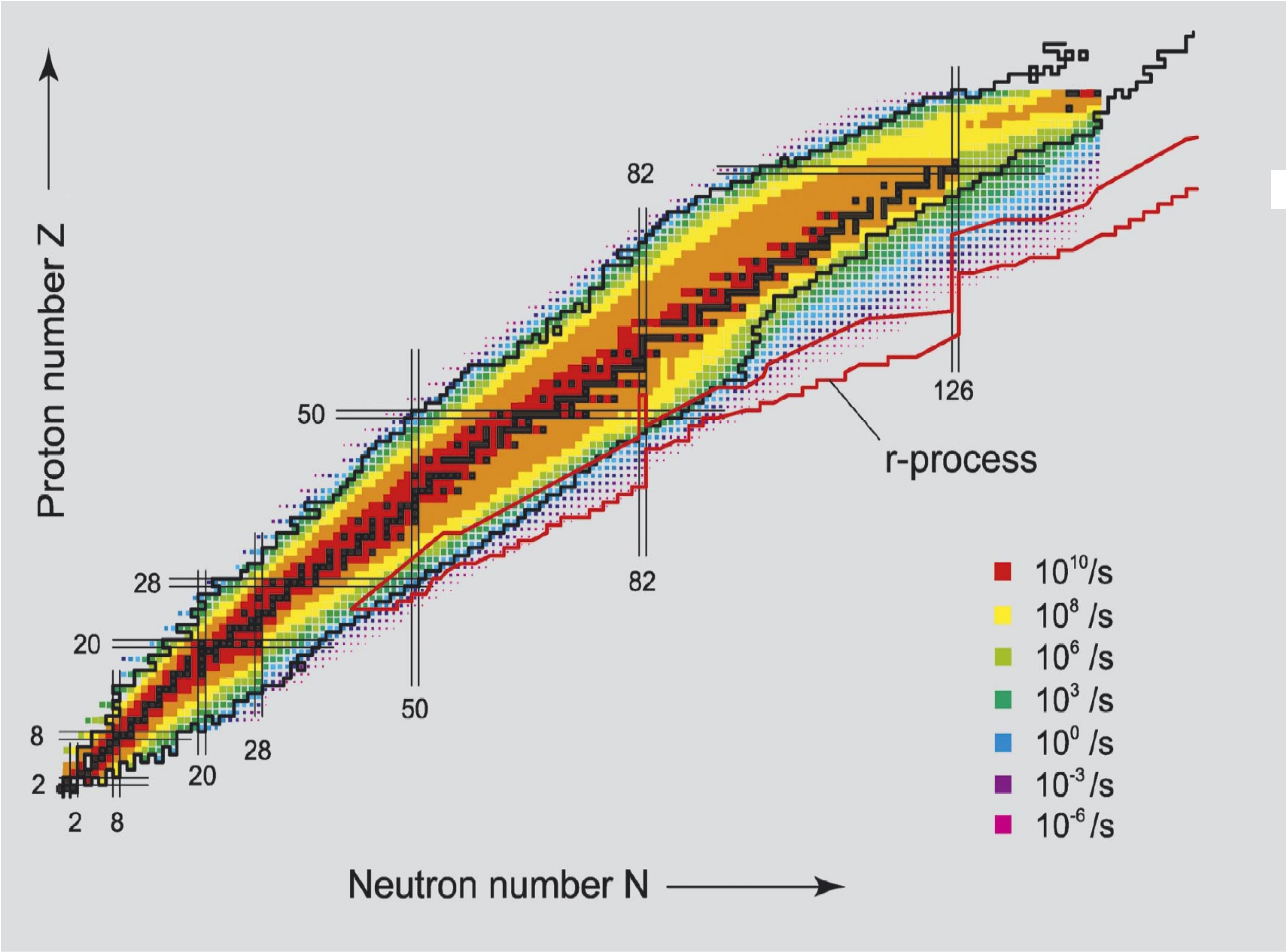

P. Roussel-Chomaz

Reactions with Relativistic Radioactive Beams

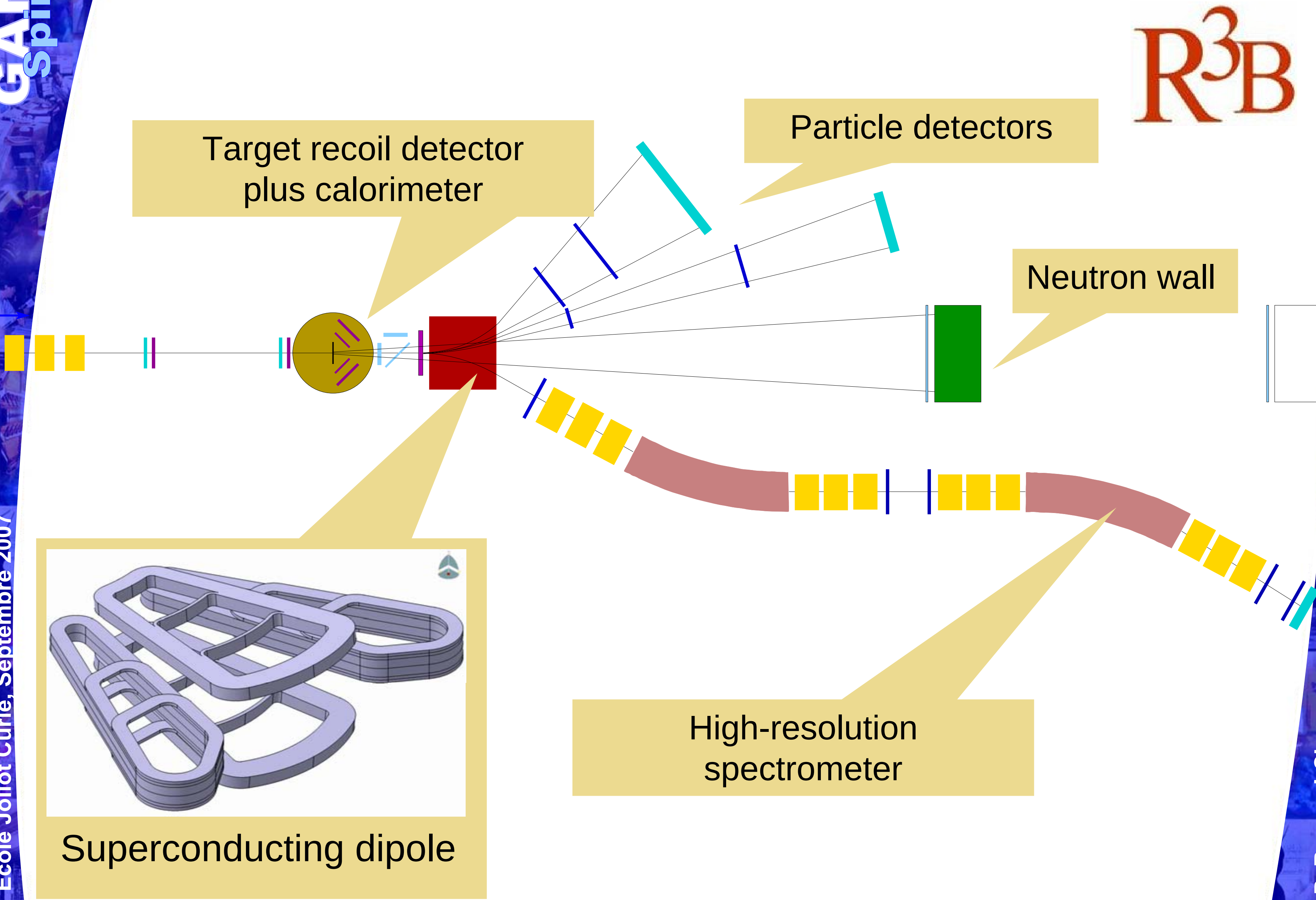

P. Roussel-Chomaz

Experiments at Storage Rings: EXL and ELISe

- Mass measurements
- Reactions with internal targets
  - ☺ Elastic p scatt.
  - ☺ (p,p') (α,α')
  - ☺ transfer
- Electron scattering
  - ☺ elastic scattering
  - ☺ inelastic

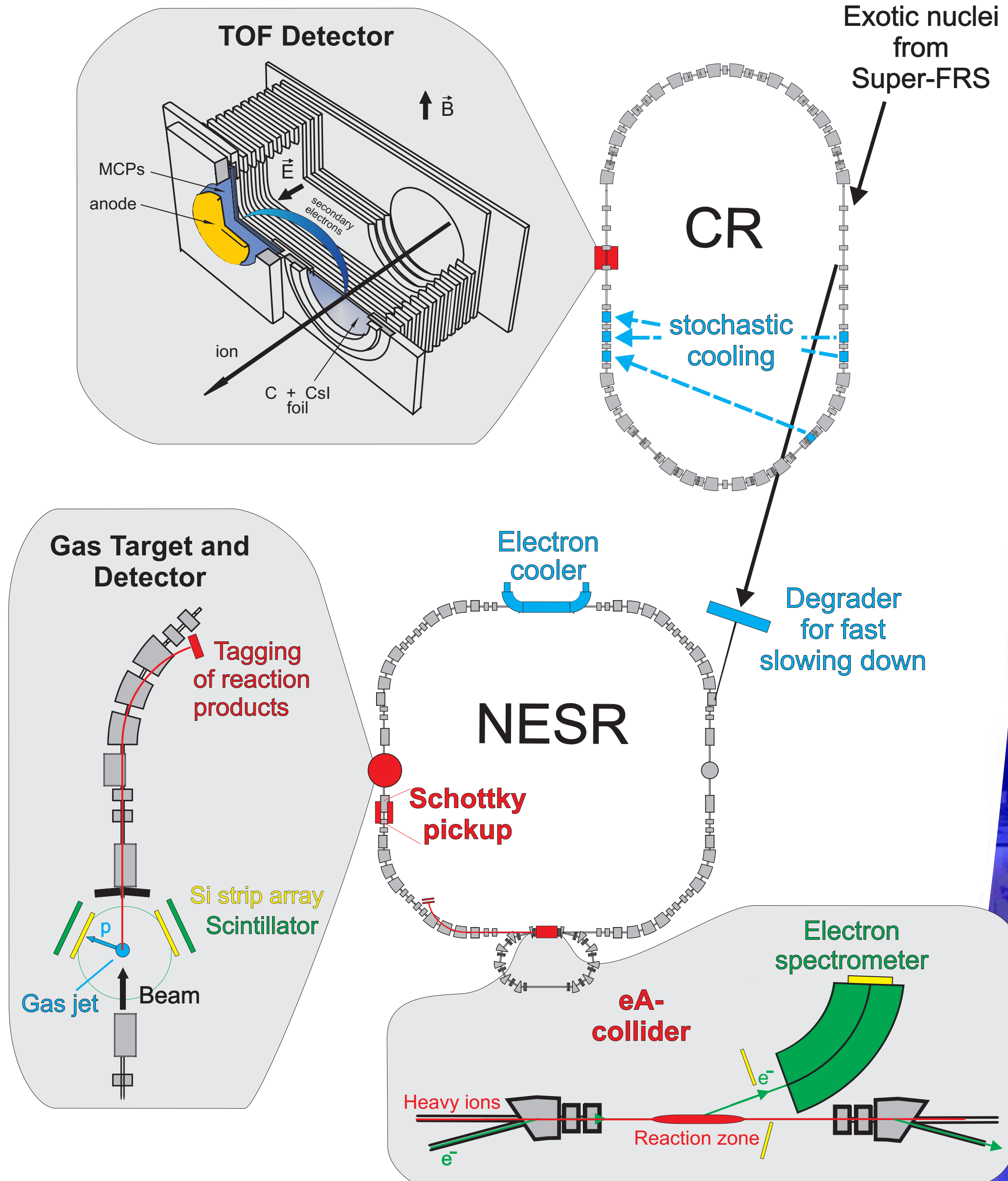

Exotic Nuclei Studied in Light-Ion Induced Reactions at NESR

EXL

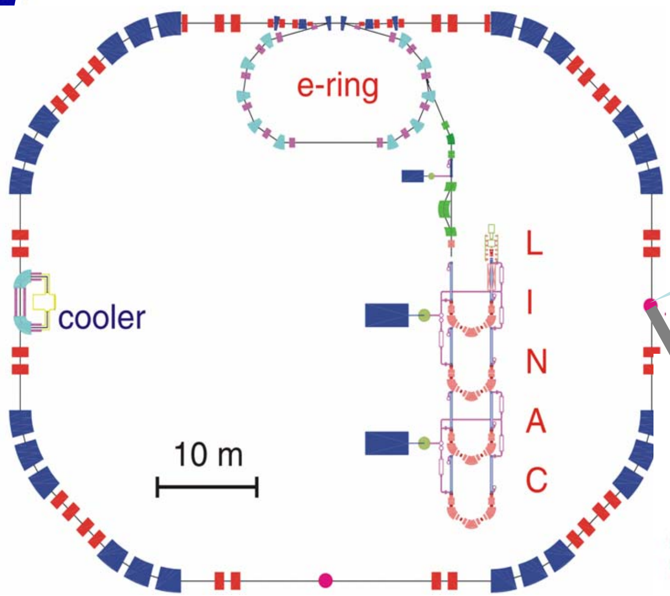

NESR

Internal target

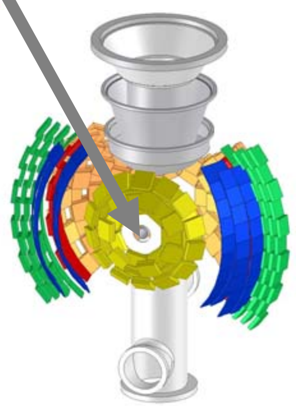

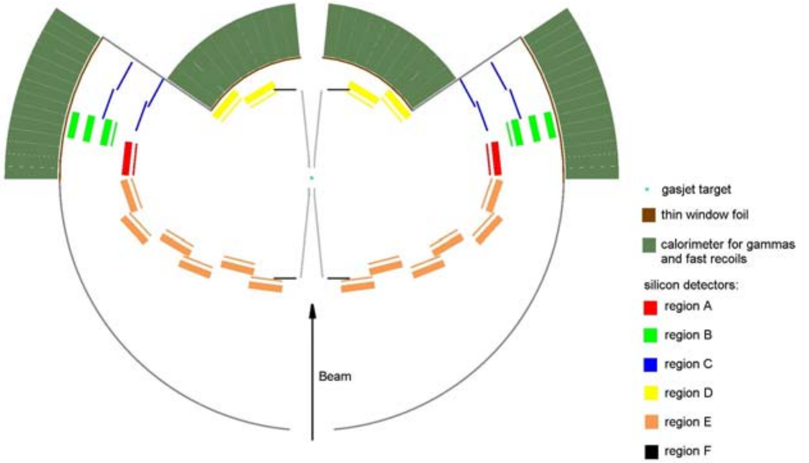

Target-Recoil and Gamma Detector around internal target

P. Roussel-Chomaz

The Electron-Ion (eA) Collider

ELISe

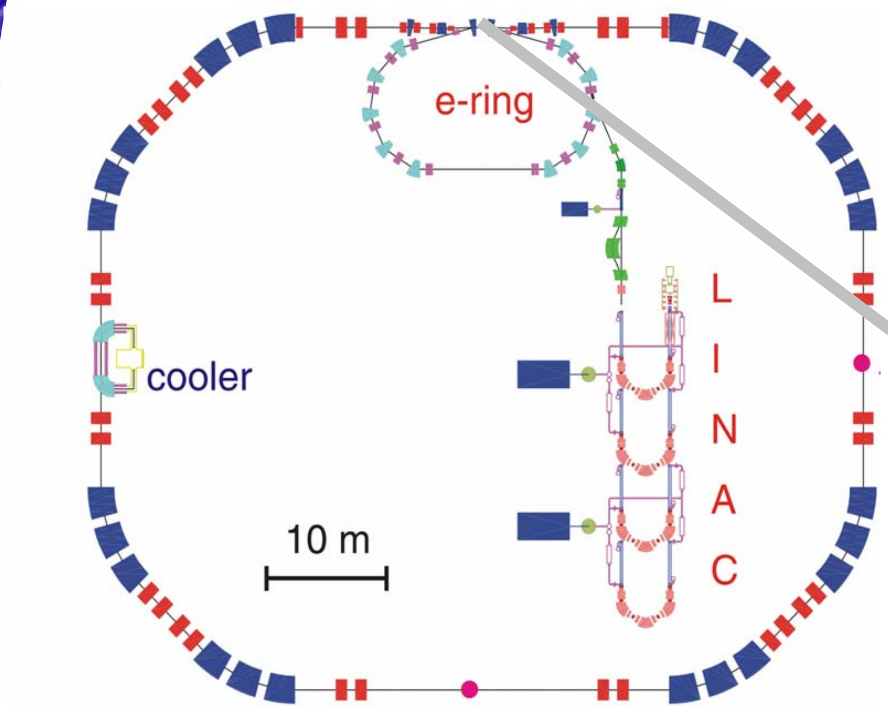

Electron spectrometer
$\Delta p/p=10^{-4}$
gap 25 cm
weight 90 t

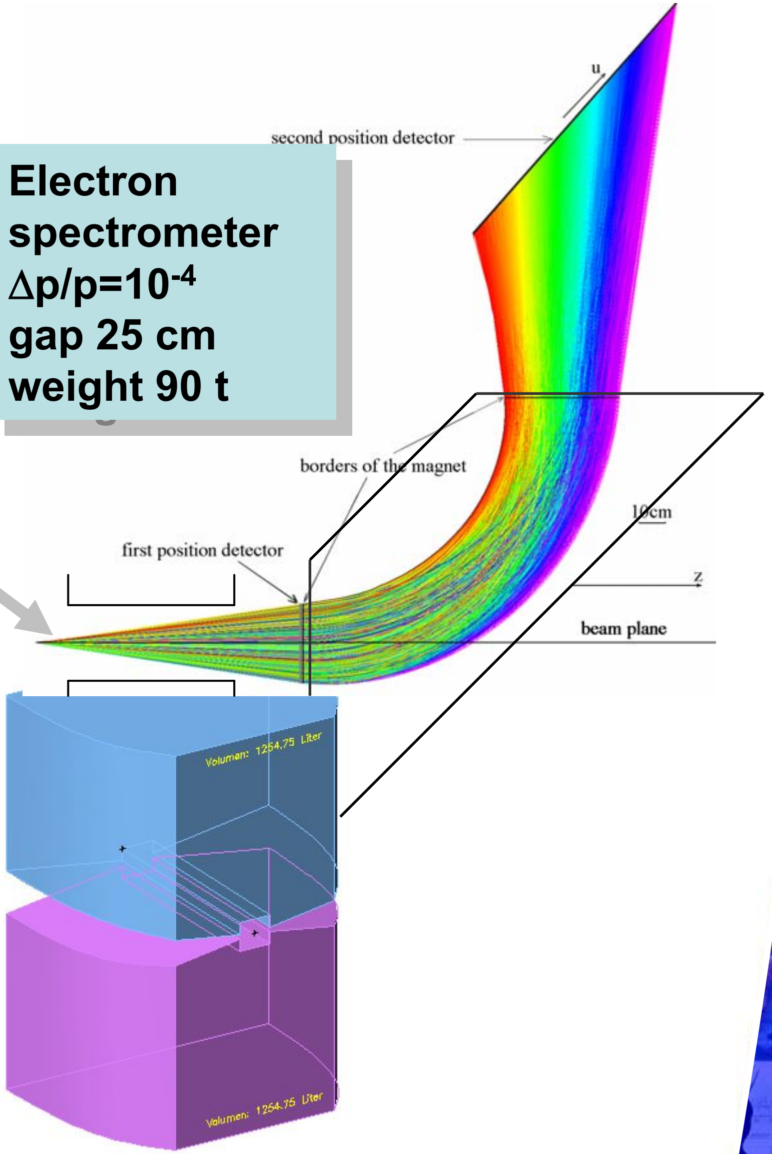

SPIRAL 2 Layout

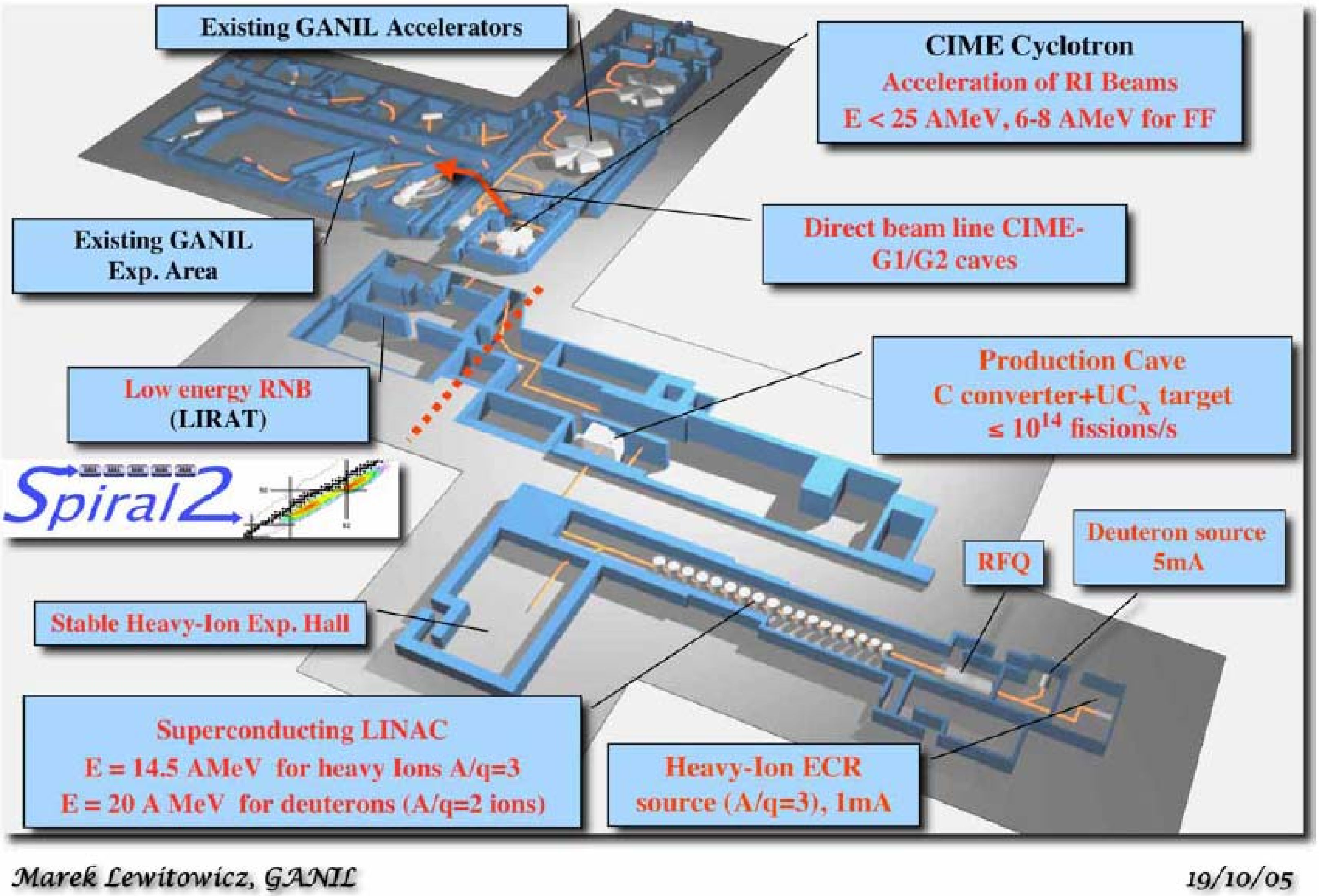

Regions of the Chart of Nuclei Accessible with SPIRAL 2 Beams

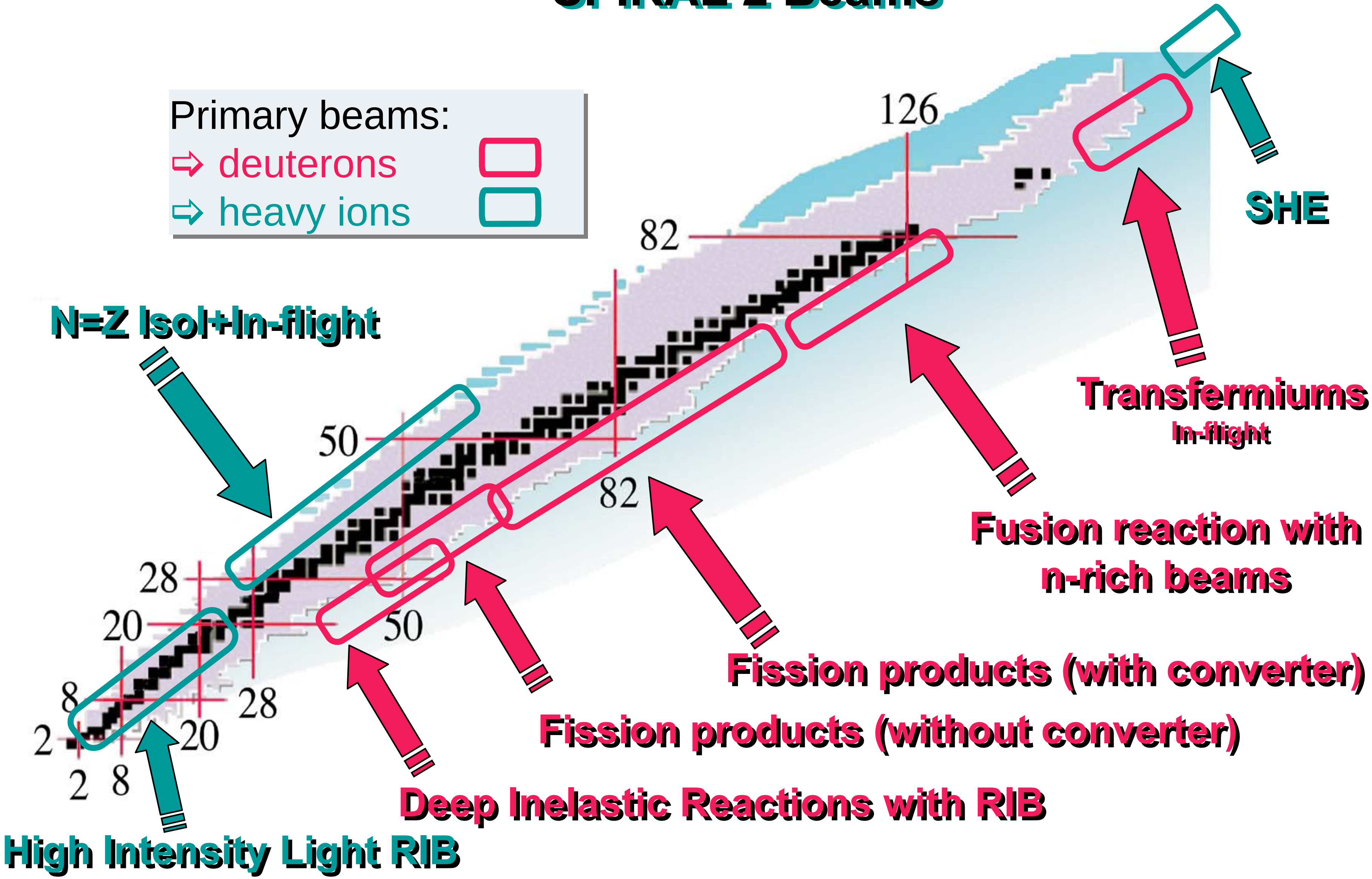

SPIRAL 2 production method

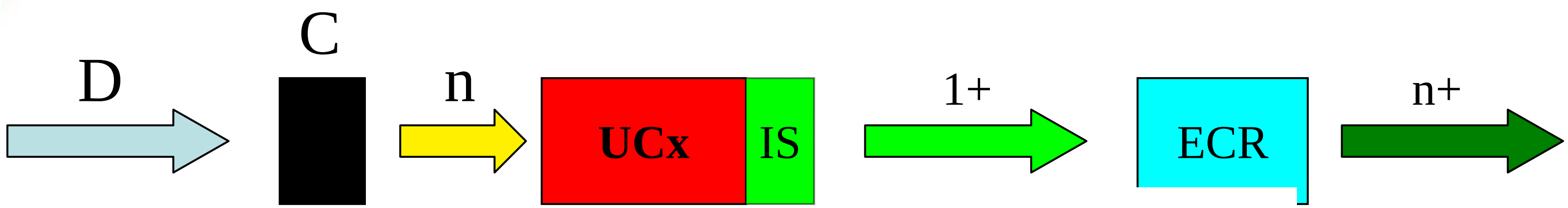

d (40 MeV, 4.3 mA) + C + UC (2.3g/cm^3, 363g, individuelle)

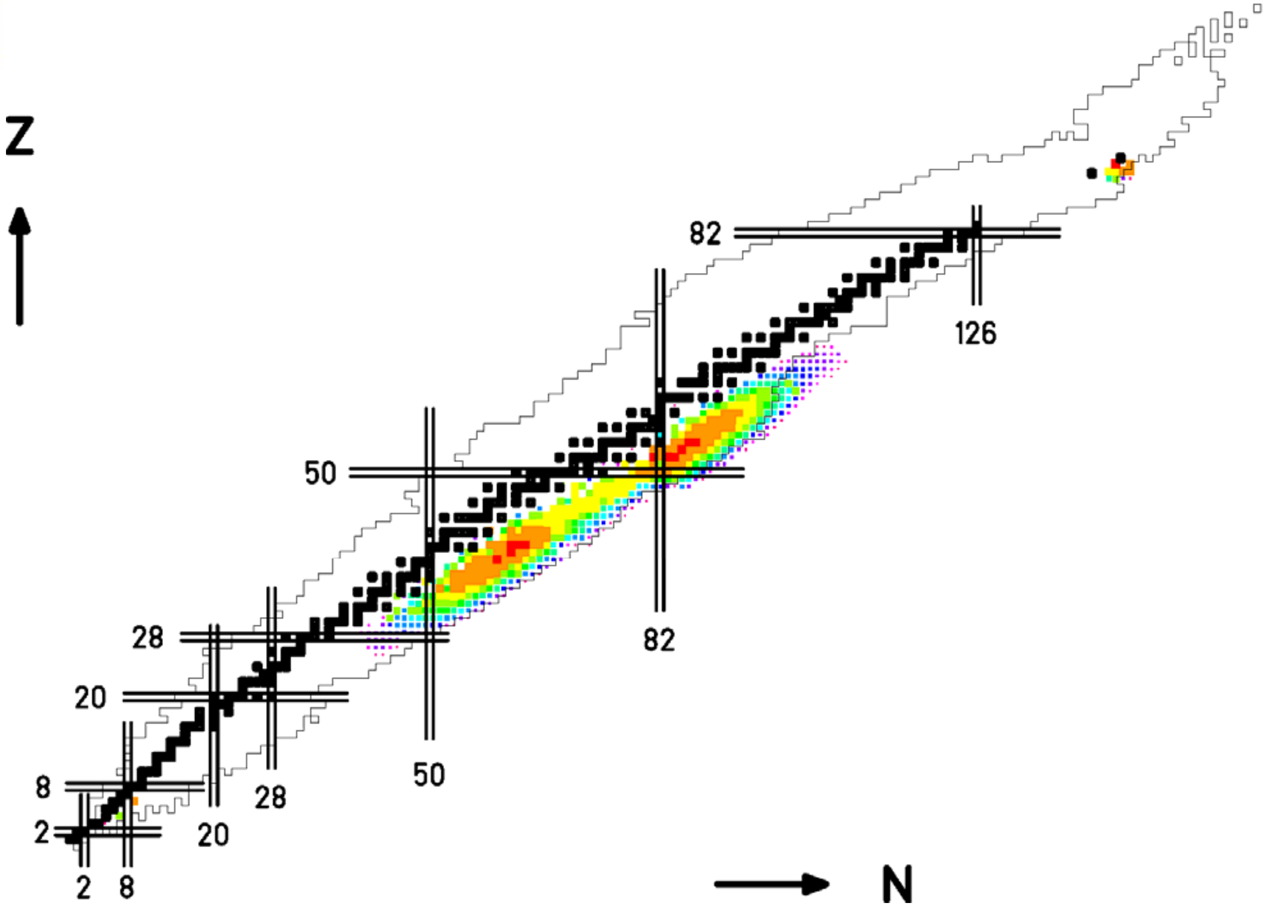

In target 10^{13}

- 10^4–10^5 pps
- 10^5–10^6 pps
- 10^6–10^7 pps
- 10^7–10^8 pps
- 10^8–10^9 pps
- 10^9–10^{10} pps
- 10^{10}–10^{11} pps
- 10^{11}–10^{12} pps

x 0.01-1%

Fission yields

With converter

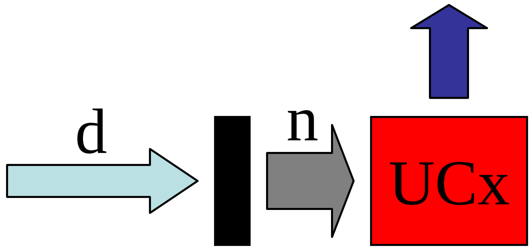

4.5 mA 10^{13} f/s ρ=2.3g/cm^3 V=240cm^3

5 mA 5.10^{13} f/s ρ=11g/cm^3 V=240cm^3

5 mA 2.10^{14} f/s ρ=11g/cm^3 V=1000cm^3 6kW (limit)

Fission of ^{239}U E_x= 20 MeV

40 MeV deuterons, 5 mA $\Rightarrow$ **200 kW** in the converter

Without converter

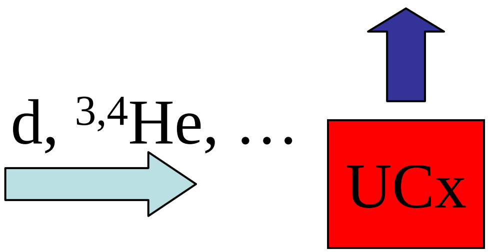

0.15mA 5.10^{12} f/s 6kW

Fission of ^{240}Pu,... $E_x \geq$ 50 MeV

acces to a wider mass region

Production of neutron deficient and (super) heavy

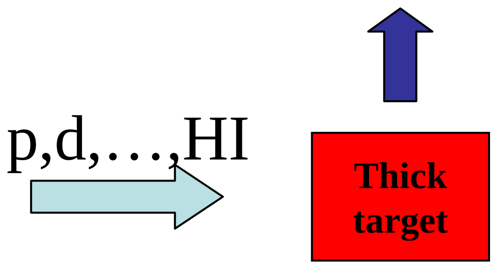

Fusion-evaporation and transfer reactions residues produced by thick target method (like ISOL@GSI) exemple 1/s $^{100}Sn\ 1^{+}$

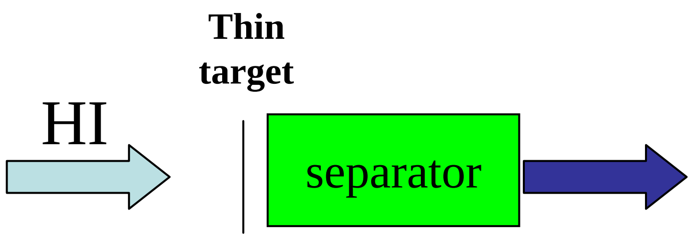

Fusion-evaporation residues produced by thin target method (In-Flight) example: 3×10^{4} /s $^{80}Zr\ 1^{+}$

Spectroscopy of N=Z A≈100, spectroscopy of SH, SHE production...

Primary Heavy Ion beams at 14.5A MeV of 1 mA, up to Ar

Expected Intensities

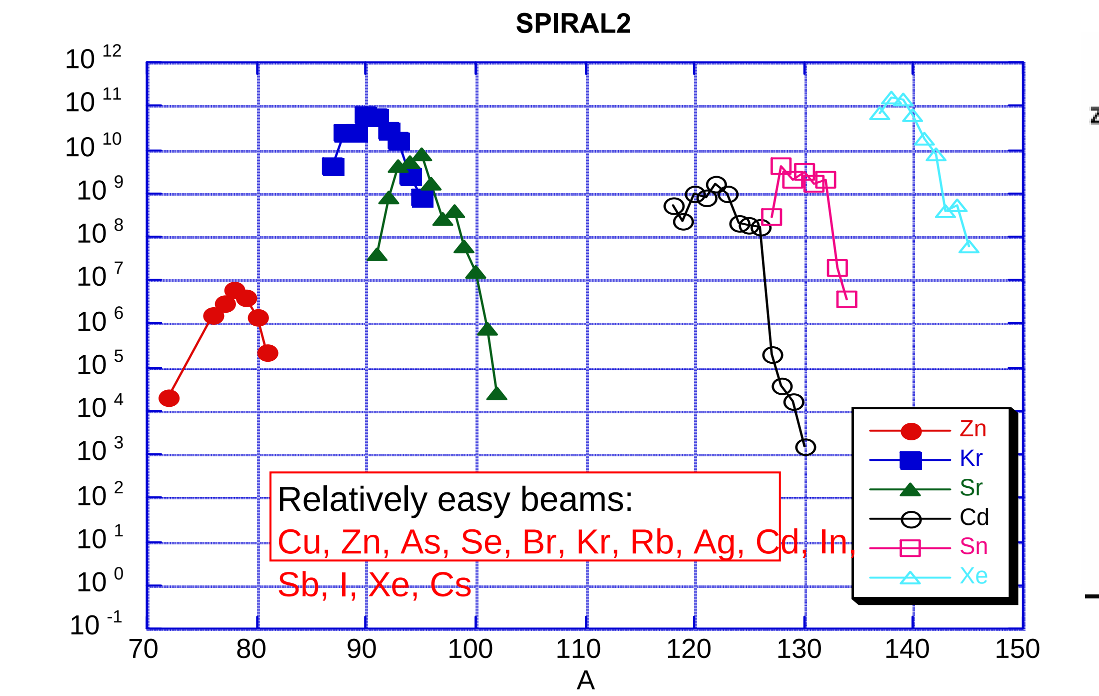

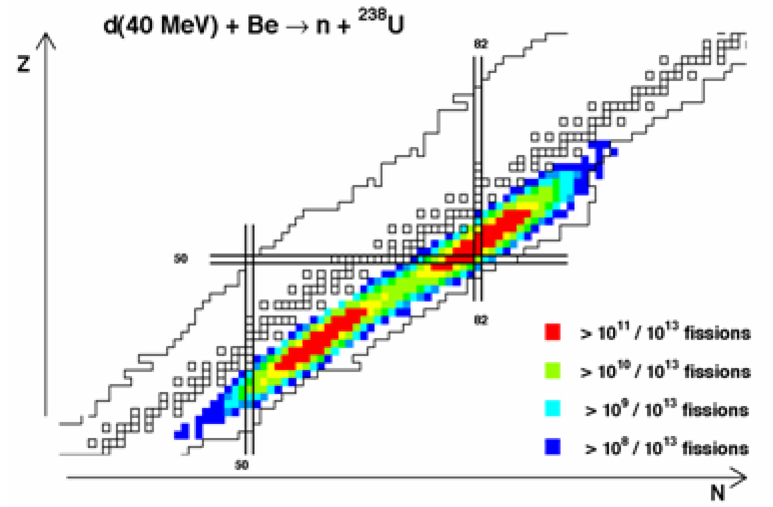

Isotope	A/Z	$T_{1/2}$, s	Production reaction
^{6}He	3.0	0.81	^{9}Be(nα)^{6}He
^{8}He	4.0	0.12	^{9}Be(^{13}C,^{14}O)^{8}He
^{8}Li	2.7	0.84	^{11}B(nα)^{8}Li or ^{9}Be(d,^{3}He)^{8}Li
^{9}Li	3.0	0.18	^{11}B(n,^{3}He)^{9}Li or ^{9}Be(^{7}Li,^{7}Be)^{9}Li
^{11}Be	2.8	13.8	^{11}B(n,p)^{11}Be
^{15}C	2.5	2.45	^{9}Be(^{7}Li,p)^{15}C
^{16}N	2.3	7.13	^{16}O(n,p)^{16}N or ^{10}B(^{7}Li,p)^{16}N
^{18}N	2.6	0.62	^{18}O(n,p)^{18}N
^{19}O	2.4	26.9	^{19}F(n,p)^{19}O
^{20}O	2.5	13.5	^{19}F(nγ)^{20}O or ^{19}F(d,n)^{20}O
^{23}Ne	2.3	37.2	^{19}F(^{6}Li,2p)^{23}Ne or ^{24}Mg(n,2p)^{23}Ne
^{25}Ne	2.5	0.60	^{26}Mg(^{13}C,^{14}O)^{25}Ne or ^{26}Mg(n,2p)^{25}Ne
^{25}Na	2.3	59.1	^{25}Mg(^{12}C,^{12}N)^{25}Na or ^{25}Mg(n,p)^{25}Na
^{26}Na	2.4	1.08	^{26}Mg(d,^{2}He)^{26}Na or ^{26}Mg(n,p)^{26}Na

^{9}Be(n,α)^{6}He ~ 10^{13} pps

^{14}N(d,n)^{15}O ~ 10^{12} pps

P. Roussel-Chomaz

Future Equipment for SPIRAL2

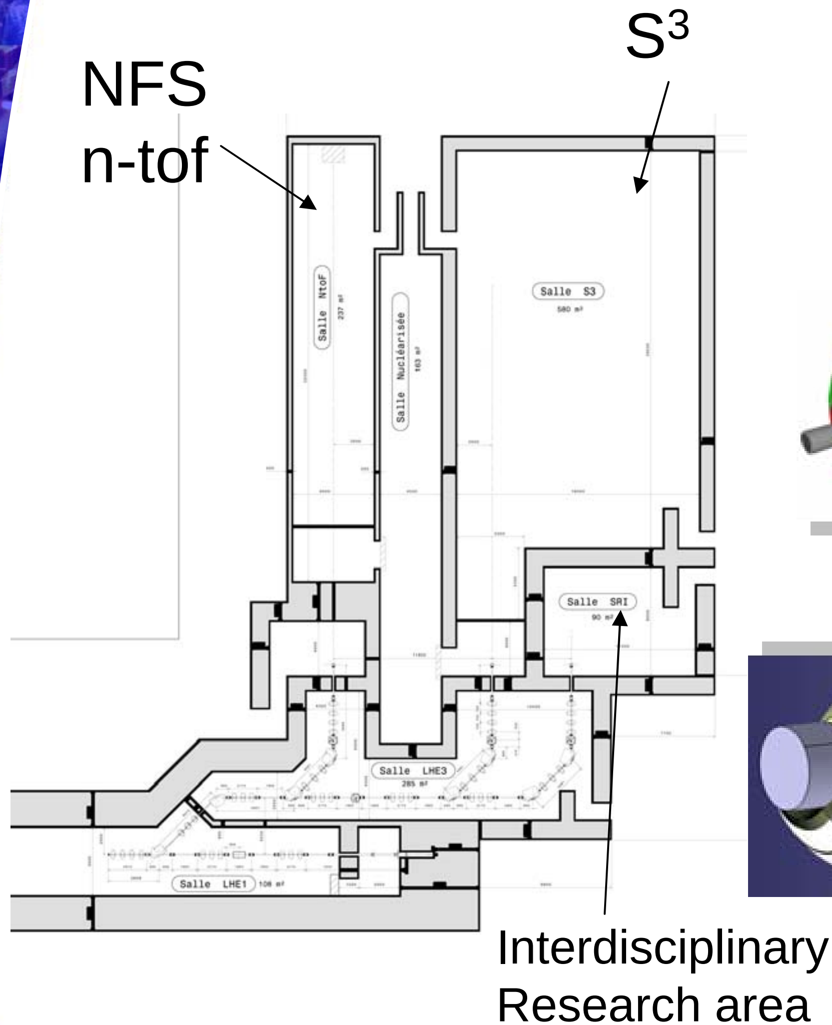

S3

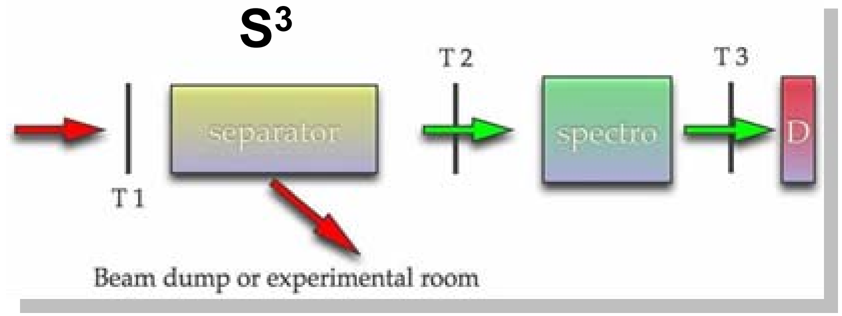

AGATA

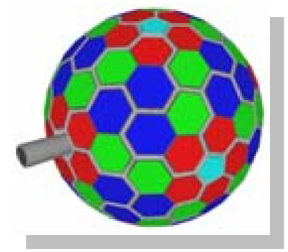

EXOGAM 2

ACTAR

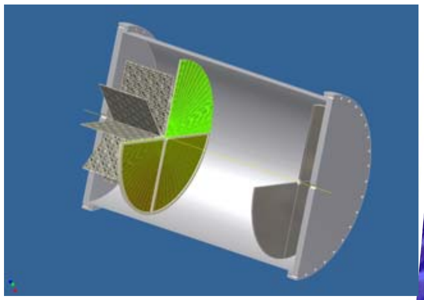

PARIS

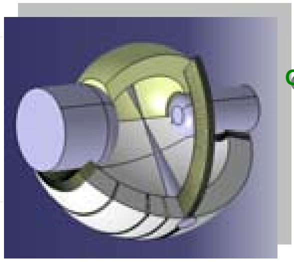

GASPARD

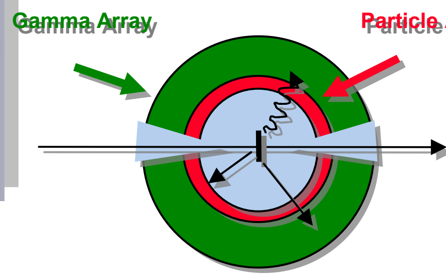

FAZIA

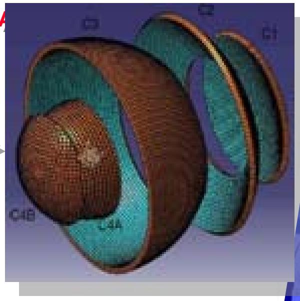

European RNB Facilities Road Map

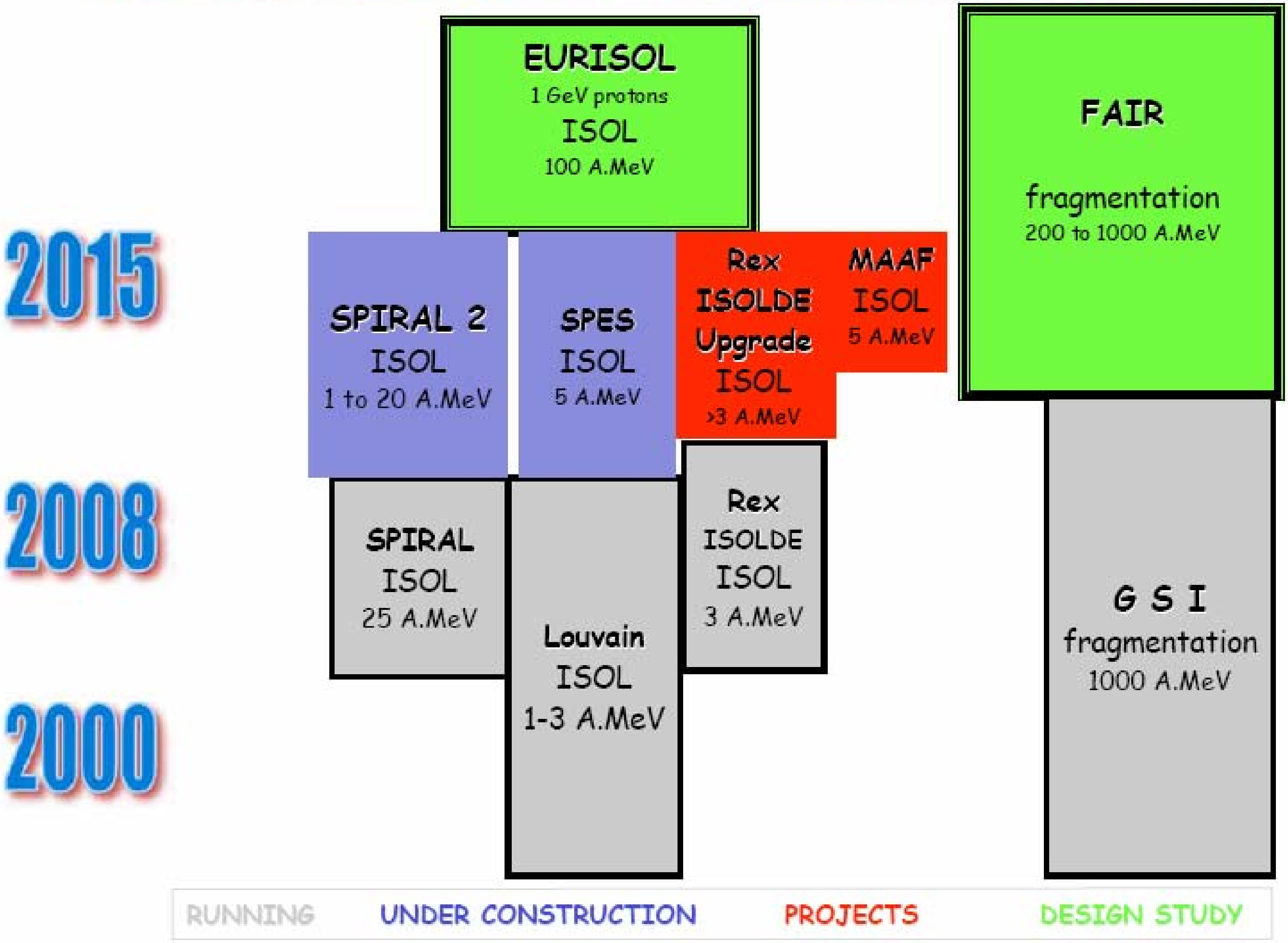

The EURISOL Concept

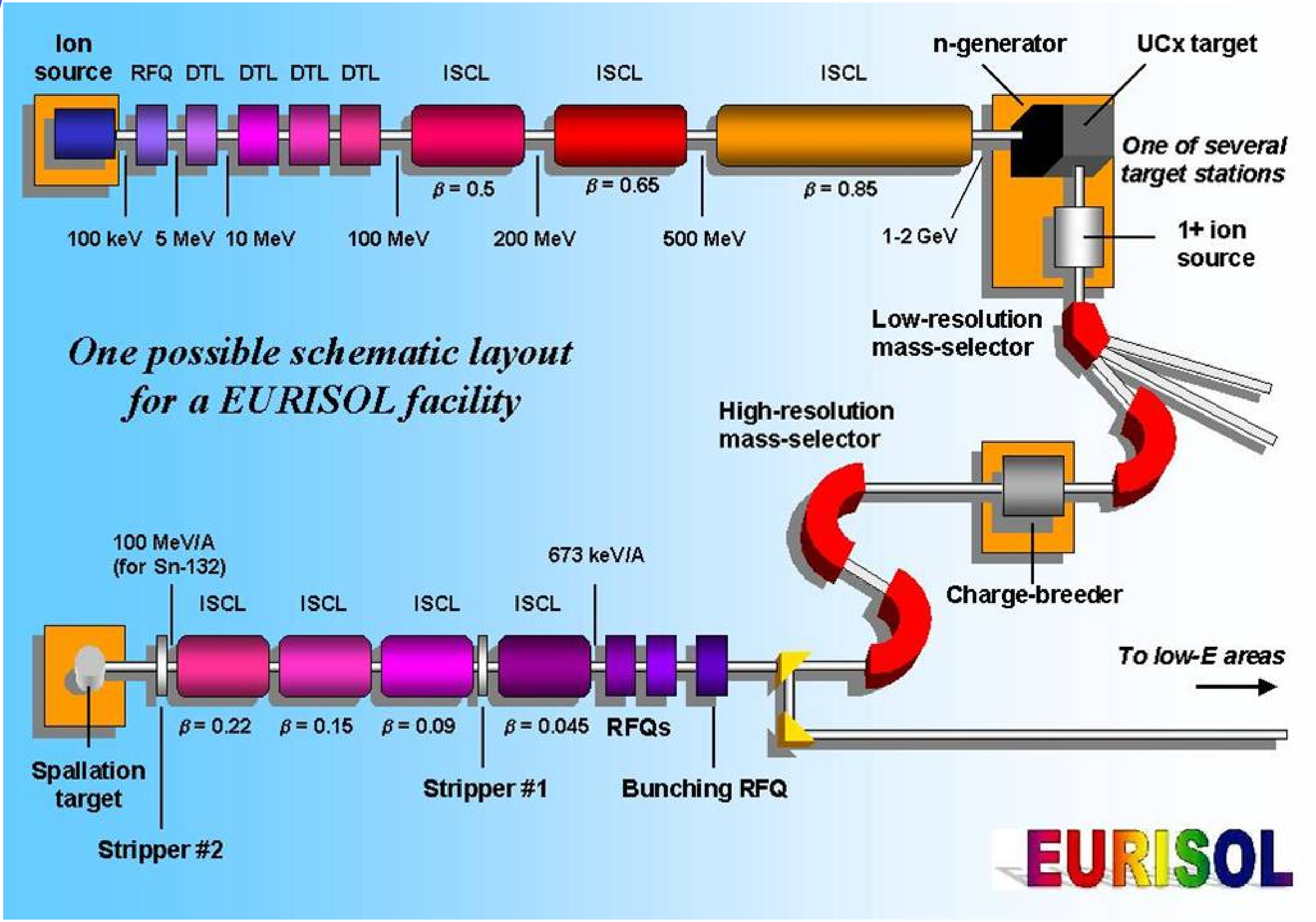

Some beam intensities

Calculations for EURISOL : Helge Ravn

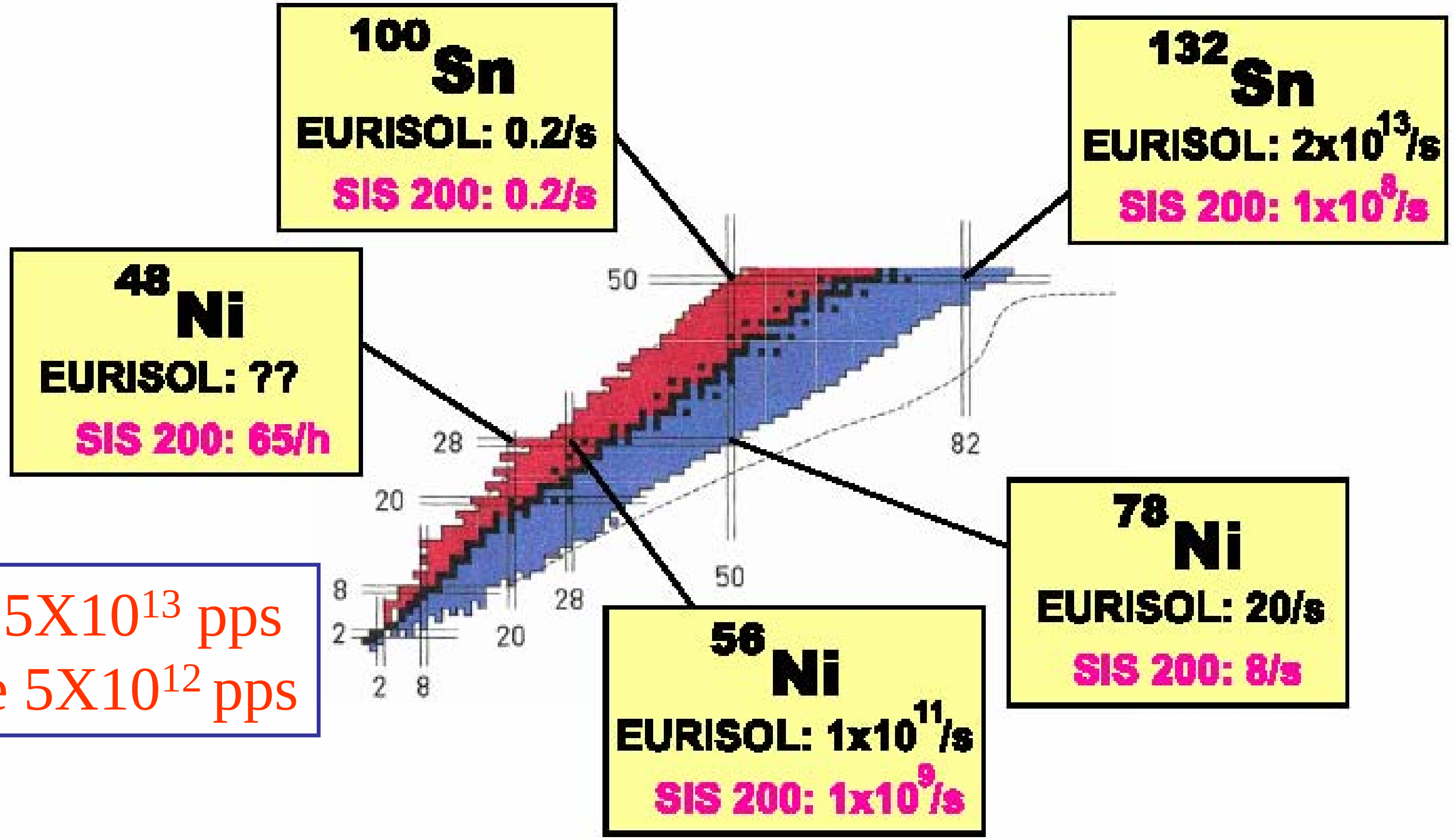

Fig. 5.2: The region of the chart of nuclides that illustrates the interesting doubly-magic nuclei far from stability and a comparison of their projected rates (as in figure 5.1) at EURISOL and the future GSI facility ('SIS 200').

^{6}He 5X10^{13} pps
^{18}Ne 5X10^{12} pps

Yields after acceleration

Comparison between facilities

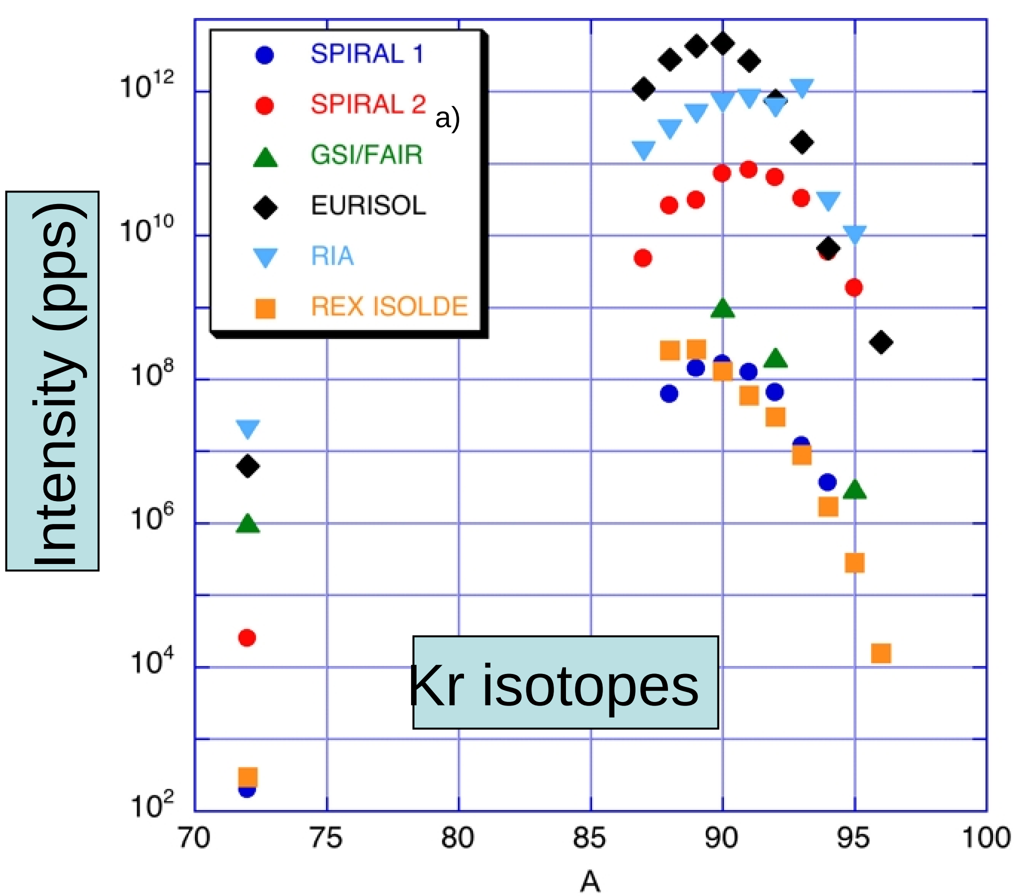

a) Yield for in-flight production of fission fragments at relativistic energy

The end…

A possible schematic layout for a EURISOL facility

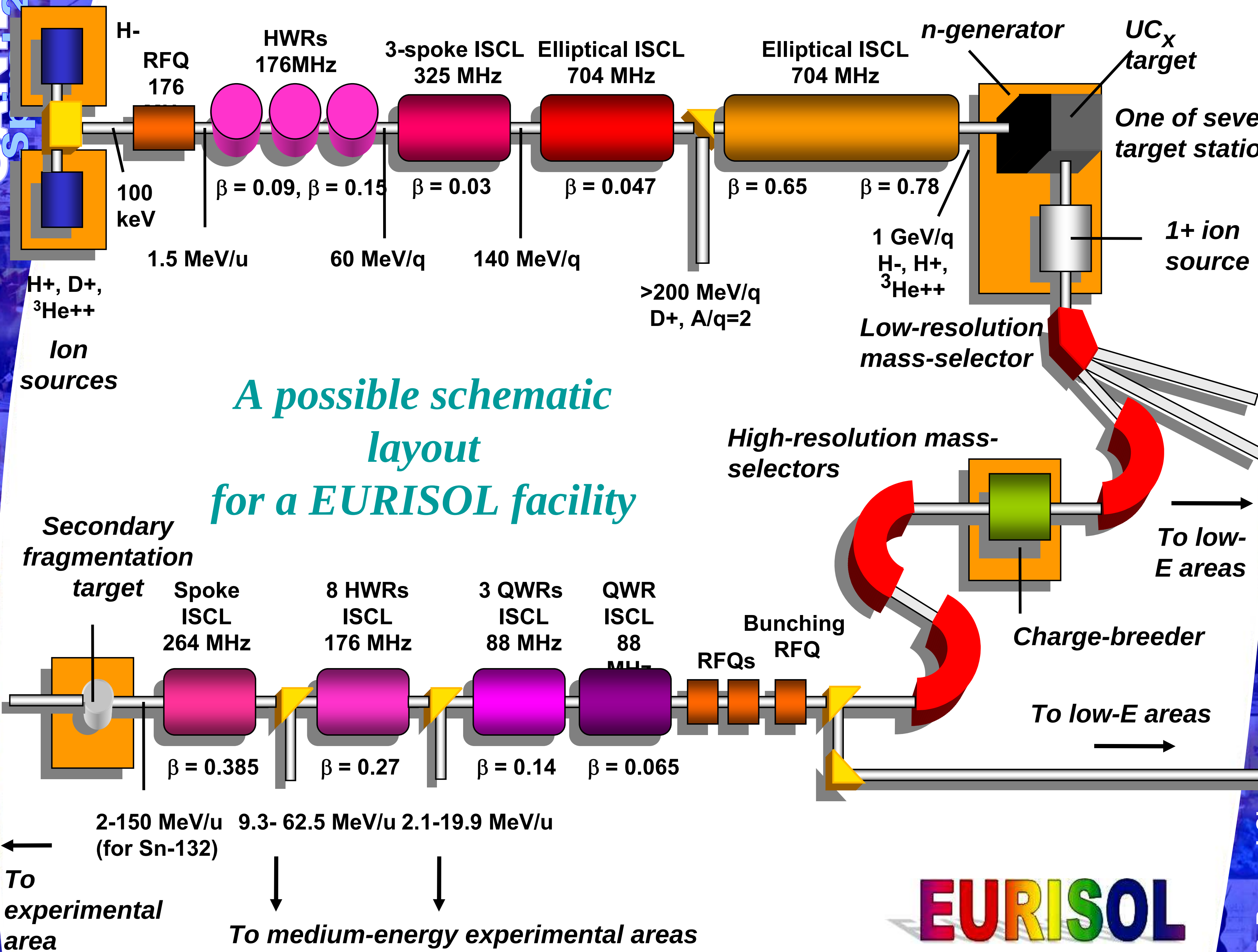

EURISOL

Coulomb Excitation: Experiment

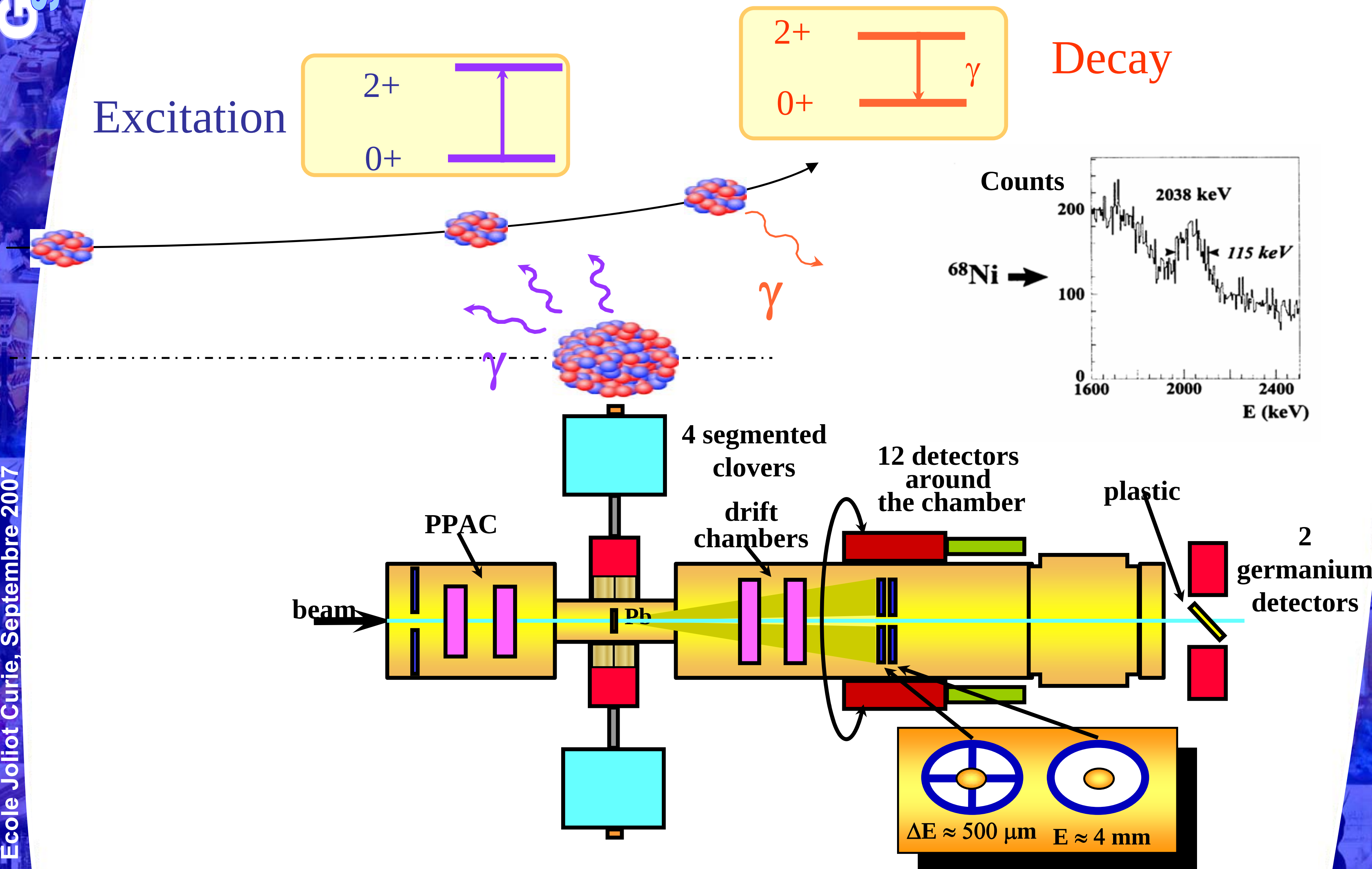

Exclusive nucleon removal reactions

Cross section leading to a final state n :

$$\sigma(n) = \Sigma_j\, C^2S(j,n)\ \sigma_{sp}(j,B_n)$$

J.Tostevin, J. Phys. G25 (1999) 735

Spectroscopic factor

Single particle removal cross section

Deduced from the experiment
or taken from shell model

Eikonal model, sum of stripping and
diffractive dissociation.
(Jeff Tostevin)

$\sigma_{sp} = \sigma_{stripping} + \sigma_{diffraction}$

Calculated in the eikonal model (integration over straight line trajectory,
ingredients are n-T and C-T interaction potentials) E>50 MeV/A

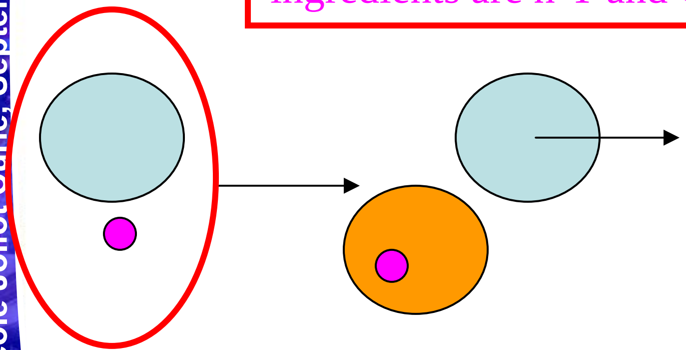

stripping

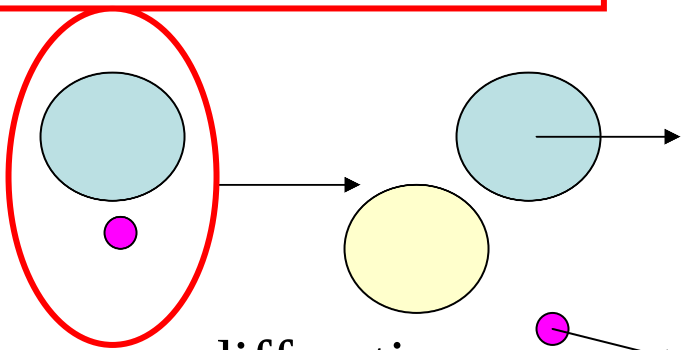

diffraction

P. Roussel-Chomaz